Figures and tables

Figures

(Figure 3.4) Sel Ayre: relative pollen diagram showing selected taxa as percentages of total pollen and spores (from Birks and Peglar, 1979; Lowe, 1984).

(Figure 3.5) Burn of Aith: relative pollen diagram showing selected taxa as percentages of total pollen (from Birnie, 1981).

(Figure 3.6) Garths Voe: relative pollen diagram showing selected taxa as percentages of total pollen (from Birnie, 1981).

(Figure 4.1) Location map and principal features of the glaciation of Orkney, including patterns of striations, directions of transport of erratics and shelly till localities (from Sutherland, 1991b).

(Figure 4.2) Section at Muckle Head, Orkney. The raised beach gravel, which rests on a rock platform, incorporates large flagstone blocks and is overlain in turn by a head deposit and till. (Photo: D. G. Sutherland.)

(Figure 4.3) Location map of North Hoy.

(Figure 4.4) Solifluction terraces on Ward Hill, Hoy. The turf-banked terraces are orientated approximately parallel with the contours. (Photo: J E. Gordon.)

(Figure 5.1) Location map and principal features of the glaciation of Caithness, including patterns of striations, ice-moulded landforms, distribution of erratics and shelly till (from Peach and Horne, 1881c; Sissons, 1967a; Sutherland, 1984a).

(Figure 5.2) Loch of Winless: relative pollen diagram showing selected taxa as percentages of total pollen (from Peglar, 1979). Note that the data are plotted against a radiocarbon time-scale.

(Figure 6.1) Location map and principal glacial features of the north-west Highlands (modified from Johnstone and Mykura, 1989).

(Figure 6.2) The Gairloch Moraine and associated landforms (from Robinson and Ballantyne, 1979).

(Figure 6.3) The Gairloch Moraine, in the valley of the River Sand north-west of Gairloch, comprises a low ridge of boulders. (Photo: J E. Gordon.)

(Figure 6.4) Geomorphology of the Achnasheen area (from Sissons, 1982a).

(Figure 6.5) Glaciofluvial terraces at Achnasheen. (British Geological Survey photograph B915.)

(Figure 6.6) The An Teallach area, showing principal glacial features and the limits of former glaciers (from Ballantyne, 1987b).

(Figure 6.7) The east flank of An Teallach. A clear lateral moraine and drift limit (centre) mark the extent of the Loch Lomond Readvance glacier that occupied the corrie of Toll an Lochain. The ice-scoured Torridonian sandstone of the lower slopes contrasts with the frost-shattered slopes of the mountain ridge and the quartzite blockslopes on Glas Mheall Liath. (British Geological Survey photograph D2102.)

(Figure 6.8) Periglacial landforms and deposits on the northern plateau of An Teallach (from Ballantyne, 1984).

(Figure 6.9) The Baosbheinn protalus rampart and associated landforms, showing the upper boulder ridge (AB) and lower ridges (CD and EF) (from Ballantyne, 1986a).

(Figure 6.10) Protalus rampart on the north-west flank of Baosbheinn. The view also shows the rock avalanche scar, the two lower Wester Ross Readvance moraine ridges and a Loch Lomond Readvance moraine intersecting the latter at the base of the mountain. (Cambridge University Collection: copyright reserved.)

(Figure 6.12) Beinn Alligin, a Torridonian sandstone mountain in Wester Ross, rises above an ice-scoured surface of Lewisian gneiss to the west. A lateral moraine (centre left) marks the limit of a Loch Lomond Readvance glacier and is

succeeded on the lower slopes by hummocky moraine; fluted drift can also be seen in the centre and to the right of the photograph. A large rock avalanche scar is prominent below the summit of Sgurr Mhor. The resulting deposit on the corrie floor includes a low tongue of boulders extending beyond the main part of the deposit. (Cambridge University Collection: copyright reserved.)

(Figure 6.11) Geomorphology of Toll a'Mhadaidh, Beinn Alligin, showing rockslide debris and principal glacial landforms (from Sissons, 1977d). formation, as they take the form of protalus lobes (see Wahrhaftig and Cox, 1959; Liestøl, 1961; Outcalt and Benedict, 1965; White, 1976; Lindner and Marks, 1985; Martin and Whalley, 1987; Whalley and Martin, 1992) that have apparently developed as a result of deformation of ice within rockfall talus accumulations. The only other features in Britain that may be of similar origin to that at Beinn Alligin are at Moelwyn Mawr in North Wales (Campbell and Bowen, 1989) and Beinn an Lochain in Argyll (Holmes, 1984; Maclean, 1991).

(Figure 6.13) Geomorphology of Coire a'Cheud-chnoic (from Hodgson, 1987).

(Figure 6.14) Hummocky moraine at Coire a'Cheud-chnoic in Glen Torridon. A clear drift limit on the valley side demarcates the Loch Lomond Readvance deposits below, from the ice-scoured bedrock slopes above. (British Geological Survey photograph D2737.)

(Figure 6.15) Diagrammatic reconstruction of the lithostratigraphy of the Creag nan Uamh caves, showing proposed relationships between certain of the layers (from Lawson, 1983).

(Figure 6.16) Cam Loch: relative pollen diagram, showing selected taxa as percentages of total pollen (from Pennington, 1977a).

(Figure 6.17) Loch Sionascaig: relative pollen diagram, showing selected taxa as percentages of total pollen (from Pennington *et al.*, 1972).

(Figure 6.18) Lochan an Druim: relative pollen diagram, showing selected taxa as percentages of total pollen (from Birks, 1980). Note that the data are plotted against a radiocarbon time-scale.

(Figure 6.19) Loch Maree: relative pollen diagram, showing selected taxa as percentages of total pollen (from Birks, 1972b).

(Figure 7.1) Location map of the Inverness area and generalized directions of ice movement.

(Figure 7.2) Section at Dalcharn showing the Dalcharn 'gravel formation' and the Dalcharn 'biogenic formation' (bottom left), overlain by a sequence of tills (right). (Photo: D. G. Sutherland.)

(Figure 7.3) Sediment logs and stratigraphy at Dalcharn (from Merritt and Auton, 1990).

(Figure 7.4) Relative pollen diagram for the Dalcharn 'biogenic formation', showing selected taxa only as percentage of total land pollen (from Walker, 1990a).

(Figure 7.5) Sediment logs of the Allt Odhar and adjacent sections (from Merritt, 1990c).

(Figure 7.6) Section at Allt Odhar showing the Odhar Peat resting on the Odhar Gravel and overlain by the Paraglacial Member of the Moy Formation. (Photo: D. G. Sutherland.)

(Figure 7.7) Relative pollen diagram for the Odhar Peat, showing selected taxa as percentages of total land pollen (from Walker, 1990b).

(Figure 7.8) Clava: lithological succession at the 'Main Pit' (from Horne *et al.*, 1894).

(Figure 7.9) Geomorphology of the Ardersier area (from Firth, 1989b).

(Figure 7.10) Geomorphology of the Struie meltwater channels, Strathrory (from J. S. Smith, 1968; Leftley, 1991).

(Figure 7.11) Geomorphology of the Kildrummie Kames esker system between High Wood and Meikle Kildrummie (from mapping by C. A. Auton for the British Geological Survey 1:50,000 Geological Sheet 84W (Fortrose), in press).

7.12 The Kildrummie Kames esker system viewed towards the east. Two areas of braided ridges (right foreground and centre distance) are linked by a single ridge. (Cambridge University Collection: copyright reserved.)

(Figure 7.13) Geomorphology of the eastern part of the Kildrummie Kames in the vicinity of Meikle Kildrummie (from Firth, 1984).

(Figure 7.14) Geomorphology of the Littlemill esker system between Inverarnie and Daviot (from mapping by J. W. Merritt for the British Geological Survey 1:50,000 Geological Sheet 84W (Fortrose), in press).

(Figure 7.15) Geomorphology of the Torvean area (from Firth, 1984). The terrace fragments include kame terraces (T161–T171), Lateglacial outwash and river terraces (T172–179, T159), and Holocene river terraces (T180–181).

(Figure 7.16) The Findhorn terraces at Ballachrochin. (British Geological Survey photograph C1415.)

(Figure 7.17) Geomorphology of Coire Dho showing landforms associated with the former ice-dammed lake (from Sissons, 197 713).

(Figure 7.18) Geomorphology of the Fort Augustus area (from Firth, 1984).

(Figure 7.19) Geomorphology of the Dores area (from Firth, 1984).

(Figure 7.20) Geomorphology of the Beauty carselands (from Firth, 1984).

(Figure 7.21) Section through the Beauly carselands at Barnyards showing the sequence of Late Devensian and Holocene deposits (frem Haggert 1986)

(Figure 7.22) Geomorphology of Munlochy Valley (from Firth, 1984).

(Figure 7.23) Periglacial landforms and deposits on the summit ridge of Ben Wyvis (from Ballantyne, 1984).

(Figure 8.1) Location map and principal features of the Quaternary geomorphology of north-east Scotland (from Hall and Connell, 1991).

(Figure 8.2) Schematic cross-section through the Moss of Cruden ridge. Borehole and pit data are from McMillan and Aitken (1981), Hall and Connell (1982) and A. M. Hall *et al*. (unpublished data).

(Figure 8.3) Weathered granite at Pittodrie overlain by soliflucted deposits. (Photo: J E. Gordon.)

(Figure 8.4) Kirkhill and Leys: lithostratigraphy.

(Figure 8.5) Kirkhill Quarry, south-east face B (1984). Developed in the Kirkhill Lower Sands and Gravels is the Kirkhill Lower Buried Soil, with its striking bleached horizon. The soil is truncated and overlain by laminated organic muds and sands, and then by periglacial slope deposits of Kirkhill Gelifluctate 3. These rubble layers have been partly reworked to form the Kirkhill Upper Till. The section is about 6 m high. (Photo: J. Jarvis.)

(Figure 8.6) Sediment logs and stratigraphy in the disused railway cutting at Bellscamphie.

(Figure 8.7) Fossil podsol and overlying organic horizon at Teindland. (Photo: D. G. Sutherland.)

(Figure 8.8) Teindland: relative pollen diagram showing selected taxa as percentage of total land pollen (from Edwards *et al.*, 1976; Lowe, 1984).

(Figure 8.9) Geomorphology of the Kippet Hills (from Smith, 1984).

(Figure 8.10) Geomorphology of the Muir of Dinnet (from Clapperton and Sugden, 1972).

(Figure 8.11) Loch Kinord: relative pollen diagram showing selected taxa as percentages of total land pollen (from Vasari, 1977).

(Figure 8.12) Section along the length of the Lower Philorth Valley showing the sequence of sediments (from Smith et al., 1982).

(Figure 9.1) Location map of the eastern Grampian Mountains. The limits of the Loch Lomond Readvance glaciers are from Sissons (1972a, 1974b, 1979f) and Sissons and Grant (1972).

(Figure 9.2) Principal geomorphological features of the Cairngorm Mountains (sources include Sugden, 1968, 1970; Young, 1974, 1975a; Sissons, 1979f; J E. Gordon, unpublished data).

(Figure 9.3) Summit plateau of Ben Avon in the Cairngorms showing well-developed tors which appear to have survived glaciation. The adjacent slopes have been affected by periglacial processes and the development of solifluction lobes. (Photo: J E. Gordon.)

(Figure 9.4) Glen More and the northern flank of the Cairngorms. The assemblage of landforms in this area includes the Cairngorm plateau and adjacent slopes extensively modified by solifluction lobes and terraces (Lurchers Gully — top centre), corries cut into the upper slopes of the massif, the striking glacial breach of the Lairig Ghru (top right), a system of ice-directed meltwater channels (including open-walled features — centre) and partly wooded glaciofluvial deposits in the valley bottom.

(Figure 9.5) Loch Lomond Readvance boulder moraine in Coire an t-Sneachda in the Cairngorms. The outer part of the moraine comprises several clearly defined ridges of boulders. (Photo: J E. Gordon.)

(Figure 9.6) Loch Lomond Readvance 'hummocky moraine' on the east flank of Glen Eidart in the Cairngorms. The deposits have a clear upper limit on the valley side and show well-defined lineations, which may mark successive ice-front positions of an actively retreating glacier. (Photo: J E. Gordon.)

(Figure 9.7) Active debris flows on the slopes above the Lairig Ghru. (Photo: J E. Gordon.)

(Figure 9.8) Geomorphology of the Lochnagar area (from Shaw, 1977; Clapperton, 1986).

(Figure 9.9) Summit blockfield, blockslopes and boulder lobes on the south-east flank of Cuidhe Cròm, Lochnagar. (Photo: J E. Gordon.)

(Figure 9.10) Geomorphology of the Loch Etteridge area (from Young, 1978).

(Figure 9.11) Loch Etteridge: relative pollen diagram showing selected taxa as percentages of total land pollen. The samples for radiocarbon dating were taken from comparable lithostratigraphic horizons in an adjacent core.

(Figure 9.12) Abernethy Forest: relative pollen diagram showing selected taxa as percentages of total land pollen (from Birks and Mathewes, 1978). Regional pollen assemblage zones are from Birks (1970). Note that the data are plotted against a radiocarbon time-scale.

(Figure 9.13) Allt na Feithe Sheilich: relative pollen diagram showing selected taxa as percentages of the pollen sums indicated (from Birks, 1975).

(Figure 9.14) Coire Fee: relastive pollen diagram showing selected taxa as a percentage of total pollen (from Huntley, 1981)

(Figure 9.15) Morrone: relative pollen diagram showing selected taxa as percentages of total pollen (from Huntley, 1976).

(Figure 9.16) Geomorphology of the Allt Garbhlach–Allt Fhearnagan area of Glen Feshie (from Robertson–Rintoul, 1986a; Werritty and Brazier, 1991).

(Figure 9.17) Top: surveyed section across the base of the Glen Feshie debris cones showing boundaries between individual debris-flow units. Bottom: detailed sections at sampling sites 1–4 (from Brazier and Ballantyne, 1989).

(Figure 10.1) Location map of the south-west Highlands.

(Figure 10.2) Tangy Glen: lithological succession at Cleongart (from Horne *et al.*, 1897).

(Figure 10.3) Geomorphology of the Glenacardoch Point area.

(Figure 10.4) Coastal profile at Glenacardoch Point showing the relationships between the morphology and succession of the features and their probable sequence of formation (1–8).

(Figure 10.5) Distribution of the Main Rock Platform on the Isle of Lismore and localities mentioned in the text (from Gray and Ivanovich, 1988).

(Figure 10.6) Geomorphology of Moss of Achnacree and Achnaba (from Gray, 1975a). See text for explanation of numbers.

(Figure 10.7) Quaternary deposits of the South Shian and Balure of Shian area, Benderloch (from Peacock, 1971a, unpublished data).

(Figure 10.8) The Parallel Roads of Lochaber. The letters T, M, B and G identify the final positions of the ice-fronts damming the 355 m, 325 m, 260 m and Glen Gloy lakes respectively (from Peacock and Cornish, 1989).

(Figure 10.9) The Parallel Roads of Glen Roy on the east flank of the glen, north-east of the viewpoint, are cut in bedrock which can be seen clearly exposed in the gully in the foreground. (Photo: J.E. Gordon.)

(Figure 10.10) Geomorphology of the northern part of upper Glen Roy (from Sissons and Cornish, 1983).

(Figure 10.11) Landforms and deposits of the Treig–Laggan area (from Sissons, 1977e; Peacock and Cornish, 1989).

(Figure 10.12) Geomorphology of the Spean Bridge–Gairlochy area (from Sissons, 1979c). See text for explanation of letters.

(Figure 10.13) Loch Lomond Readvance ice limits and associated ice-dammed lakes in the Glen Roy–Glen Spean area (from Sissons, 1981d).

(Figure 10.14) Kingshouse: relative pollen diagram showing selected taxa as percentages of total land pollen (from Walker and Lowe, 1977).

(Figure 10.15) Pulpit Hill: relative pollen diagram showing selected taxa as percentages of total land pollen (from Tipping, 1991b).

(Figure 10.16) Loch Cill an Aonghais: relative pollen diagram showing selected taxa as percentages of total pollen (from Birks, 1980, after S. Peglar). Note that the data are plotted against a radiocarbon timescale.

(Figure 10.17) Top: schematic section along the length of the Eas na Broige debris cone. Bottom: detail of section at sampling sites (from Brazier *et al.*, 1988).

(Figure 11.1) Location map and principal Quaternary features of the Inner Hebrides (from Peacock, 1983b; Sissons, 1983c; Ballantyne and Benn, 1991).

(Figure 11.2) (A) Principal glacial features of the Cuillin. (B) Reconstructed Loch Lomond Readvance glaciers in central Skye (from Ballantyne, 1989a).

(Figure 11.3) Landforms of glacial and periglacial erosion are strikingly developed in the Cuillin of Skye. The serrated aspect of the main Cuillin ridge reflects intense periglacial weathering, whereas the lower slopes are heavily ice-scoured. (British Geological Survey photograph B168.)

(Figure 11.4) Detail of ice-moulded bedrock near Loch Coruisk showing glacially abraded and smoothed stoss slopes and localized joint-block removal. (Photo: D. G. Sutherland.)

(Figure 11.5) Scarisdale: localities with well-preserved p-forms (from Gray, 1981).

(Figure 11.6) P-form channels at Scarisdale, Mull. (Photo: S. Campbell.)

(Figure 11.7) The Beinn Shiantaidh rock glacier (from The Western Hills of Rum, Sròn an t-Saighdeir Dawson, 1977).

(Figure 11.8) Periglacial features on the Western Hills of Rum (from Ballantyne, 1984).

(Figure 11.9) Geomorphology of northern Islay between Rubha a'Mhail and Port Domhnuill Chruinn.

(Figure 11.10) The coast of northern Islay, south of Rubha a'Mhail, showing the High Rock Platform and its backing cliff. In the foreground the Main Rock Platform and its backing cliff are also clearly developed. (Photo: J E. Gordon.)

(Figure 11.11) Geomorphology of western Jura in the area of South Shian Bay.

(Figure 11.12) View south along the west coast of Jura between Shian Bay and Ruantallain. Lateglacial shingle ridges extend across a high rock platform and to the west of Loch a'Mhile (centre). The loch was formerly a marine inlet prior to the deposition of the shingle ridges. Note also a prominent rock platform and backing cliff (the Main Rock Platform) seaward of the high shingle ridge 'staircases'. Holocene shingle ridges also cover the Main Rock Platform. (Photo: John Dewar Studios.)

(Figure 11.13) West coast of Jura. The Sgriob na Caillich raised shoreline. (Photo: D. G. Sutherland.)

(Figure 11.14) Gribun: relative pollen diagram showing selected taxa as percentages of total land pollen (from Walker and Lowe, 1987).

(Figure 11.15) Loch an t-Suidhe: relative pollen diagram showing selected taxa as percentages of total land pollen (from Lowe and Walker, 1986a).

(Figure 11.16) Loch Ashik: Lateglacial relative pollen diagram showing selected taxa as percentages of total land pollen (from Walker and Lowe, 1991).

(Figure 11.17) Loch Ashik: Holocene relative pollen diagram showing selected taxa as percentages of total pollen (from Birks and Williams, 1983). Note that the data are plotted against a radiocarbon time-scale.

(Figure 11.18) Loch Cleat: Holocene relative pollen diagram showing selected taxa as percentages of total pollen (from Birks and Williams, 1983). Note that the data are plotted against a radiocarbon time-scale.

(Figure 11.19) Loch Meodal: Holocene relative pollen diagram showing selected taxa as percentages of total pollen (from Birks and Williams, 1983). Note that the data are plotted against a radiocarbon time-scale.

(Figure 12.1) Location map and principal Quaternary features of the Outer Hebrides (from Peacock, 1984a).

(Figure 12.2) Quaternary deposits of north-west Lewis (from Peacock, 1984a).

(Figure 12.3) Toa Gilson: sequence of sediments (from Sutherland and Walker, 1984).

(Figure 12.4) Section at Toa Galson, north-west Lewis, showing the interglacial peat resting on bedrock and overlain by sand, head and the Galson Beach deposits. The upper part of the beach deposits has been affected by cryoturbation. (Photo: D. G. Sutherland.)

(Figure 12.5) Relative pollen diagram for the peat deposit at Toa Galson showing selected taxa as percentages of total land pollen (from Sutherland and Walker, 1984). The location of the sample is shown in Figure 12.3.

(Figure 12.6) Tolsta Head: sediments and relative pollen diagram showing selected taxa as percentages of total pollen (from von Weymarn and Edwards, 1973; Birnie, 1983; Lowe, 1984).

(Figure 12.7) Landforms and deposits of the Glen Valtos–Uig area (from Peacock, 1984a).

(Figure 12.8) Glen Valtos meltwater channel. The channel has the form of a single, narrow gorge. (Photo: D. G. Sutherland.)

(Figure 12.9) Profile across the intertidal deposits at Borve, showing the sediment sequence and its variations (from Ritchie, 1985).

(Figure 12.10) Gleann Mor, Hirta: relative pollen diagram showing selected taxa as percentages of total land pollen (from Walker, 1984a).

(Figure 13.1) Location map of the Western Highland Boundary area.

(Figure 13.2) Landforms and deposits associated with the Loch Lomond Readvance ice limit at Aucheneck (from Rose, 1981). Inset shows the wider extent of the moraine that marks the ice limit at the southern end of Loch Lomond (from Dickson *et al.*, 1978).

(Figure 13.3) Landforms and deposits associated with the Loch Lomond Readvance ice limit at Gartness (from Rose, 1980e, 1981).

(Figure 13.4) Geilston: sequence of sediments (from Rose, 1980a).

(Figure 13.5) Rhu Point: section showing glacially deformed Clyde beds, Rhu Gravels and Holocene raised beach deposits (from Rose, 1980c).

(Figure 13.6) Geomorphology of the Western Forth Valley.

(Figure 13.7) Western Forth Valley: section along the Goodie Water (from Sissons *et al.*, 1965). See Figure 13.6 for location of section.

(Figure 13.8) Western Forth Valley: section at West Mossside, East Flanders Moss (from Sissons and Smith, 1965b). See Figure 13.6 for location of section.

(Figure 13.9) Glacial and glaciofluvial landforms of the Callander area (from Lowe, 1978, after Thompson, 1972).

(Figure 13.10) Mollands: Lateglacial and early Holocene relative pollen diagram showing selected taxa as percentages of total land pollen (from Lowe, 1978).

(Figure 13.11) Mollands: main Holocene relative pollen diagram showing selected taxa as percentages of total land pollen (from Lowe, 1982a).

(Figure 13.12) Core from the basal sediments at Tynaspirit. From the left, the sequence comprises Late Devensian minerogenic sediments, organic Lateglacial Interstadial sediments, Loch Lomond Stadial silts and clays, and early Holocene organic lake muds. (Photo: M. J. C. Walker.)

(Figure 13.13) Tynaspirit: relative pollen diagram showing selected taxa as percentages of total land pollen (from Lowe, 1978).

(Figure 14.1) Location map of the Eastern Highland Boundary area.

(Figure 14.2) Map and section of Late glacial deposits in the Almond Valley (from Paterson, 1974).

(Figure 14.3) Sketch section of glacial deposits at Shochie Burn (unscaled) (from Paterson, 1974).

(Figure 14.4) Lateglacial and Holocene raised marine deposits in the Dryleys area.

(Figure 14.5) Section at Maryton. Laminated Late Devensian marine clays are overlain by peat then a layer of grey, micaceous, silty, fine sand interpreted as a tsunami deposit. Above the latter is silty peat then carse clay. (Photo: D. E. Smith.)

(Figure 14.6) Marylon: relative pollen diagram showing selected taxa as percentages of total pollen (from Smith *et al.*, 1980).

(Figure 14.7) Raised shorelines and intertidal shore platform at Milton Ness.

(Figure 14.8) Terraces of the River North Esk and West Water in the Edzell area (from Maizels, 1983a).

(Figure 14.9) Stormont Loch: relative pollen diagram for core SGI showing selected taxa as percentages of total land pollen (from Caseldine, 1980a).

(Figure 15.1) Location map of the Fife and the Lower Tay area.

(Figure 15.2) Inferred stratigraphy of the Errol beds at Inchcoonans claypit (from Paterson *et al.*, 1981).

(Figure 15.3) Silver Moss: section along the gully showing the sequence of sediments (from Morrison *et al.,* 1981).

(Figure 15.4) Silver Moss: relative pollen diagram showing selected taxa as percentages of total pollen and spores (from Morrison *et al.*, 1981).

(Figure 15.5) Geomorphology of the Pitlowie gullies (from Morrison *et al.*, 1981). The sediment sequence along the line AB is shown in Figure 15.6.

(Figure 15.6) Pitlowie: section along the Hole of Clien gully showing the sequence of sediments and radiocarbon dates (from Smith et al., 1985b).

(Figure 15.7) Black Loch: relative pollen diagram at coring site BL II showing selected taxa as percentages of total land pollen (from Whittington *et al.*, 1990). *Cannabis sativa* is not represented in this diagram but in the other cores occurs in zones equivalent to BL II j.

(Figure 16.1) Location map of the western Central Lowlands.

(Figure 16.2) Nith Bridge: sequence of sediments (from Holden and Jardine, 1980).

(Figure 16.3) Geomorphology of the Carstairs area (from McLellan, 1969).

(Figure 16.4) Carstairs Kames showing the interlinked form of the ridges and mounds, with intervening kettle holes. (© British Crown copyright 1992/MOD reproduced with the permission of the Controller of Her Britannic Majesty's Stationery Office.)

(Figure 16.5) Clochodrick Stone. (Photo: J E. Gordon.)

(Figure 16.6) Stone stripes are particularly well developed on Tinto Hill. (Photo: J E. Gordon.)

(Figure 17.1) Location map of the Lothians and Borders area.

(Figure 17.2) Part of the smoothed and grooved rock surface at Agassiz Rock, Edinburgh, which has been attributed to glacial abrasion. The form of the rock surface bears a strong resemblance to glacially abraded surfaces elsewhere in Scotland and in modern glacial environments (Photo: J E. Gordon.)

(Figure 17.3) Blackford Hill crag and tail, showing a till clast fabric in the tail, the Corbie's Craig crag and tail and the direction of ice movement inferred from the striations at Agassiz Rock (from Kirby, 1969b).

(Figure 17.4) Indicators of ice movement in the Lothians area recorded up until 1863 (from Kirby, 1969b).

(Figure 17.5) The meltwater channel system at Carlops. The detailed pattern of channels immediately to the south-west of the village (main diagram) forms part of a more extensive glacial drainage system represented by channels and glaciofluvial deposits (inset) (from Sissons, 1963b).

(Figure 17.6) The main meltwater channel at Carlops showing the anastomosing form of the channel system and the isolated interfluve 'islands' between constituent channels. (Photo: J E. Gordon.)

(Figure 17.7) Geomorphology of the meltwater channel system at Rammer Cleugh (from Sissons, 1958a).

(Figure 17.8) Loch Lomond Readvance moraines at Loch Skene (from May, 1981).

(Figure 17.9) Beanrig Moss: relative pollen diagram showing selected taxa as percentages of total land pollen (from Webb and Moore, 1982).

(Figure 17.10) Din Moss: relative pollen diagram showing selected taxa as percentages of the pollen sums indicated (from Hibbert and Switsur, 1976).

(Figure 17.11) Intertidal shore platform at Dunbar, which has been planed across a series of Devonian–Carboniferous and Carboniferous sediments and agglomerates. (Photo: J E. Gordon.)

(Figure 18.1) Location map of south-west Scotland and generalized directions of ice movement.

(Figure 18.2) Loch Lomond Readvance moraines and ice limits at the Tauchers (from Cornish, 1981).

(Figure 18.3) Redkirk Point: sediment succession (from Bishop and Coope, 1977).

(Figure 18.4) Newbie: sediment succession (from Jardine, 1980b).

(Figure 18.5) Geomorphology of the Loch Dungeon area (from Cornish, 1981).

(Figure 18.6) A Loch Dungeon: relative pollen diagram from the loch showing selected taxa as percentages of the pollen sums indicated (from Birks, 1972a). B Loch Dungeon: relative pollen diagram from adjacent peat profile showing selected taxa as percentages of the pollen sums indicated (from Birks, 1975).

(Figure 18.7) Round Loch of Glenhead: relative pollen diagram showing selected taxa from core RLGH3 as percentages of total land pollen. Values of herbs except Gramineae and Cyperaceae are expanded X 10. Peatland indicators are based on the sum of *Calluna*, *Potentilla*, *Sphagnum* and Cyperaceae (from Jones, 1987).

(Figure 18.8) Round Loch of Glenhead: relative pollen diagram showing selected taxa from core S18, from a peat deposit adjacent to the loch, as percentages of total pollen. Values of the herbs, Gramineae (4049 p.m), Liguliflorae, *Artemisia*, Cruciferae and *Potentilla* are expanded x 10. Peatland indicators are based on the sum of *Calluna*, *Potentilla*, *Sphagnum* and Cyperaceae (from Jones, 1987).

Tables

References

(Figure 1.1) Location of sites and areas described.

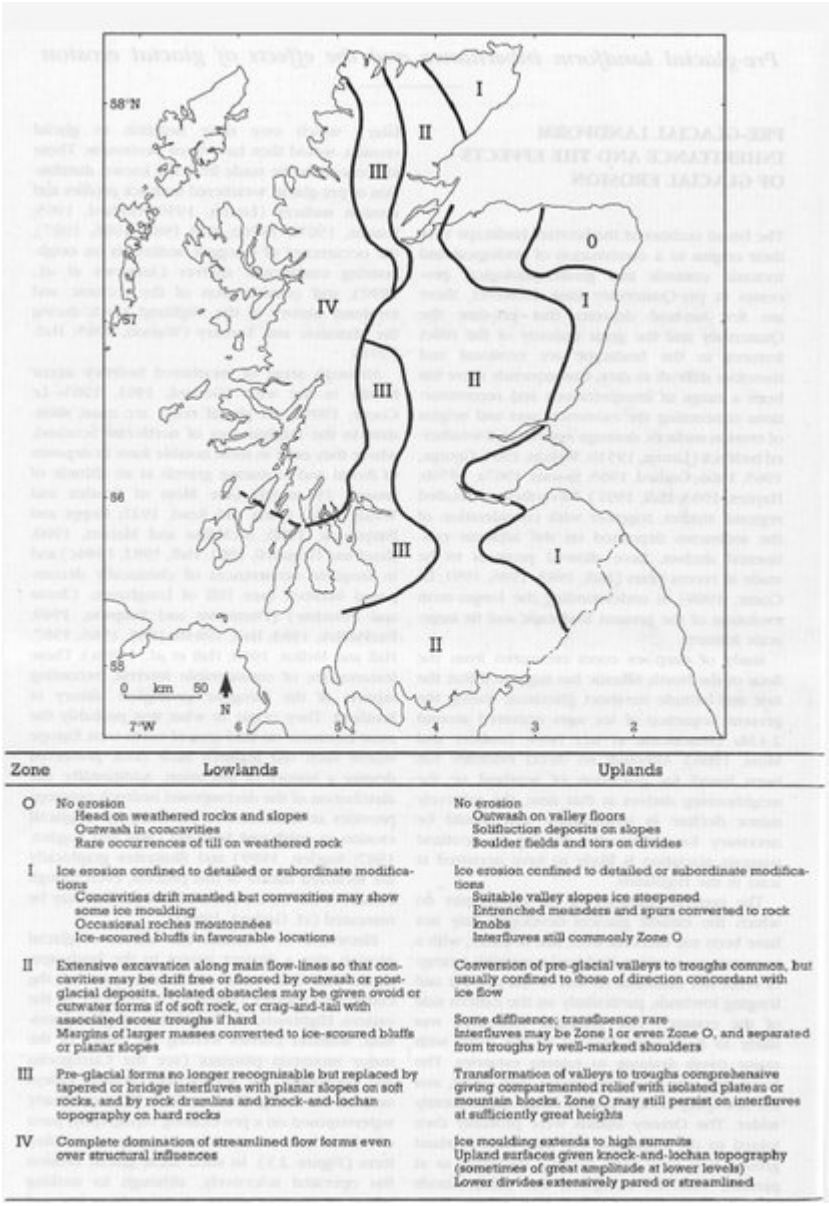

Zone	Lowlands	Uplands
O	No erosion Head on weathered rocks and slopes Outwash in concavities Rare occurrences of till on weathered rock	No erosion Outwash on valley floors Solifluction deposits on slopes Boulder fields and tors on divides
I	Ice erosion confined to detailed or subordinate modifications Concavities drift mantled but convexities may show some ice moulding Occasional roches moutonnées Ice-scoured bluffs in favourable locations	Ice erosion confined to detailed or subordinate modifications Suitable valley slopes ice steepened Entrenched meanders and spurs converted to rock knobs Interfluves still commonly Zone O
II	Extensive excavation along main flow-lines so that concavities may be drift free or floored by outwash or post-glacial deposits. Isolated obstacles may be given ovoid or cutwater forms if of soft rock, or crag-and-tail with associated scour troughs if hard Margins of larger masses converted to ice-scoured bluffs or planar slopes	Conversion of pre-glacial valleys to troughs common, but usually confined to those of direction concordant with ice flow Some diffluence; transfluence rare Interfluves may be Zone I or even Zone O, and separated from troughs by well-marked shoulders
III	Pre-glacial forms no longer recognisable but replaced by tapered or bridge interfluves with planar slopes on soft rocks, and by rock drumlins and knock-and-lochan topography on hard rocks	Transformation of valleys to troughs comprehensive giving compartmented relief with isolated plateaux or mountain blocks. Zone O may still persist on interfluves at sufficiently great heights
IV	Complete domination of streamlined flow forms even over structural influences	Ice moulding extends to high summits Upland surfaces given knock-and-lochan topography (sometimes of great amplitude at lower levels) Lower divides extensively pared or streamlined

(Figure 2.1) Zones of glacial erosion (from Clayton, 1974).

(Figure 2.2) Distribution of rock basins On the Scottish mainland and neighbouring shelves.

(Figure 2.3) The western Cairngorms, with Ben Macdui (centre) viewed from the east, showing the diversity of the geomorphology of the eastern Highlands. Rounded plateau surfaces with tors (on Beinn Mheadhoin, lower left), solifluction lobes and weathered bedrock contrast strikingly with landforms of glacial erosion, including corries, the glacial troughs of Loch Avon (foreground) and the Lairig Ghru (middle distance), and the truncated spur of the Devil's Point (top, left of centre). Locally, parts of the plateau are ice scoured, as between Ben Macdui and Loch Avon. 'Hummocky moraine' can also be seen at the head of Loch Avon. (Cambridge University Collection: copyright reserved.)

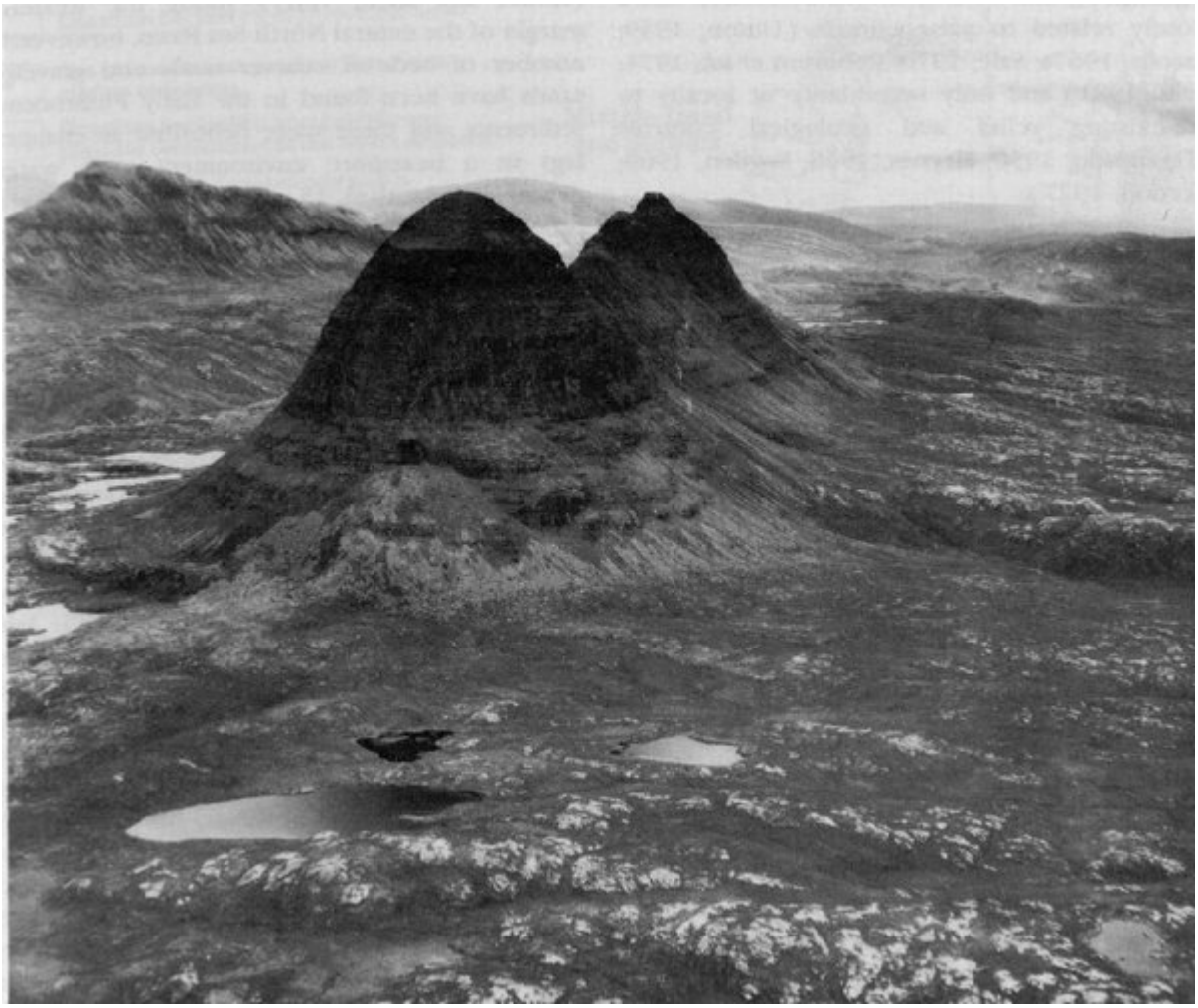

(Figure 2.4) Suilven, with Canisp in the background (left), shows the striking relationships between geology and relief in north-west Scotland. These isolated mountains of Torridonian sandstone rise above the intensively ice-scoured surface of Lewisian gneiss. (© British Crown copyright 1992/MOD reproduced with the permission of the Controller of Her Britannic Majesty's Stationery Office.)

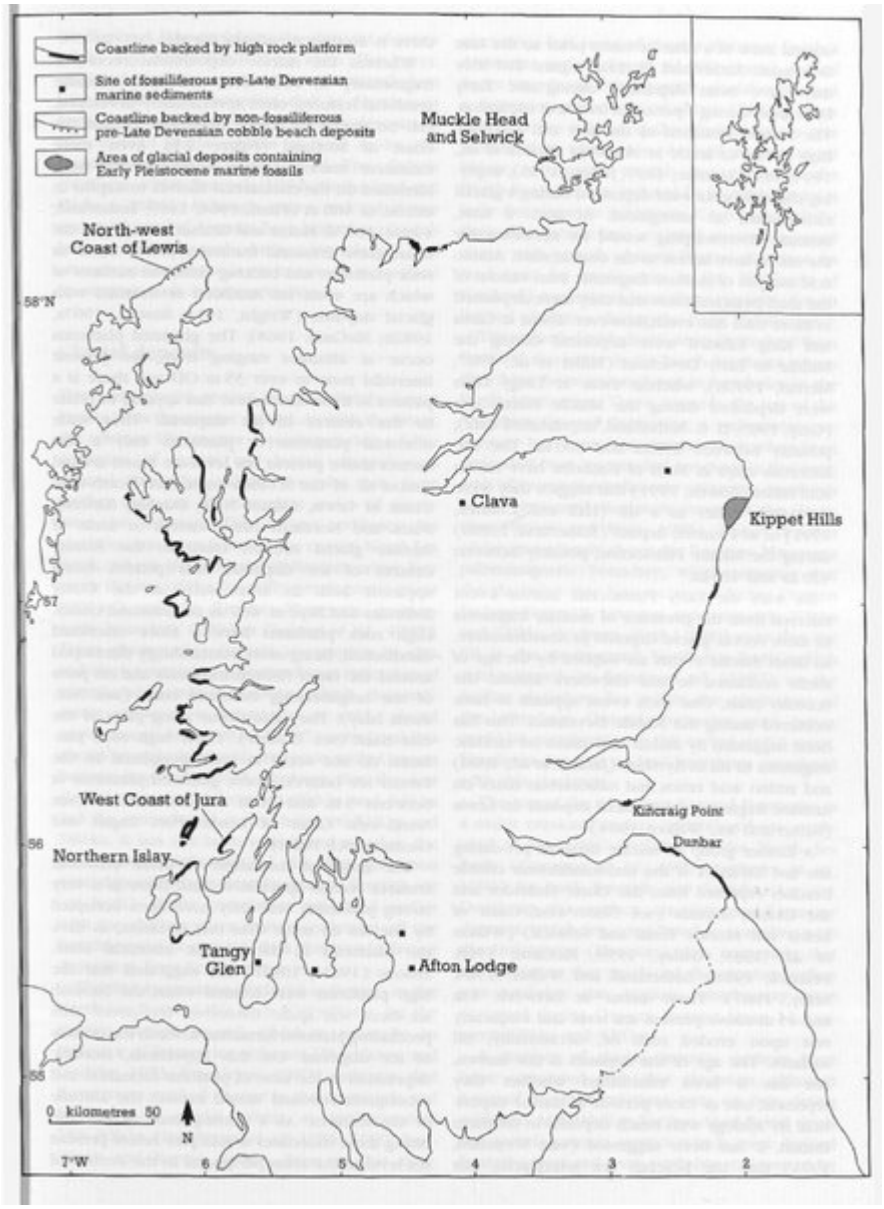

(Figure 2.5) Distribution of pre-Late Devensian marine deposits and high rock platforms.

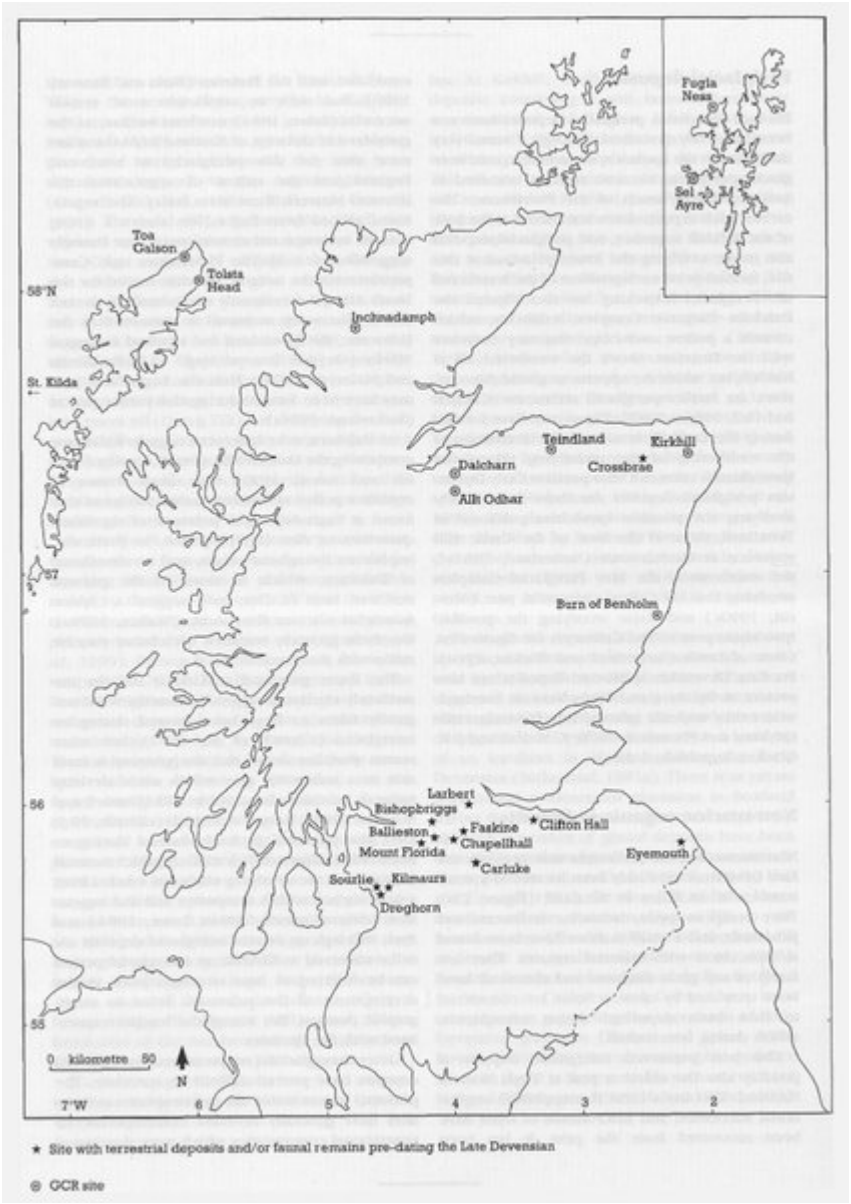

(Figure 2.6) Location of sites where pre-Late Devensian fossils or organic non-marine sediments have been found. Details of non-GCR sites are given in Sutherland (1984a).

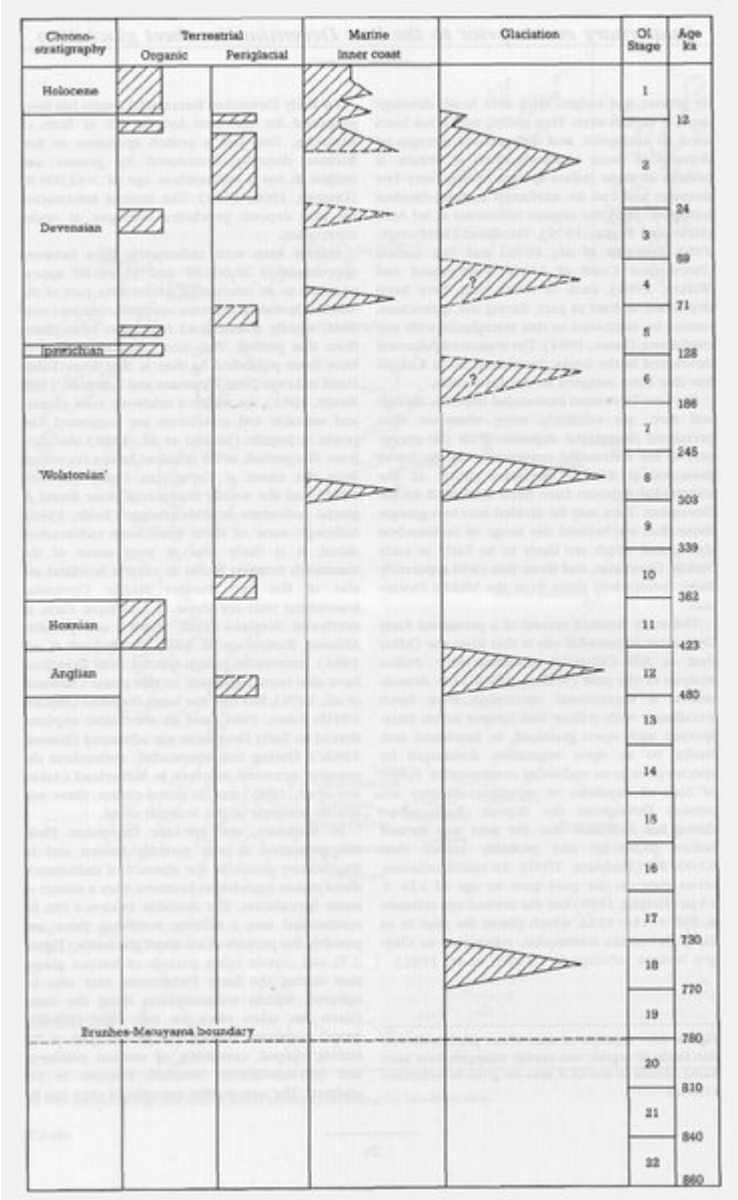

(Figure 2.7) Summary of the principal glacial, periglacial, marine and terrestrial depositional events recognized in the Quaternary record in Scotland. Note that the time-scale is not linear. Only those events that can be related to specific deposits on land or on the adjacent continental shelves are plotted.

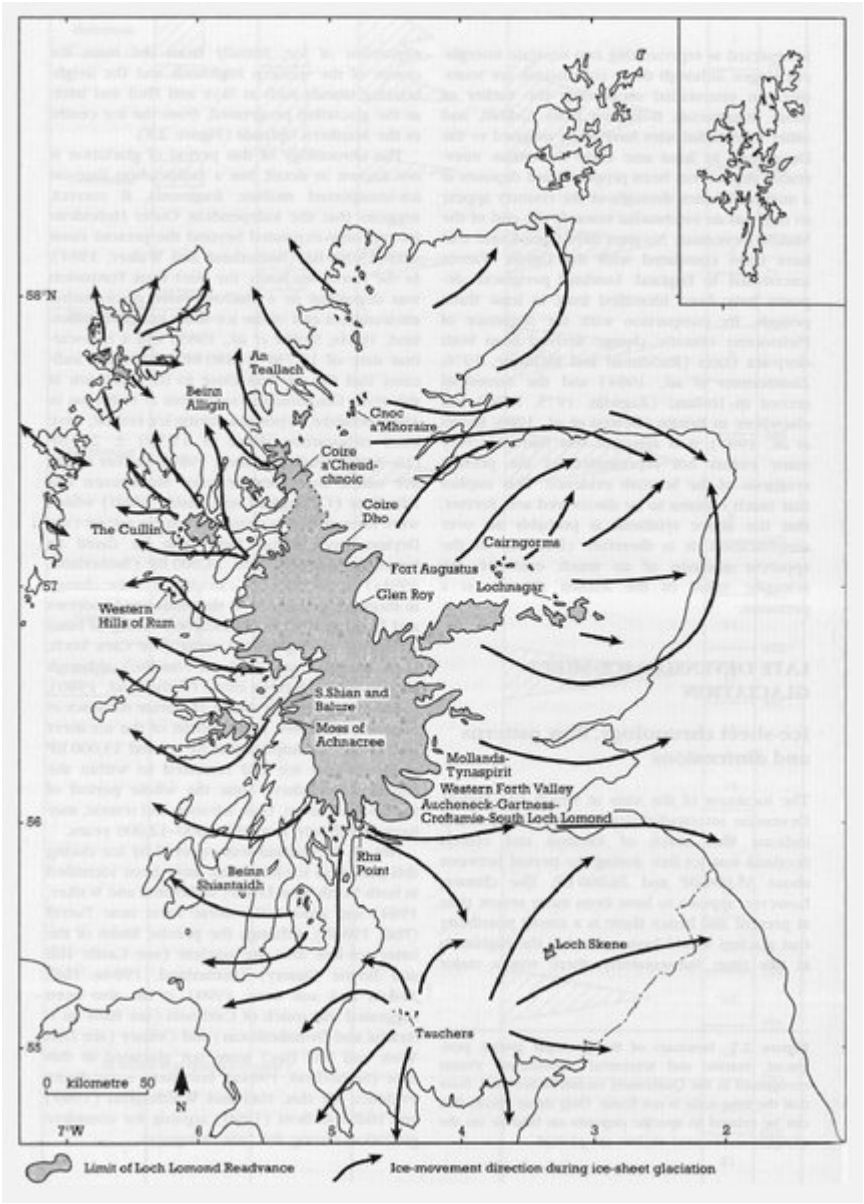

(Figure 2.8) Ice-sheet flow patterns and Loch Lomond Readvance glaciers.

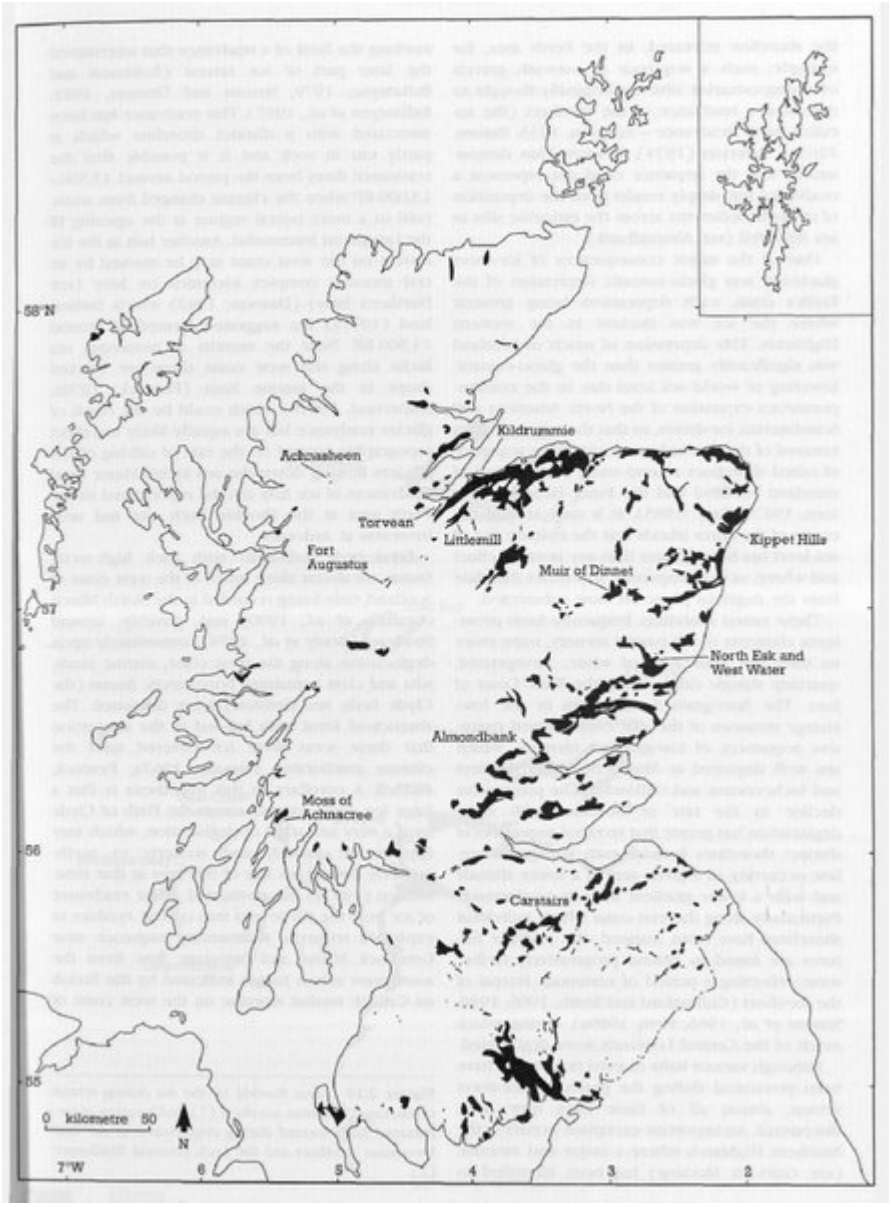

(Figure 2.9) Distribution of glaciofluvial deposits.

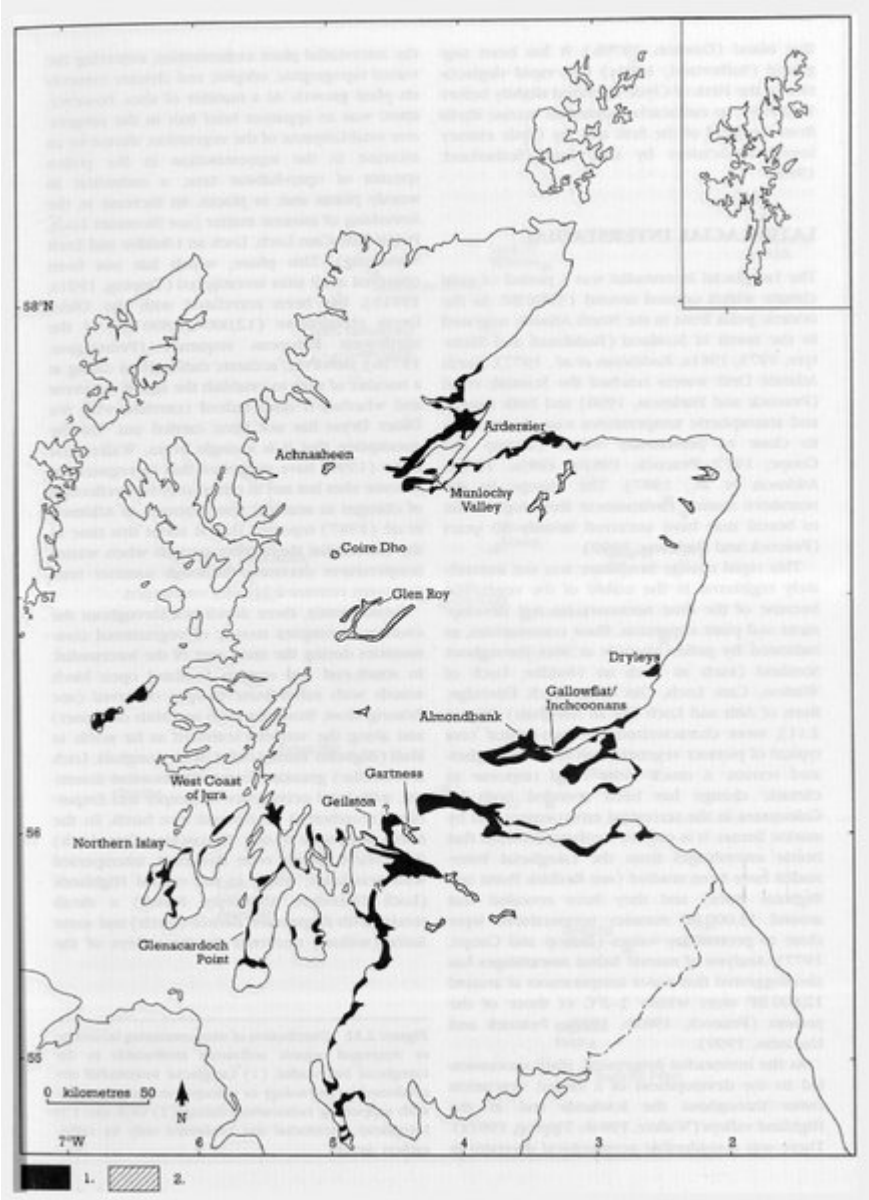

(Figure 2.10) Areas flooded by the sea during retreat of the Late Devensian ice-sheet (1), and location of ice-dammed lakes formed during deglaciation of the Late Devensian ice-sheet and the Loch Lomond Readvance (2).

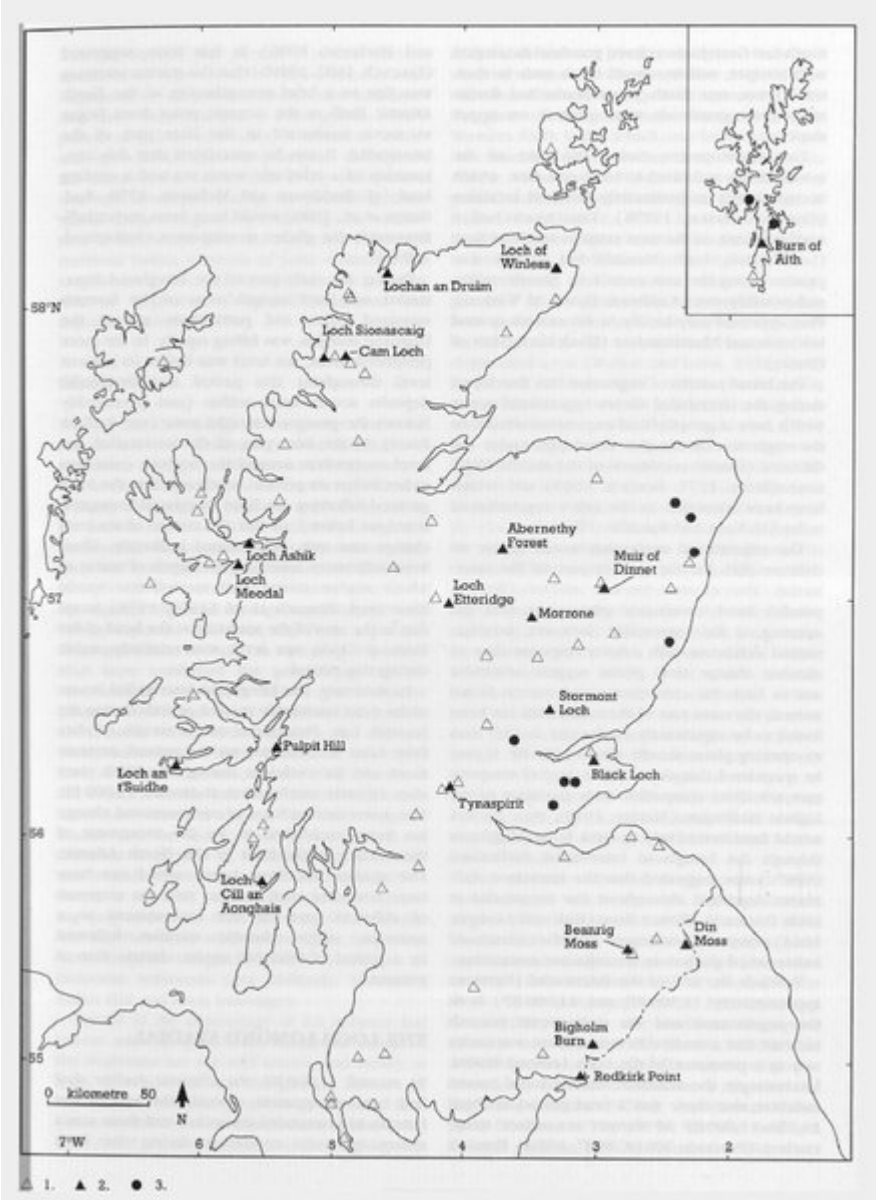

(Figure 2.11) Distribution of sites containing lacustrine or terrestrial organic sediments attributable to the Lateglacial Interstadial. (1) Lateglacial Interstadial site confirmed by palynology or coleopteran analyses, many with supporting radiocarbon dating; (2) GCR site; (3) Lateglacial Interstadial site confirmed only by radiocarbon dating.

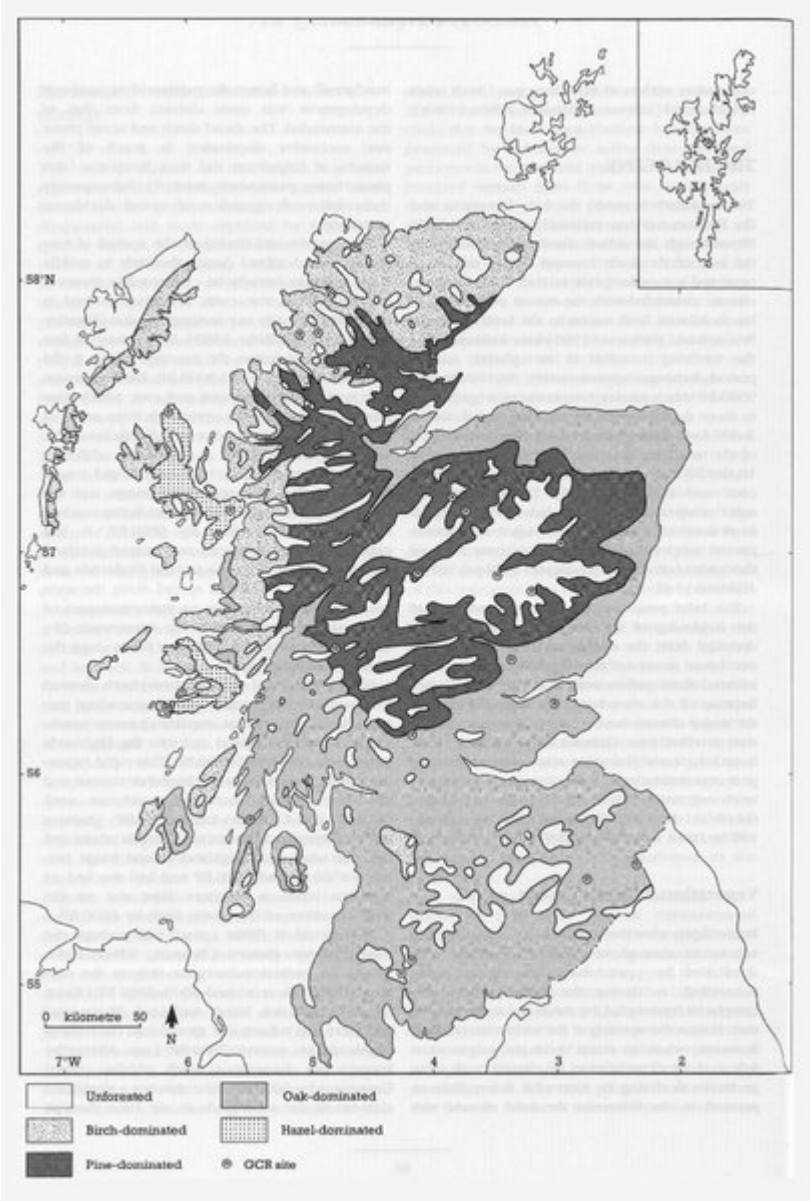

(Figure 2.12) Forest zones at approximately 5000 BP (from Bennett, 1989), and GCR sites with palynological data for the Holocene.

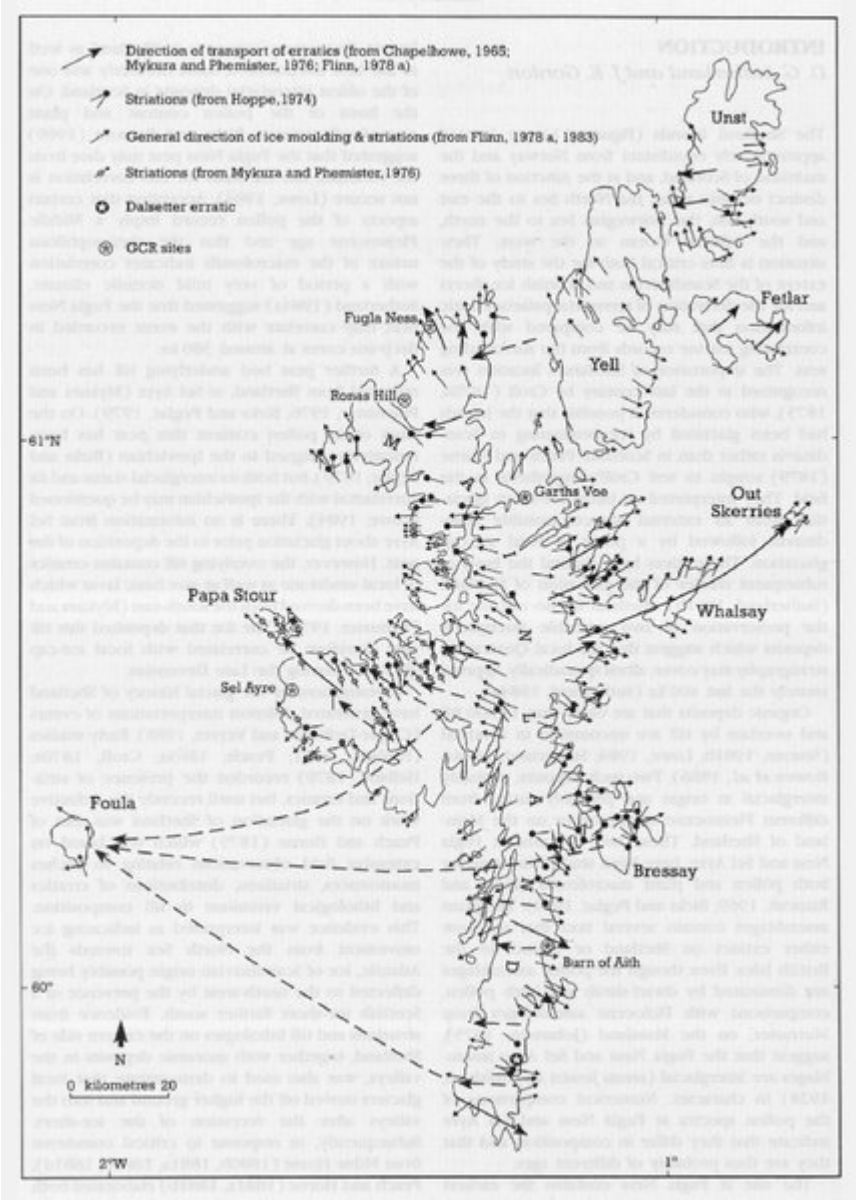

(Figure 3.1) Location map and principal features of the glaciation of Shetland, including pat-terns of striations, directions of transport of erratics and general directions of ice moulding (from Sutherland, 1991b).

(Figure 3.2) Sediment sequence at Fugla Ness, Shetland, showing interglacial peat (lower left) overlain by slope deposits, with till at the top. (Photo: J E. Gordon.)

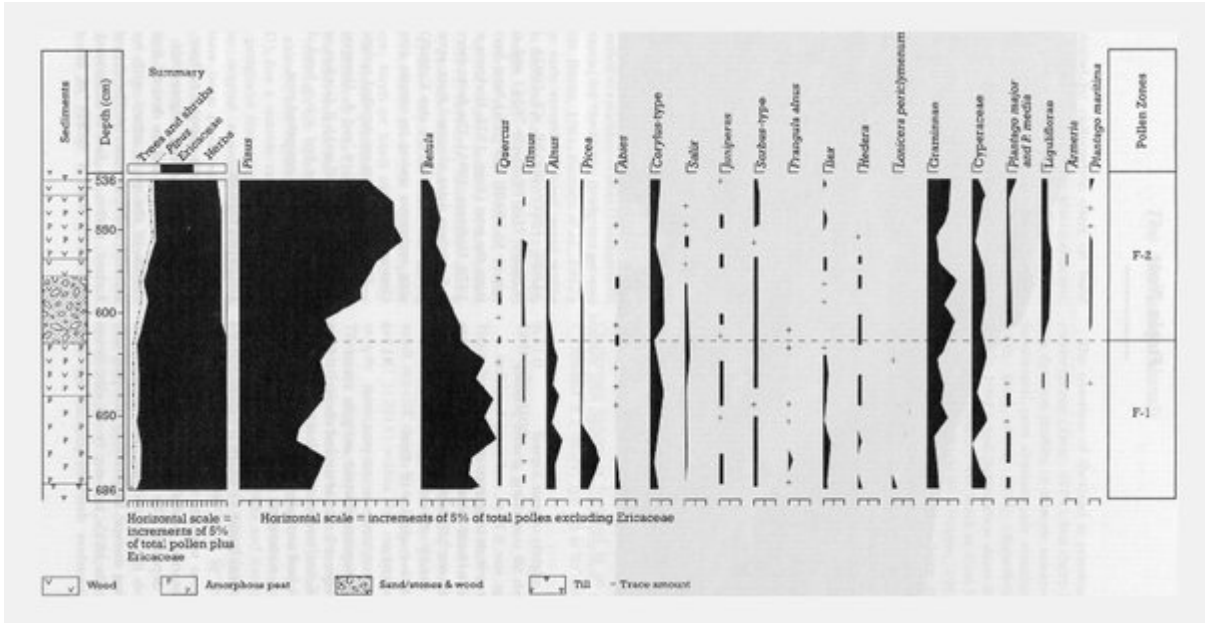

(Figure 3.3) Fugla Ness: relative pollen diagram showing selected taxa based on sum of total pollen excluding Ericaceae (from Birks and Ransom, 1969; Lowe, 1984).

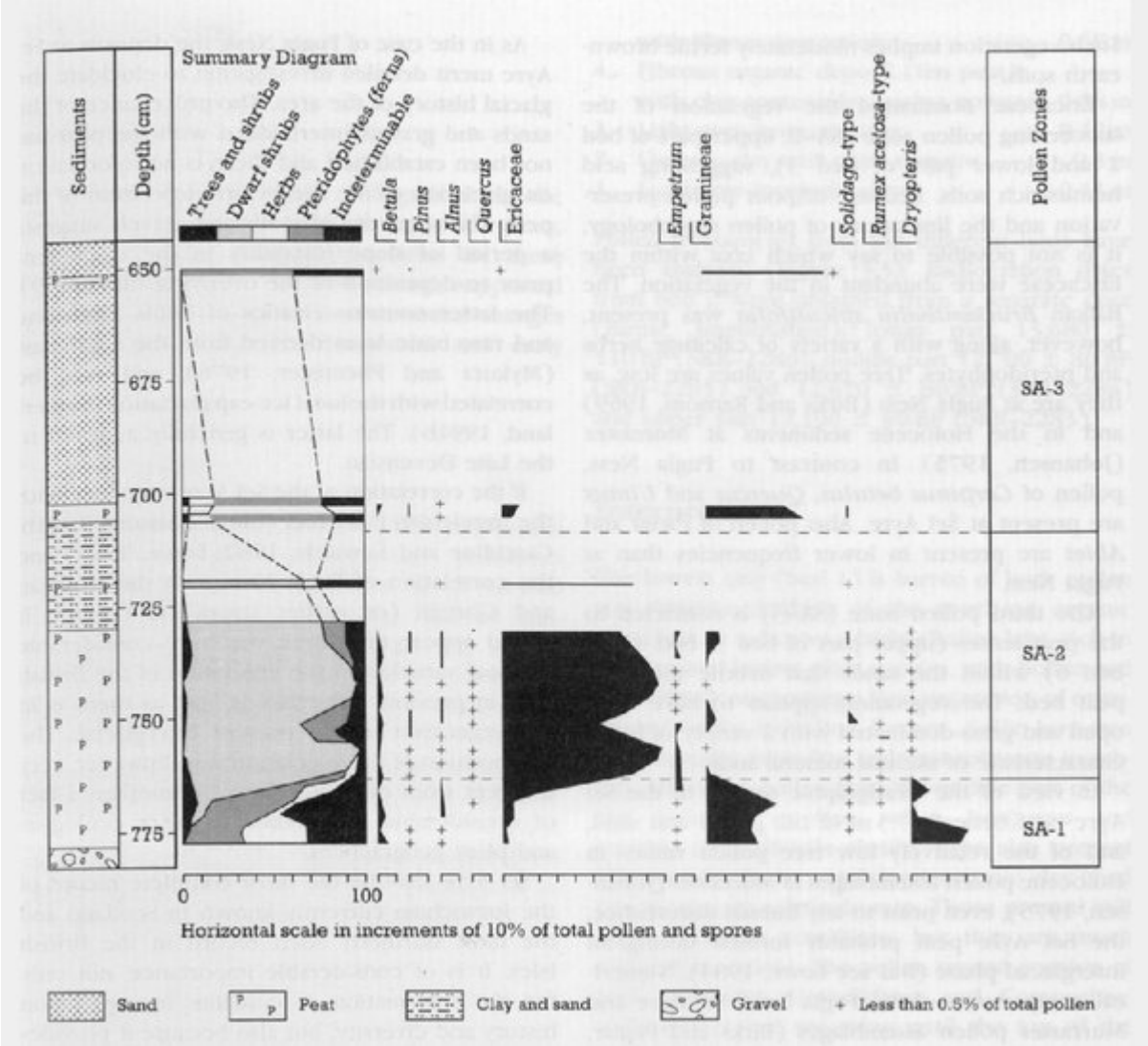

(Figure 3.4) Sel Ayre: relative pollen diagram showing selected taxa as percentages of total pollen and spores (from Birks and Peglar, 1979; Lowe, 1984).

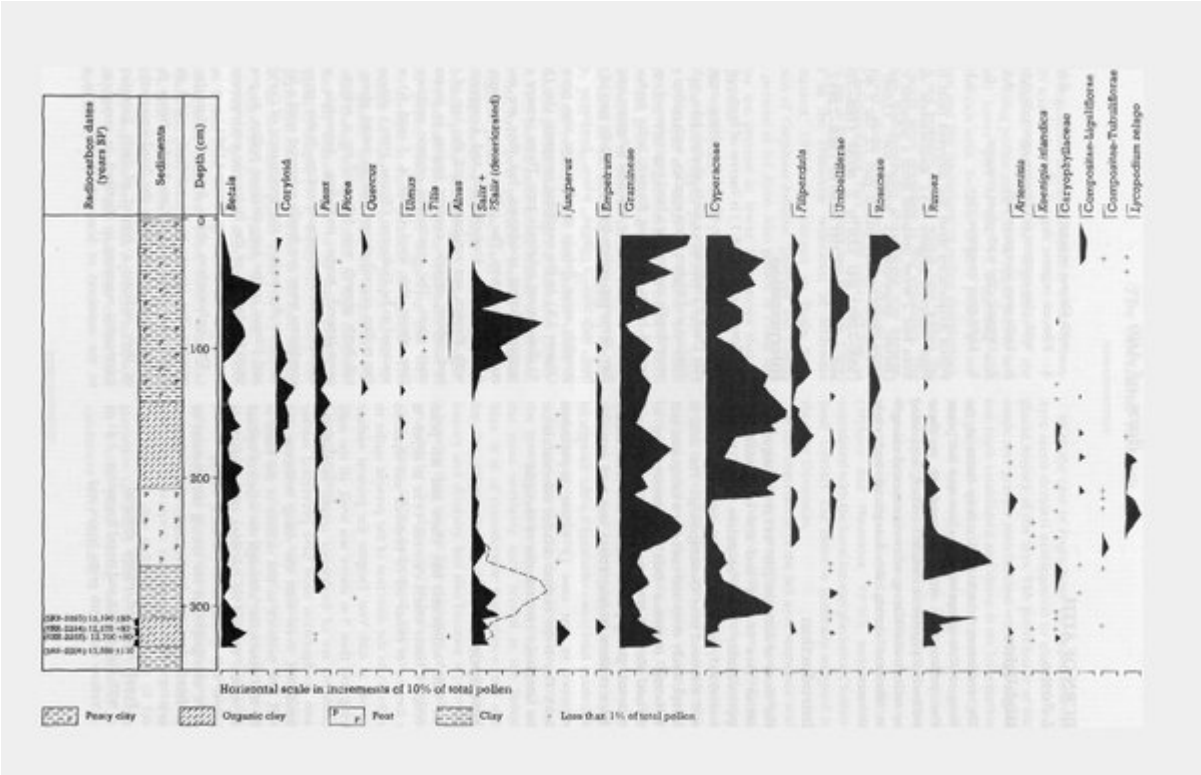

(Figure 3.5) Burn of Aith: relative pollen diagram showing selected taxa as percentages of total pollen (from Birnie, 1981).

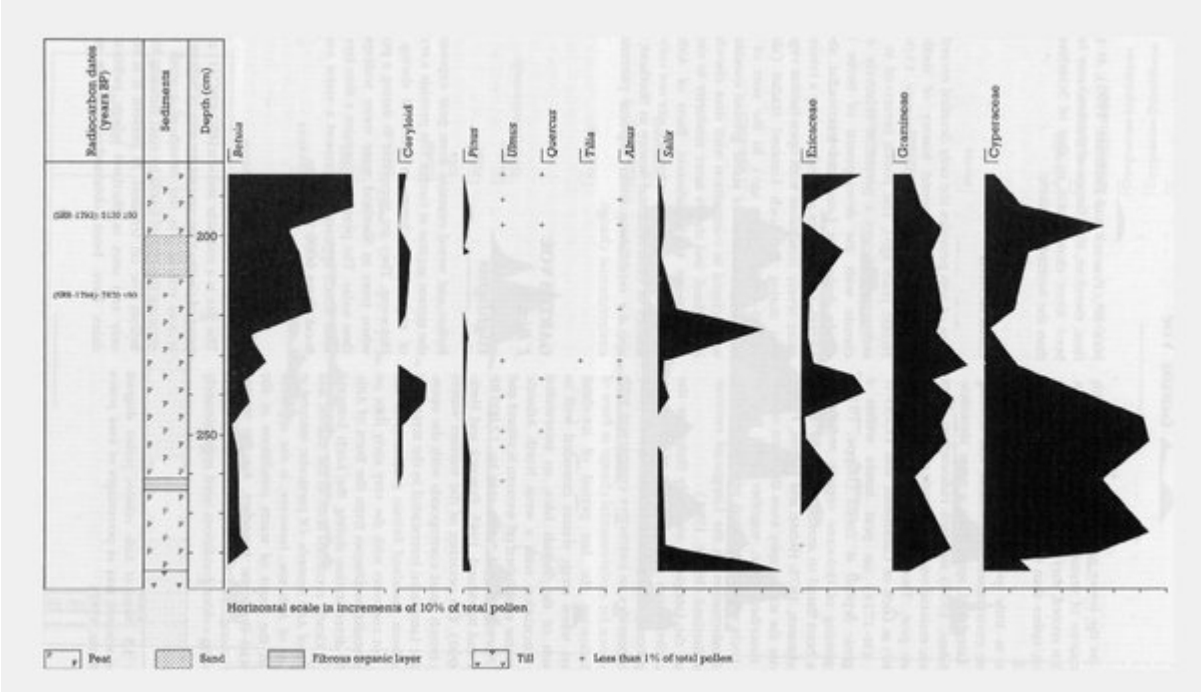

(Figure 3.6) Garths Voe: relative pollen diagram showing selected taxa as percentages of total pollen (from Birnie, 1981).

(Figure 4.1) Location map and principal features of the glaciation of Orkney, including patterns of striations, directions of transport of erratics and shelly till localities (from Sutherland, 1991b).

(Figure 4.2) Section at Muckle Head, Orkney. The raised beach gravel, which rests on a rock platform, incorporates large flagstone blocks and is overlain in turn by a head deposit and till. (Photo: D. G. Sutherland.)

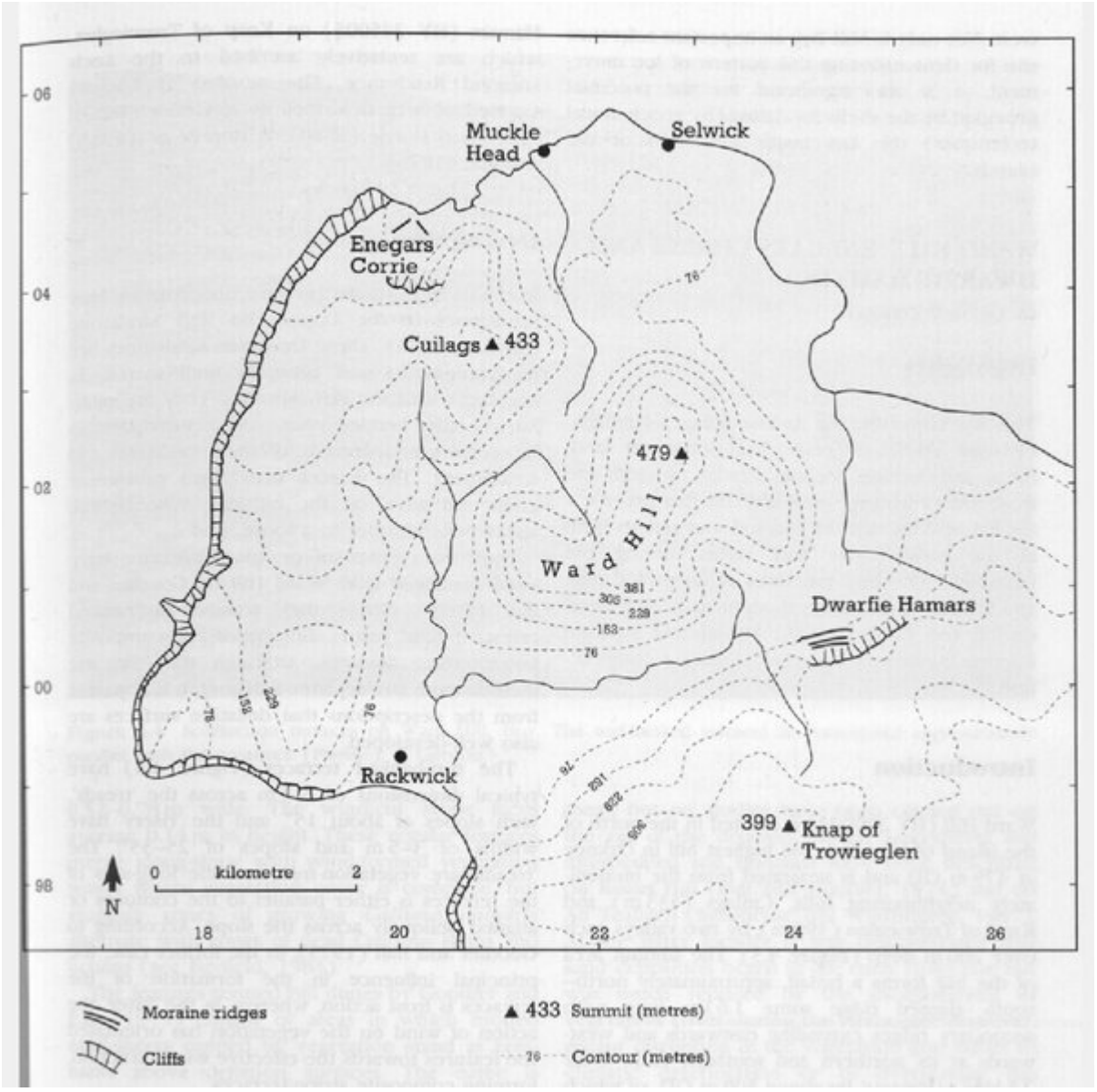

(Figure 4.3) Location map of North Hoy.

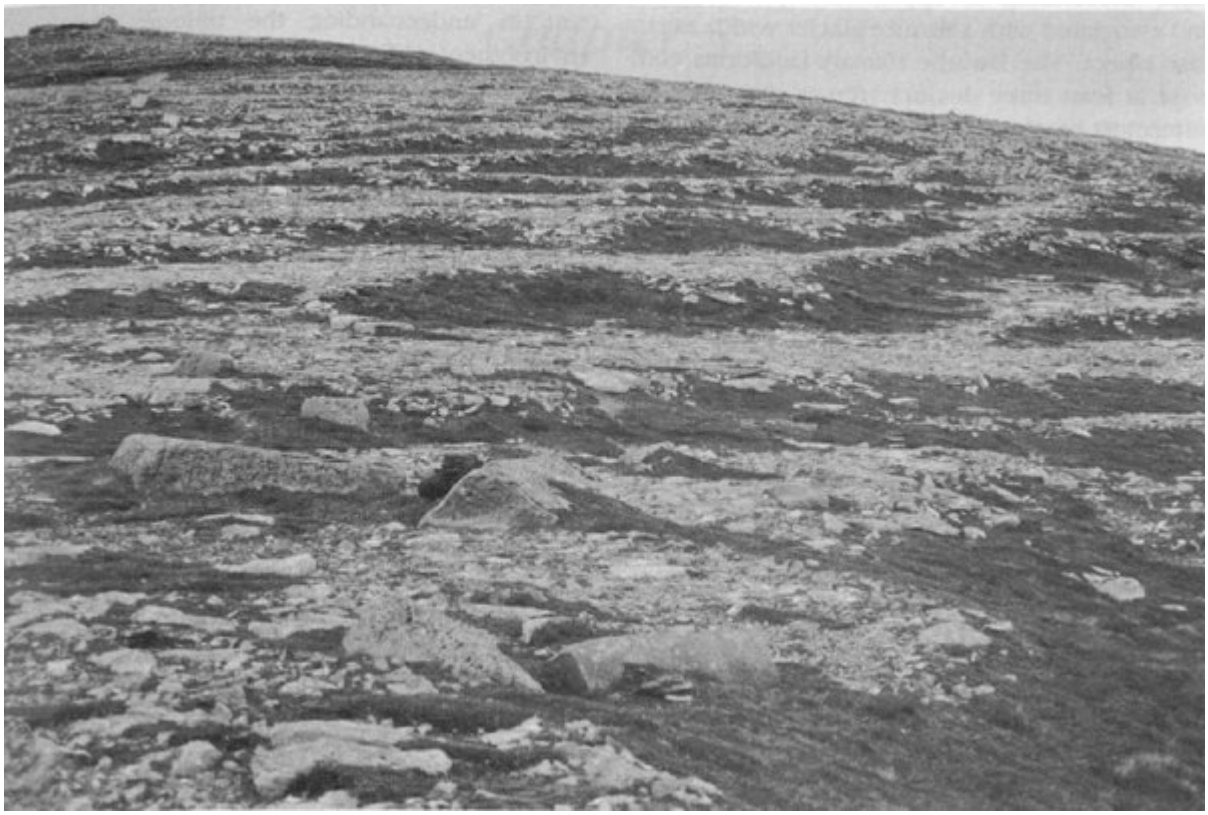

(Figure 4.4) Solifluction terraces on Ward Hill, Hoy. The turf-banked terraces are orientated approximately parallel with the contours. (Photo: J E. Gordon.)

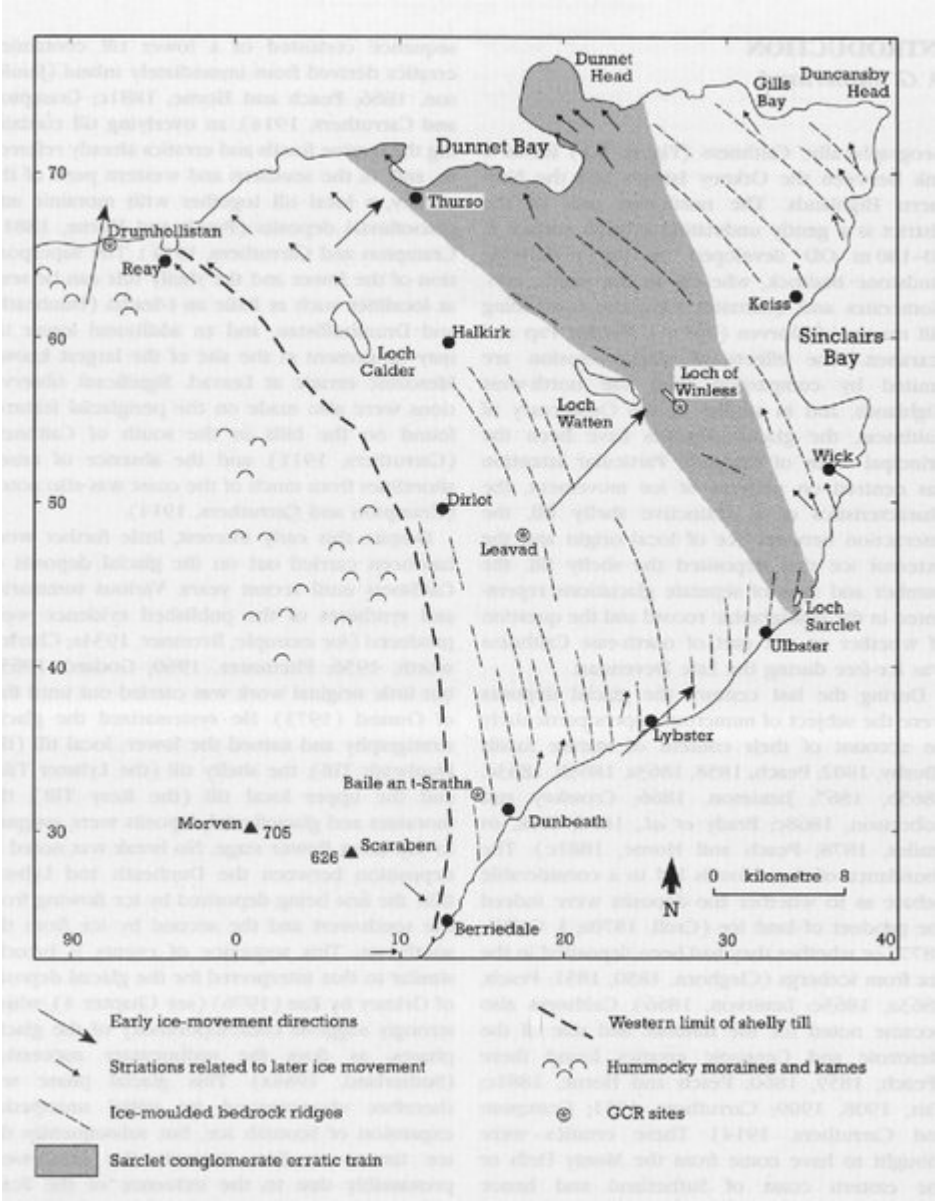

(Figure 5.1) Location map and principal features of the glaciation of Caithness, including patterns of striations, ice-moulded landforms, distribution of erratics and shelly till (from Peach and Horne, 1881c; Sissons, 1967a; Sutherland, 1984a).

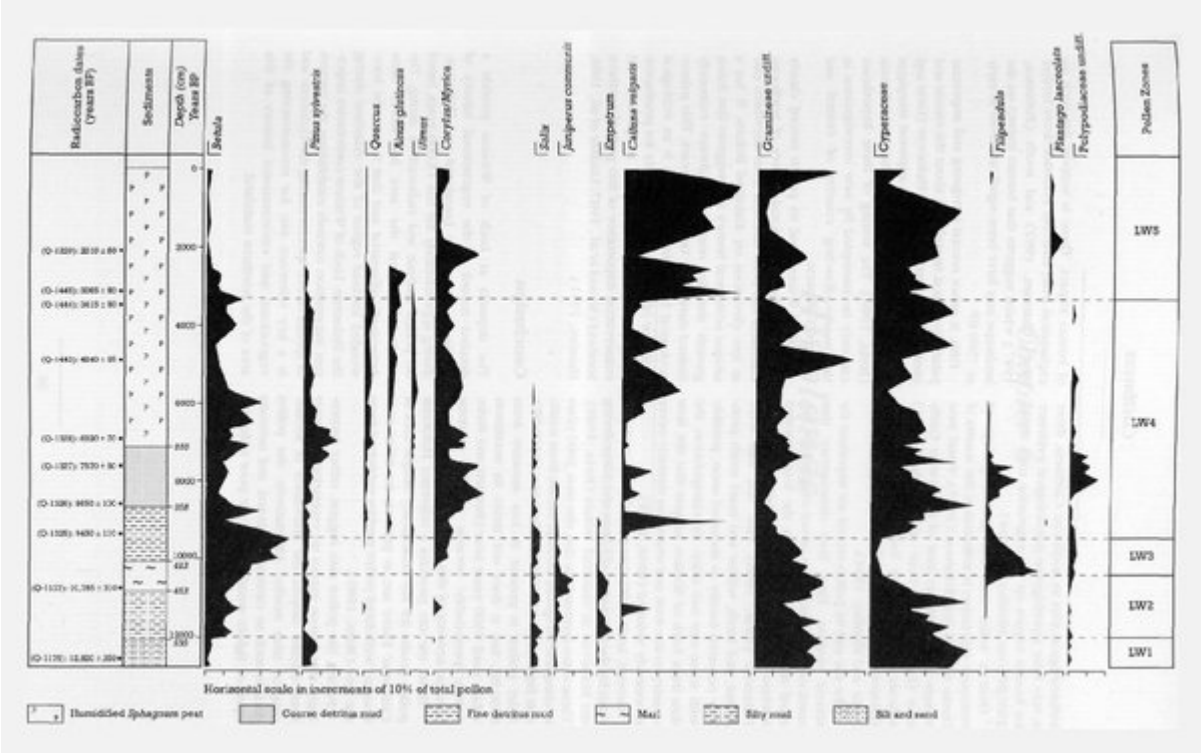

(Figure 5.2) Loch of Winless: relative pollen diagram showing selected taxa as percentages of total pollen (from Peglar, 1979). Note that the data are plotted against a radiocarbon time-scale.

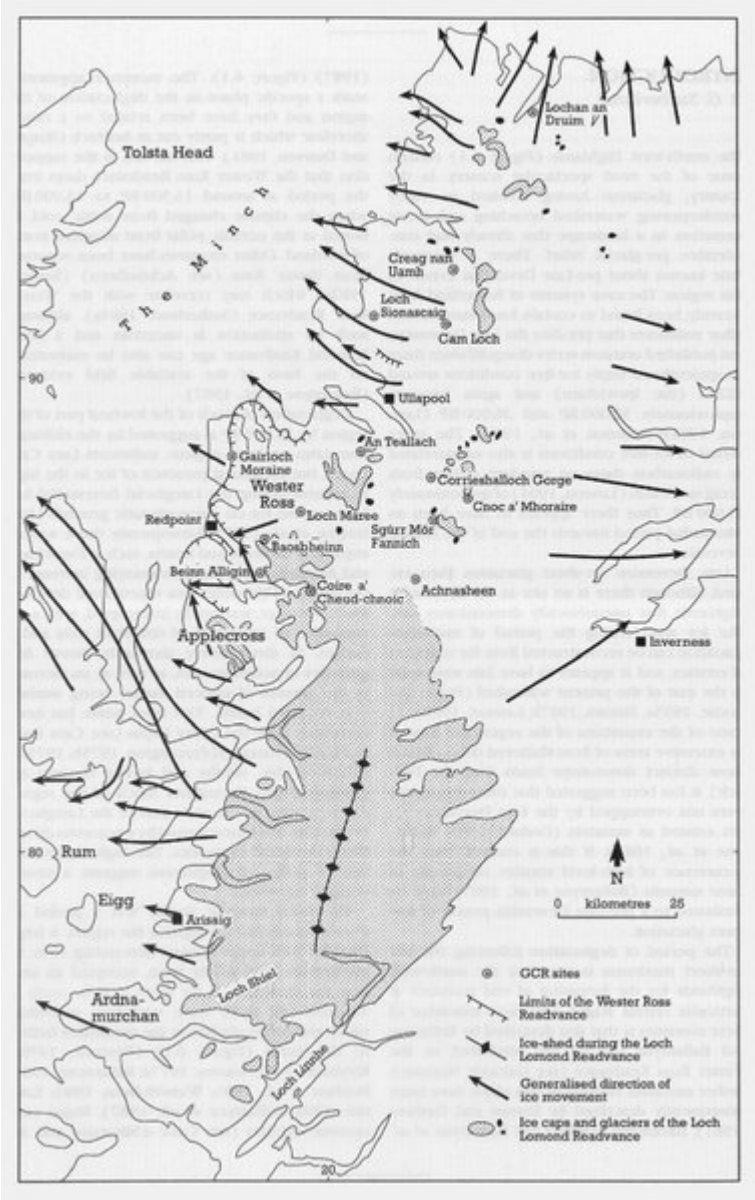

(Figure 6.1) Location map and principal glacial features of the north-west Highlands (modified from Johnstone and Mykura, 1989).

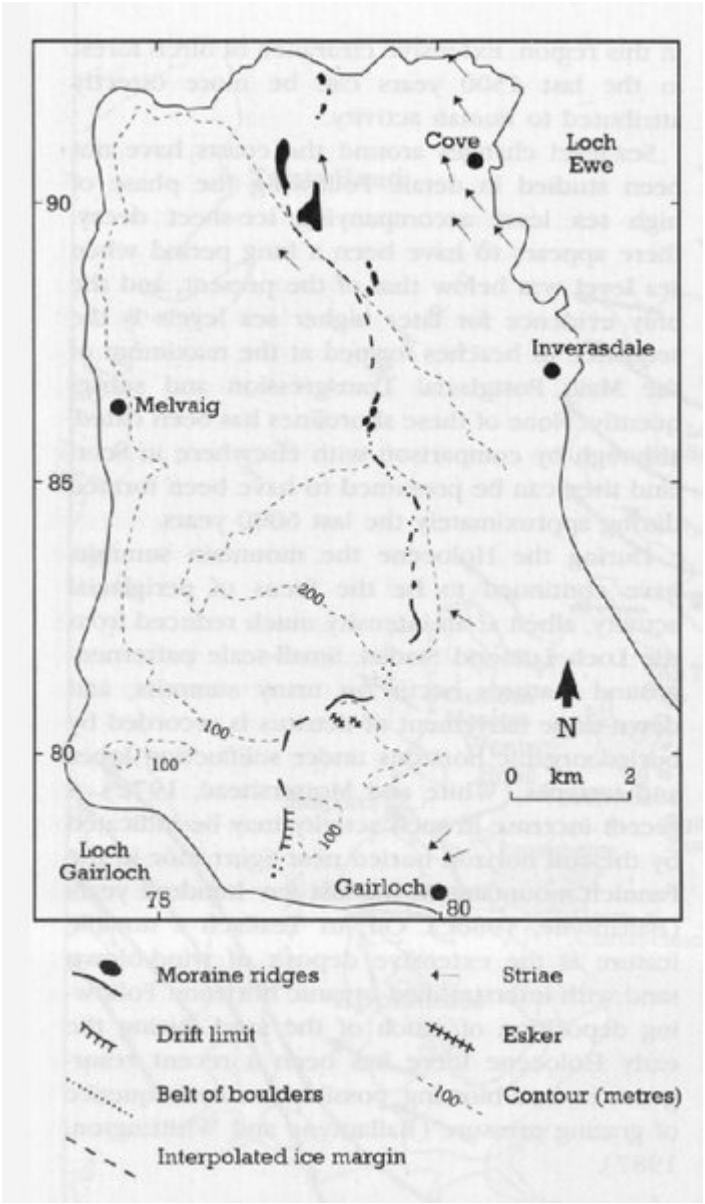

(Figure 6.2) The Gairloch Moraine and associated landforms (from Robinson and Ballantyne, 1979).

(Figure 6.3) The Gairloch Moraine, in the valley of the River Sand north-west of Gairloch, comprises a low ridge of boulders. (Photo: J E. Gordon.)

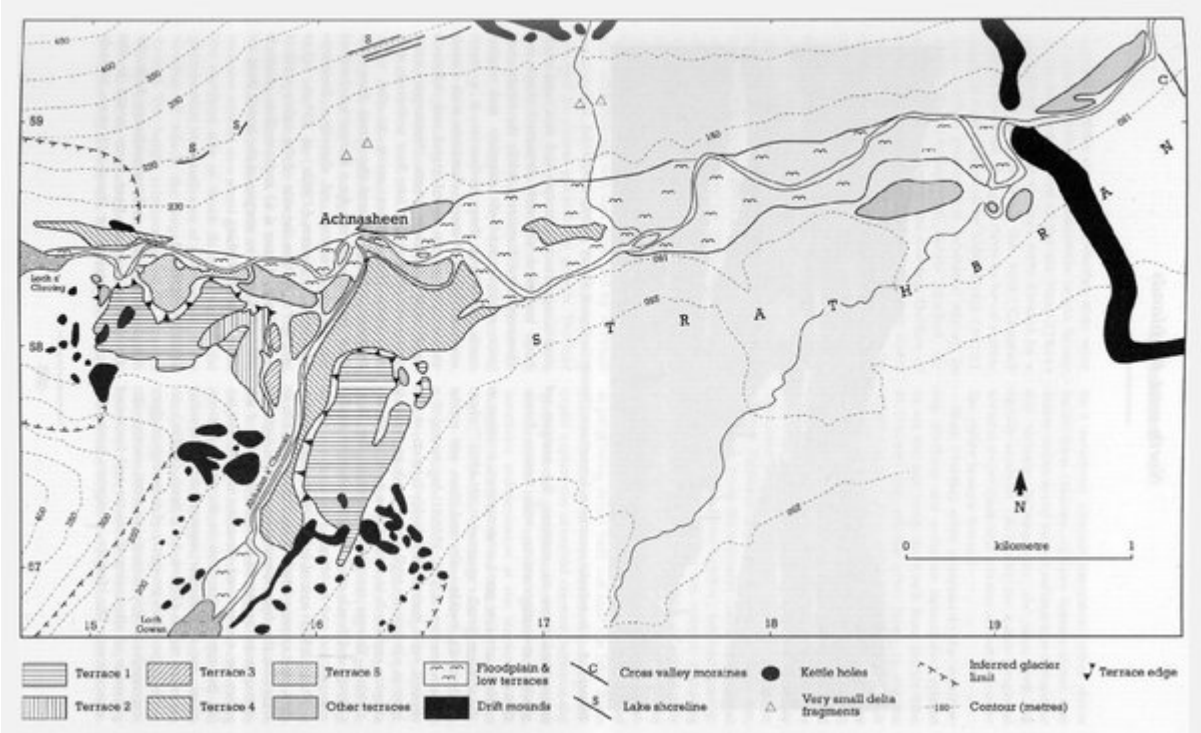

(Figure 6.4) Geomorphology of the Achnasheen area (from Sissons, 1982a).

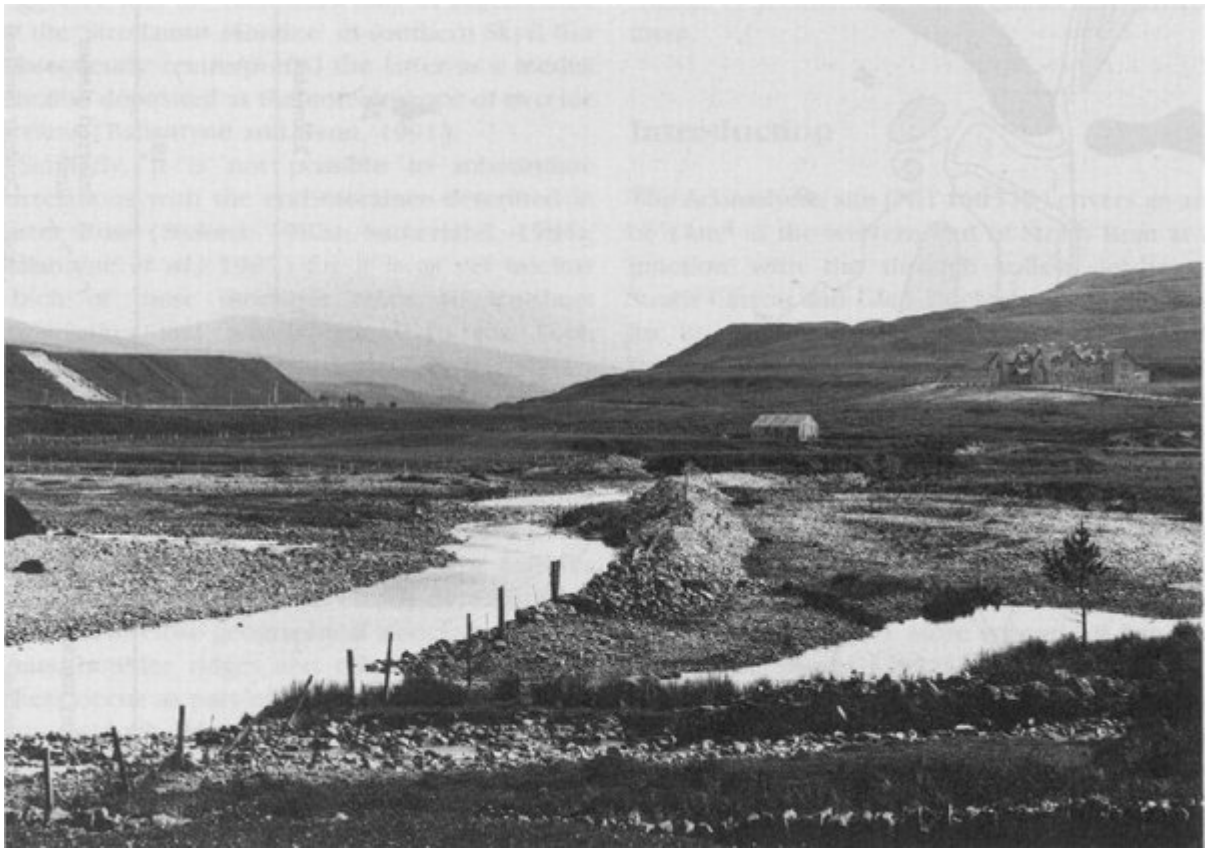

(Figure 6.5) Glaciofluvial terraces at Achnasheen. (British Geological Survey photograph B915.)

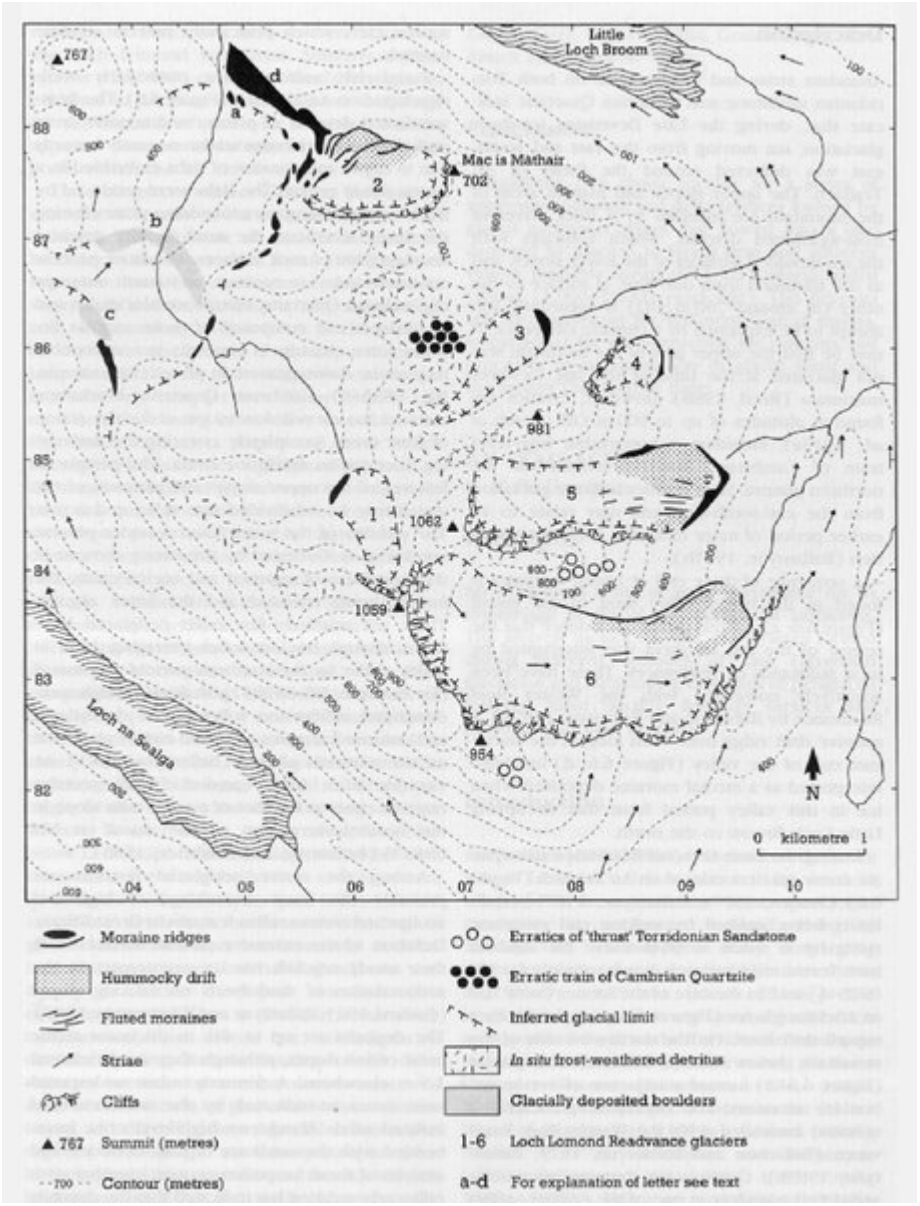

(Figure 6.6) The An Teallach area, showing principal glacial features and the limits of former glaciers (from Ballantyne, 1987b).

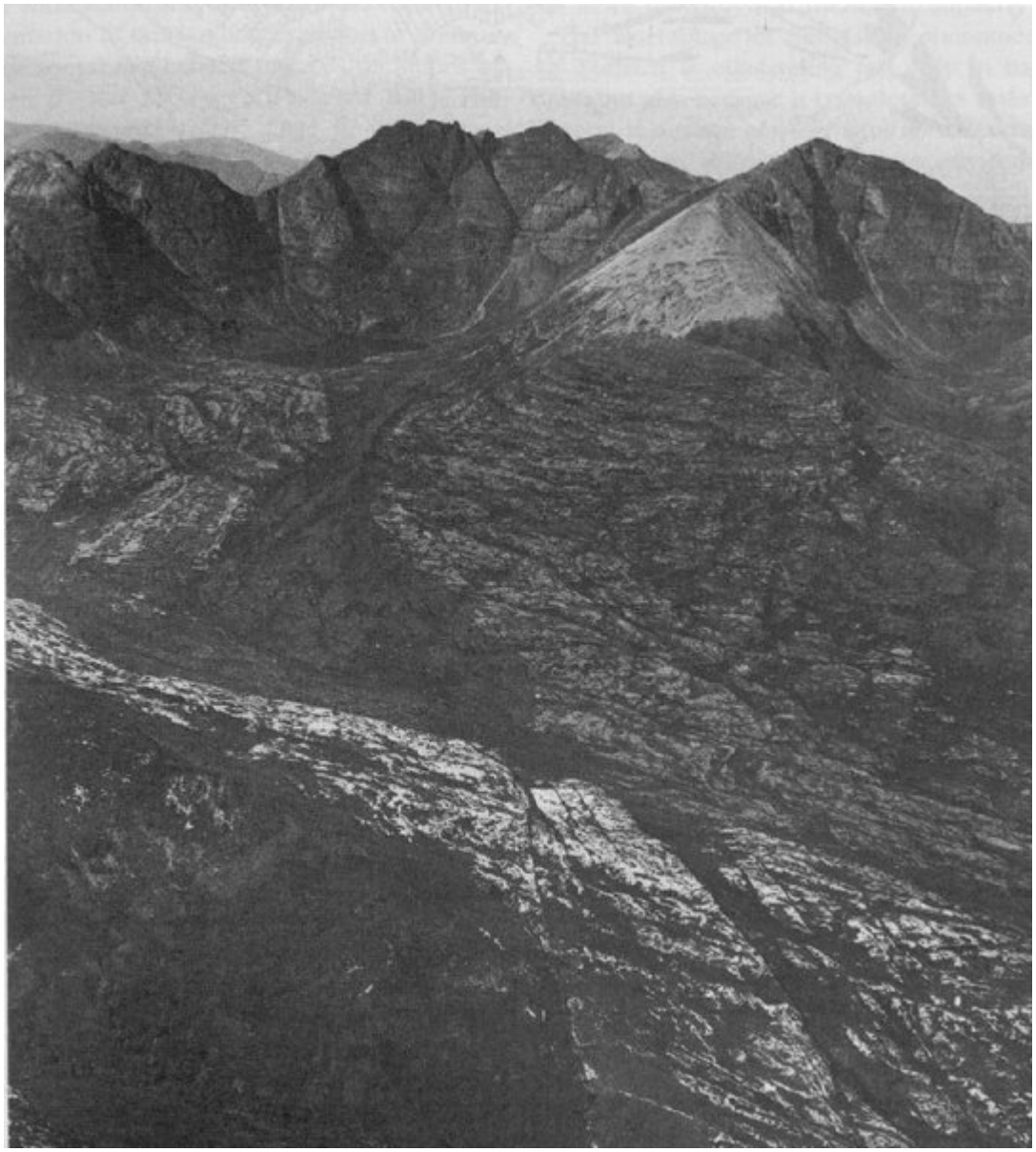

(Figure 6.7) The east flank of An Teallach. A clear lateral moraine and drift limit (centre) mark the extent of the Loch Lomond Readvance glacier that occupied the corrie of Toll an Lochain. The ice-scoured Torridonian sandstone of the lower slopes contrasts with the frost-shattered slopes of the mountain ridge and the quartzite blockslopes on Glas Mheall Liath. (British Geological Survey photograph D2102.)

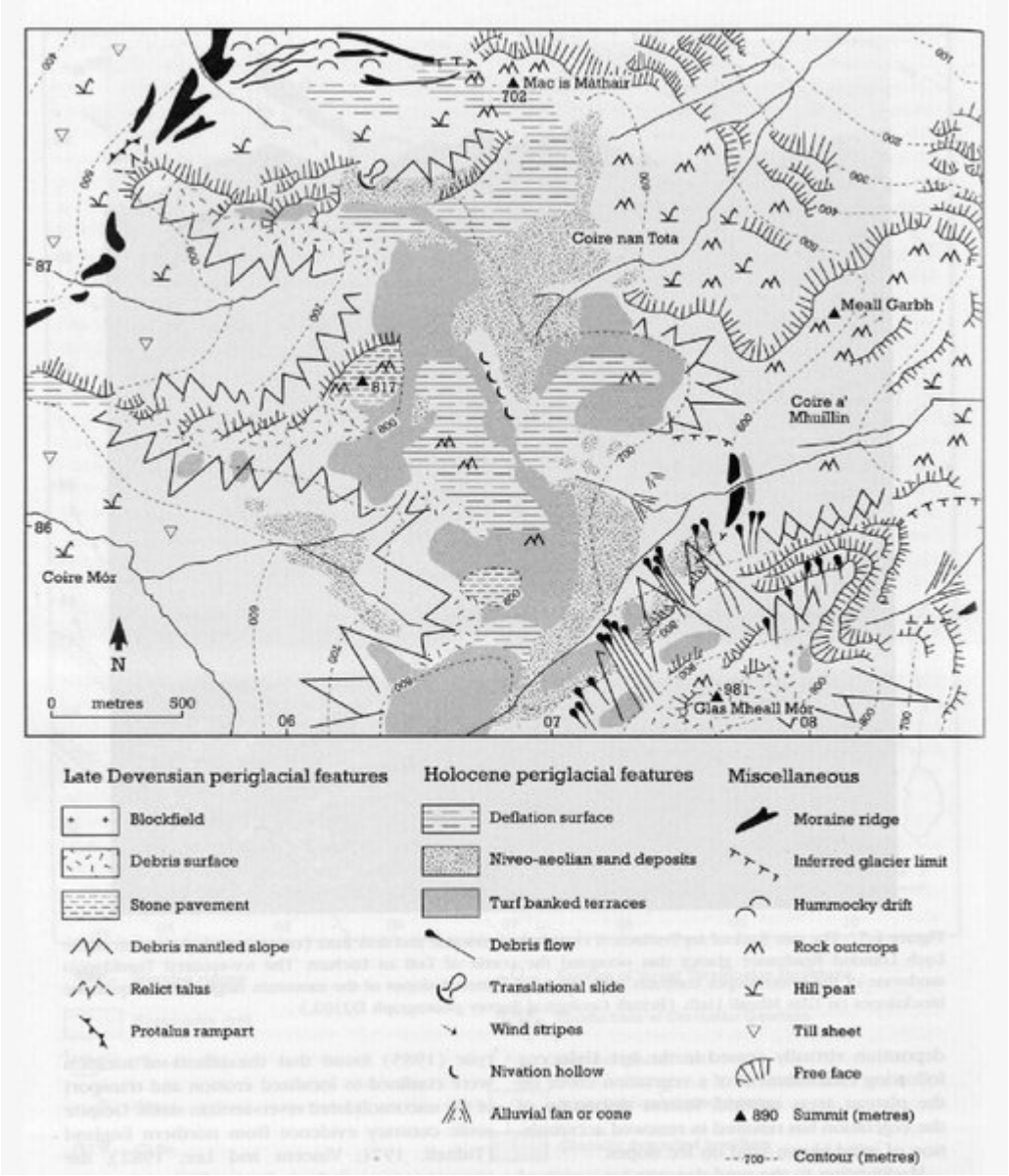

(Figure 6.8) Periglacial landforms and deposits on the northern plateau of An Teallach (from Ballantyne, 1984).

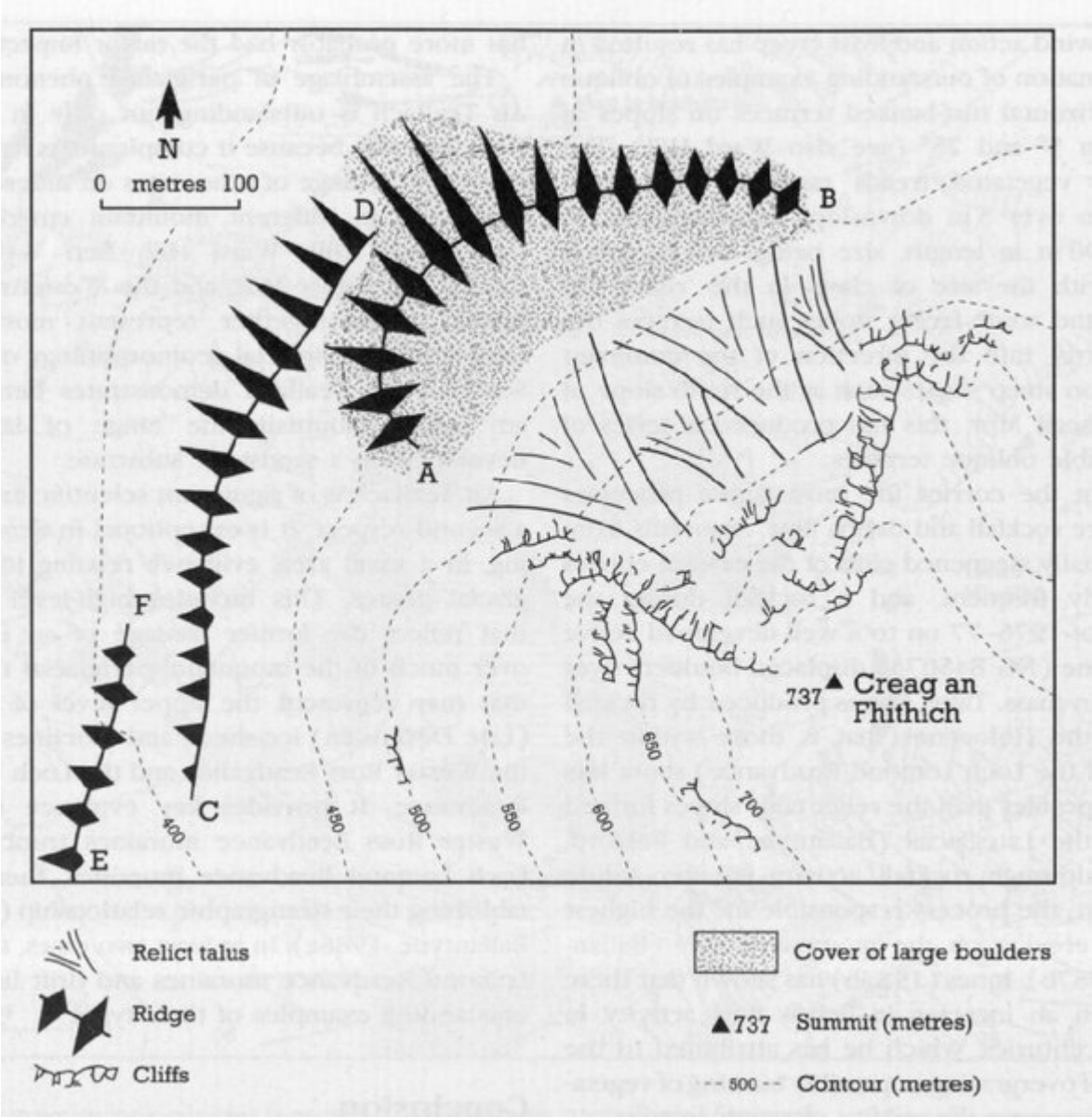

(Figure 6.9) The Baosbheinn protalus rampart and associated landforms, showing the upper boulder ridge (AB) and lower ridges (CD and EF) (from Ballantyne, 1986a).

(Figure 6.10) Protalus rampart on the north-west flank of Baosbheinn. The view also shows the rock avalanche scar, the two lower Wester Ross Readvance moraine ridges and a Loch Lomond Readvance moraine intersecting the latter at the base of the mountain. (Cambridge University Collection: copyright reserved.)

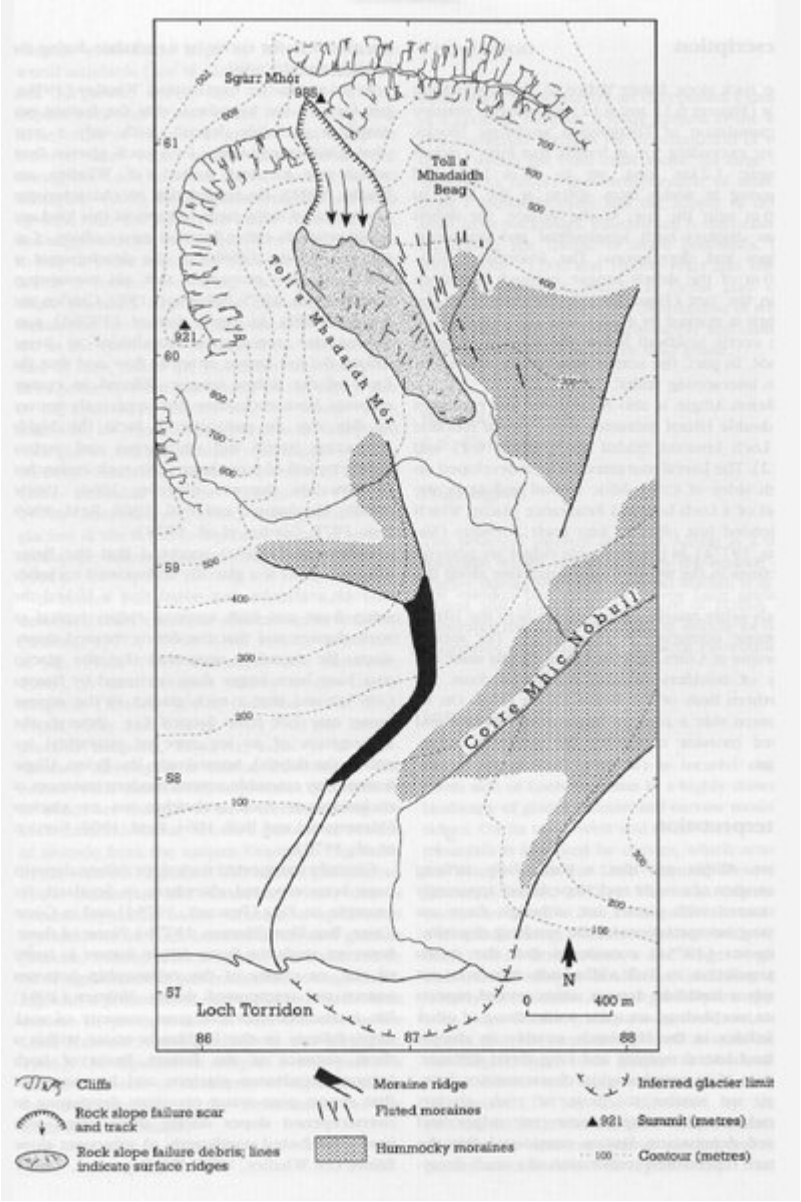

(Figure 6.12) Beinn Alligin, a Torridonian sandstone mountain in Wester Ross, rises above an ice-scoured surface of Lewisian gneiss to the west. A lateral moraine (centre left) marks the limit of a Loch Lomond Readvance glacier and is succeeded on the lower slopes by hummocky moraine; fluted drift can also be seen in the centre and to the right of the photograph. A large rock avalanche scar is prominent below the summit of Sgurr Mhor. The resulting deposit on the corrie floor includes a low tongue of boulders extending beyond the main part of the deposit. (Cambridge University Collection: copyright reserved.)

(Figure 6.11) Geomorphology of Toll a'Mhadaidh, Beinn Alligin, showing rockslide debris and principal glacial landforms (from Sissons, 1977d). formation, as they take the form of protalus lobes (see Wahrhaftig and Cox, 1959; Liestøl, 1961; Outcalt and Benedict, 1965; White, 1976; Lindner and Marks, 1985; Martin and Whalley, 1987; Whalley and Martin, 1992) that have apparently developed as a result of deformation of ice within rockfall talus accumulations. The only other features in Britain that may be of similar origin to that at Beinn Alligin are at Moelwyn Mawr in North Wales (Campbell and Bowen, 1989) and Beinn an Lochain in Argyll (Holmes, 1984; Maclean, 1991).

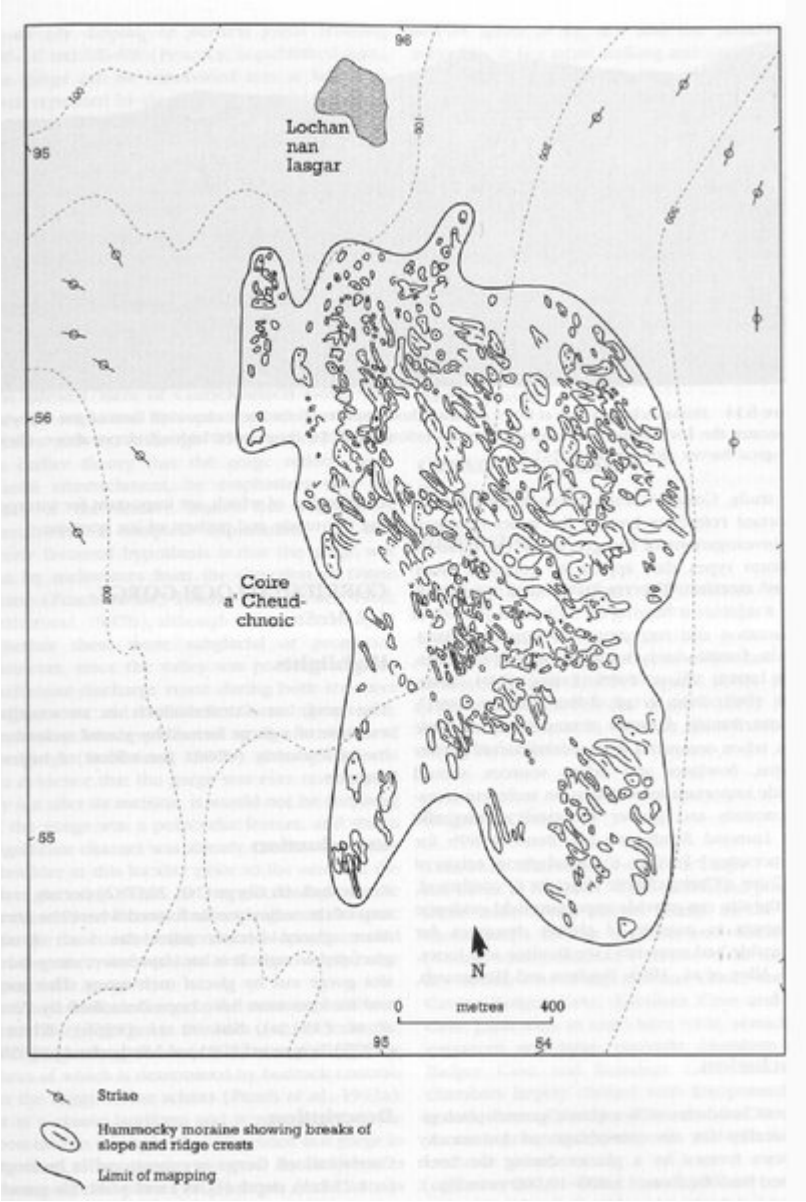

(Figure 6.13) Geomorphology of Coire a'Cheud-chnoic (from Hodgson, 1987).

(Figure 6.14) Hummocky moraine at Coire a'Cheud-chnoic in Glen Torridon. A clear drift limit on the valley side demarcates the Loch Lomond Readvance deposits below, from the ice-scoured bedrock slopes above. (British Geological Survey photograph D2737.)

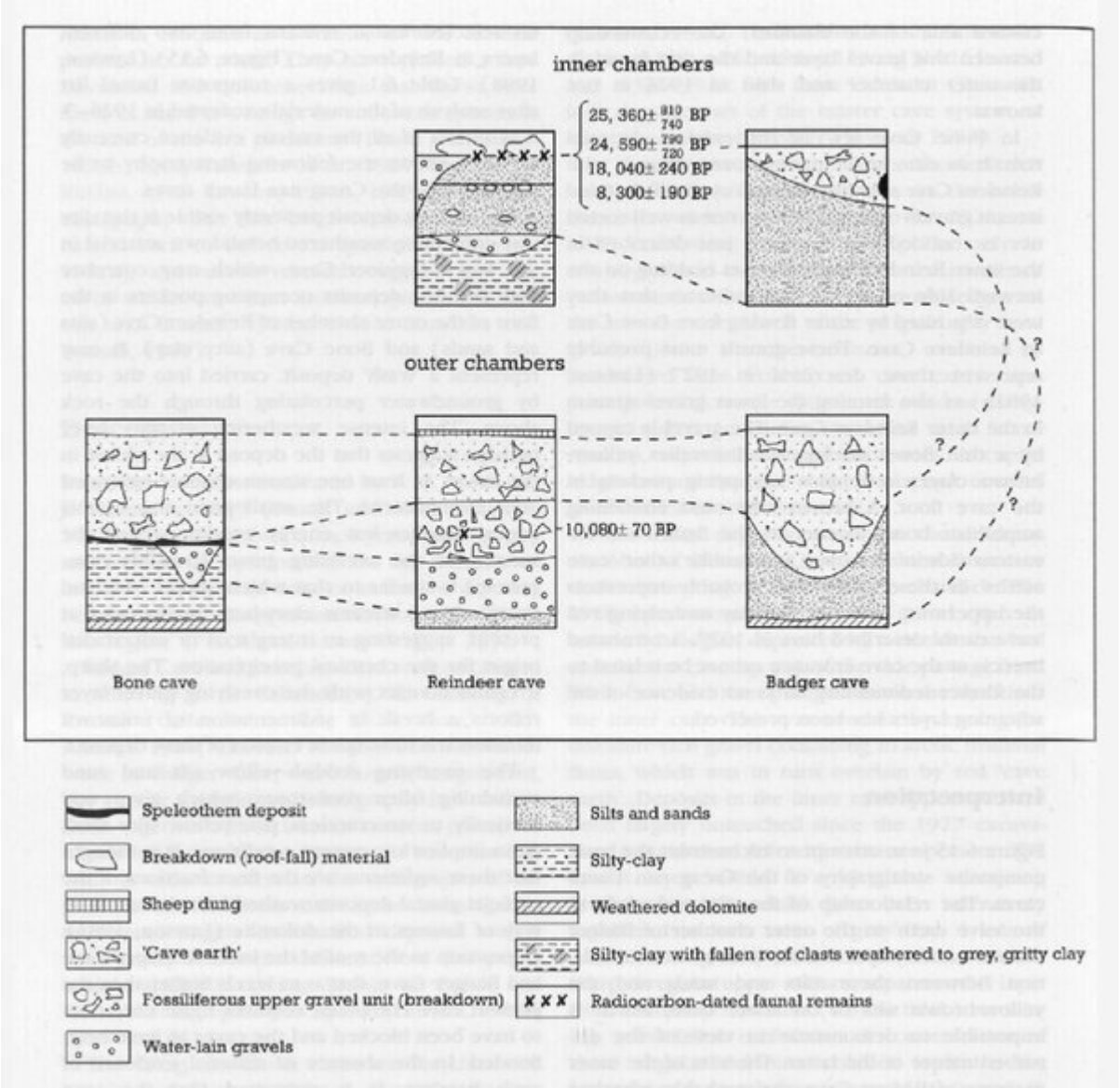

(Figure 6.15) Diagrammatic reconstruction of the lithostratigraphy of the Creag nan Uamh caves, showing proposed relationships between certain of the layers (from Lawson, 1983).

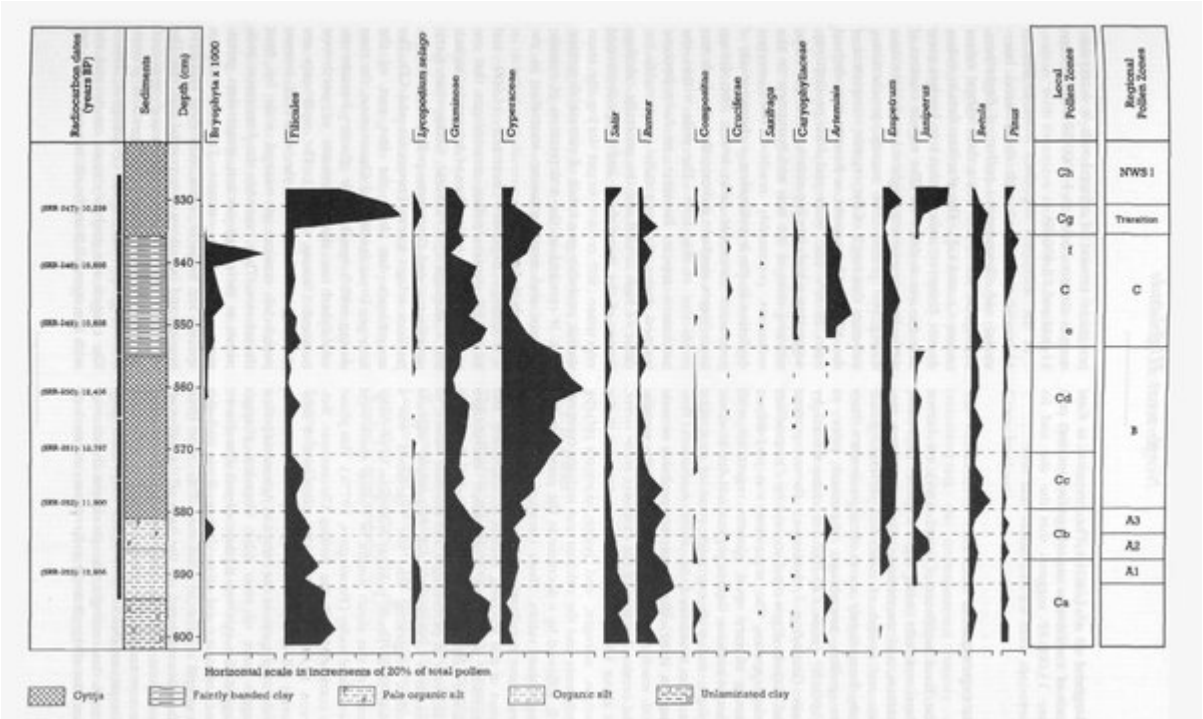

(Figure 6.16) Cam Loch: relative pollen diagram, showing selected taxa as percentages of total pollen (from Pennington, 1977a).

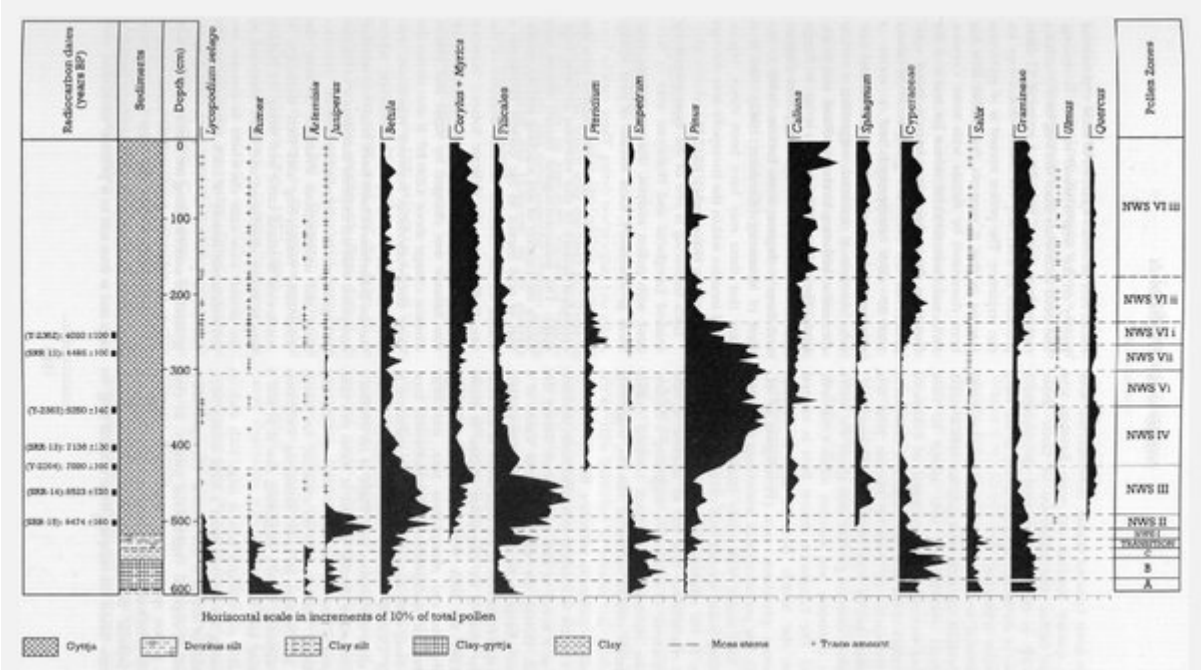

(Figure 6.17) Loch Sionascaig: relative pollen diagram, showing selected taxa as percentages of total pollen (from Pennington et al., 1972).

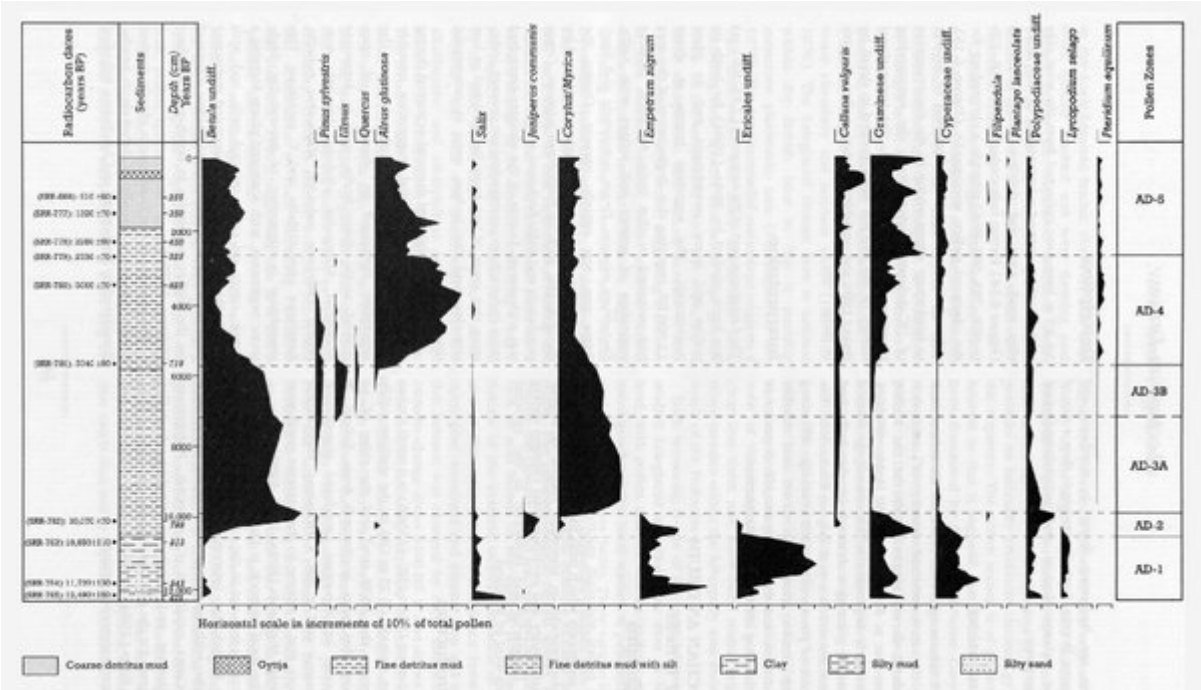

(Figure 6.18) Lochan an Druim: relative pollen diagram, showing selected taxa as percentages of total pollen (from Birks, 1980). Note that the data are plotted against a radiocarbon time-scale.

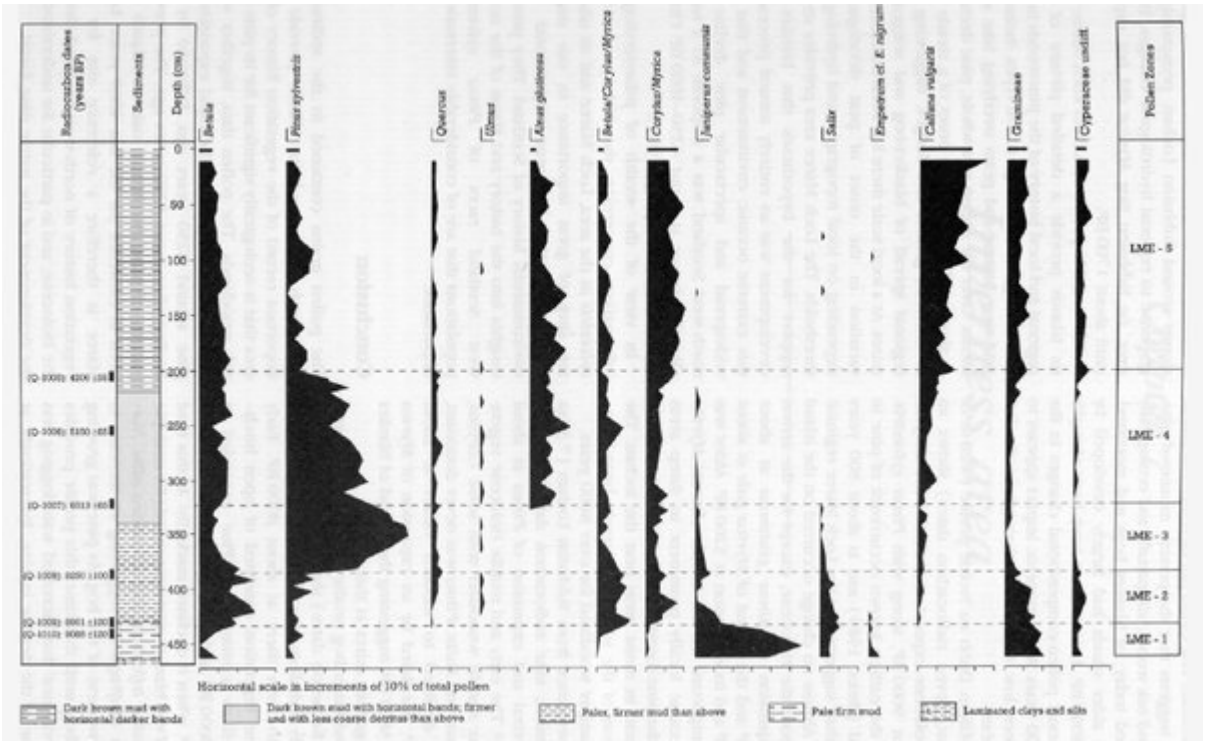

(Figure 6.19) Loch Maree: relative pollen diagram, showing selected taxa as percentages of total pollen (from Birks, 1972b).

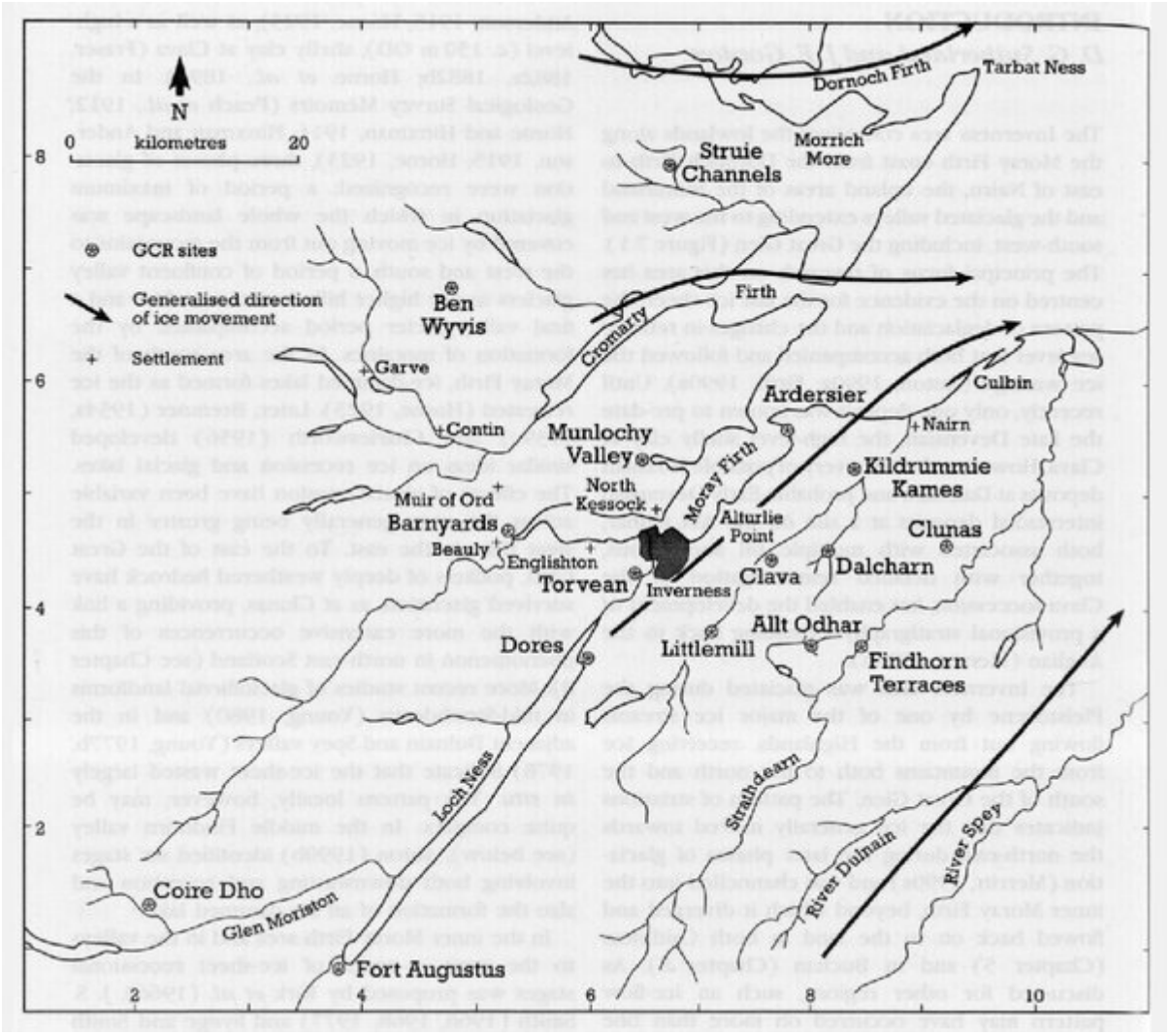

(Figure 7.1) Location map of the Inverness area and generalized directions of ice movement.

(Figure 7.2) Section at Dalcharn showing the Dalcharn 'gravel formation' and the Dalcharn 'biogenic formation' (bottom left), overlain by a sequence of tills (right). (Photo: D. G. Sutherland.)

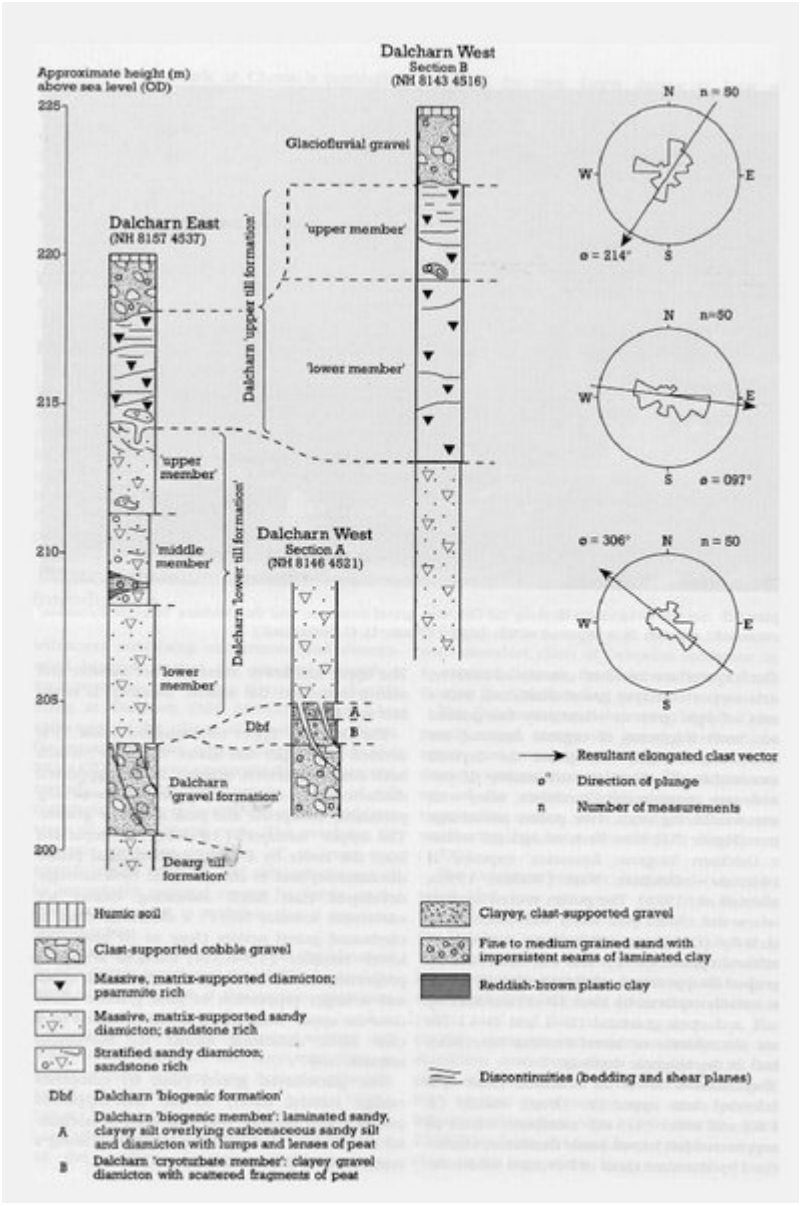

(Figure 7.3) Sediment logs and stratigraphy at Dalcharn (from Merritt and Auton, 1990).

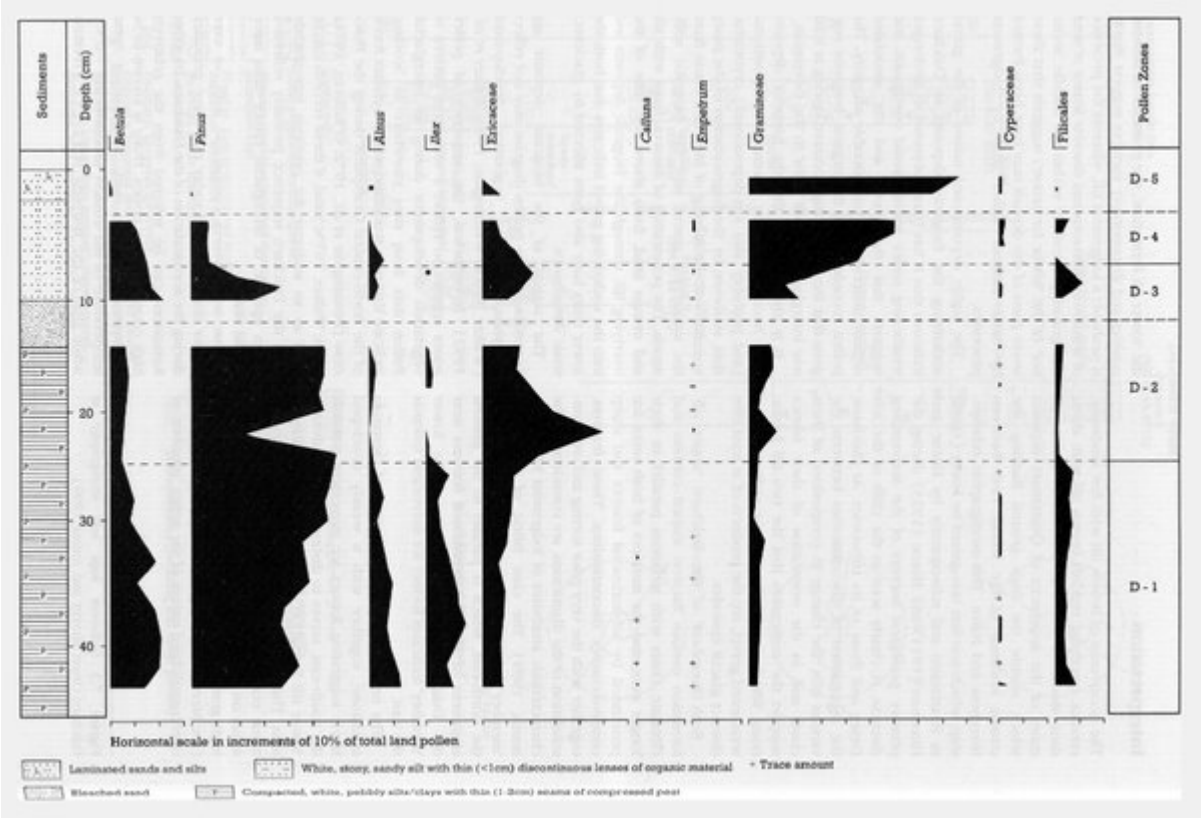

(Figure 7.4) Relative pollen diagram for the Dalcharn 'biogenic formation', showing selected taxa only as percentage of total land pollen (from Walker, 1990a).

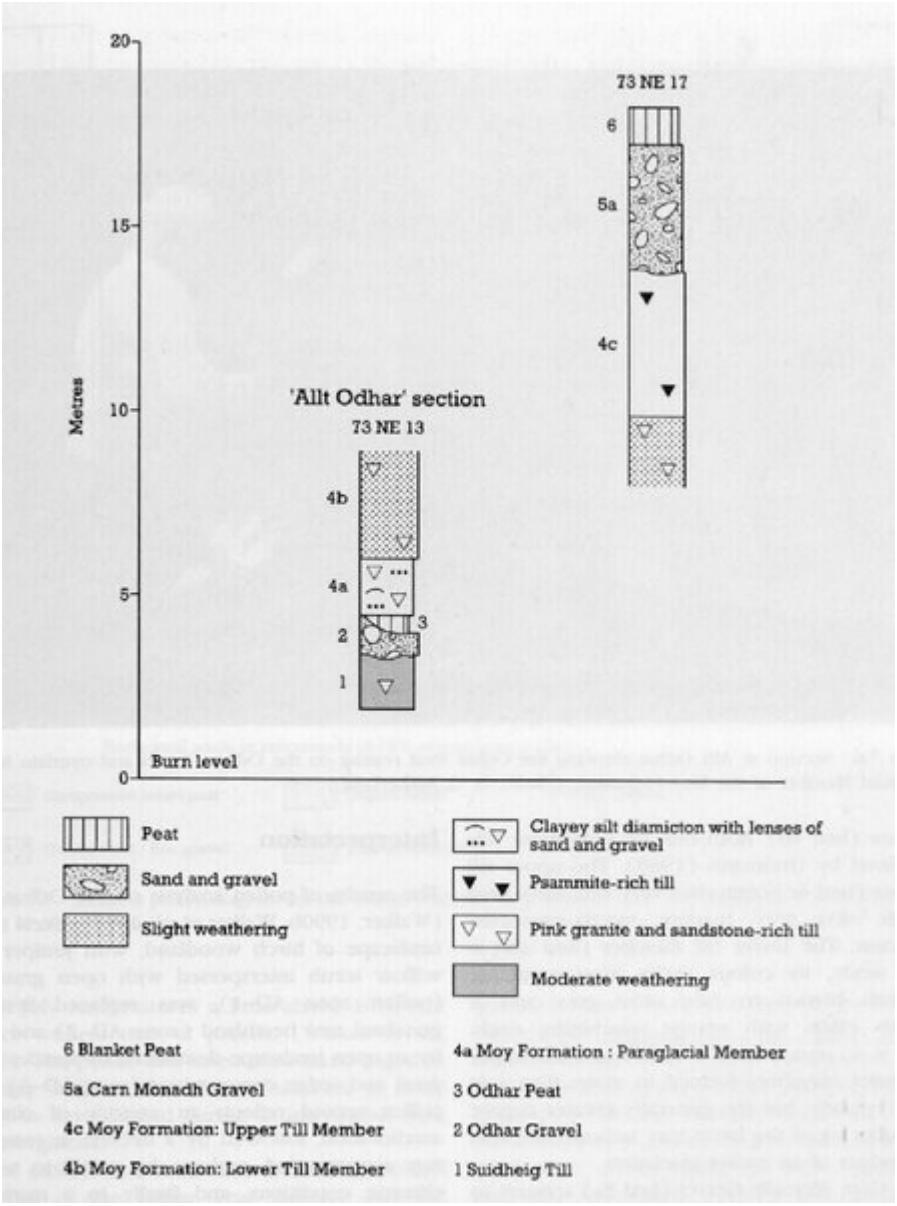

(Figure 7.5) Sediment logs of the Allt Odhar and adjacent sections (from Merritt, 1990c).

(Figure 7.6) Section at Allt Odhar showing the Odhar Peat resting on the Odhar Gravel and overlain by the Paraglacial Member of the Moy Formation. (Photo: D. G. Sutherland.)

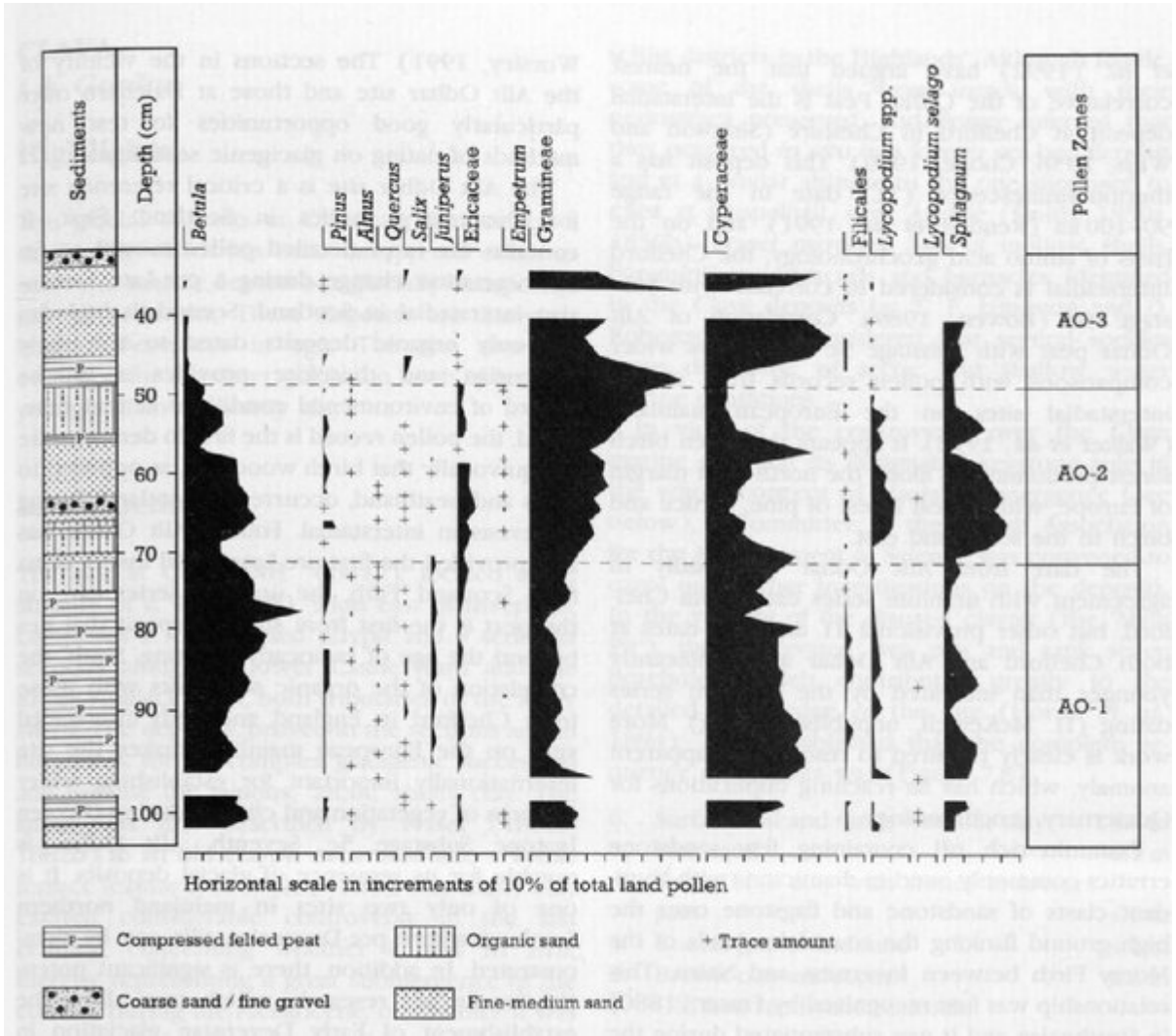

(Figure 7.7) Relative pollen diagram for the Odhar Peat, showing selected taxa as percentages of total land pollen (from Walker, 1990b).

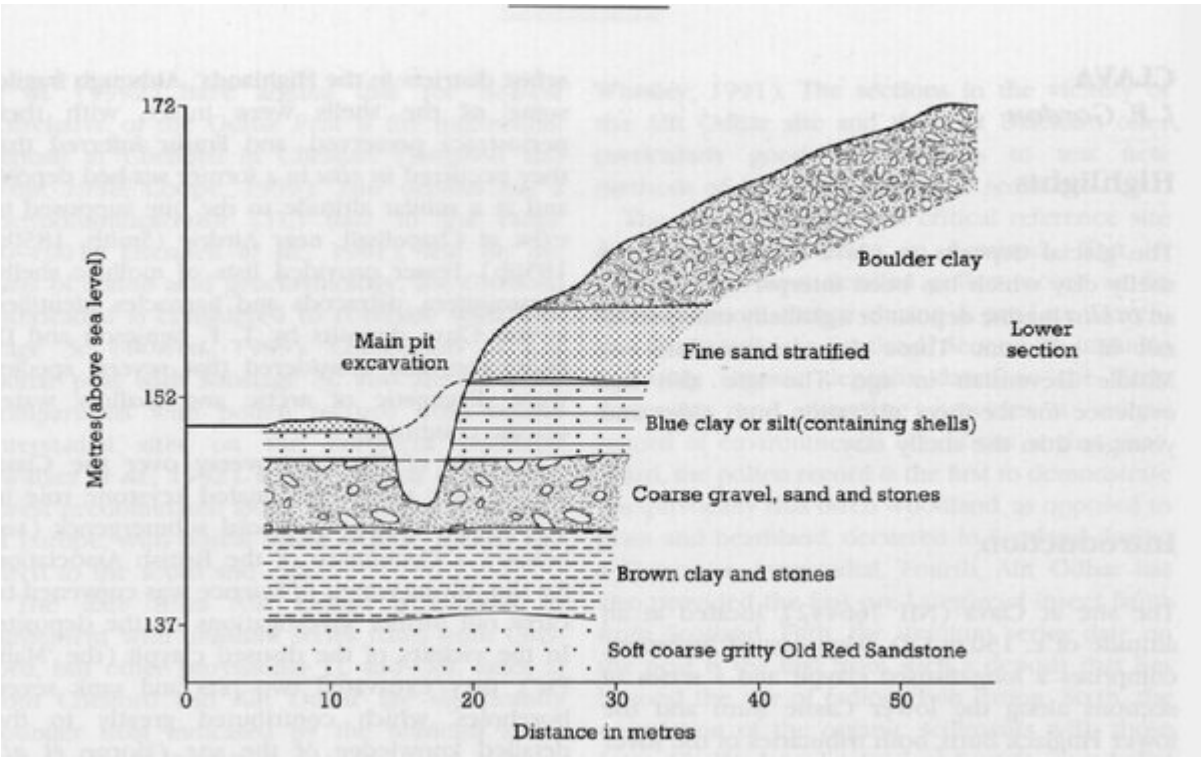

(Figure 7.8) Clava: lithological succession at the 'Main Pit' (from Horne et al., 1894).

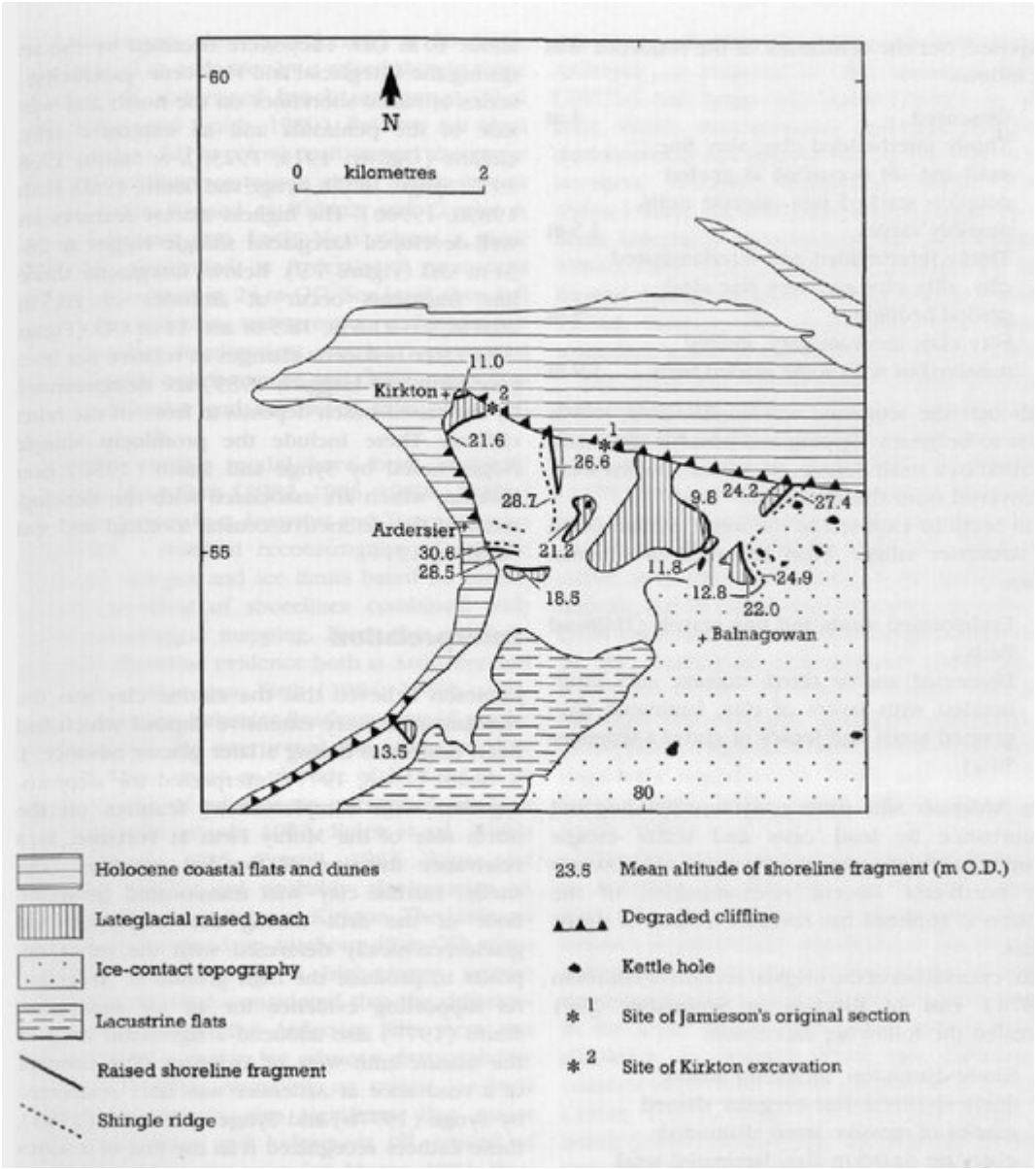

(Figure 7.9) Geomorphology of the Ardersier area (from Firth, 1989b).

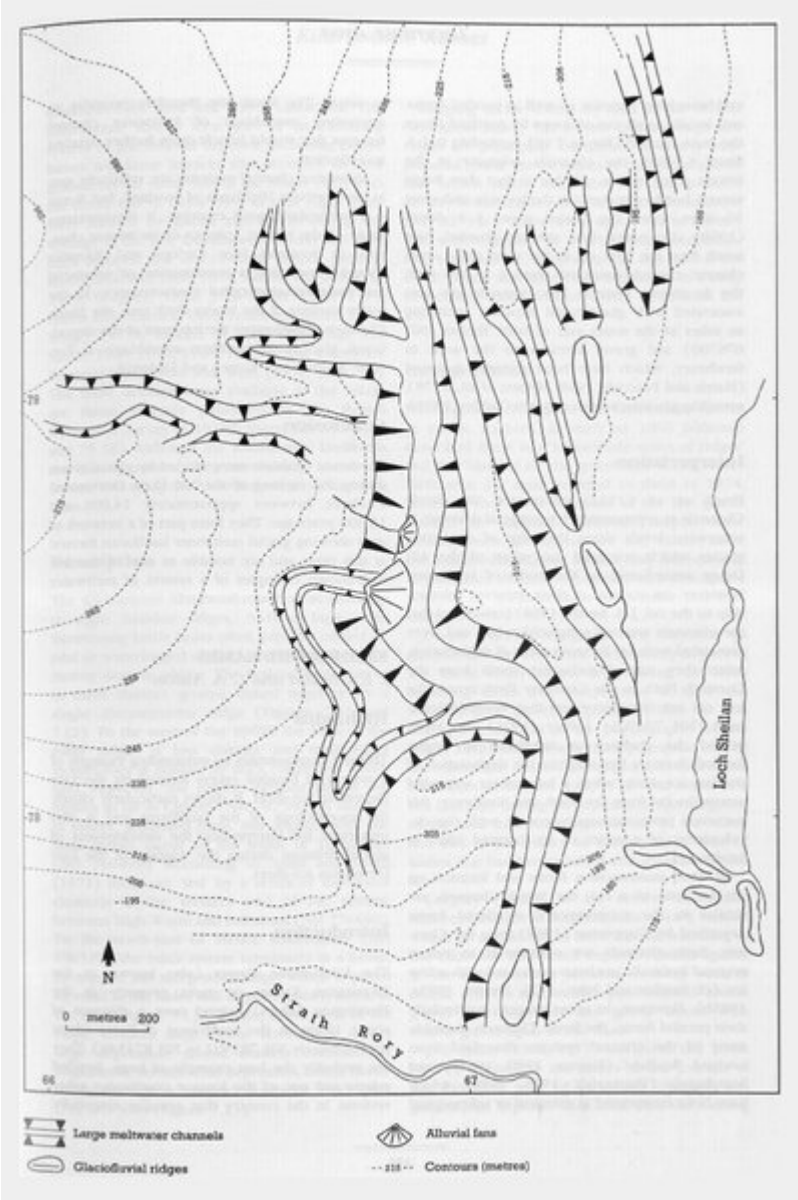

(Figure 7.10) Geomorphology of the Struie meltwater channels, Strathrory (from J. S. Smith, 1968; Leftley, 1991).

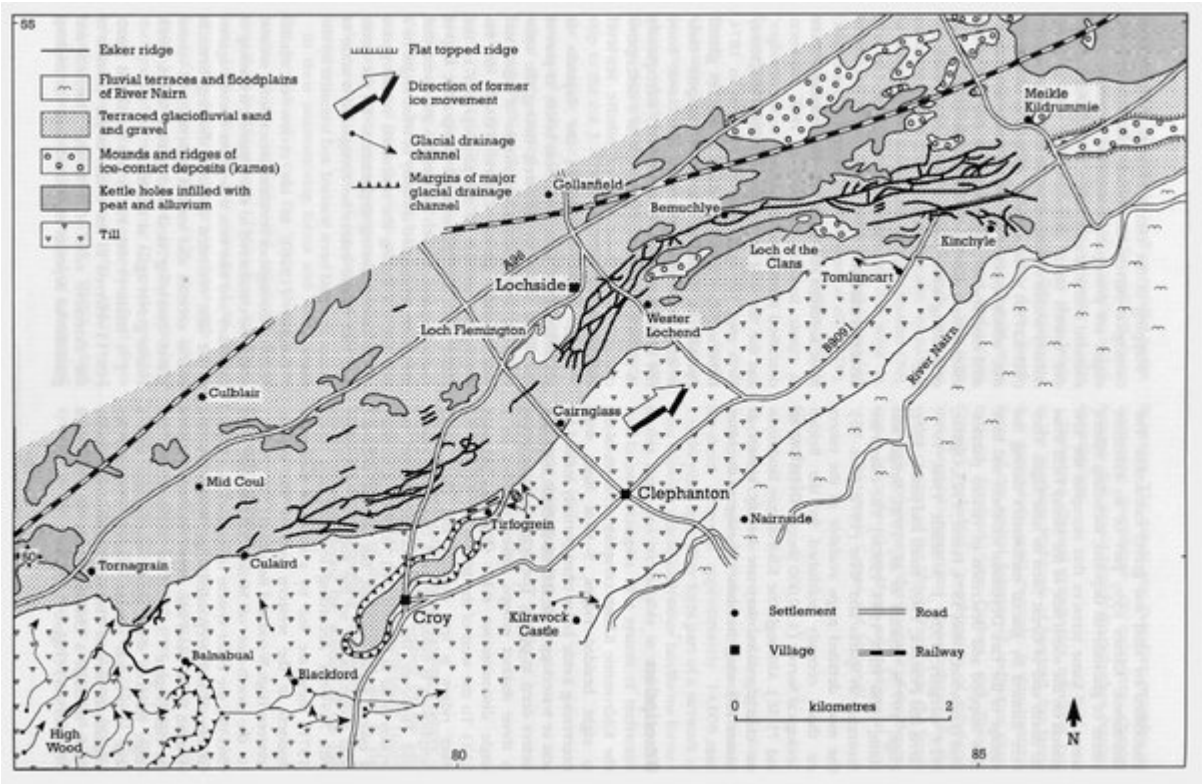

(Figure 7.11) Geomorphology of the Kildrummie Kames esker system between High Wood and Meikle Kildrummie (from mapping by C. A. Auton for the British Geological Survey 1:50,000 Geological Sheet 84W (Fortrose), in press).

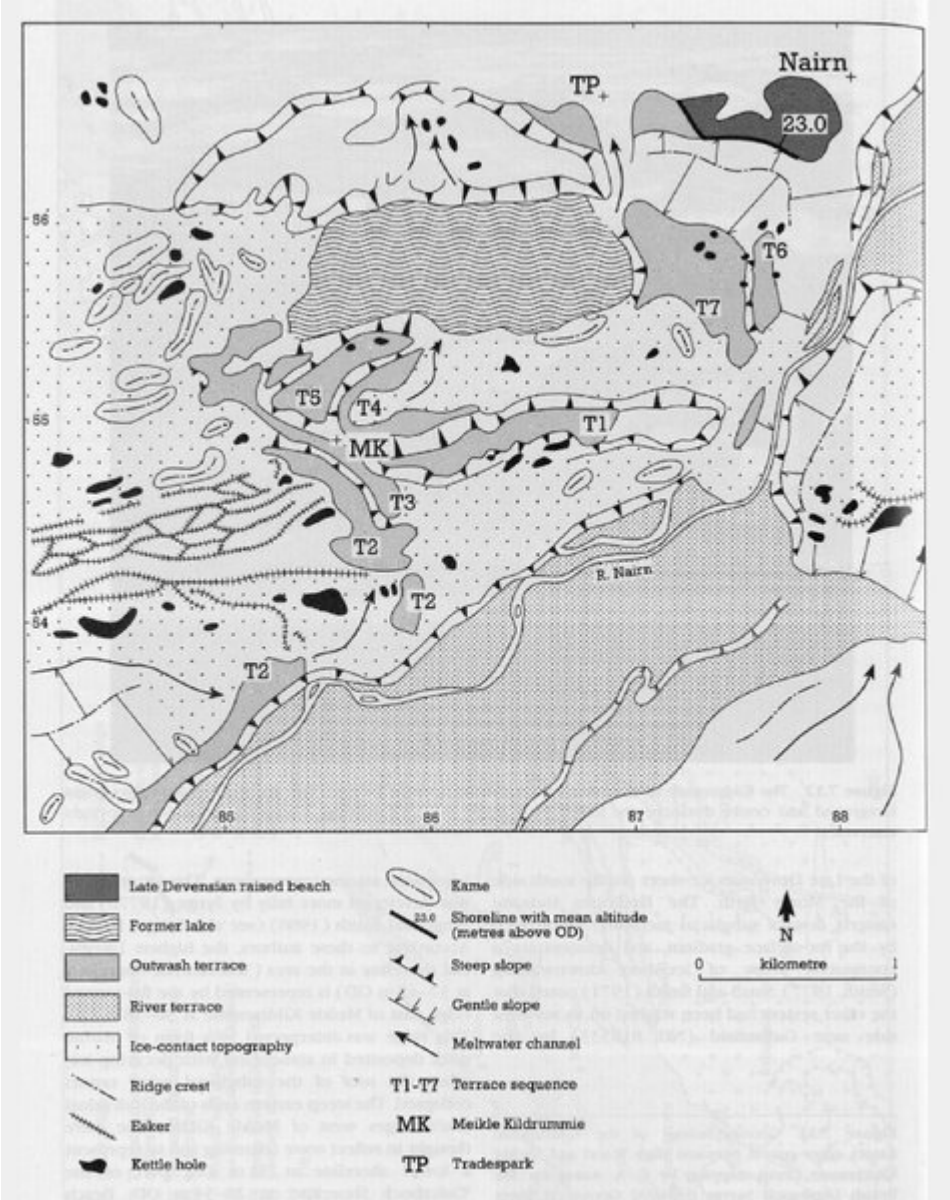

(Figure 7.13) Geomorphology of the eastern part of the Kildrummie Kames in the vicinity of Meikle Kildrummie (from Firth, 1984).

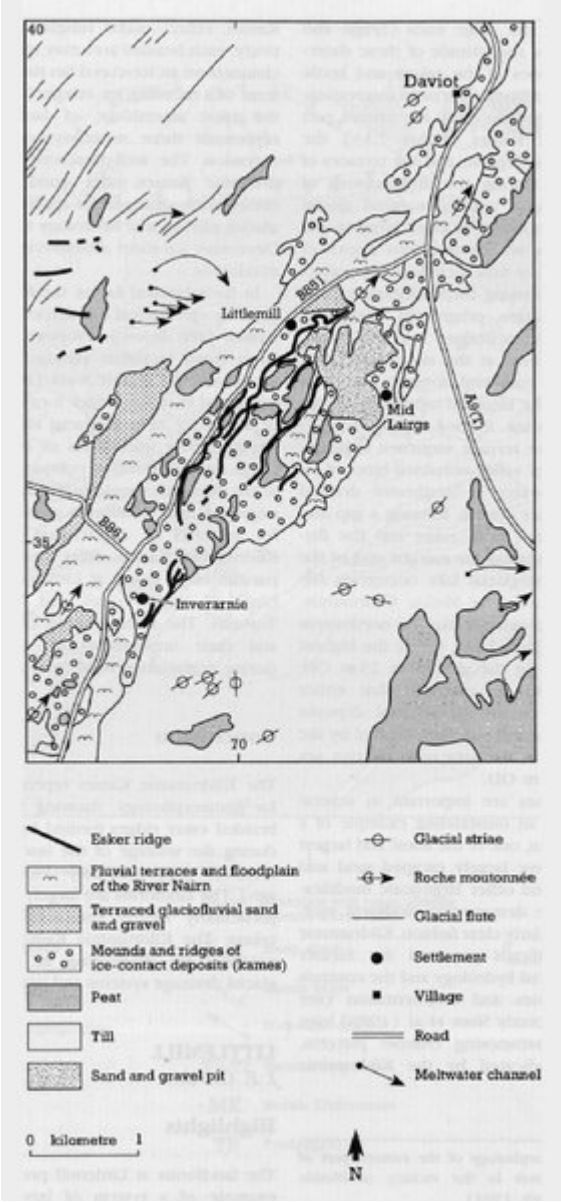

(Figure 7.14) Geomorphology of the Littlemill esker system between Inverarnie and Daviot (from mapping by J. W. Merritt for the British Geological Survey 1:50,000 Geological Sheet 84W (Fortrose), in press).

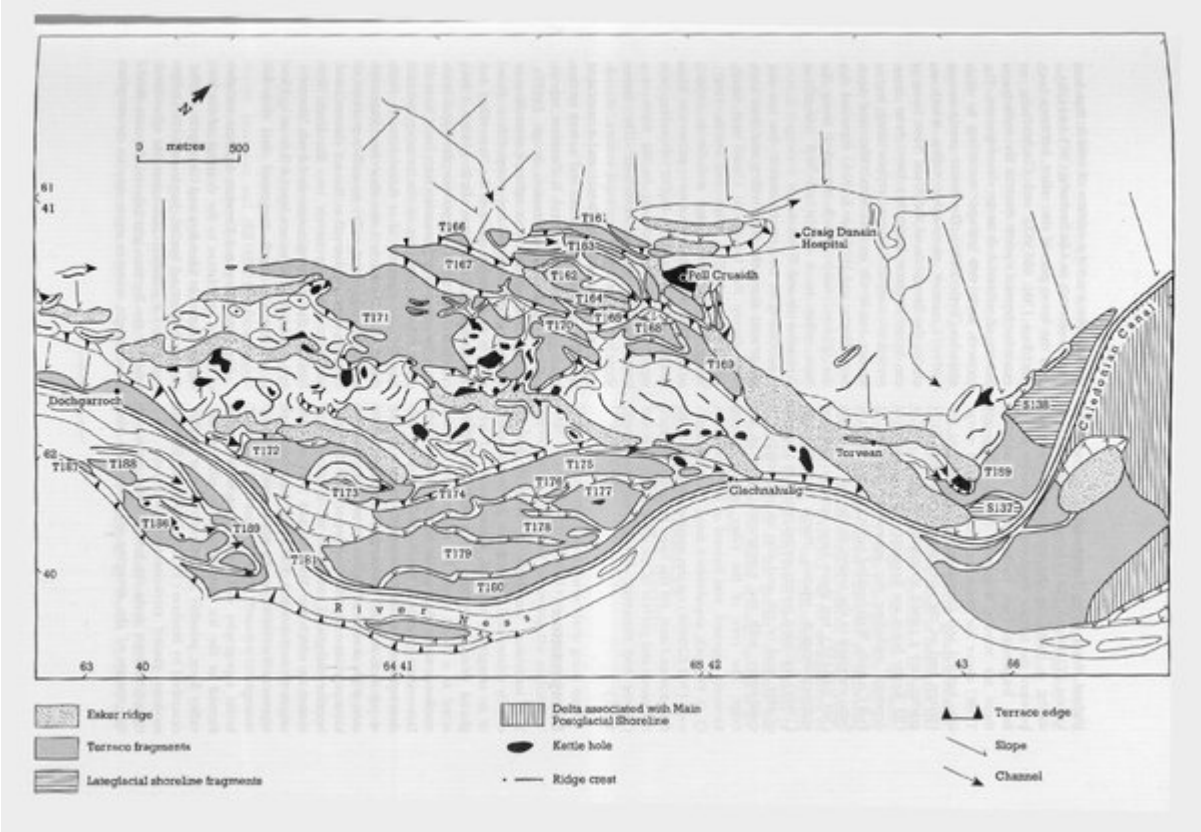

(Figure 7.15) Geomorphology of the Torvean area (from Firth, 1984). The terrace fragments include kame terraces (T161–T171), Lateglacial outwash and river terraces (T172–179, T159), and Holocene river terraces (T180–181).

(Figure 7.16) The Findhorn terraces at Ballachrochin. (British Geological Survey photograph C1415.)

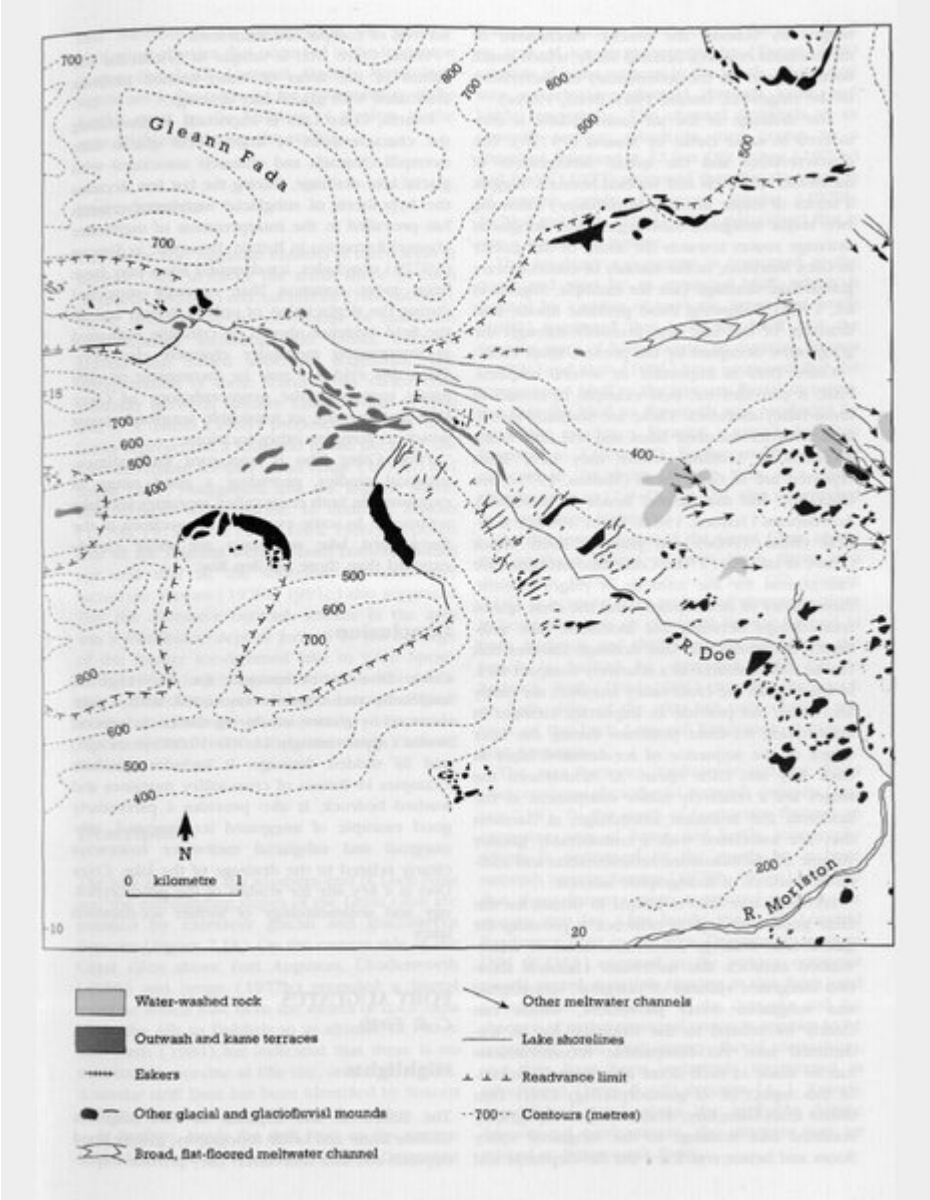

(Figure 7.17) Geomorphology of Coire Dho showing landforms associated with the former ice-dammed lake (from Sissons, 197 713).

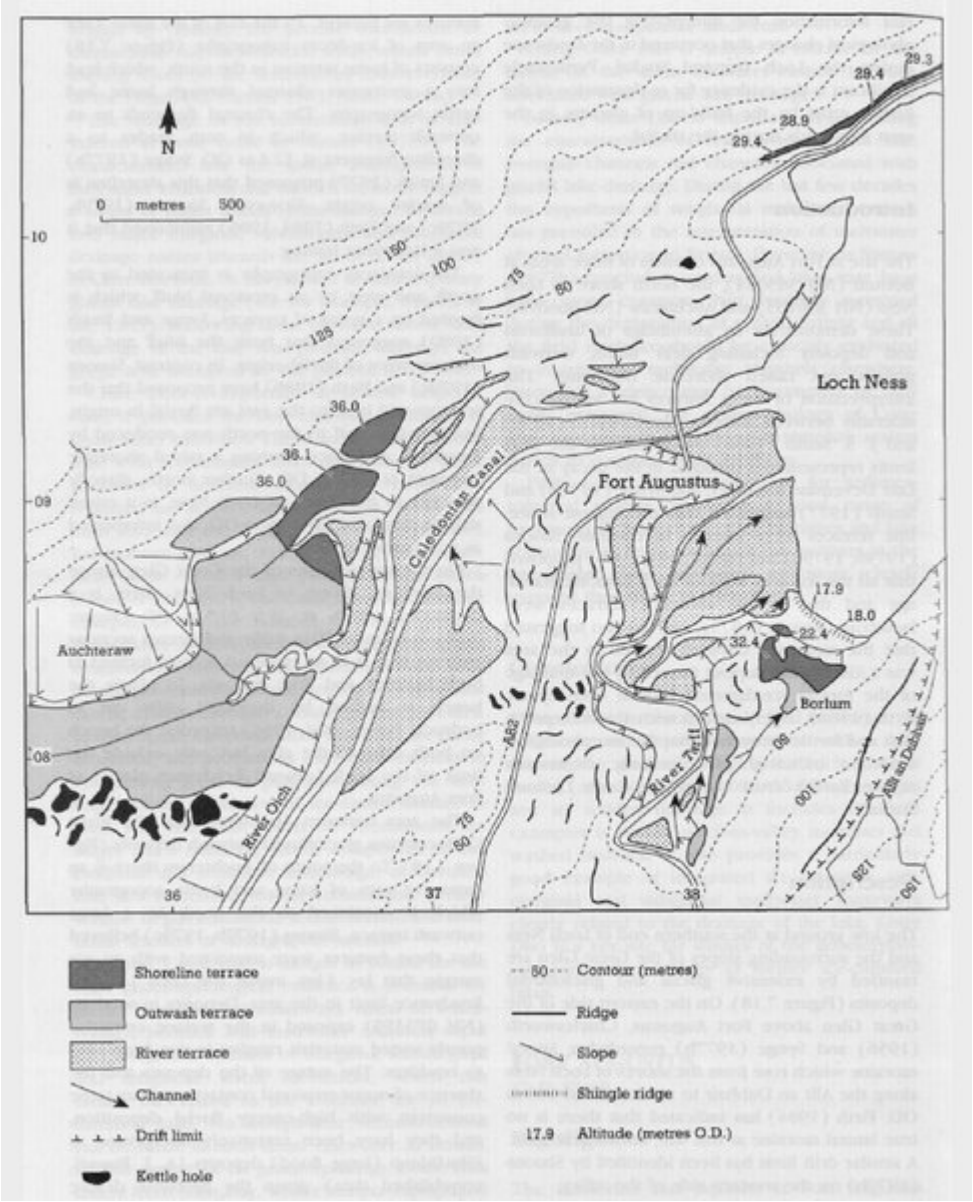

(Figure 7.18) Geomorphology of the Fort Augustus area (from Firth, 1984).

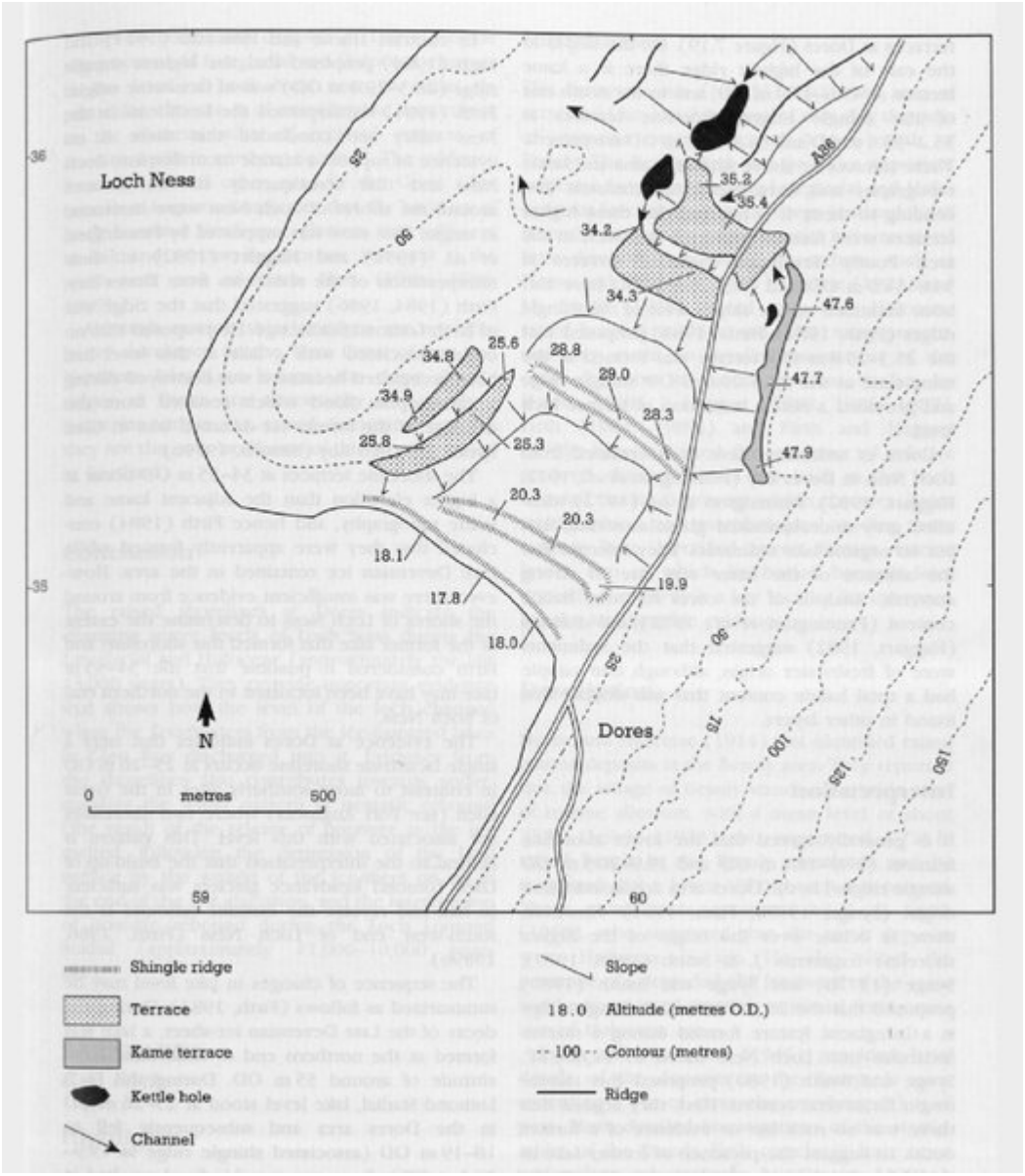

(Figure 7.19) Geomorphology of the Dores area (from Firth, 1984).

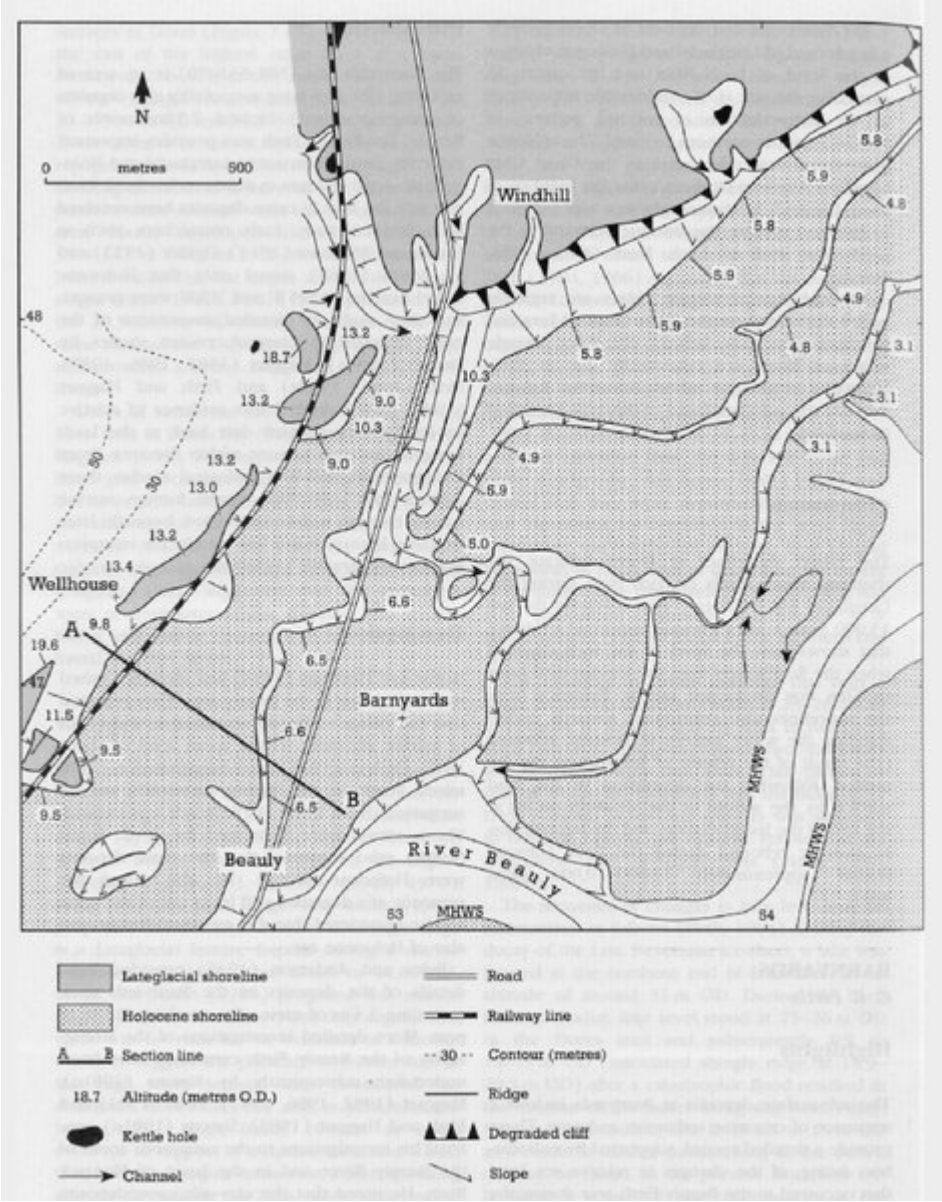

(Figure 7.20) Geomorphology of the Beauty carselands (from Firth, 1984).

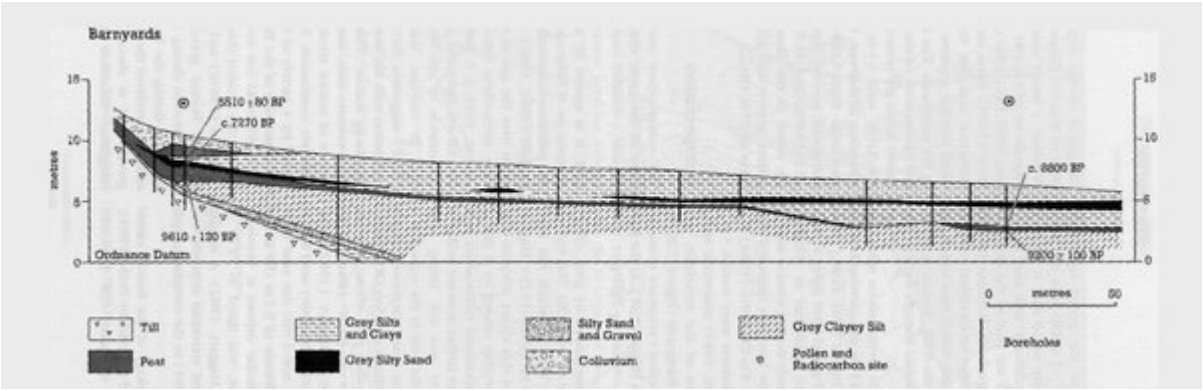

(Figure 7.21) Section through the Beauly carselands at Barnyards showing the sequence of Late Devensian and Holocene deposits (frem Haggert 1986)

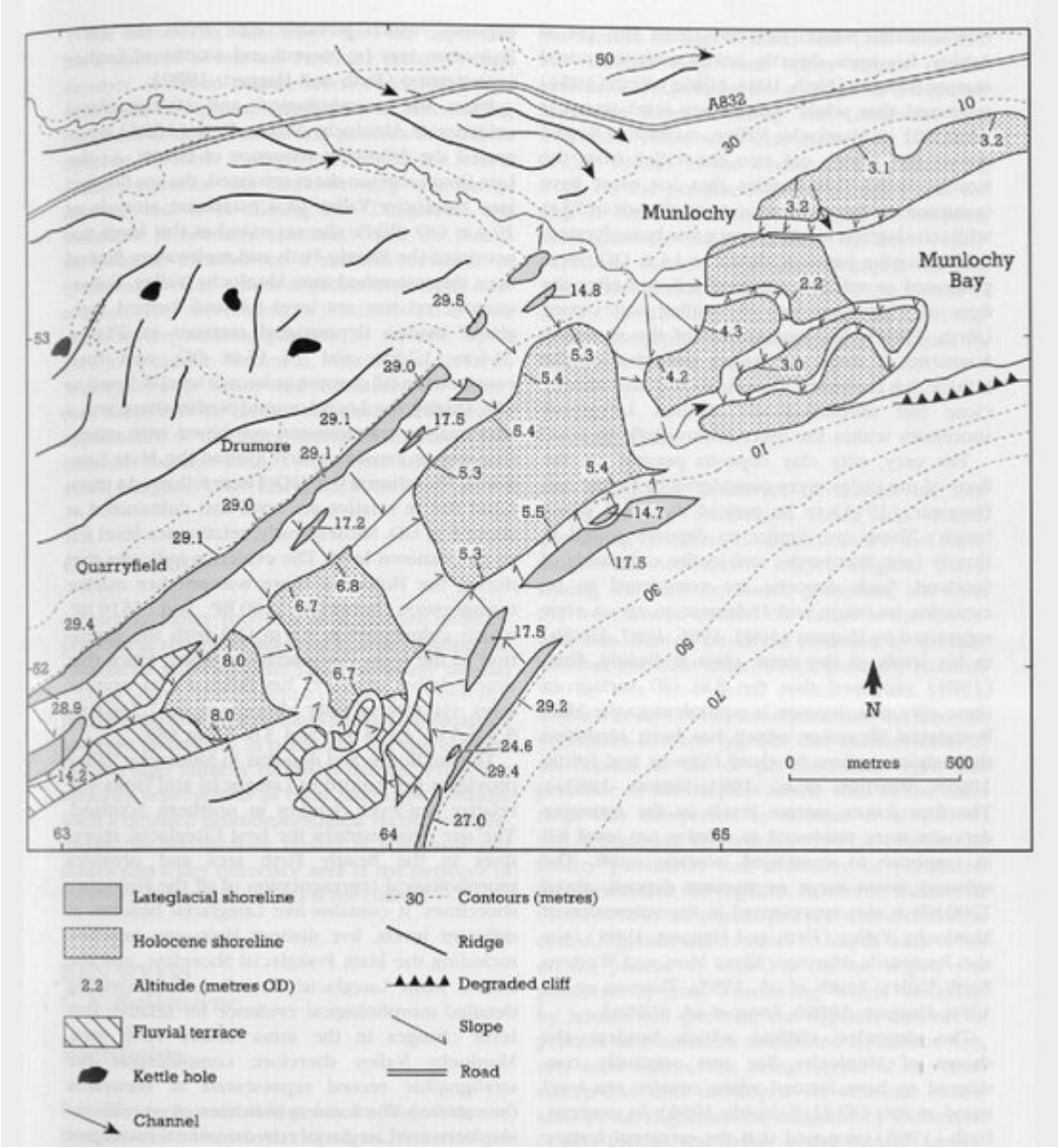

(Figure 7.22) Geomorphology of Munlochy Valley (from Firth, 1984).

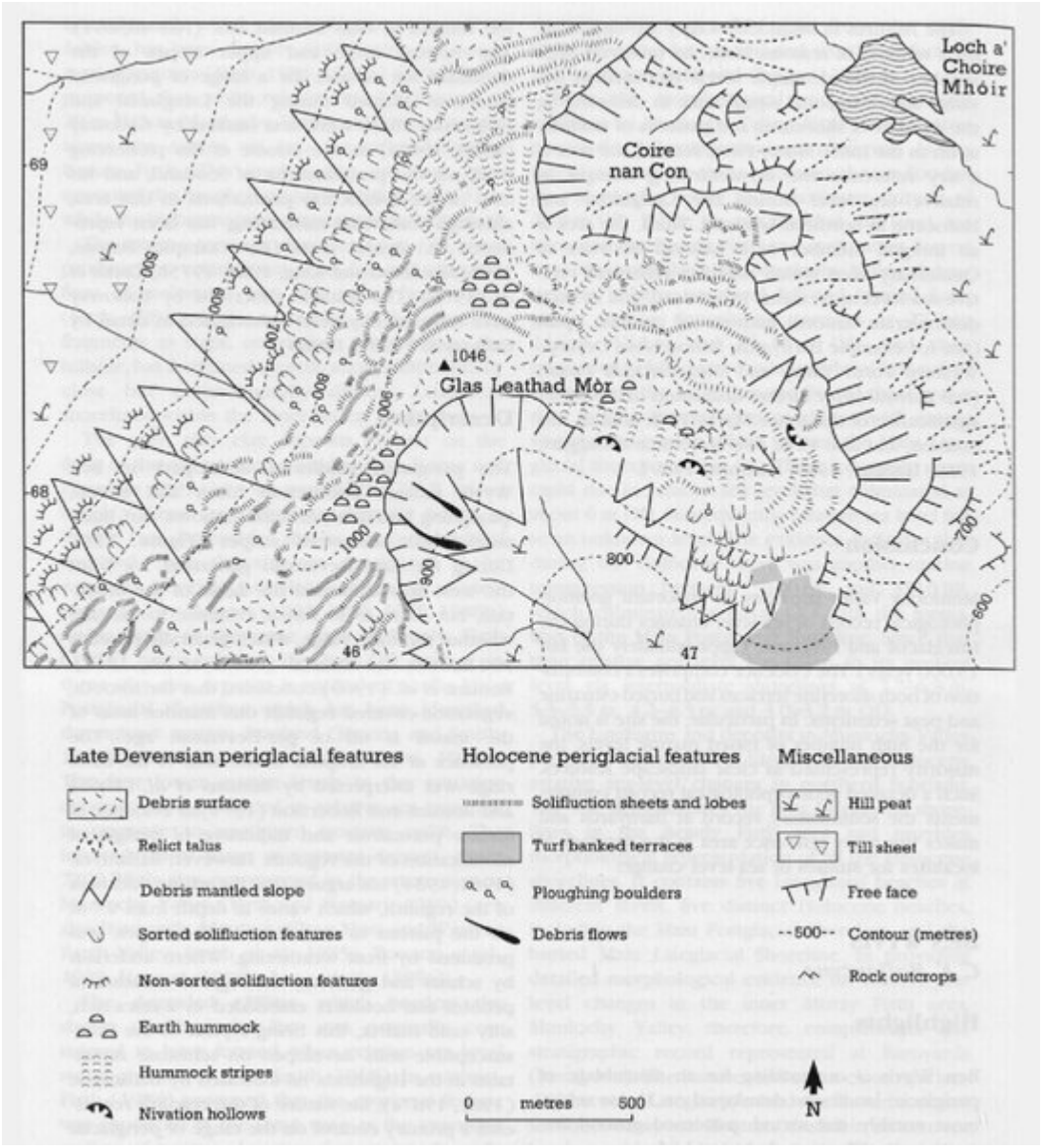

(Figure 7.23) Periglacial landforms and deposits on the summit ridge of Ben Wyvis (from Ballantyne, 1984).

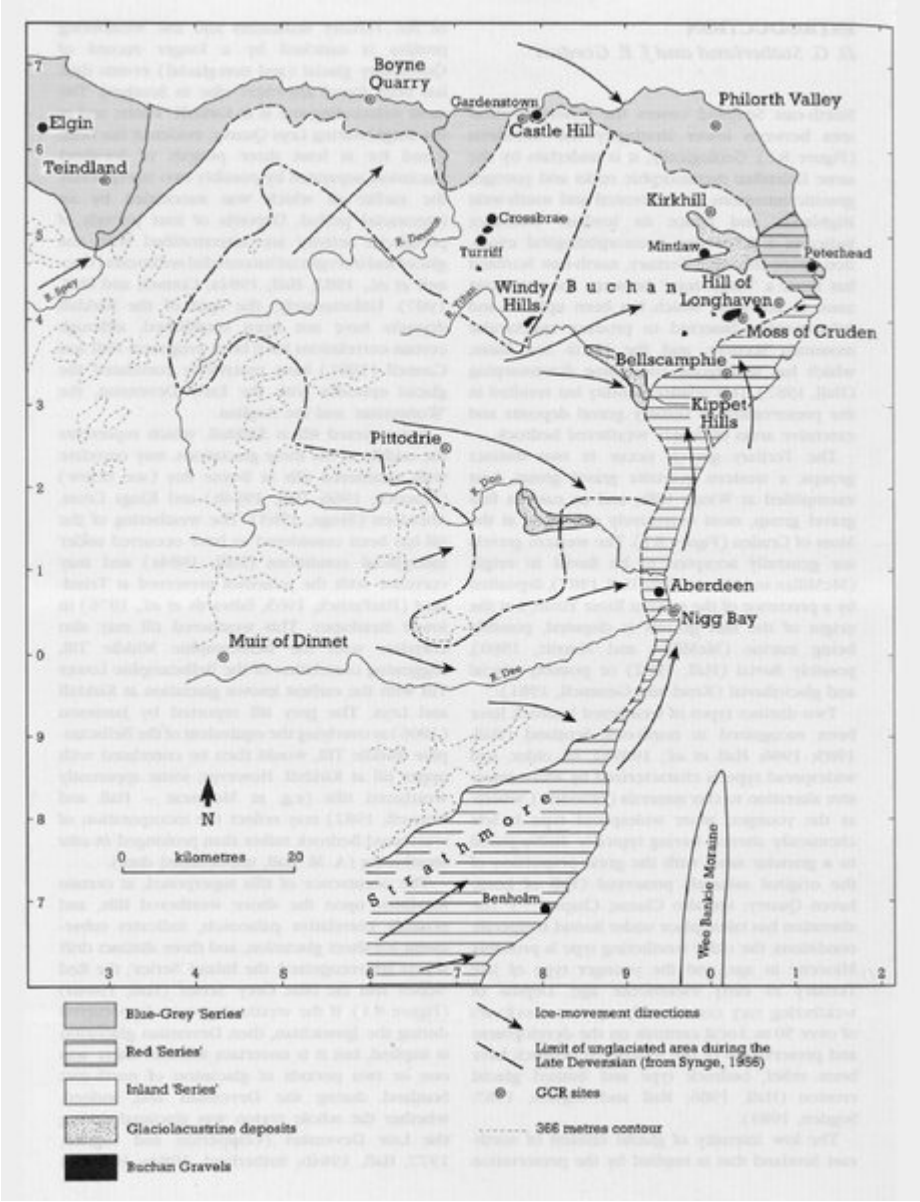

(Figure 8.1) Location map and principal features of the Quaternary geomorphology of north-east Scotland (from Hall and Connell, 1991).

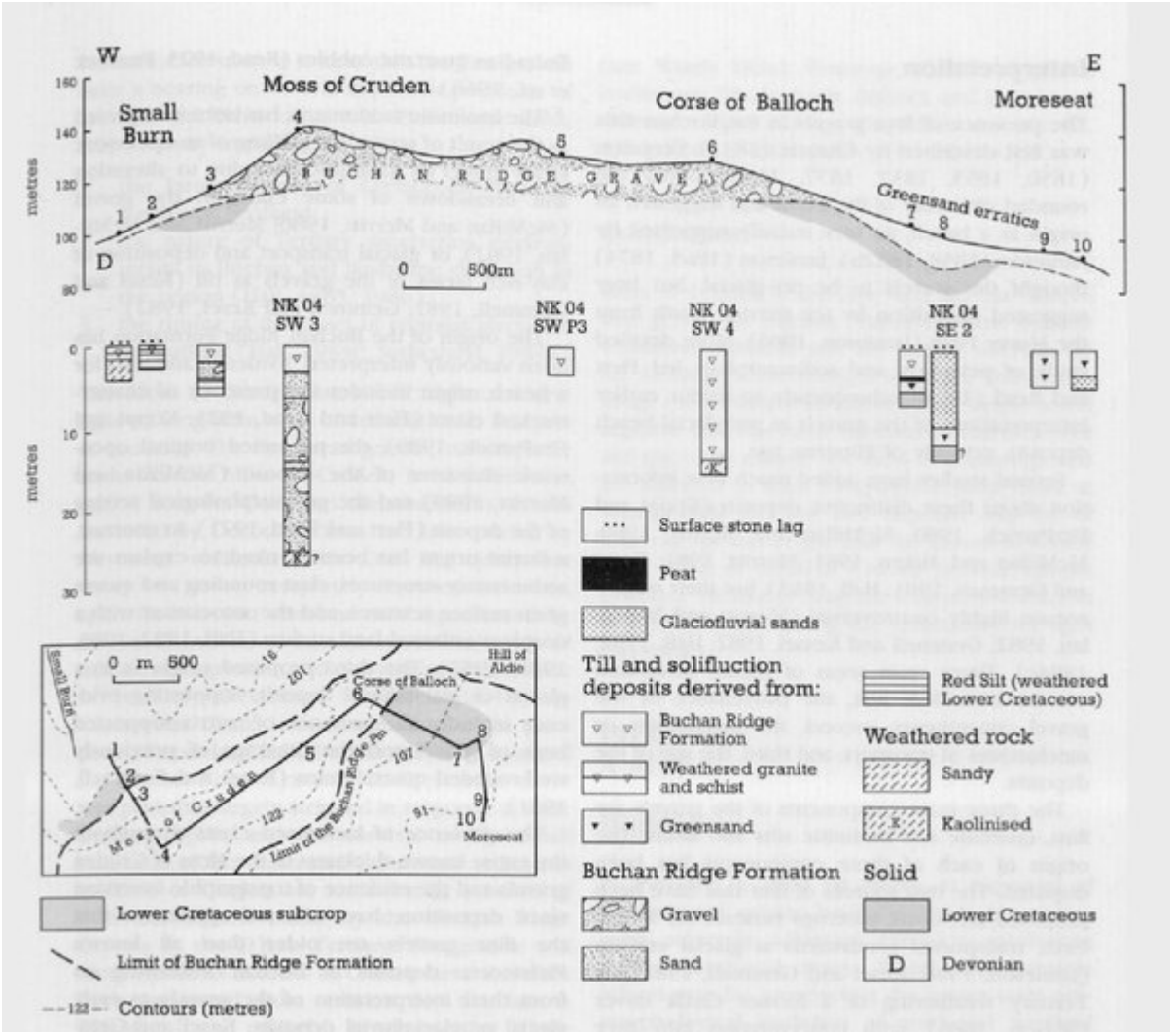

(Figure 8.2) Schematic cross-section through the Moss of Cruden ridge. Borehole and pit data are from McMillan and Aitken (1981), Hall and Connell (1982) and A. M. Hall et al. (unpublished data).

(Figure 8.3) Weathered granite at Pittodrie overlain by soliflucted deposits. (Photo: J E. Gordon.)

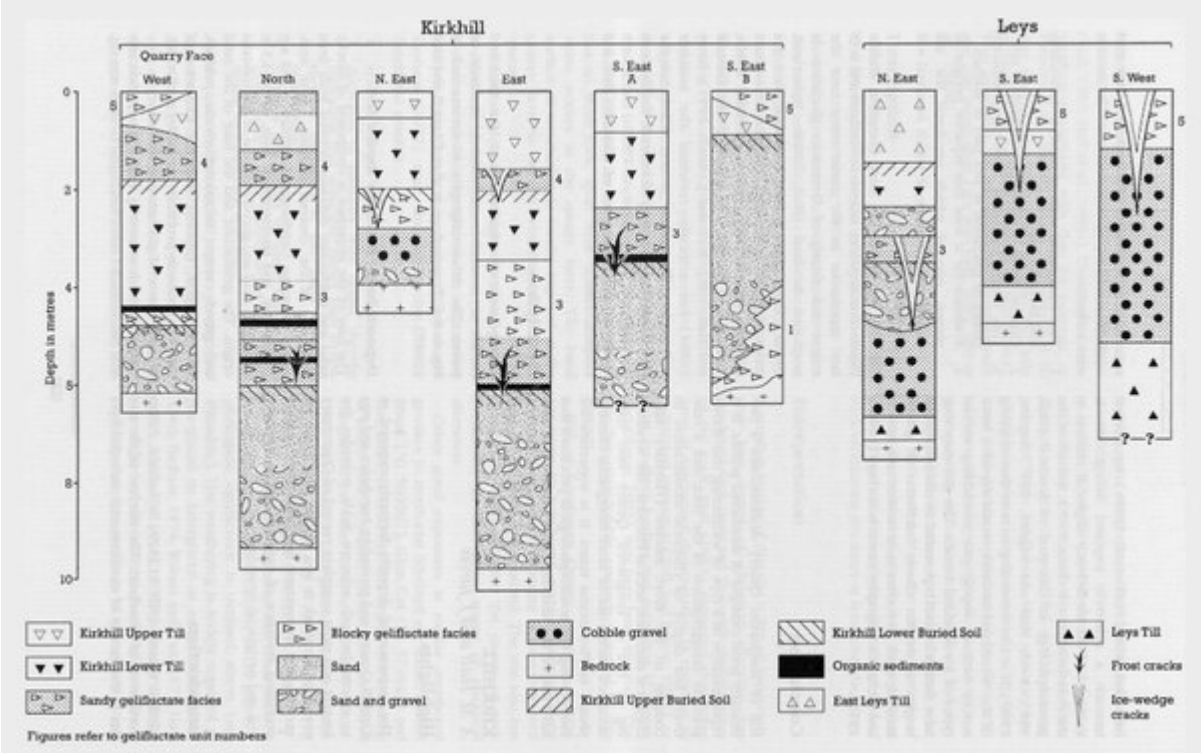

(Figure 8.4) Kirkhill and Leys: lithostratigraphy.

(Figure 8.5) Kirkhill Quarry, south-east face B (1984). Developed in the Kirkhill Lower Sands and Gravels is the Kirkhill Lower Buried Soil, with its striking bleached horizon. The soil is truncated and overlain by laminated organic muds and sands, and then by periglacial slope deposits of Kirkhill Gelifluctate 3. These rubble layers have been partly reworked to form the Kirkhill Upper Till. The section is about 6 m high. (Photo: J. Jarvis.)

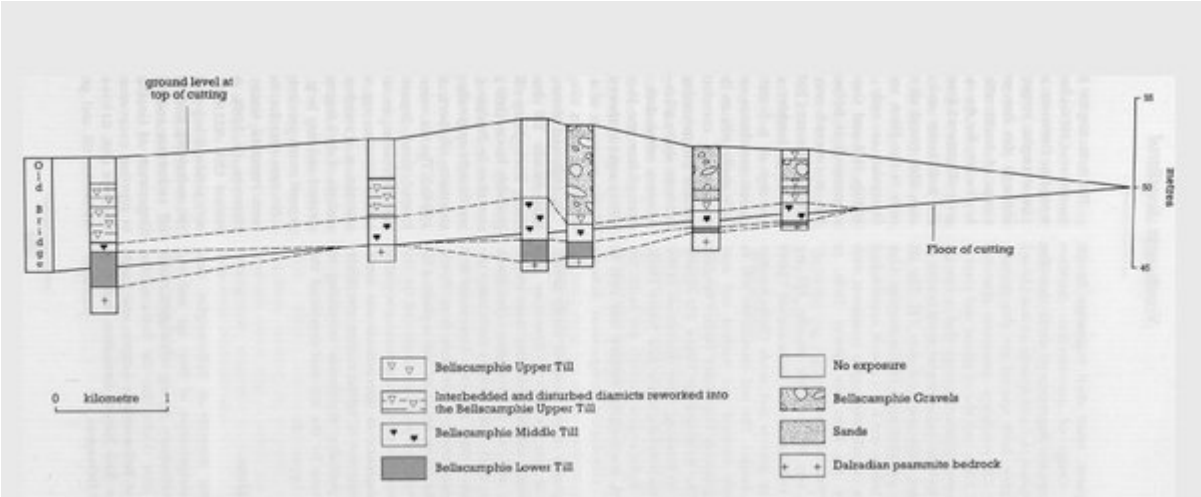

(Figure 8.6) Sediment logs and stratigraphy in the disused railway cutting at Bellscamphie.

(Figure 8.7) Fossil podsol and overlying organic horizon at Teindland. (Photo: D. G. Sutherland.)

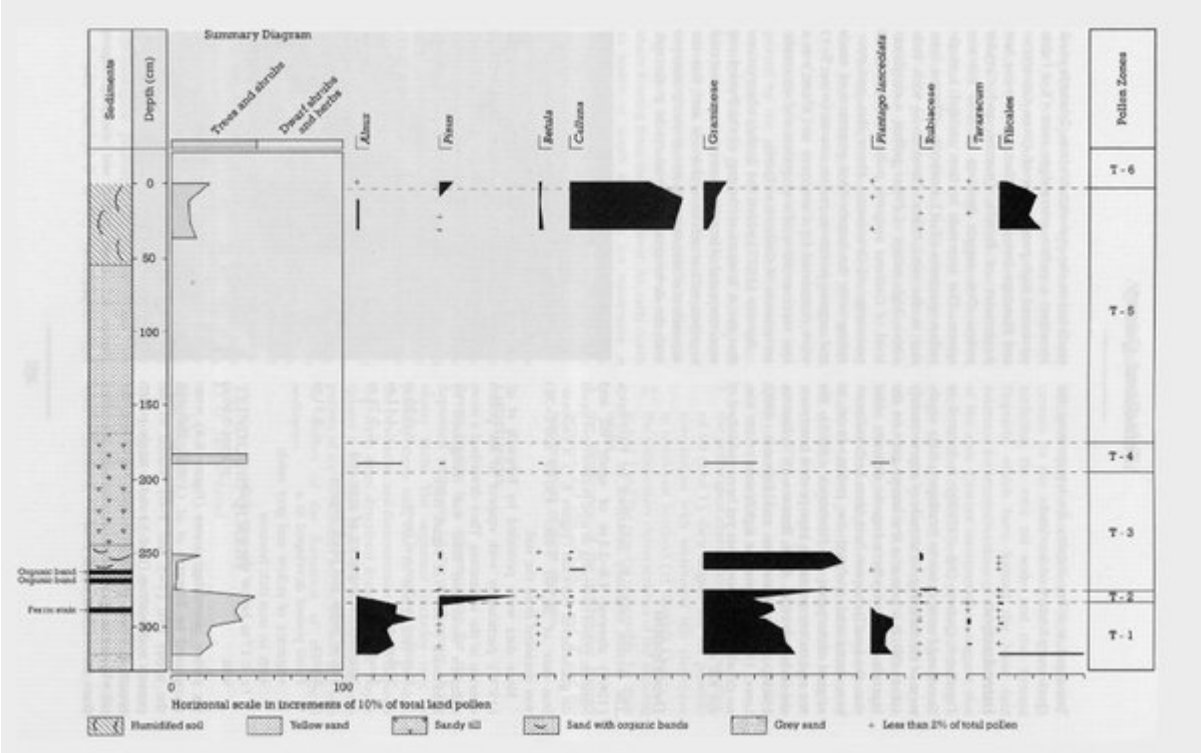

(Figure 8.8) Teindland: relative pollen diagram showing selected taxa as percentage of total land pollen (from Edwards et al., 1976; Lowe, 1984).

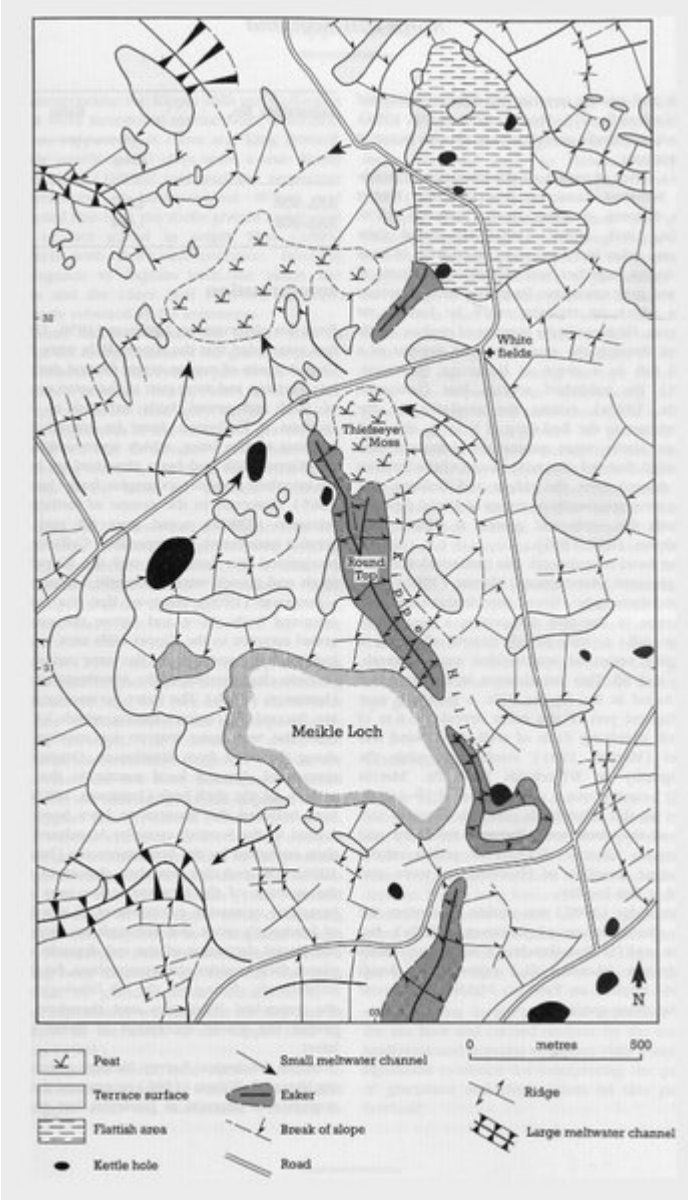

(Figure 8.9) Geomorphology of the Kippet Hills (from Smith, 1984).

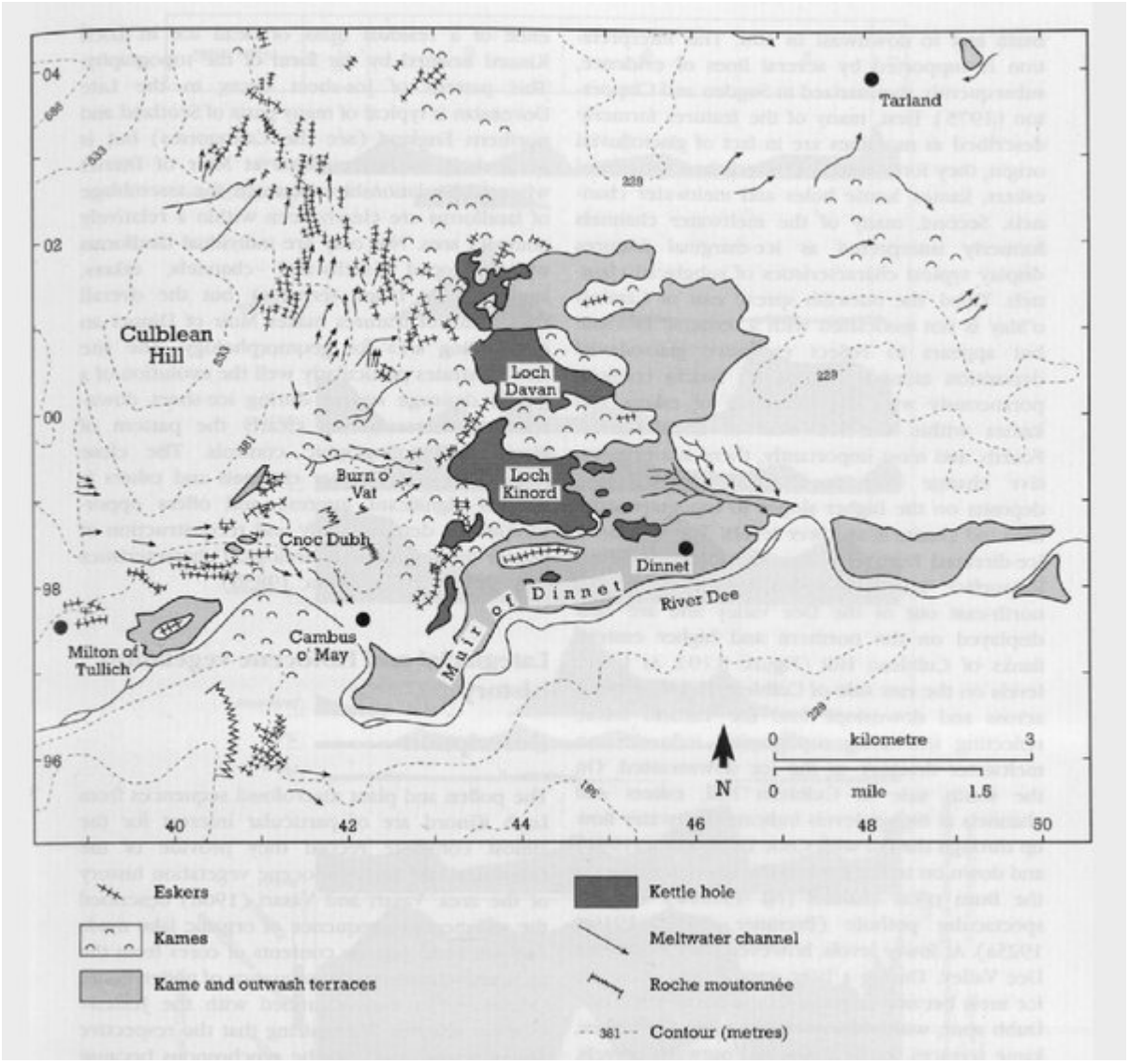

(Figure 8.10) Geomorphology of the Muir of Dinnet (from Clapperton and Sugden, 1972).

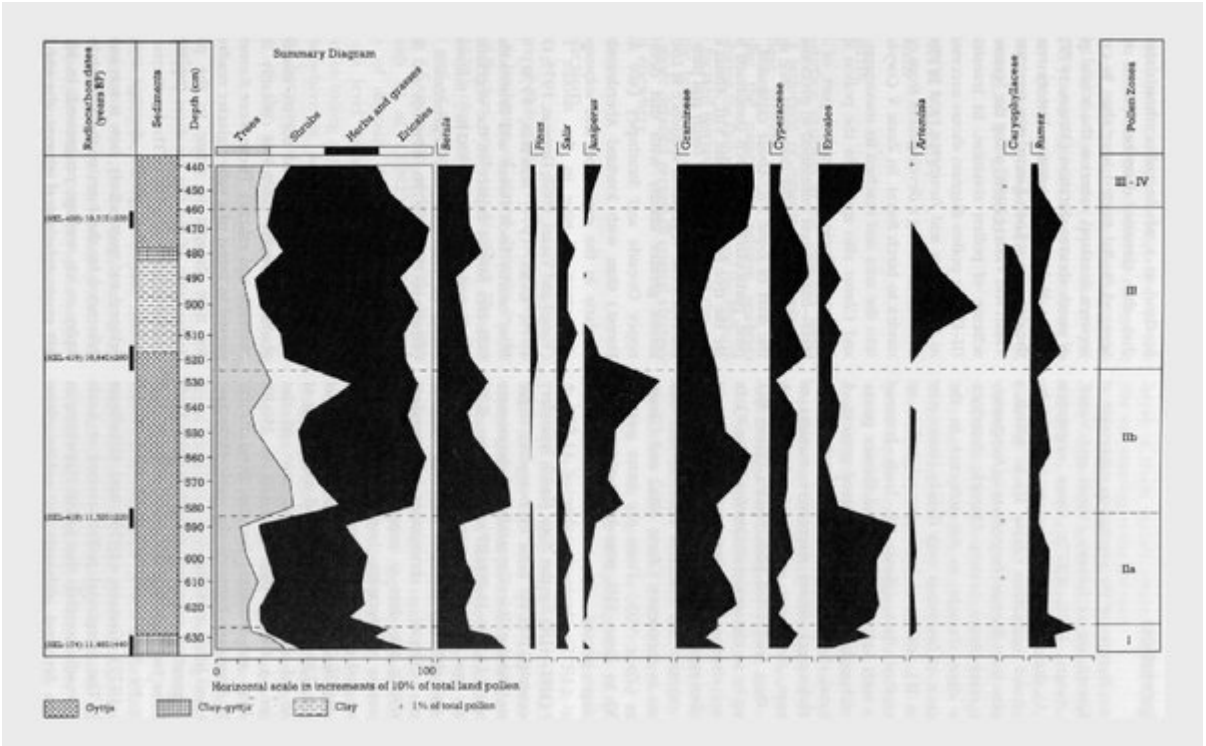

(Figure 8.11) Loch Kinord: relative pollen diagram showing selected taxa as percentages of total land pollen (from Vasari, 1977).

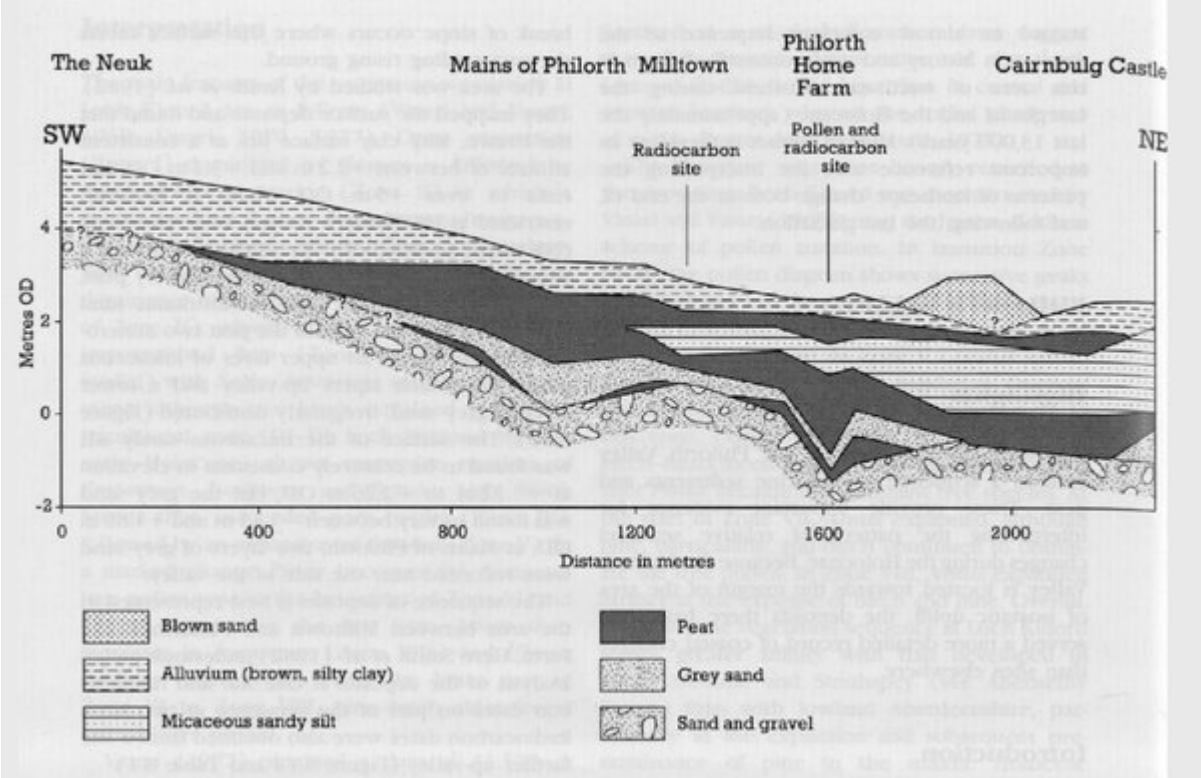

(Figure 8.12) Section along the length of the Lower Philorth Valley showing the sequence of sediments (from Smith et al., 1982).

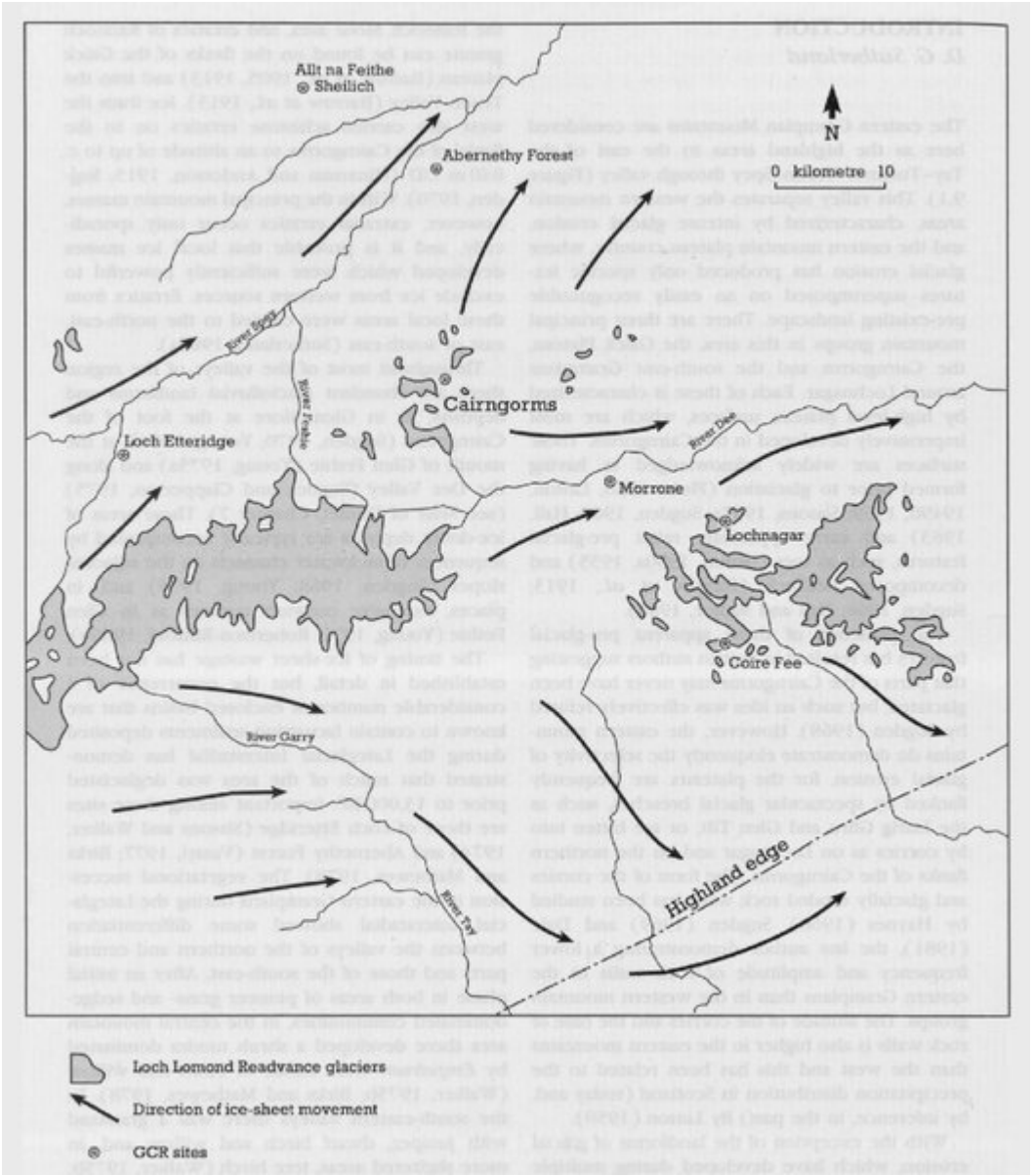

(Figure 9.1) Location map of the eastern Grampian Mountains. The limits of the Loch Lomond Readvance glaciers are from Sissons (1972a, 1974b, 1979f) and Sissons and Grant (1972).

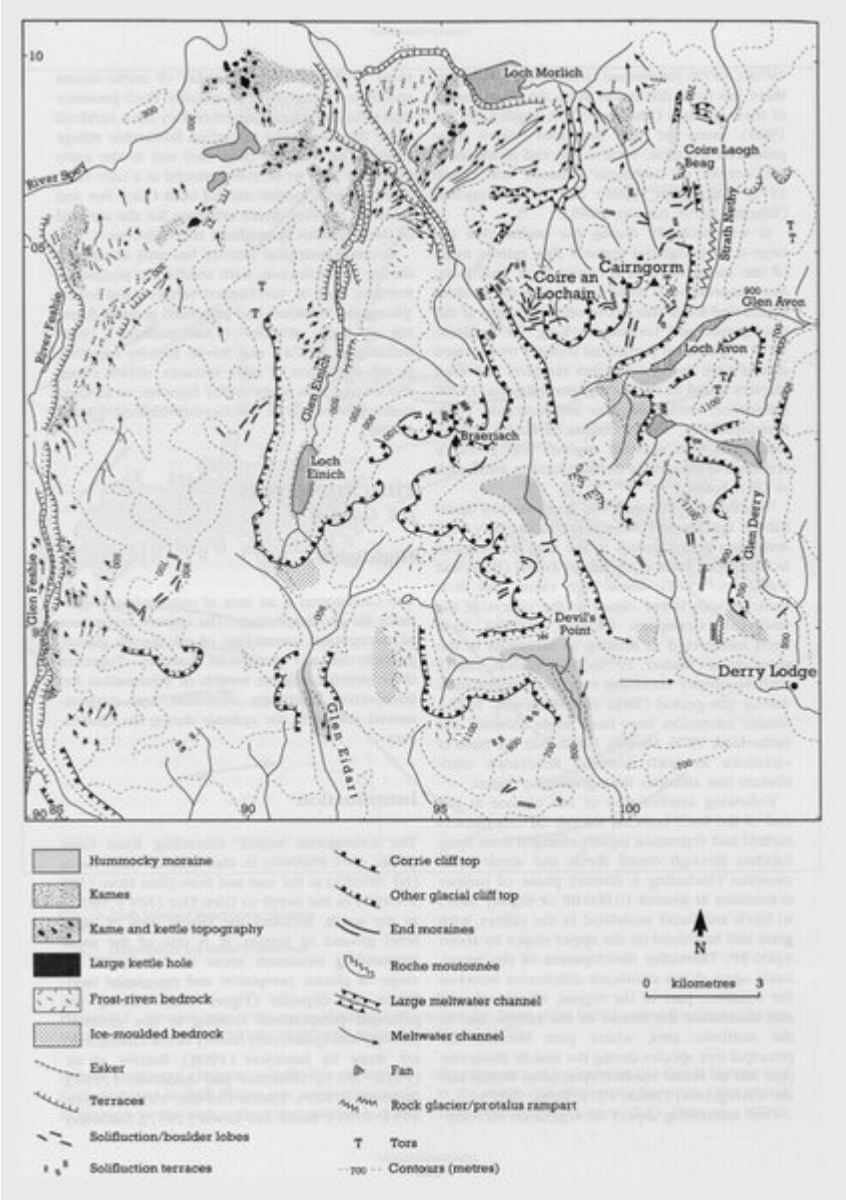

(Figure 9.2) Principal geomorphological features of the Cairngorm Mountains (sources include Sugden, 1968, 1970; Young, 1974, 1975a; Sissons, 1979f; J E. Gordon, unpublished data).

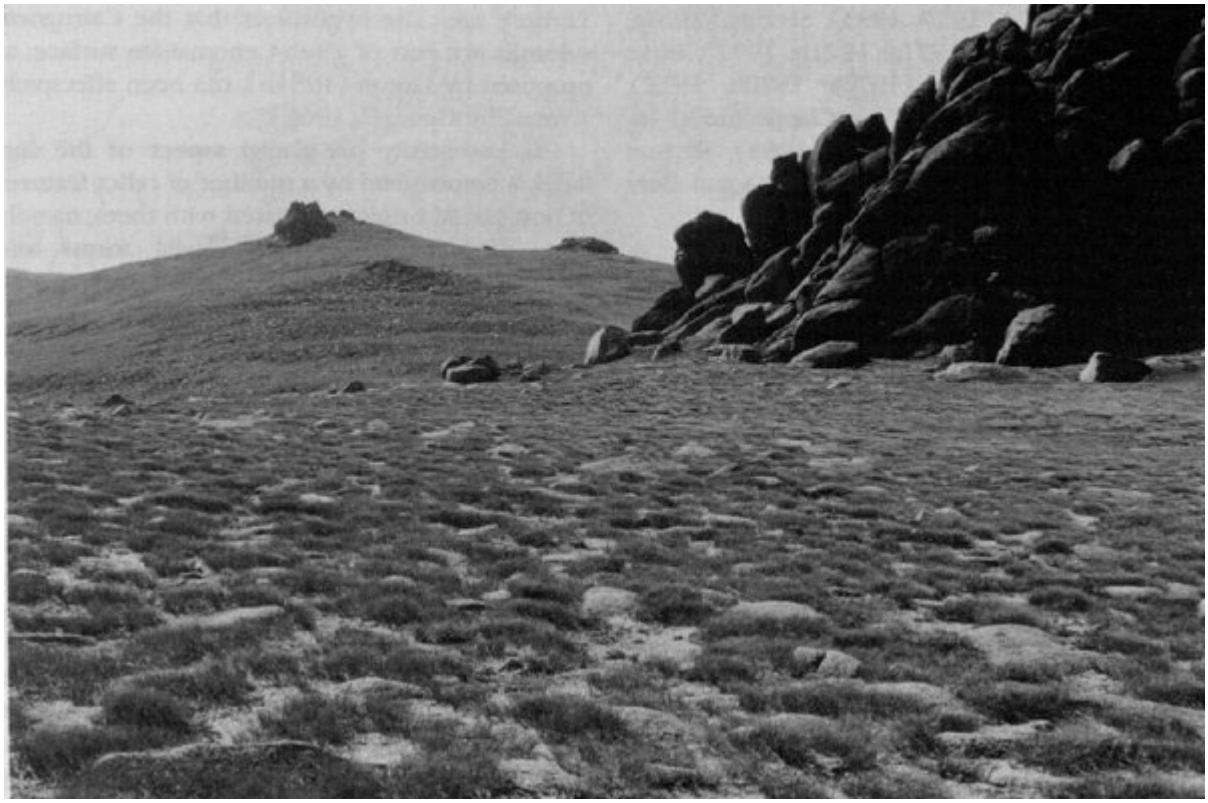

(Figure 9.3) Summit plateau of Ben Avon in the Cairngorms showing well-developed tors which appear to have survived glaciation. The adjacent slopes have been affected by periglacial processes and the development of solifluction lobes. (Photo: J E. Gordon.)

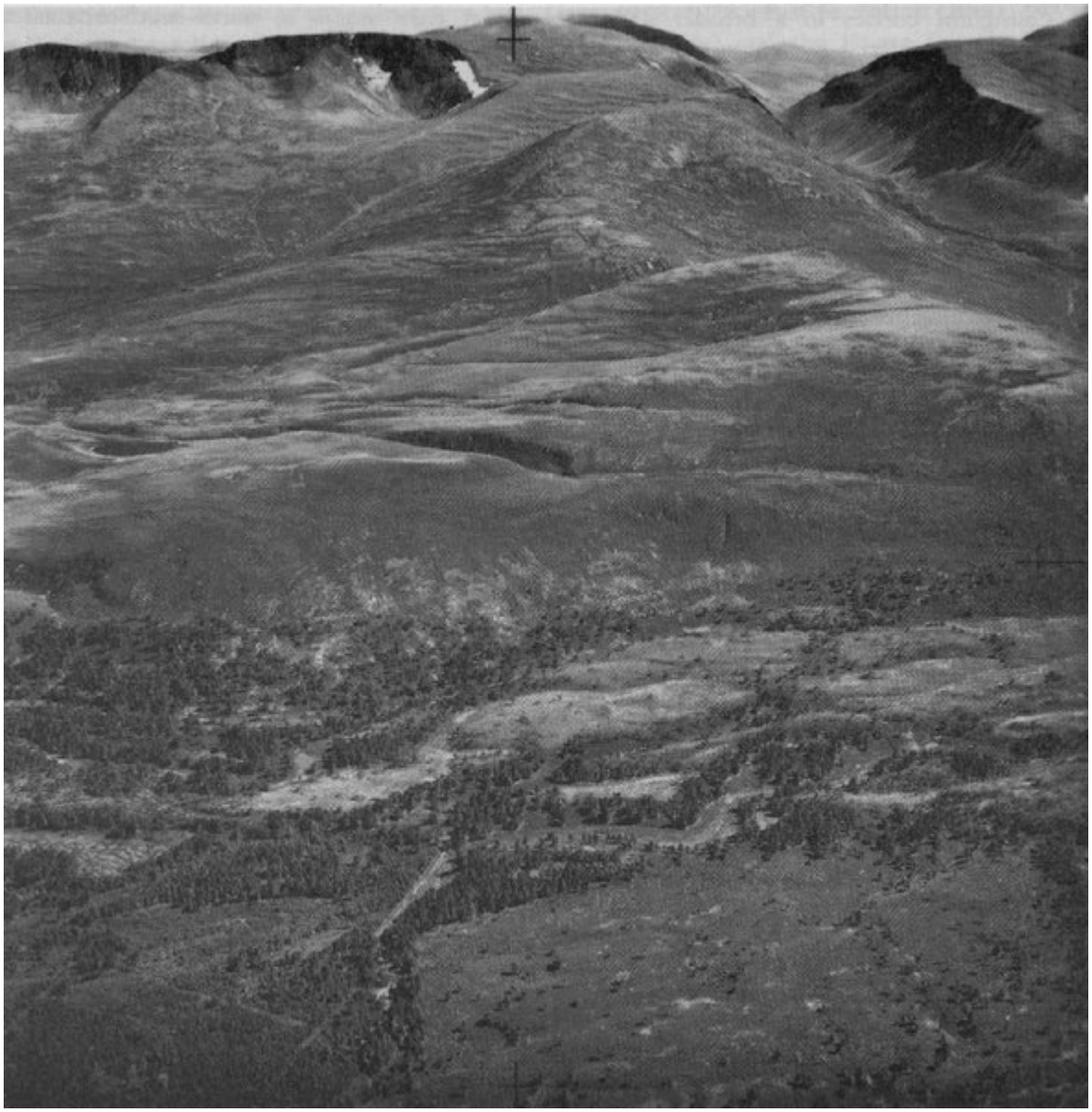

(Figure 9.4) Glen More and the northern flank of the Cairngorms. The assemblage of landforms in this area includes the Cairngorm plateau and adjacent slopes extensively modified by solifluction lobes and terraces (Lurchers Gully — top centre), corries cut into the upper slopes of the massif, the striking glacial breach of the Lairig Ghru (top right), a system of ice-directed meltwater channels (including open-walled features — centre) and partly wooded glaciofluvial deposits in the valley bottom. (© British Crown copyright 1992/MOD reproduced with the permission of the Controller of Her Britannic Majesty's Stationery Office.)

(Figure 9.5) Loch Lomond Readvance boulder moraine in Coire an t-Sneachda in the Cairngorms. The outer part of the moraine comprises several clearly defined ridges of boulders. (Photo: J E. Gordon.)

(Figure 9.6) Loch Lomond Readvance 'hummocky moraine' on the east flank of Glen Eidart in the Cairngorms. The deposits have a clear upper limit on the valley side and show well-defined lineations, which may mark successive ice-front positions of an actively retreating glacier. (Photo: J E. Gordon.)

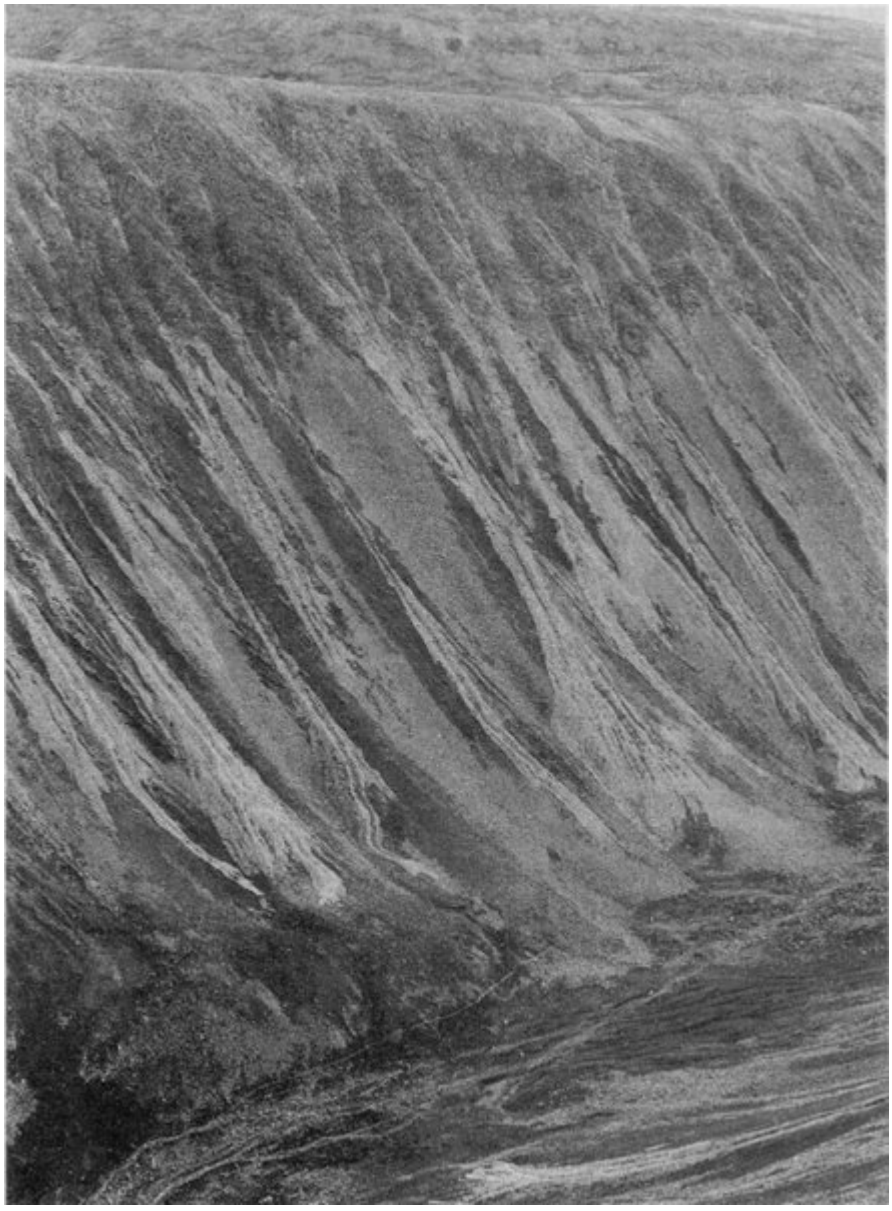

(Figure 9.7) Active debris flows on the slopes above the Lairig Ghru. (Photo: J E. Gordon.)

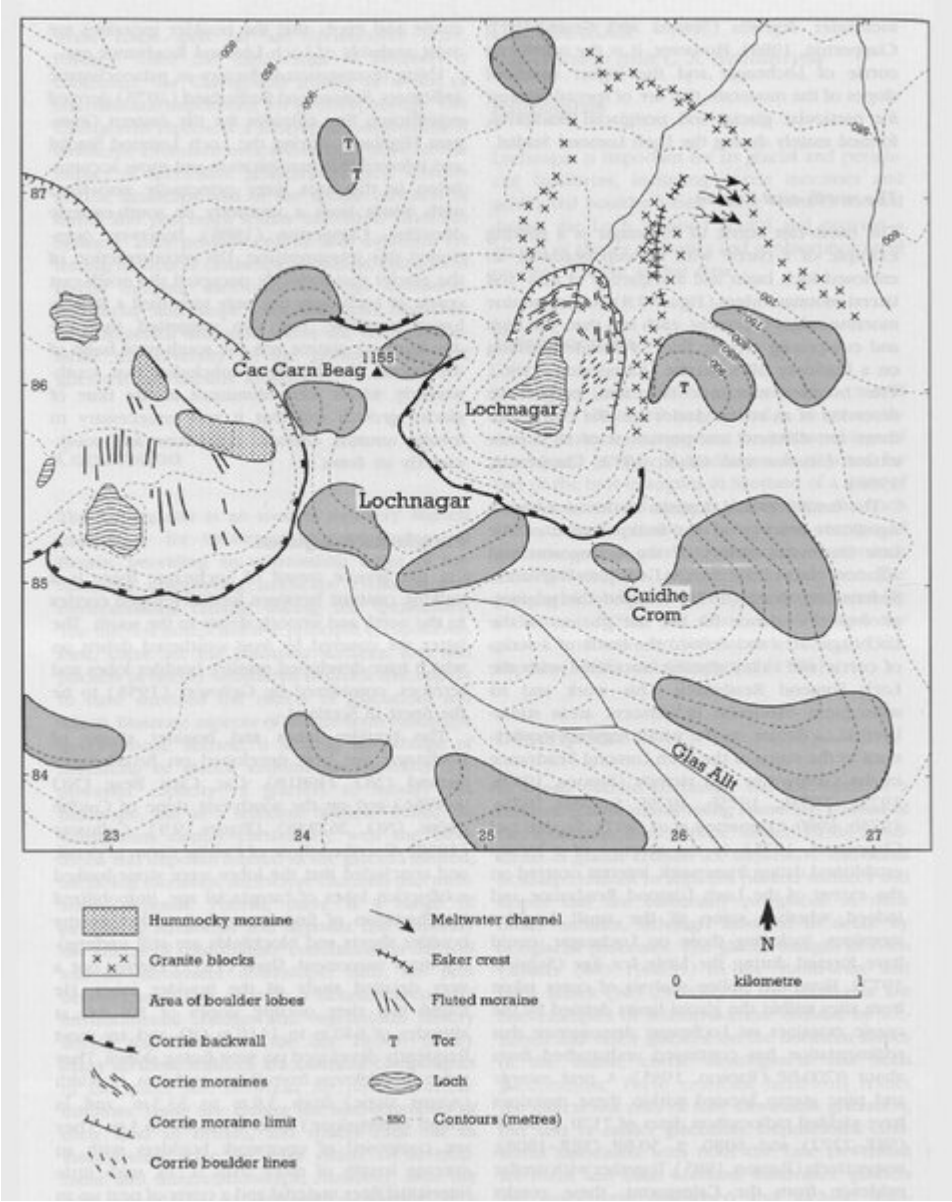

(Figure 9.8) Geomorphology of the Lochnagar area (from Shaw, 1977; Clapperton, 1986).

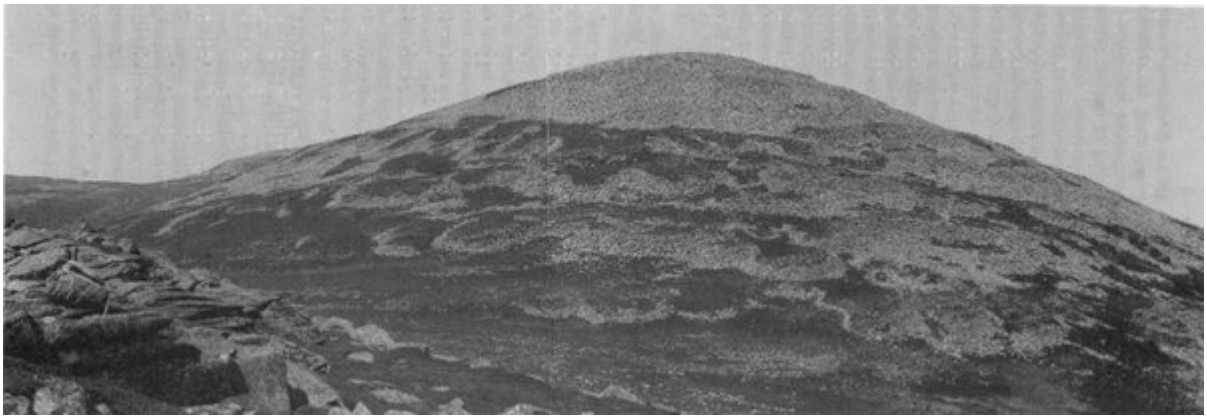

(Figure 9.9) Summit blockfield, blockslopes and boulder lobes on the south-east flank of Cuidhe Cròm, Lochnagar. (Photo: J E. Gordon.)

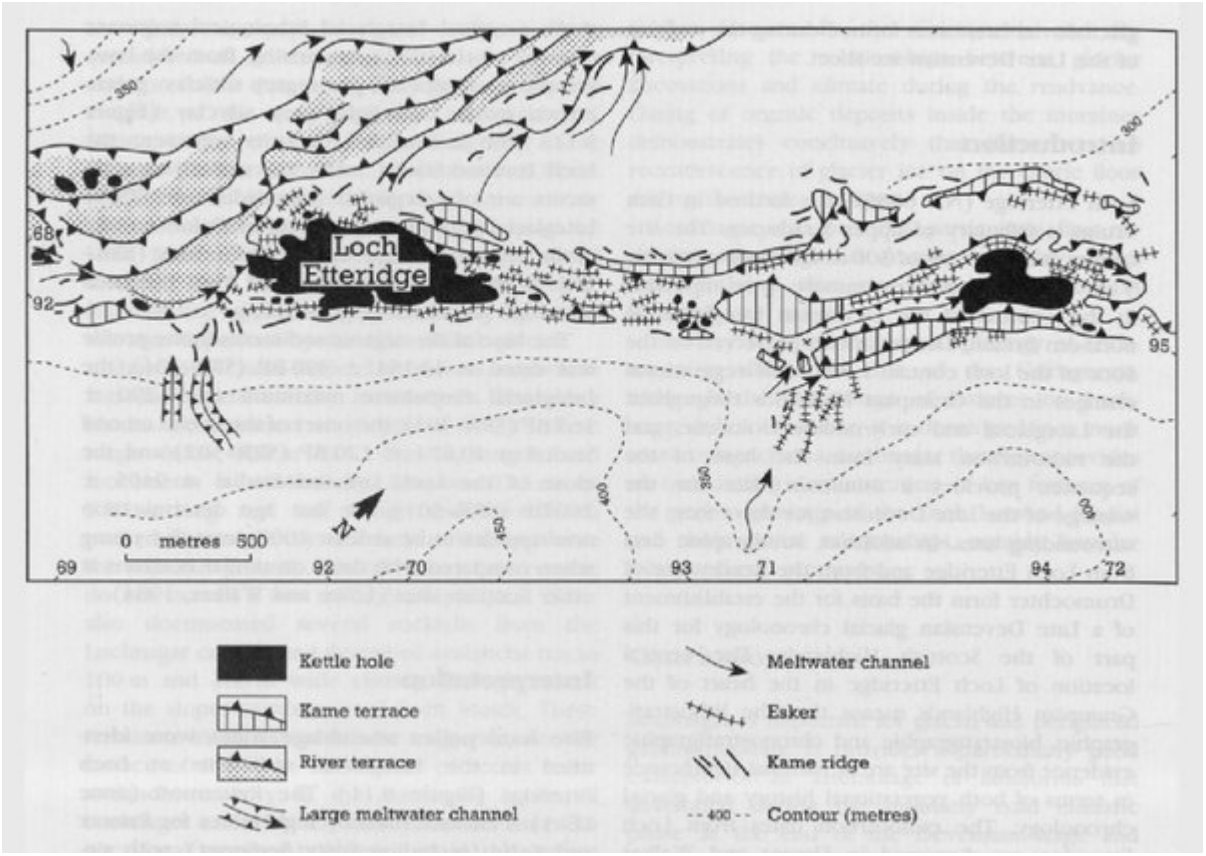

(Figure 9.10) Geomorphology of the Loch Etteridge area (from Young, 1978).

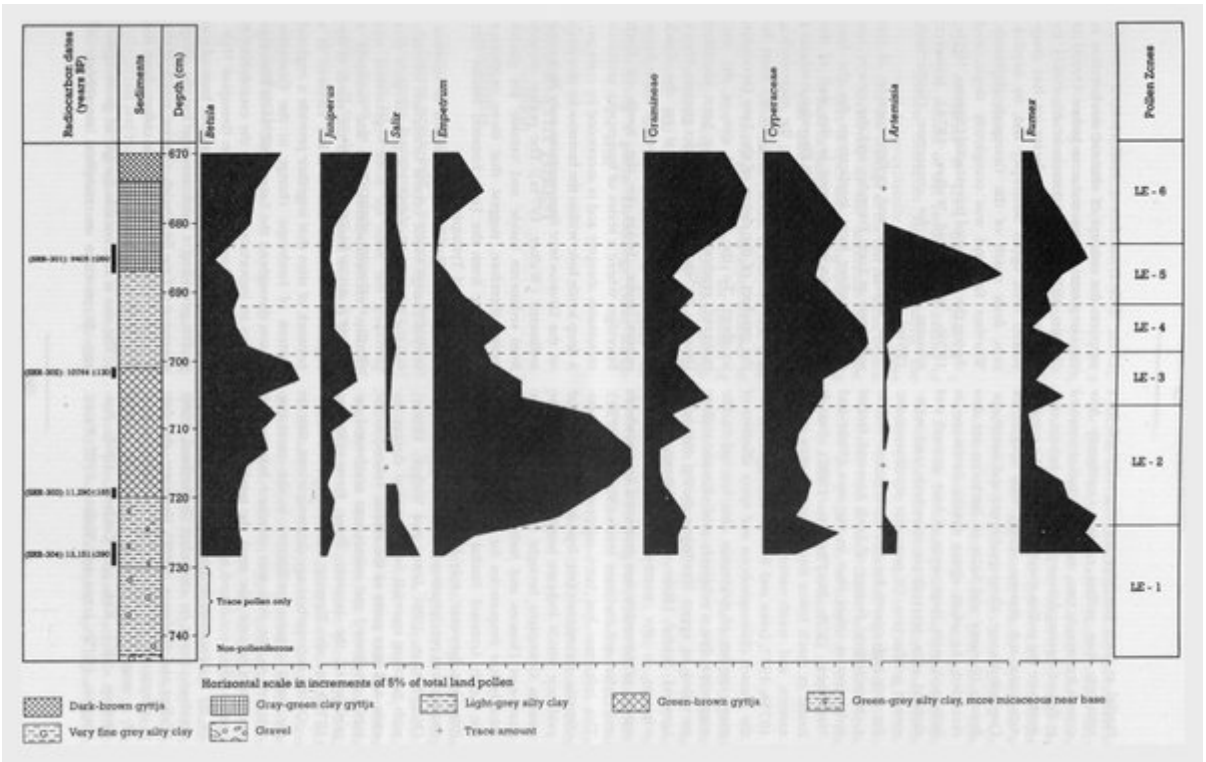

(Figure 9.11) Loch Etteridge: relative pollen diagram showing selected taxa as percentages of total land pollen. The samples for radiocarbon dating were taken from comparable lithostratigraphic horizons in an adjacent core.

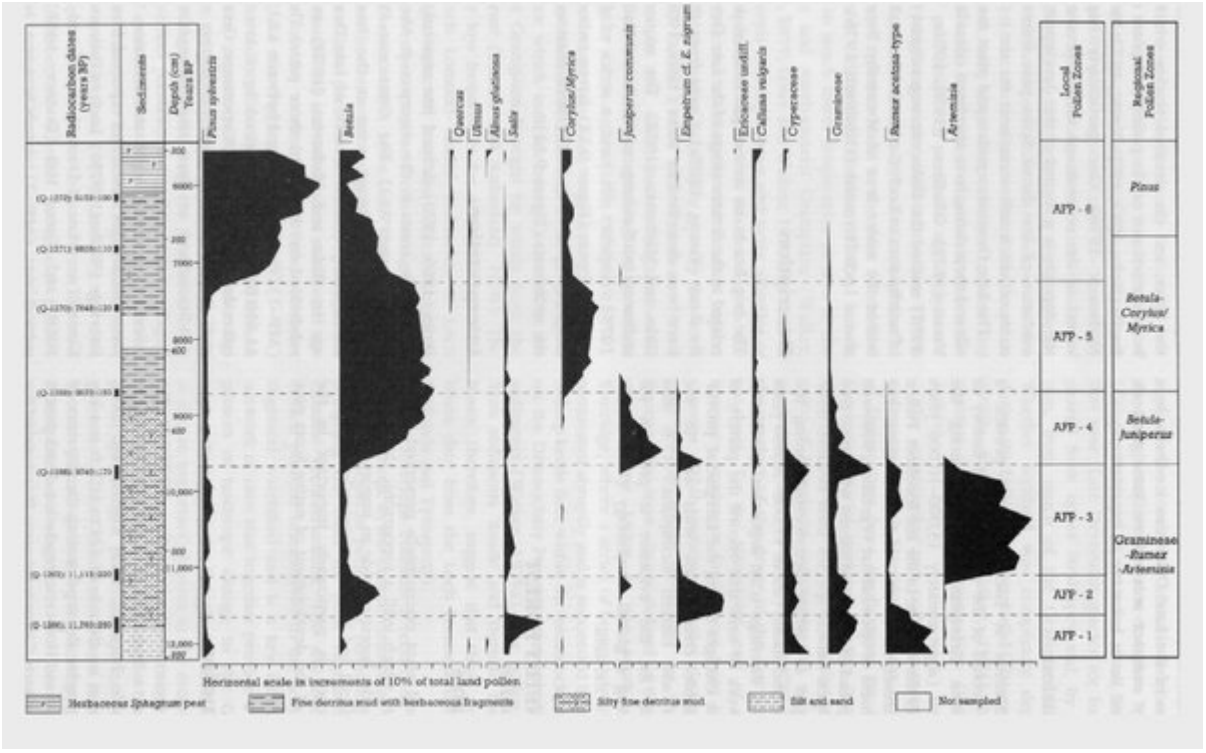

(Figure 9.12) Abernethy Forest: relative pollen diagram showing selected taxa as percentages of total land pollen (from Birks and Mathewes, 1978). Regional pollen assemblage zones are from Birks (1970). Note that the data are plotted against a radiocarbon time-scale.

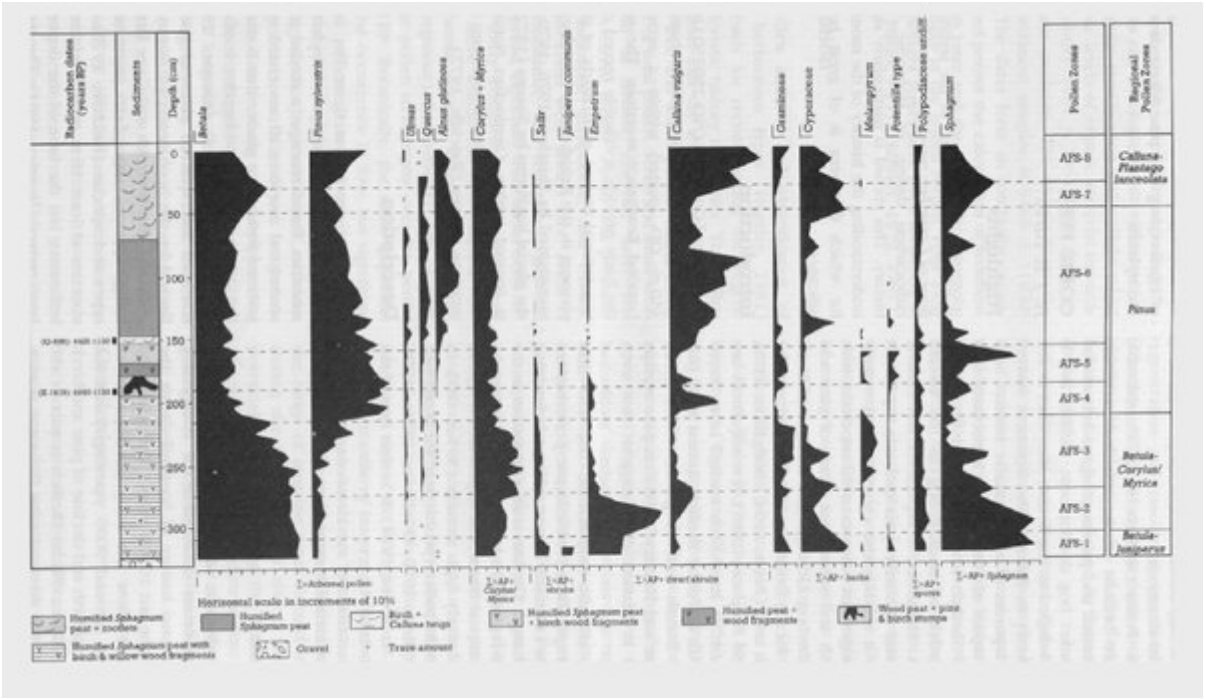

(Figure 9.13) Allt na Feithe Sheilich: relative pollen diagram showing selected taxa as percentages of the pollen sums indicated (from Birks, 1975).

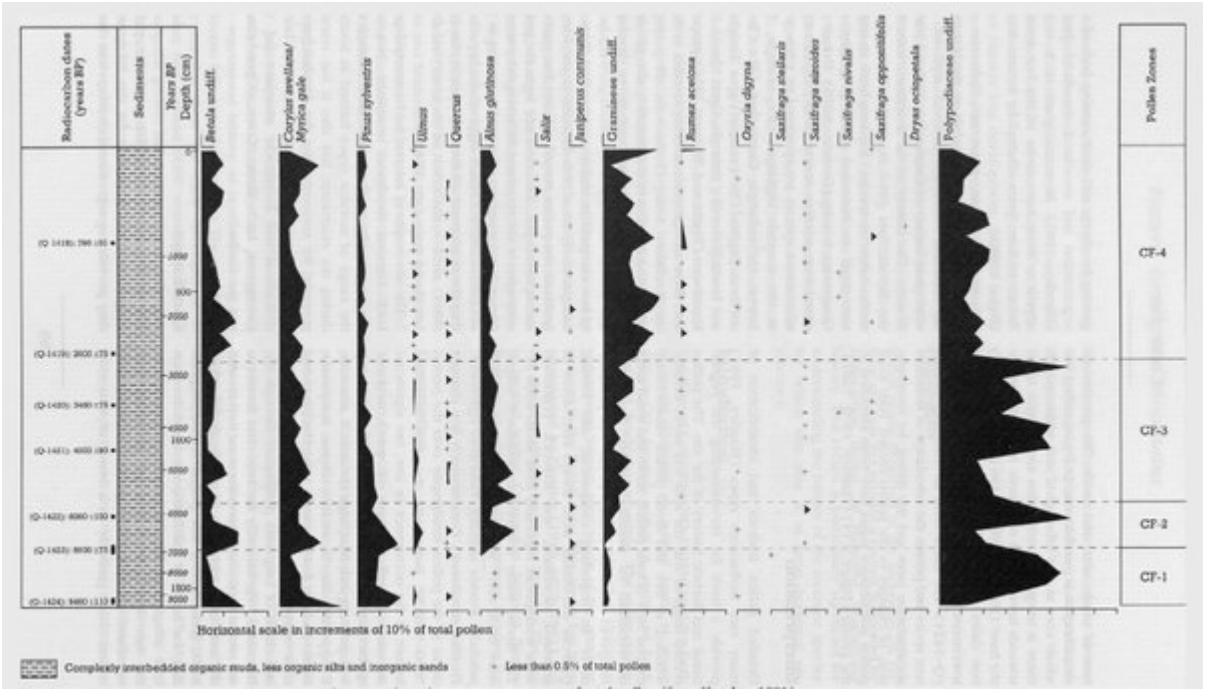

(Figure 9.14) Coire Fee: relastive pollen diagram showing selected taxa as a percentage of total pollen (from Huntley, 1981)

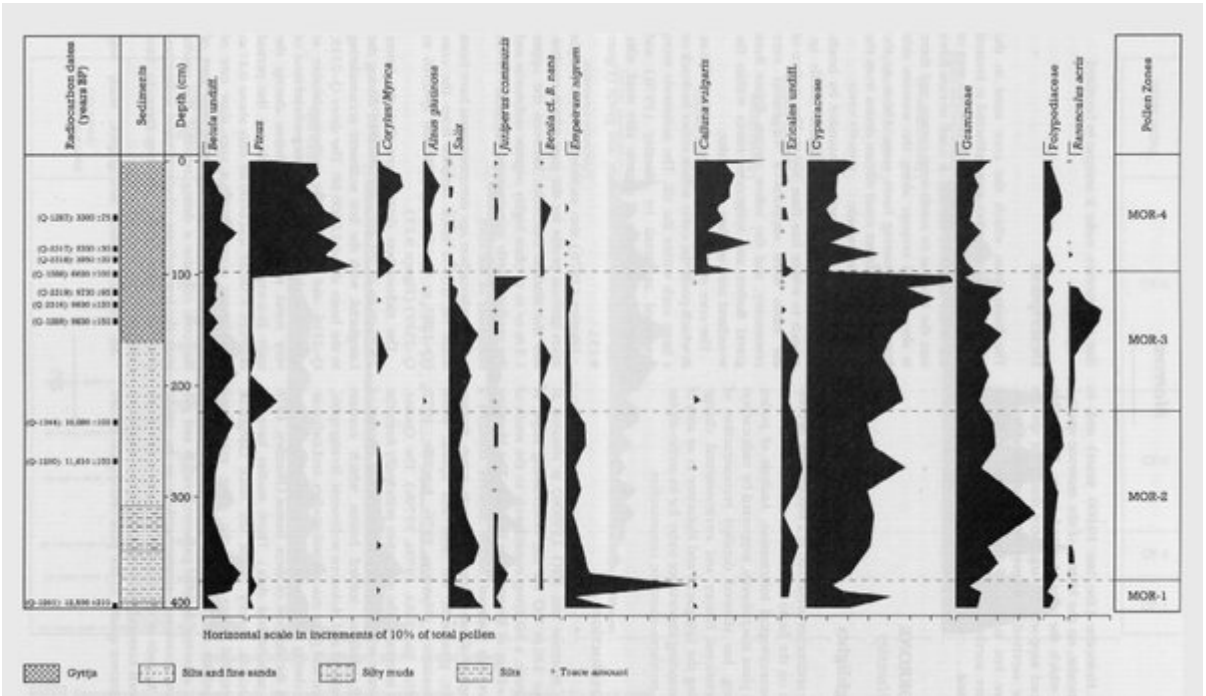

(Figure 9.15) Morrone: relative pollen diagram showing selected taxa as percentages of total pollen (from Huntley, 1976).

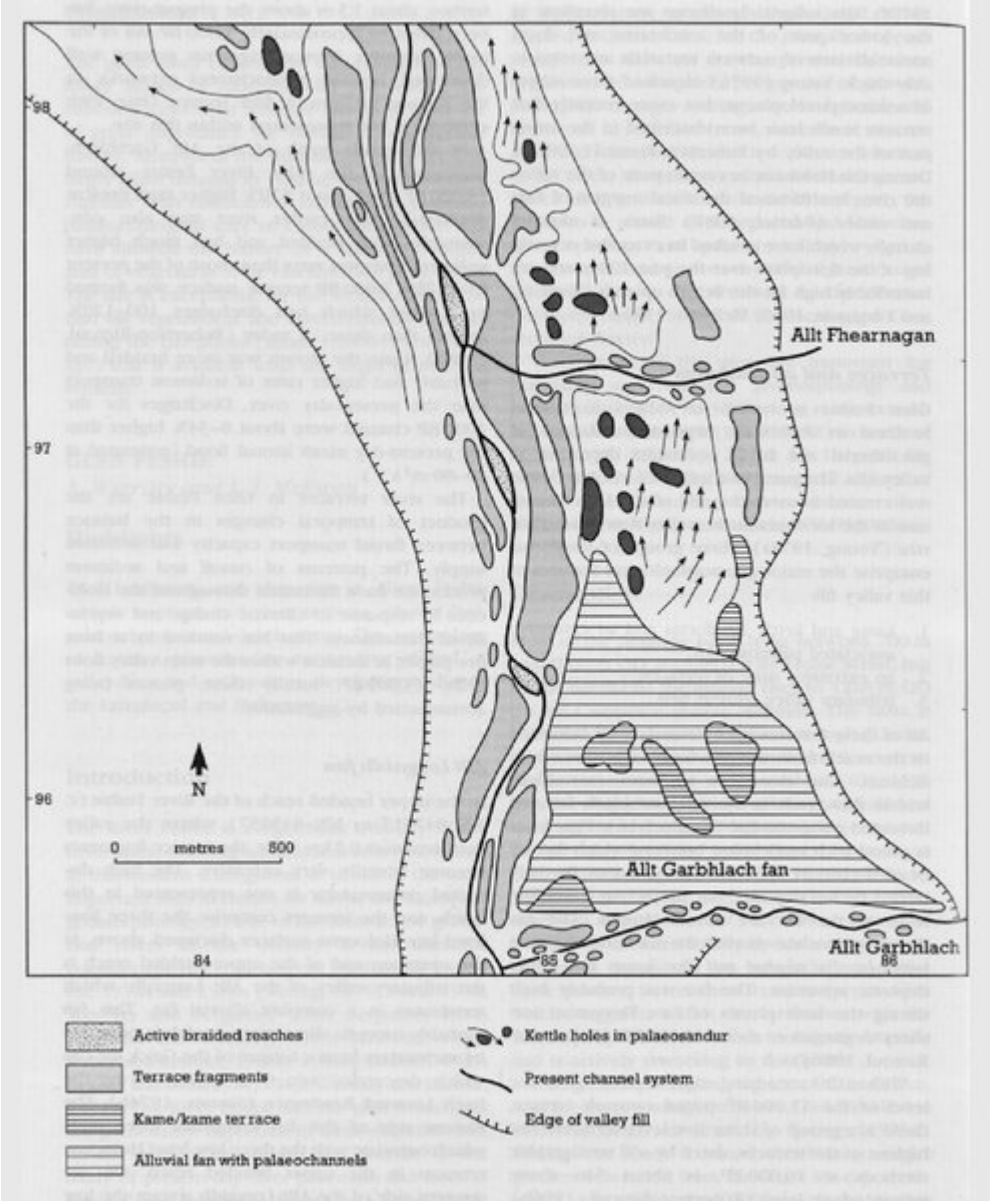

(Figure 9.16) Geomorphology of the Allt Garbhlach–Allt Fhearnagan area of Glen Feshie (from Robertson–Rintoul, 1986a; Werritty and Brazier, 1991).

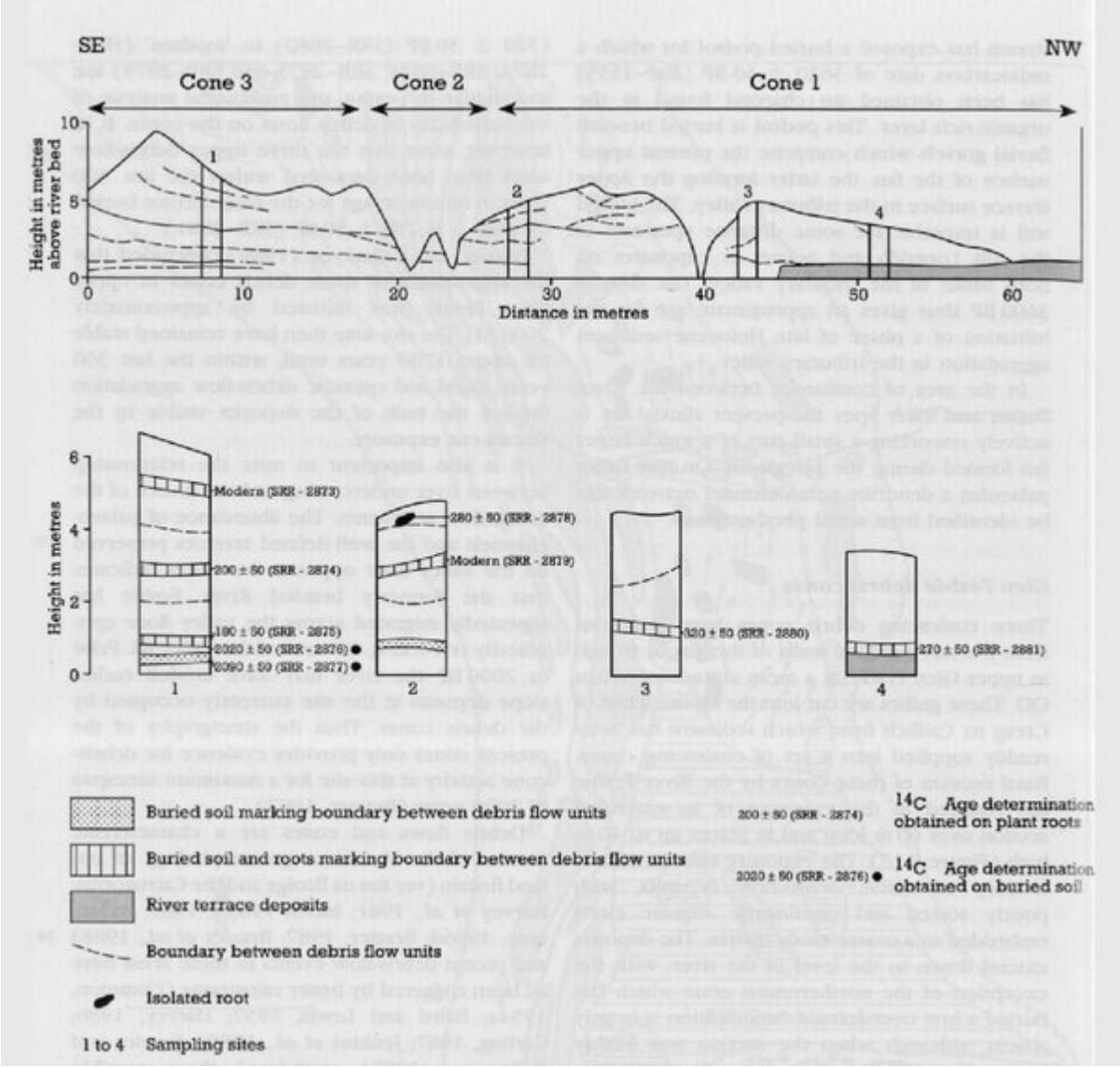

(Figure 9.17) Top: surveyed section across the base of the Glen Feshie debris cones showing boundaries between individual debris-flow units. Bottom: detailed sections at sampling sites 1–4 (from Brazier and Ballantyne, 1989).

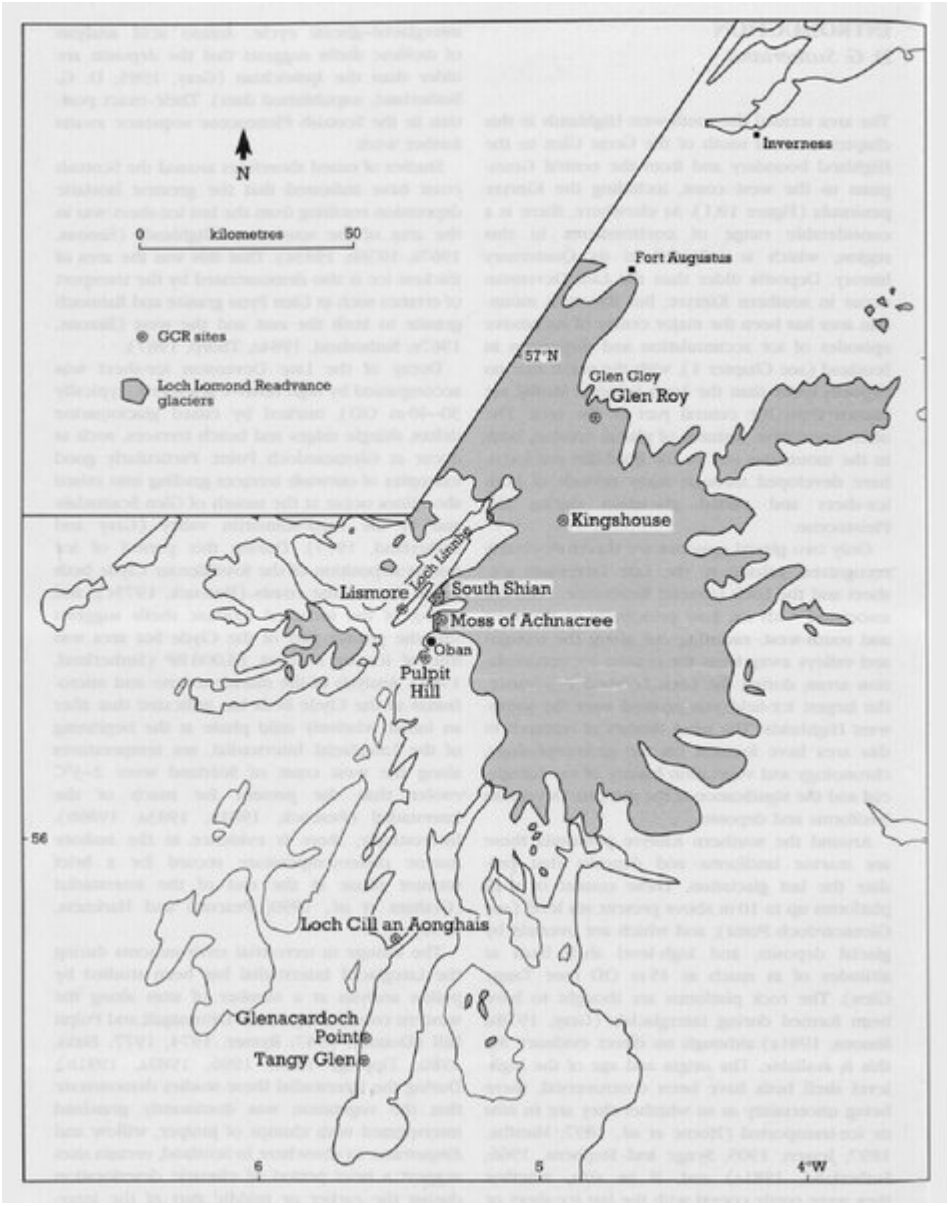

(Figure 10.1) Location map of the south-west Highlands.

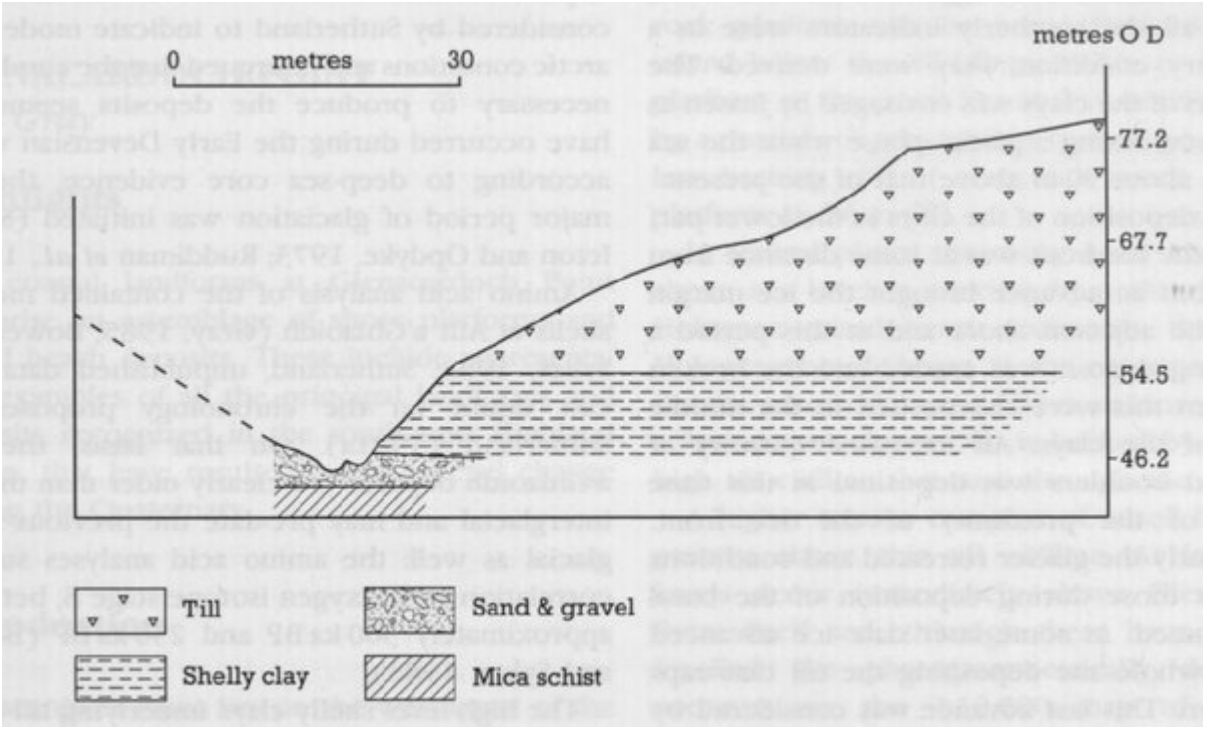

(Figure 10.2) Tangy Glen: lithological succession at Cleongart (from Horne et al., 1897).

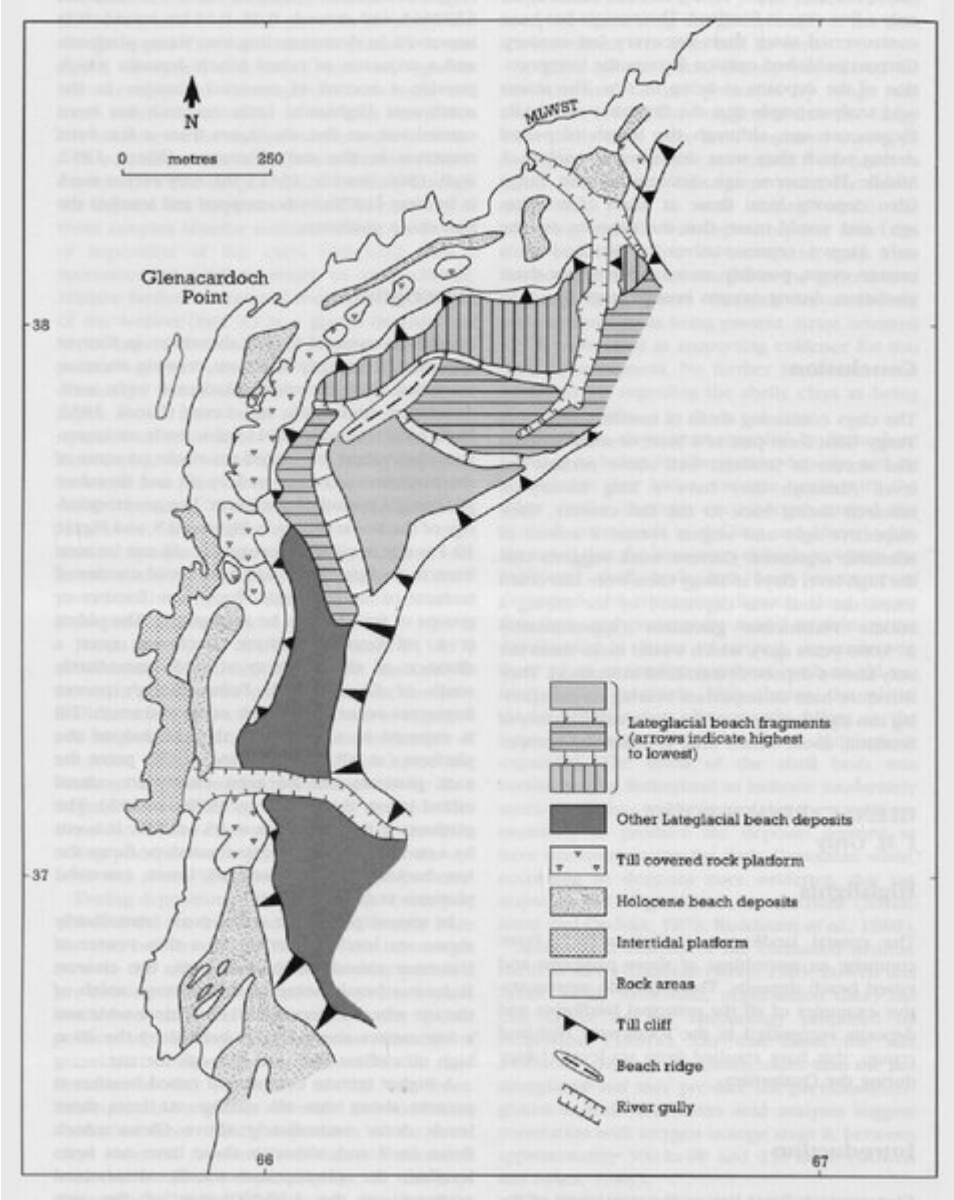

(Figure 10.3) Geomorphology of the Glenacardoch Point area.

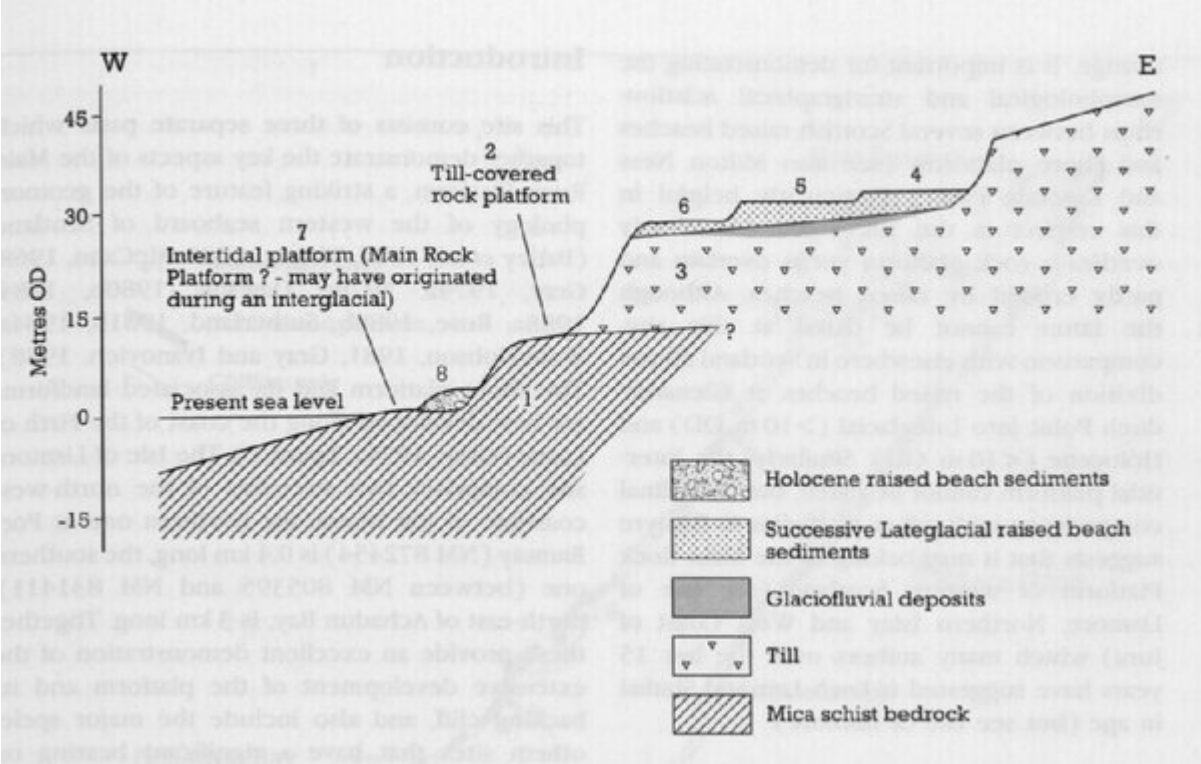

(Figure 10.4) Coastal profile at Glenacardoch Point showing the relationships between the morphology and succession of the features and their probable sequence of formation (1–8).

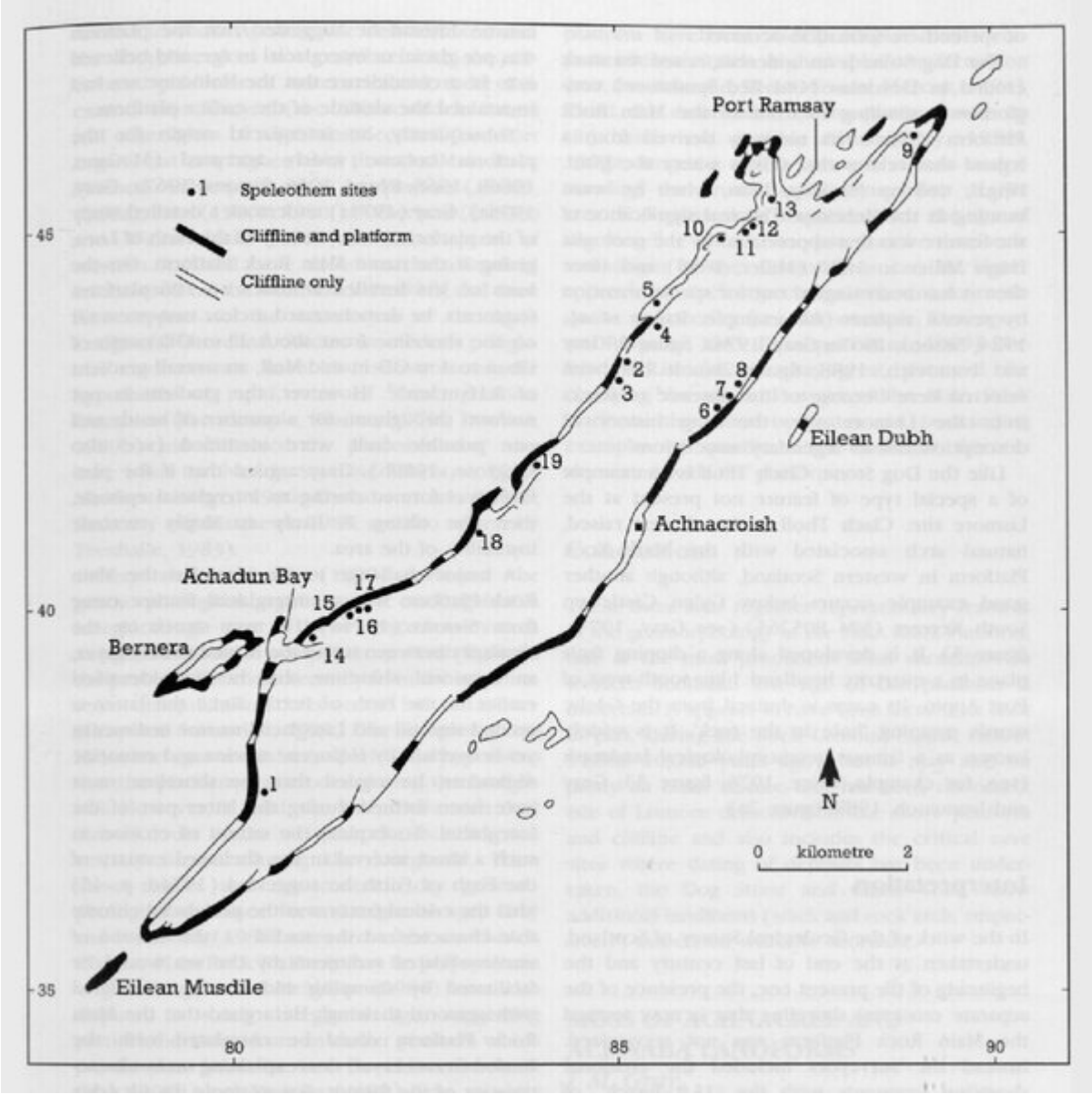

(Figure 10.5) Distribution of the Main Rock Platform on the Isle of Lismore and localities mentioned in the text (from Gray and Ivanovich, 1988).

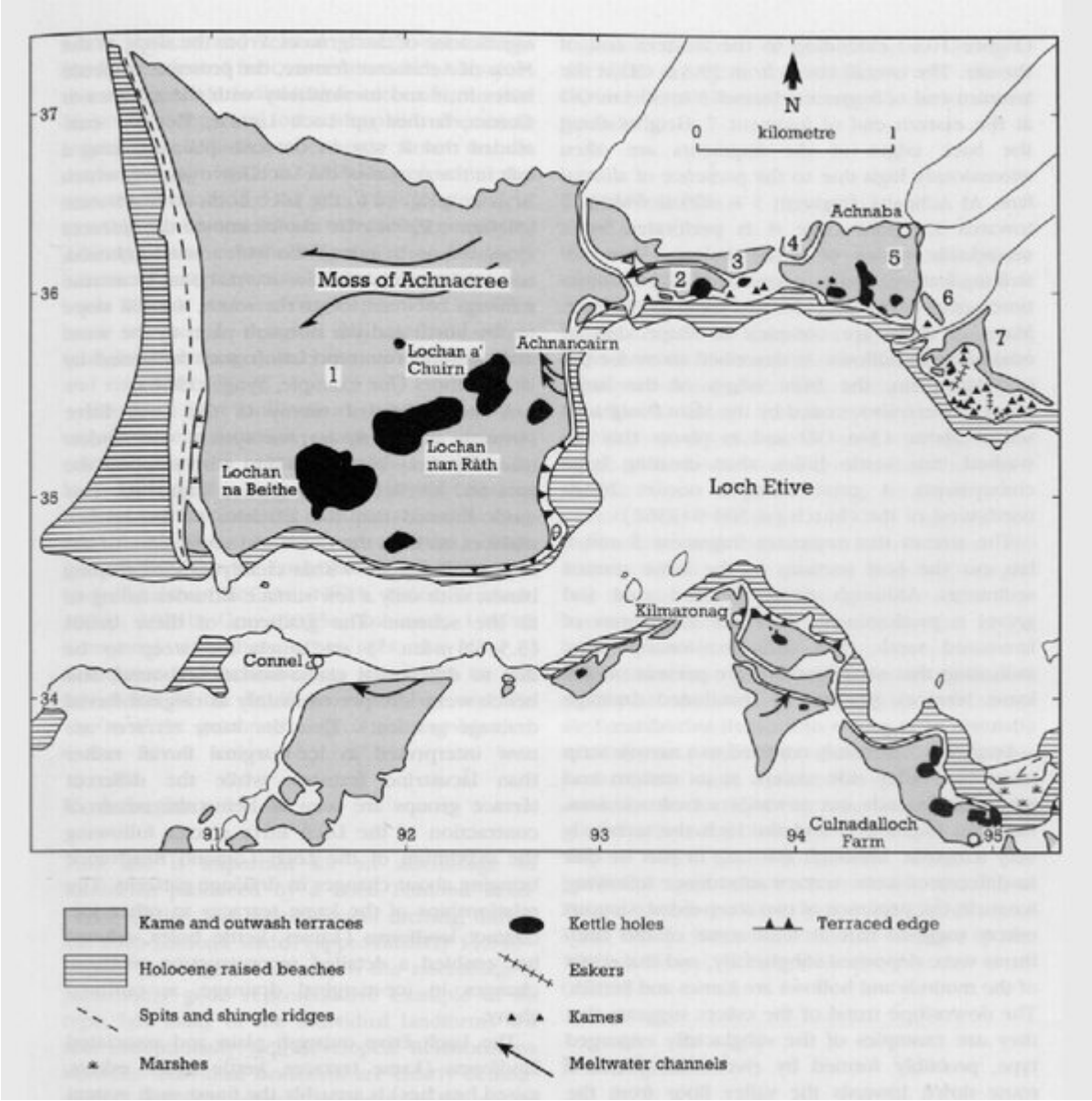

(Figure 10.6) Geomorphology of Moss of Achnacree and Achnaba (from Gray, 1975a). See text for explanation of numbers.

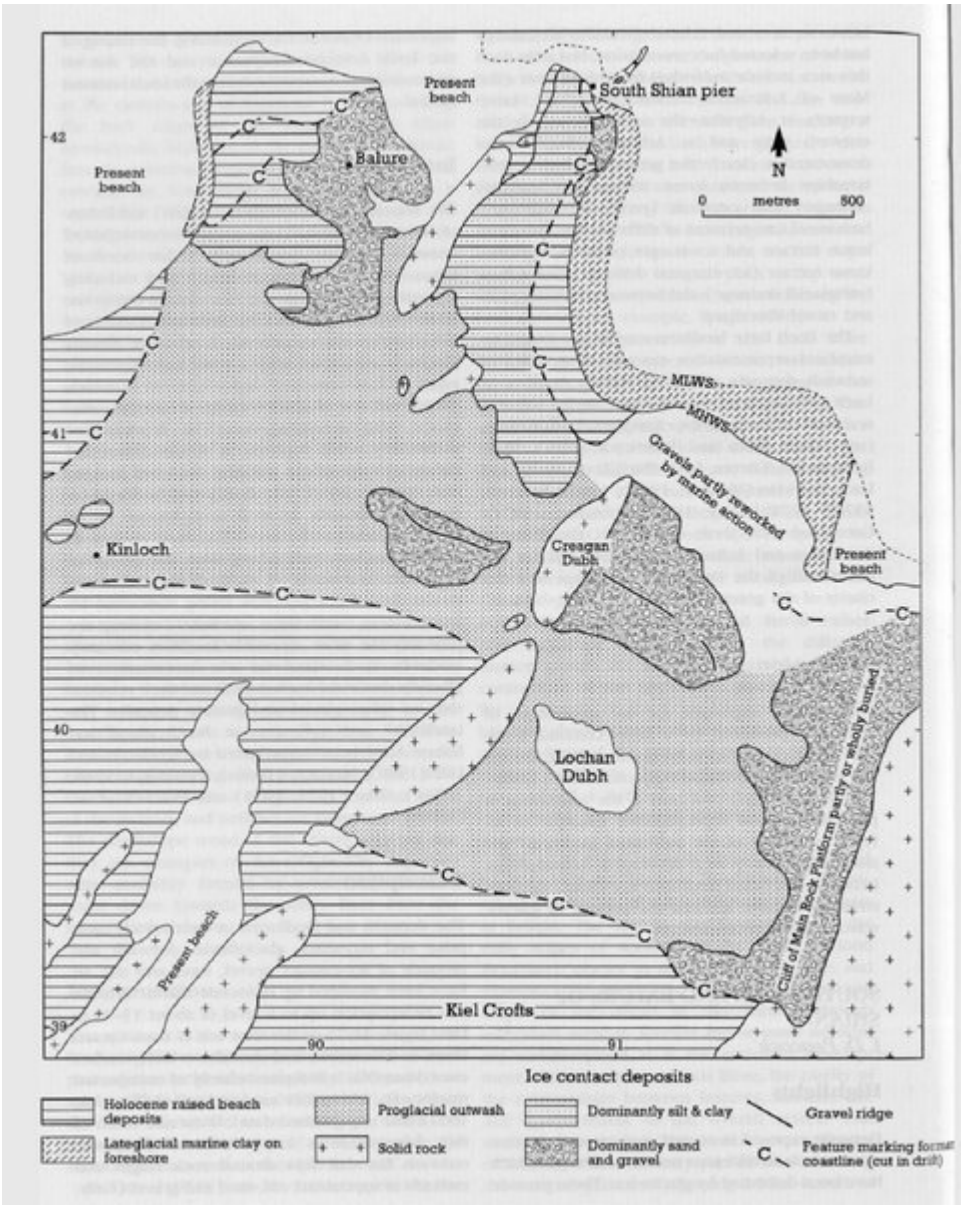

(Figure 10.7) Quaternary deposits of the South Shian and Balure of Shian area, Benderloch (from Peacock, 1971a, unpublished data).

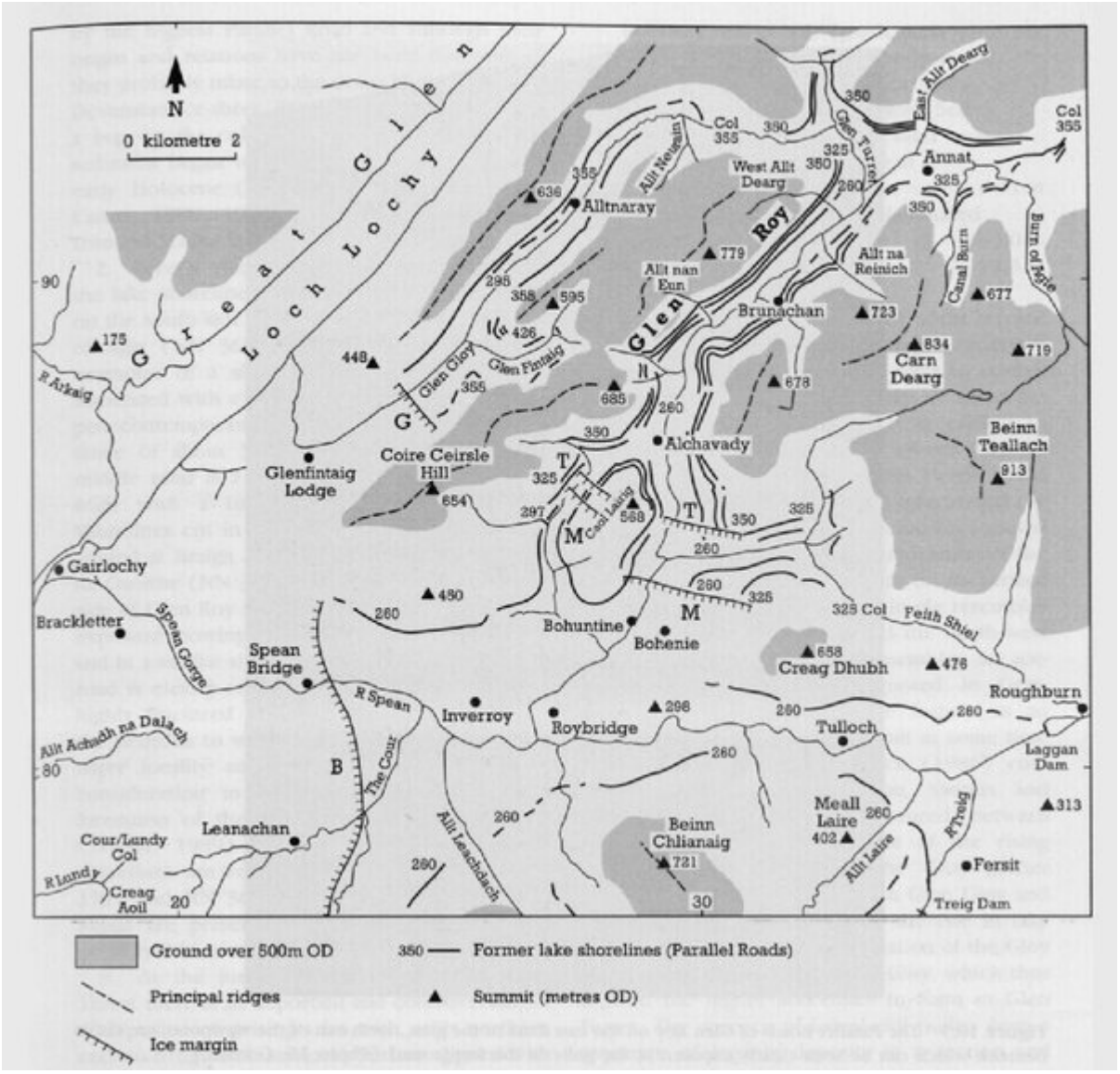

(Figure 10.8) The Parallel Roads of Lochaber. The letters T, M, B and G identify the final positions of the ice-fronts damming the 355 m, 325 m, 260 m and Glen Gloy lakes respectively (from Peacock and Cornish, 1989).

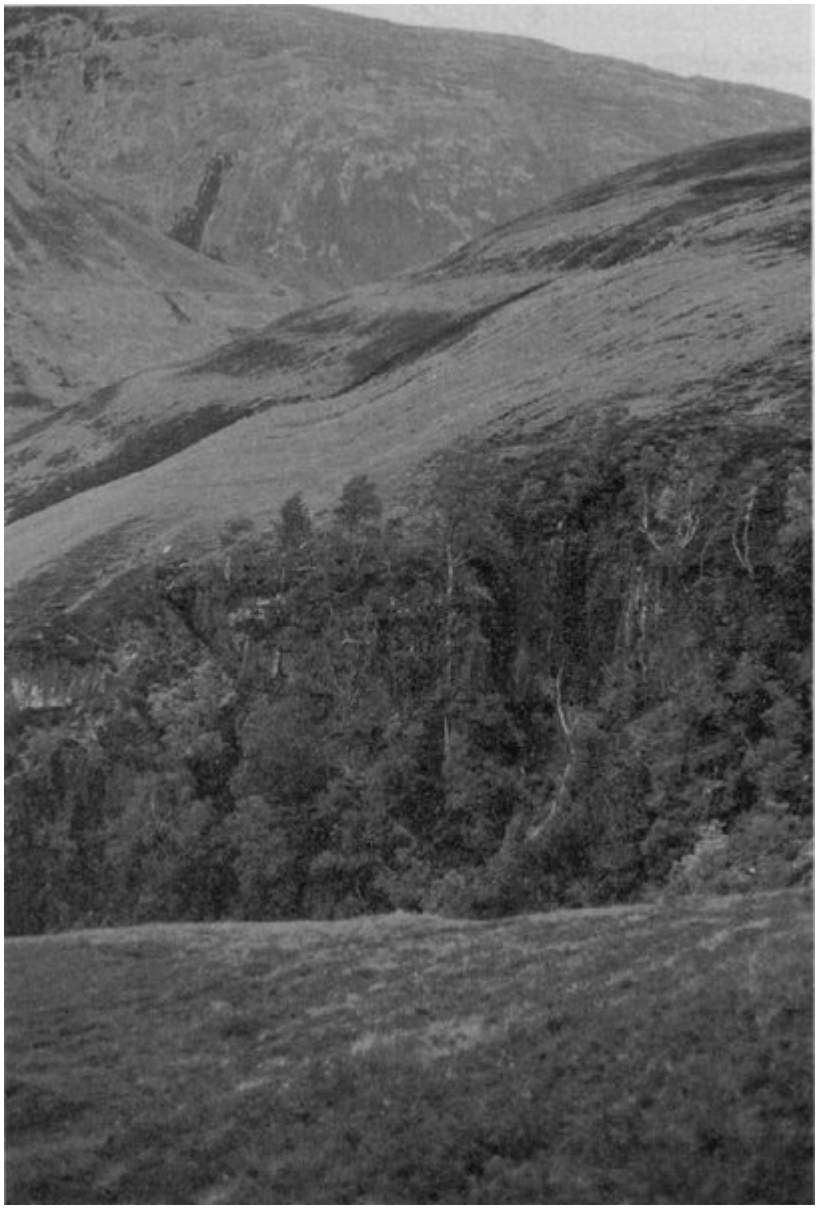

(Figure 10.9) The Parallel Roads of Glen Roy on the east flank of the glen, north-east of the viewpoint, are cut in bedrock which can be seen clearly exposed in the gully in the foreground. (Photo: J.E. Gordon.)

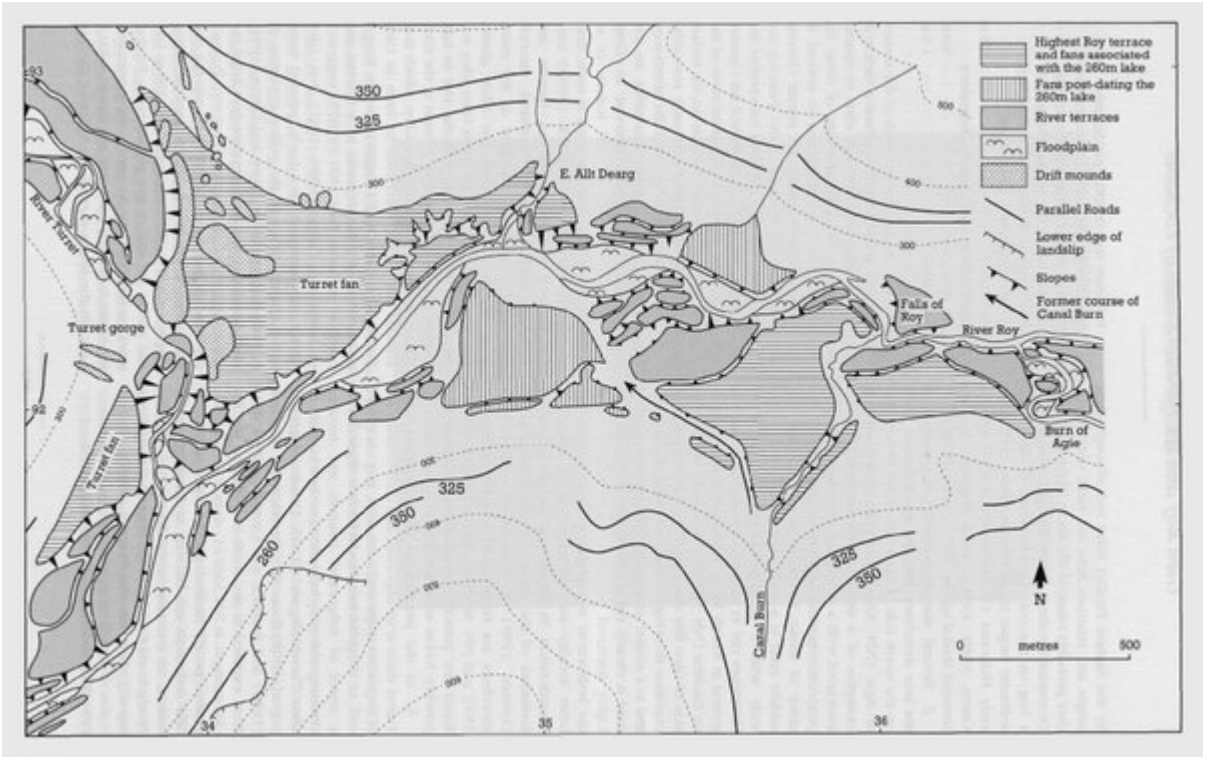

(Figure 10.10) Geomorphology of the northern part of upper Glen Roy (from Sissons and Cornish, 1983).

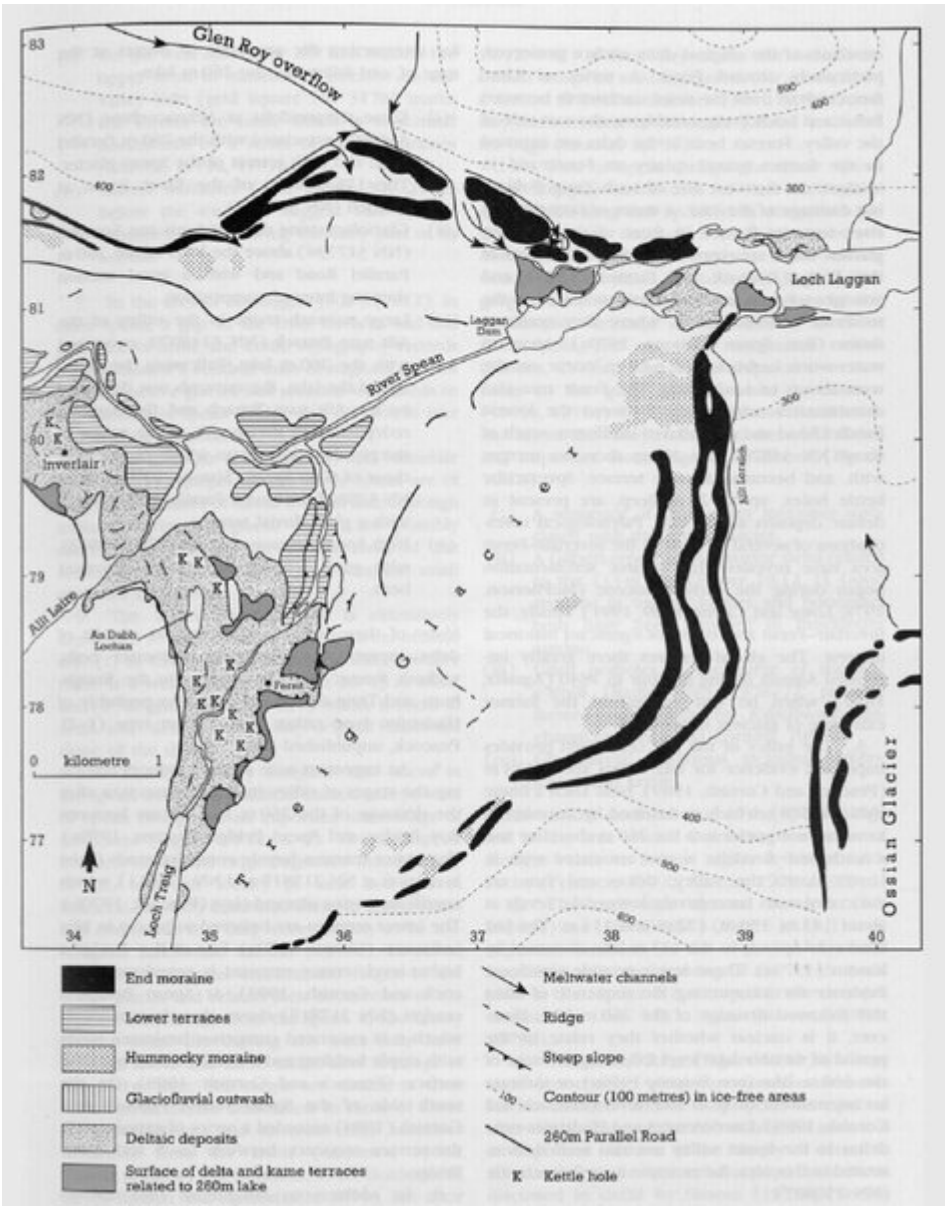

(Figure 10.11) Landforms and deposits of the Treig–Laggan area (from Sissons, 1977e; Peacock and Cornish, 1989).

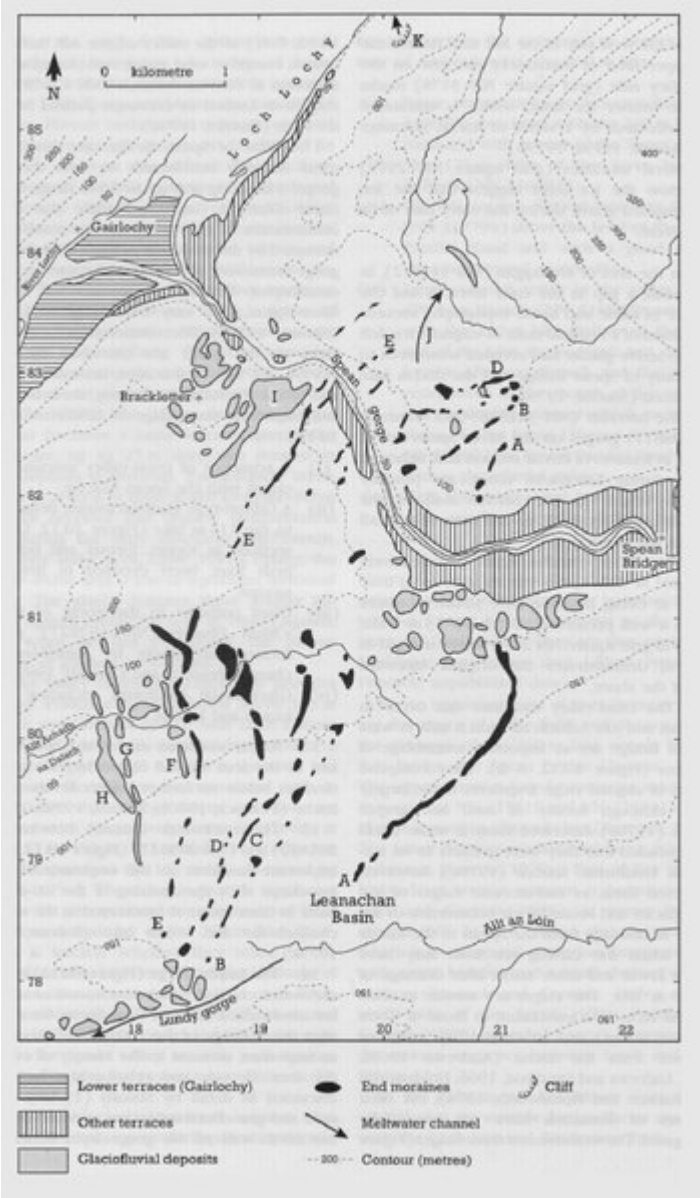

(Figure 10.12) Geomorphology of the Spean Bridge–Gairlochy area (from Sissons, 1979c). See text for explanation of letters.

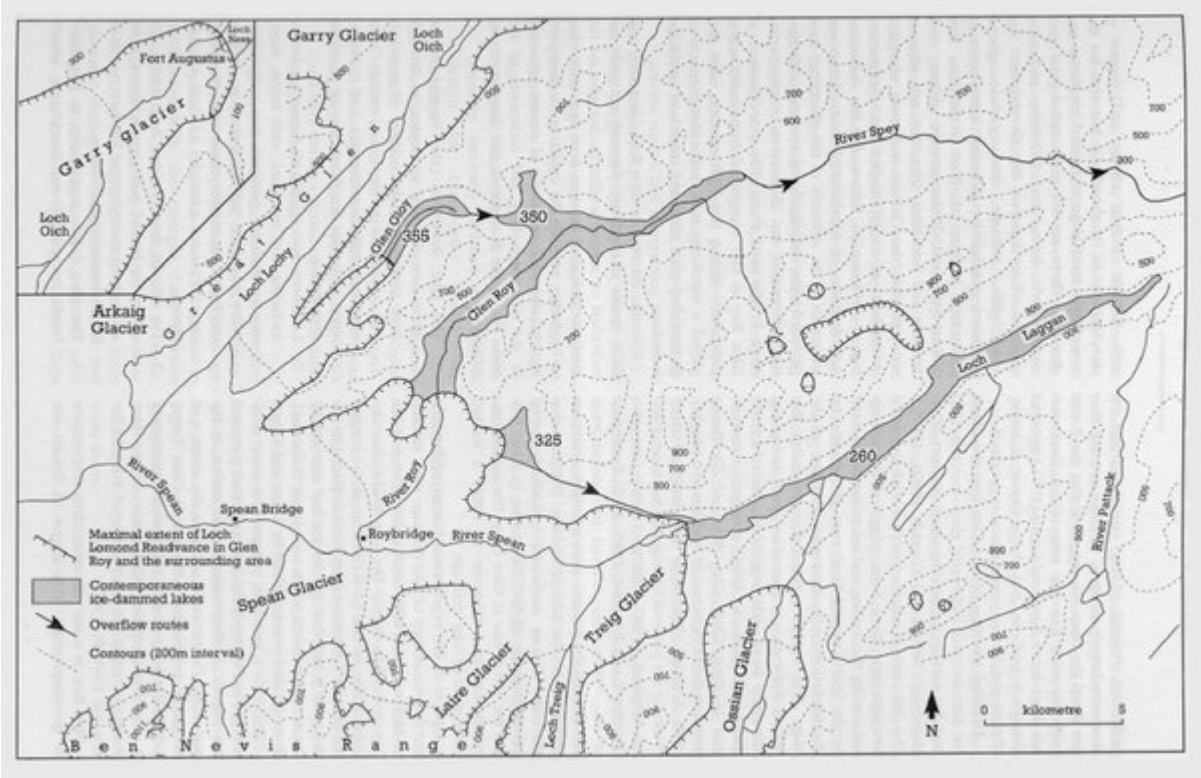

(Figure 10.13) Loch Lomond Readvance ice limits and associated ice-dammed lakes in the Glen Roy–Glen Spean area (from Sissons, 1981d).

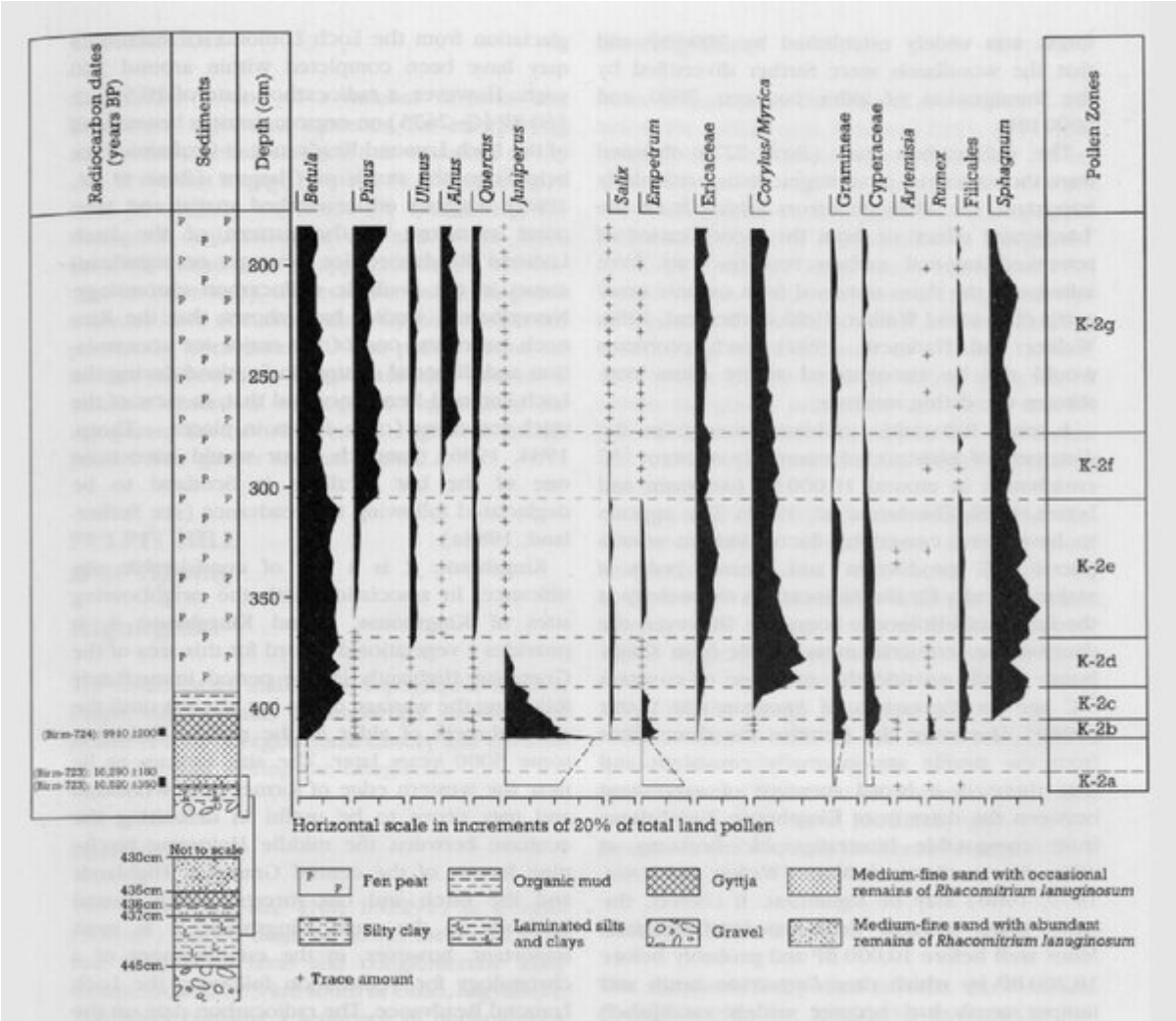

(Figure 10.14) Kingshouse: relative pollen diagram showing selected taxa as percentages of total land pollen (from Walker and Lowe, 1977).

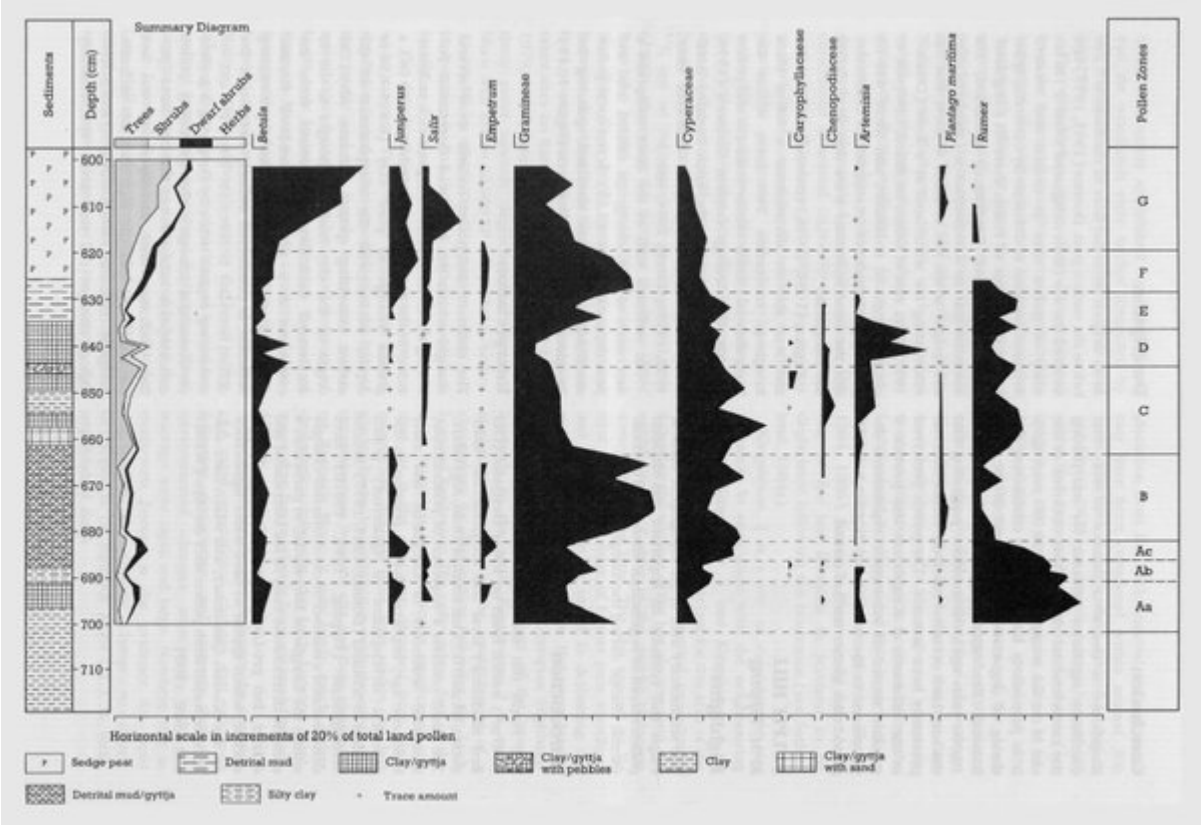

(Figure 10.15) Pulpit Hill: relative pollen diagram showing selected taxa as percentages of total land pollen (from Tipping, 1991b).

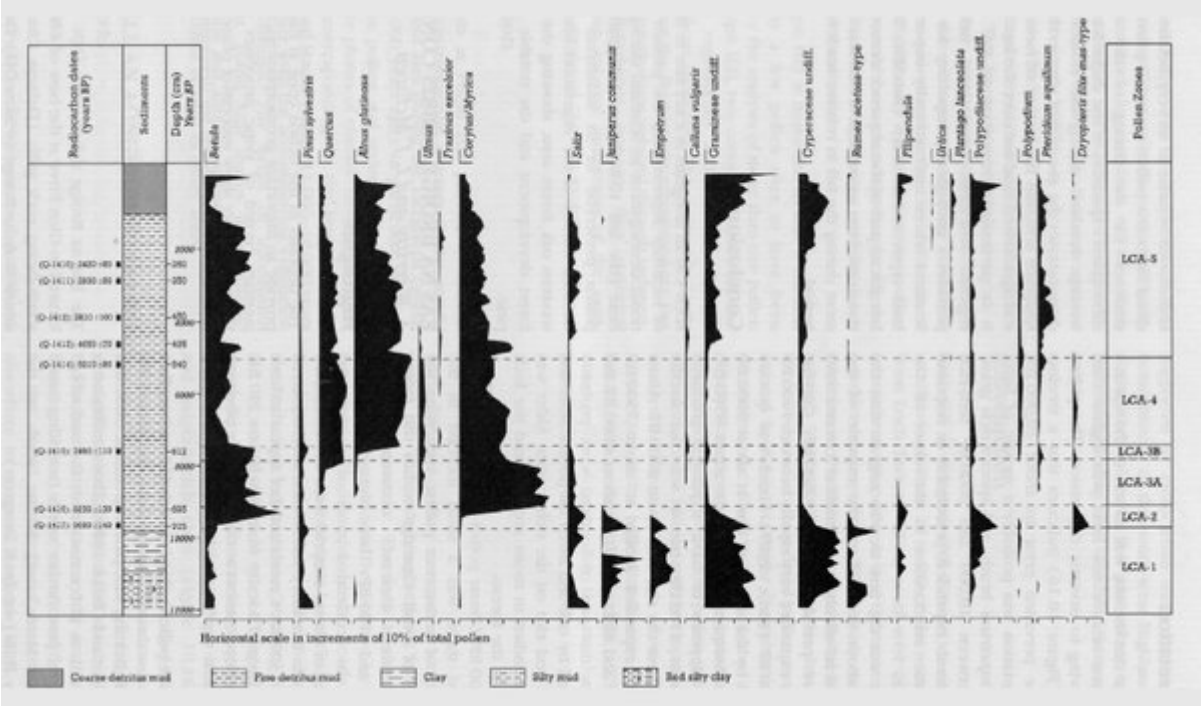

(Figure 10.16) Loch Cill an Aonghais: relative pollen diagram showing selected taxa as percentages of total pollen (from Birks, 1980, after S. Peglar). Note that the data are plotted against a radiocarbon timescale.

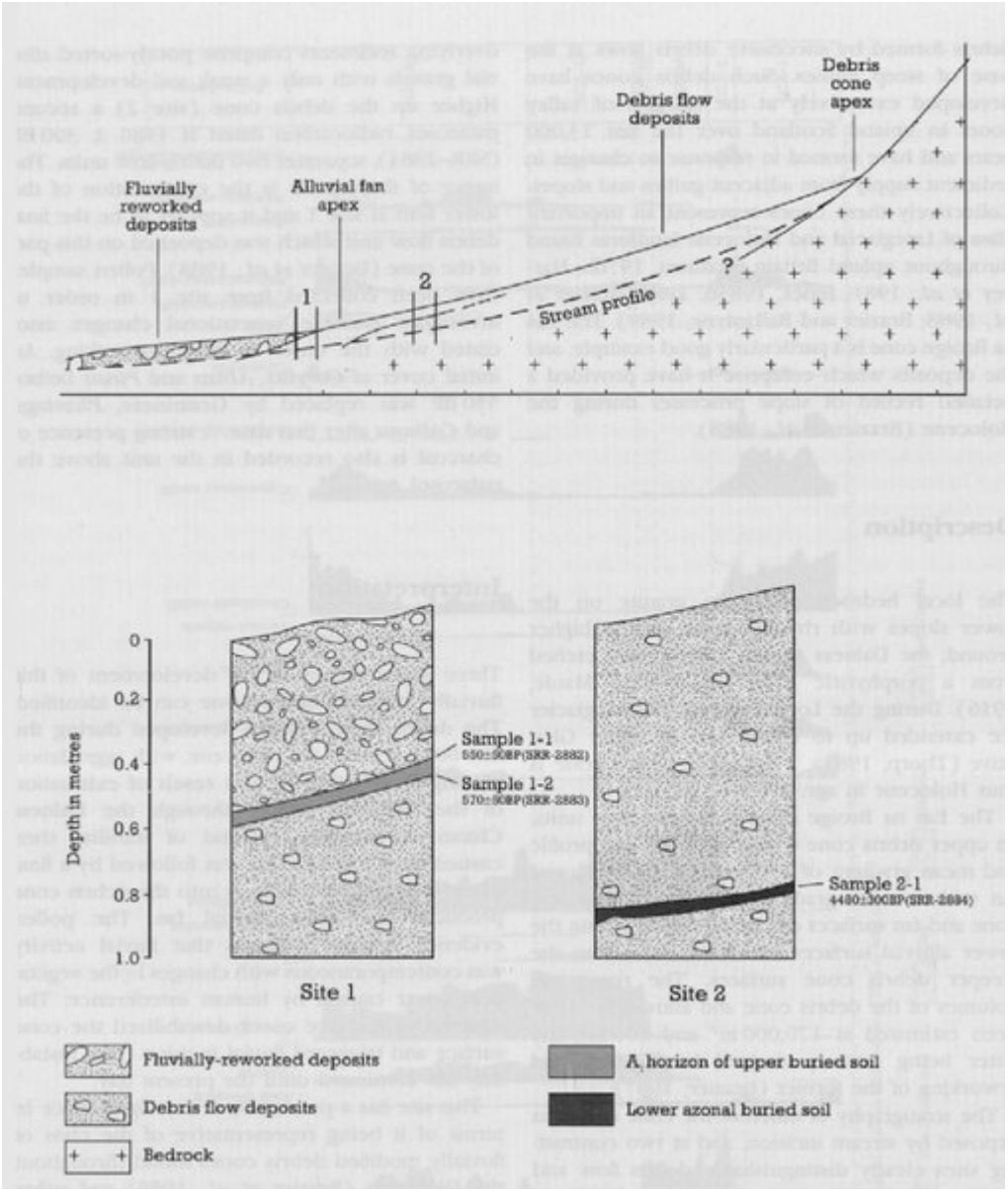

(Figure 10.17) Top: schematic section along the length of the Eas na Broige debris cone. Bottom: detail of section at sampling sites (from Brazier et al., 1988).

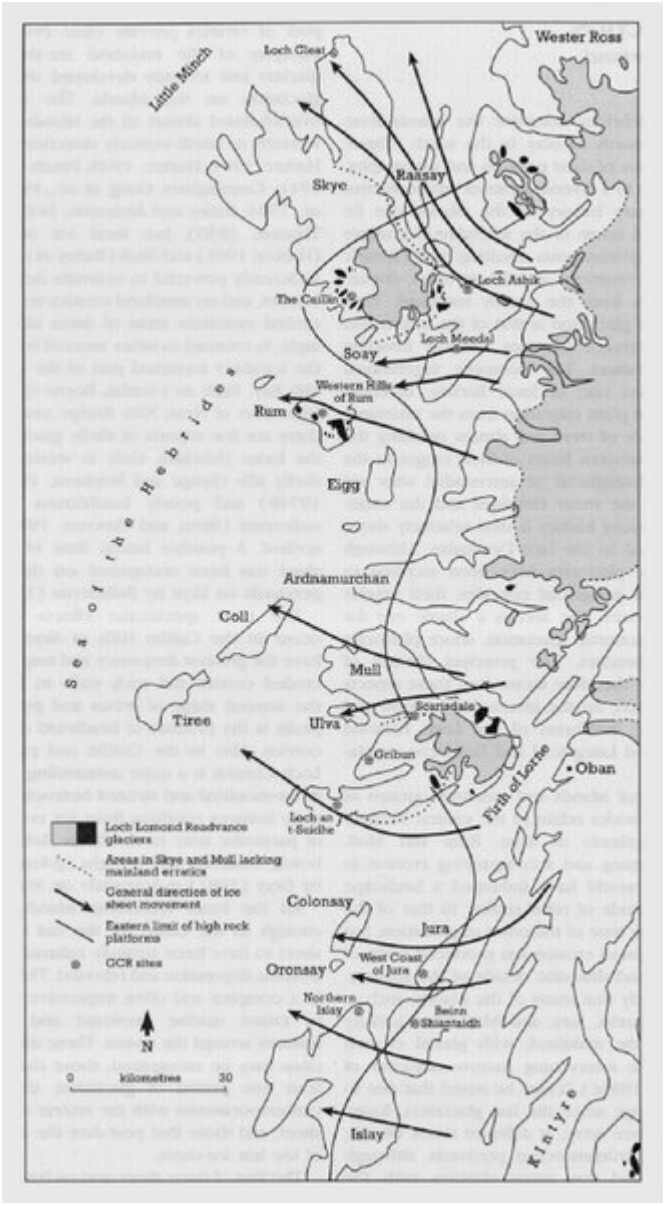

(Figure 11.1) Location map and principal Quaternary features of the Inner Hebrides (from Peacock, 1983b; Sissons, 1983c; Ballantyne and Benn, 1991).

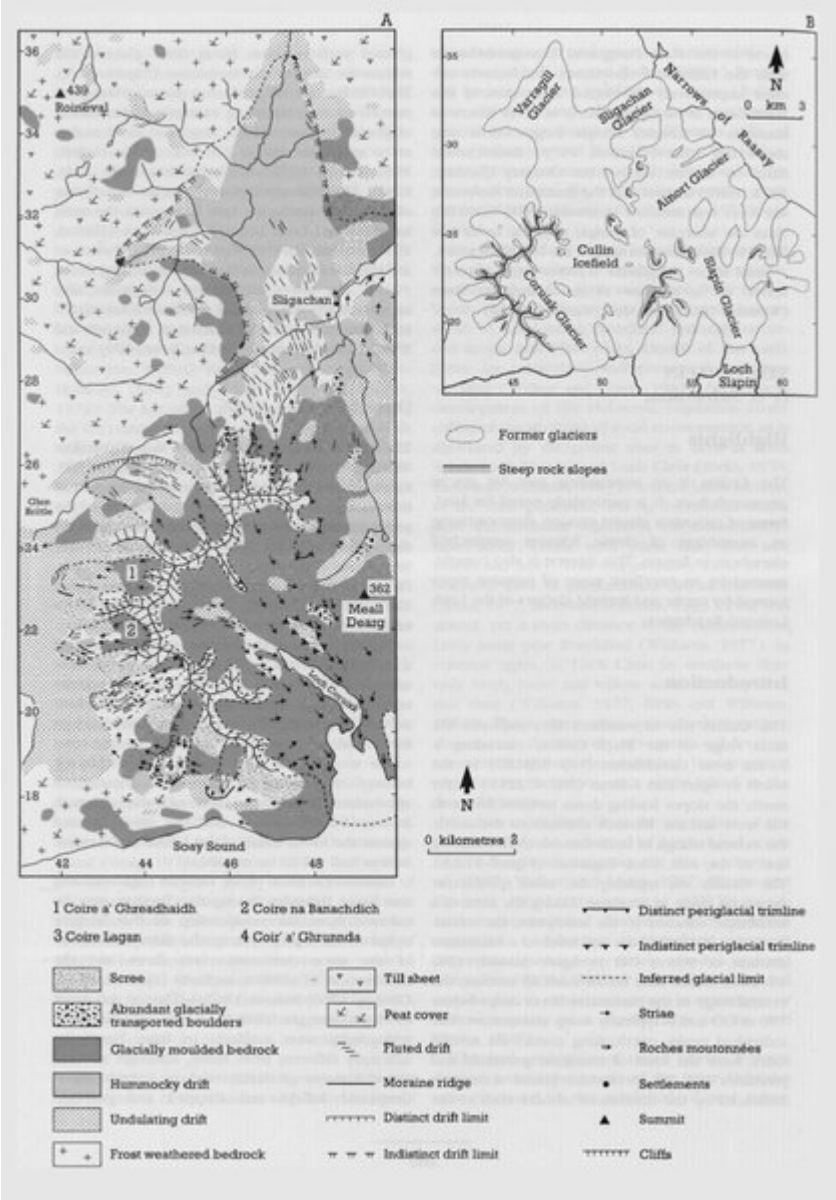

(Figure 11.2) (A) Principal glacial features of the Cuillin. (B) Reconstructed Loch Lomond Readvance glaciers in central Skye (from Ballantyne, 1989a).

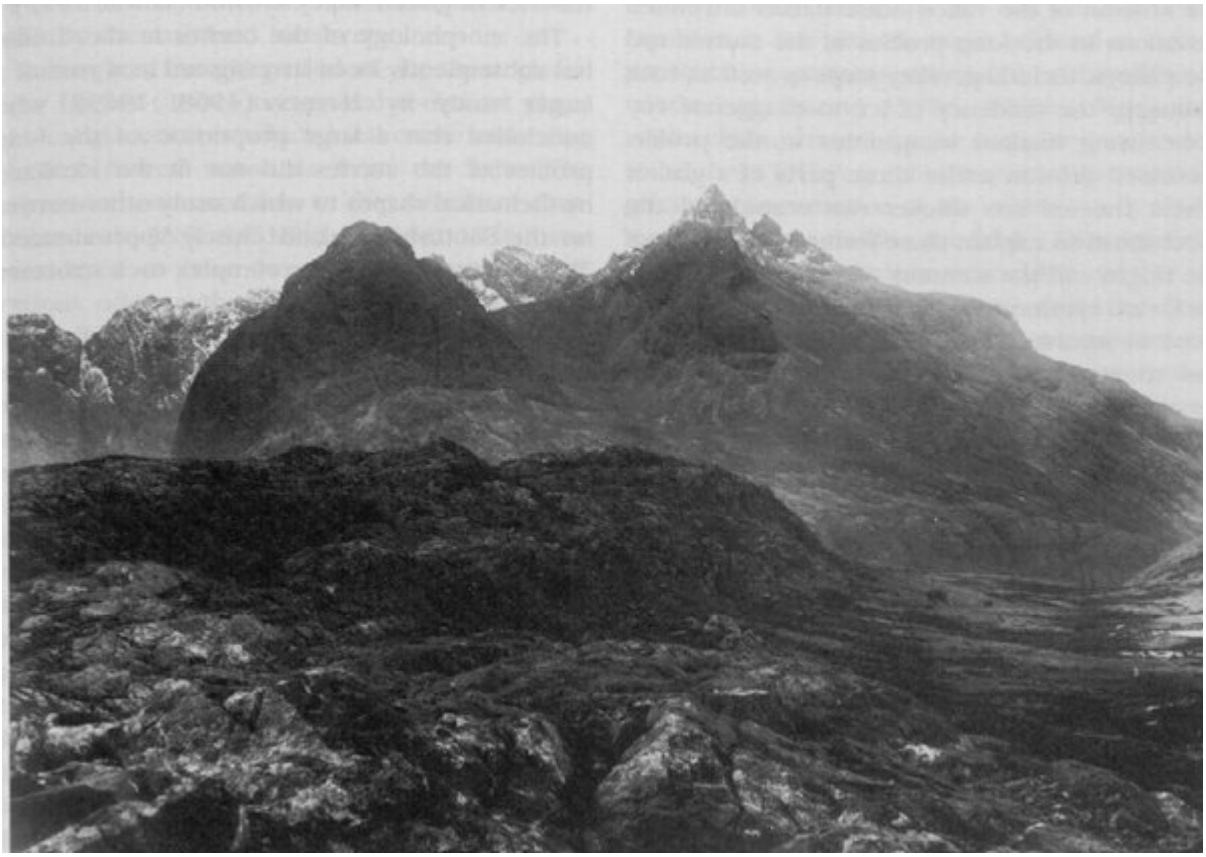

(Figure 11.3) Landforms of glacial and periglacial erosion are strikingly developed in the Cuillin of Skye. The serrated aspect of the main Cuillin ridge reflects intense periglacial weathering, whereas the lower slopes are heavily ice-scoured. (British Geological Survey photograph B168.)

(Figure 11.4) Detail of ice-moulded bedrock near Loch Coruisk showing glacially abraded and smoothed stoss slopes and localized joint-block removal. (Photo: D. G. Sutherland.)

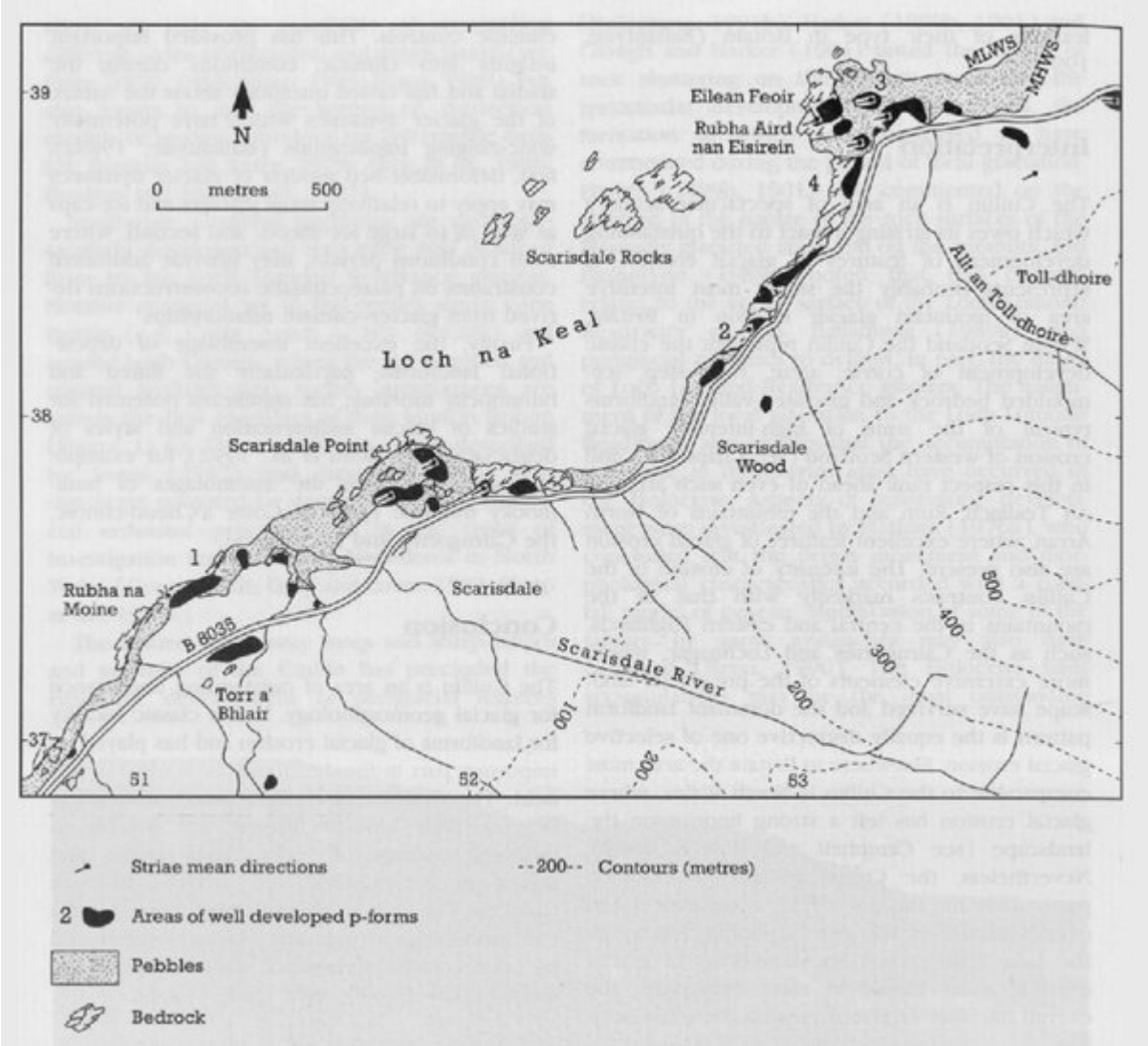

(Figure 11.5) Scarisdale: localities with well-preserved p-forms (from Gray, 1981).

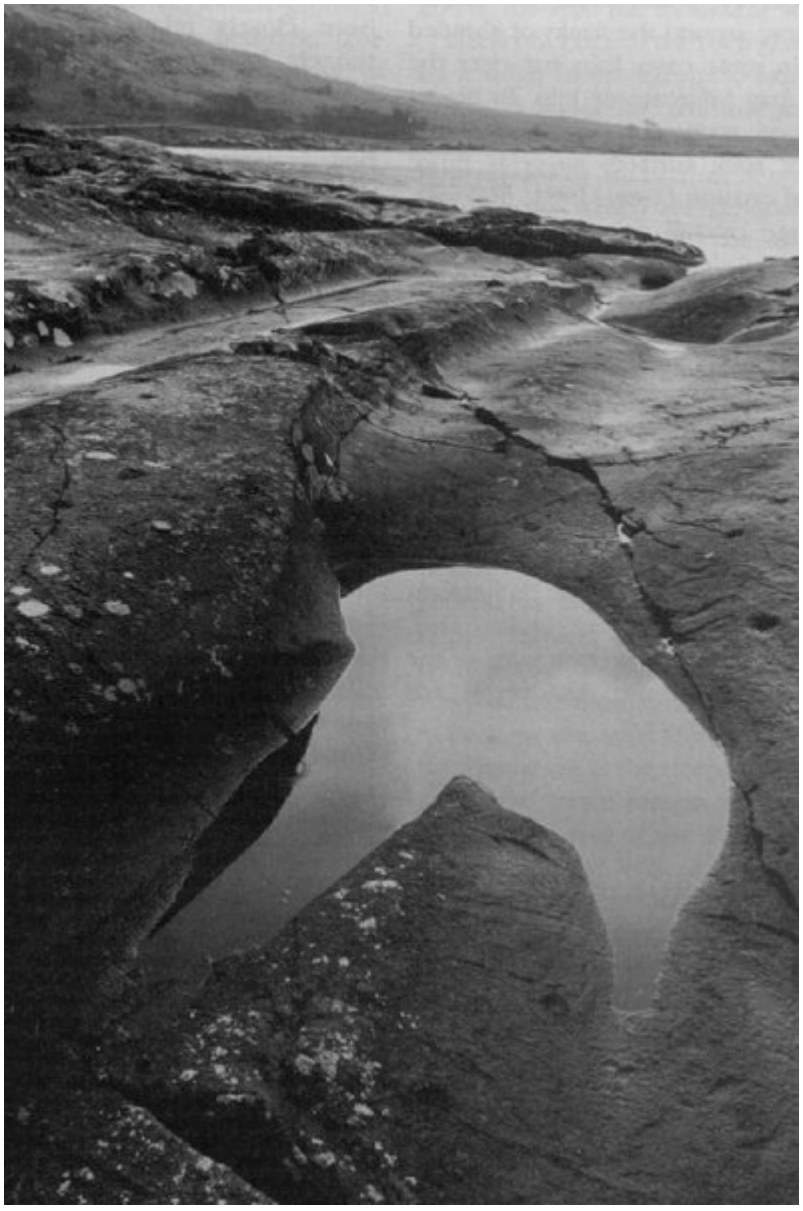

(Figure 11.6) P-form channels at Scarisdale, Mull. (Photo: S. Campbell.)

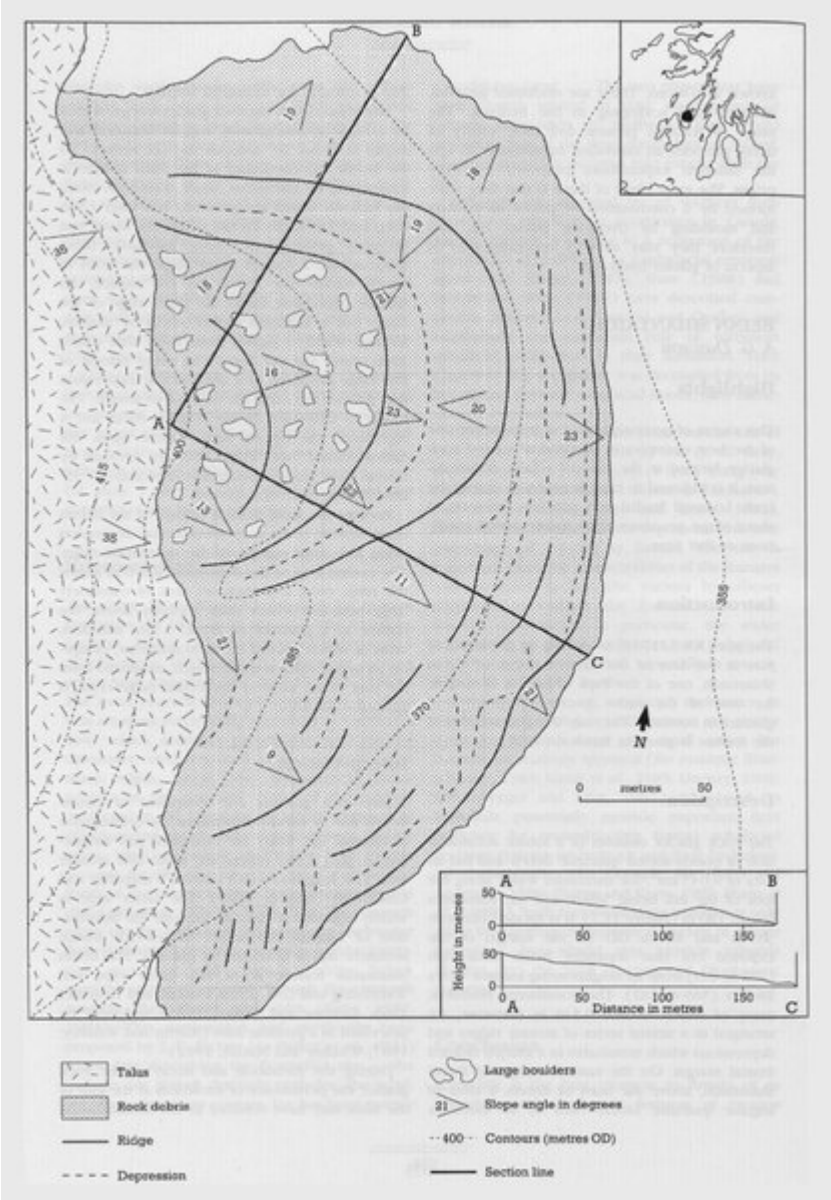

(Figure 11.7) The Beinn Shiantaidh rock glacier (from The Western Hills of Rum, Sròn an t-Saighdeir Dawson, 1977).

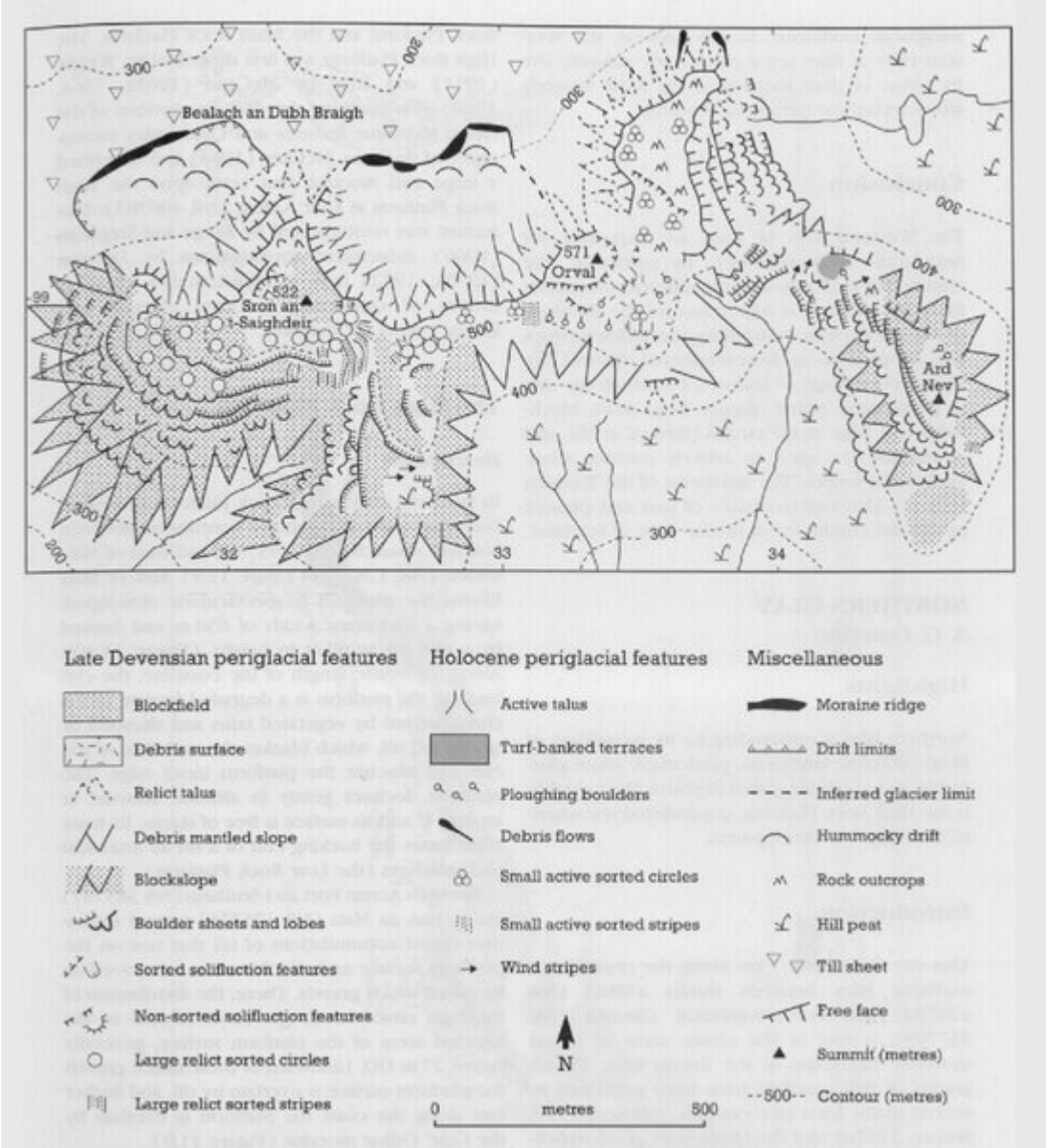

(Figure 11.8) Periglacial features on the Western Hills of Rum (from Ballantyne, 1984).

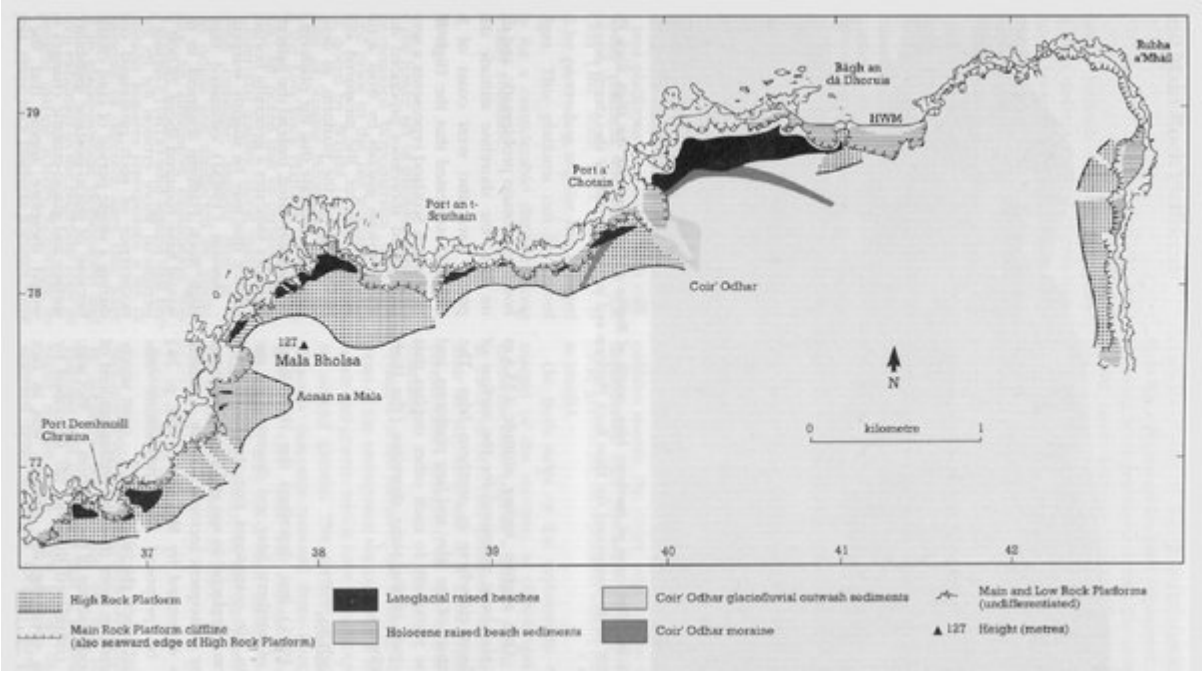

(Figure 11.9) Geomorphology of northern Islay between Rubha a'Mhail and Port Domhnuill Chruinn.

(Figure 11.10) The coast of northern Islay, south of Rubha a'Mhail, showing the High Rock Platform and its backing cliff. In the foreground the Main Rock Platform and its backing cliff are also clearly developed. (Photo: J E. Gordon.)

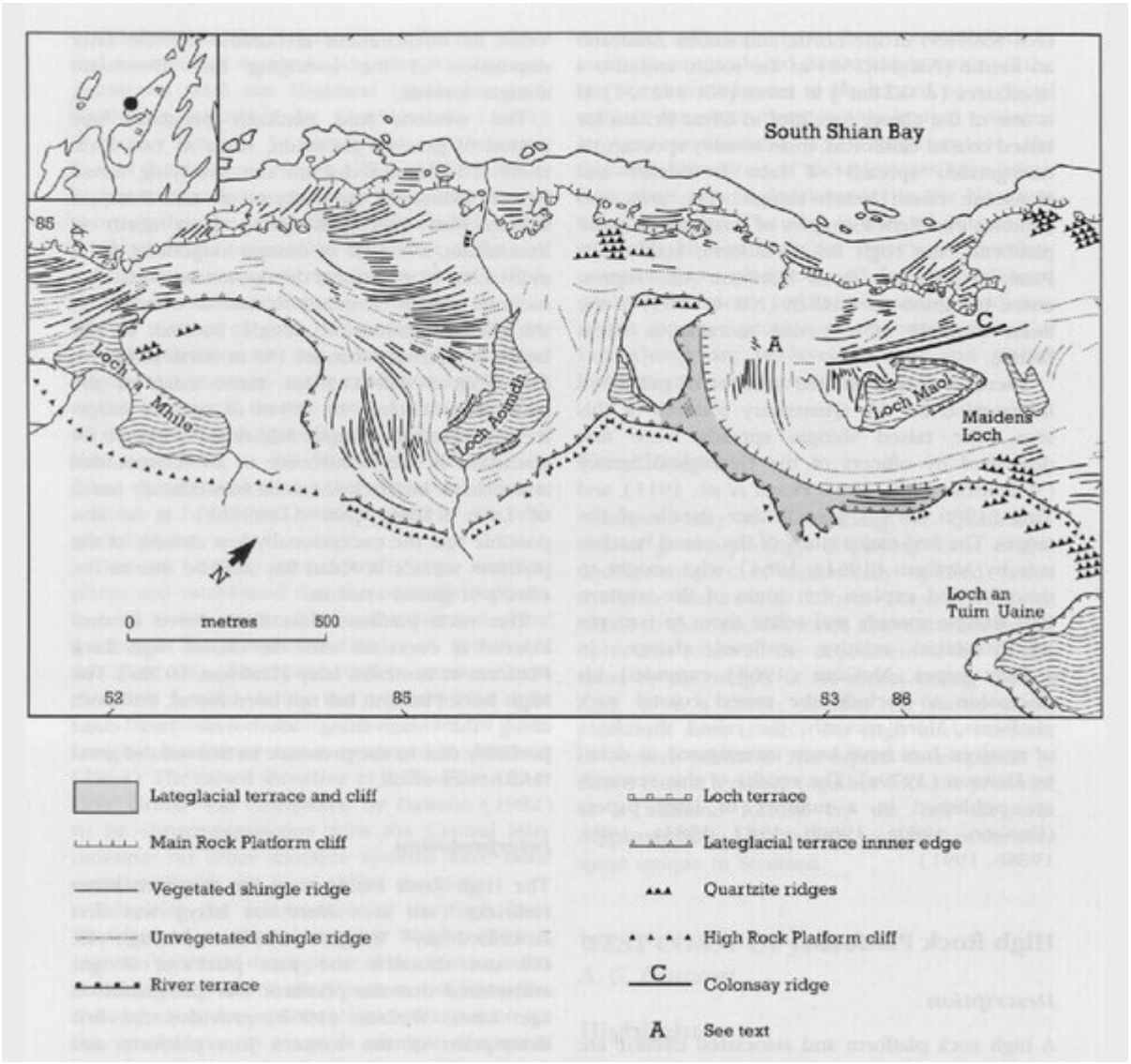

(Figure 11.11) Geomorphology of western Jura in the area of South Shian Bay.

(Figure 11.12) View south along the west coast of Jura between Shian Bay and Ruantallain. Lateglacial shingle ridges extend across a high rock platform and to the west of Loch a'Mhile (centre). The loch was formerly a marine inlet prior to the deposition of the shingle ridges. Note also a prominent rock platform and backing cliff (the Main Rock Platform) seaward of the high shingle ridge 'staircases'. Holocene shingle ridges also cover the Main Rock Platform. (Photo: John Dewar Studios.)

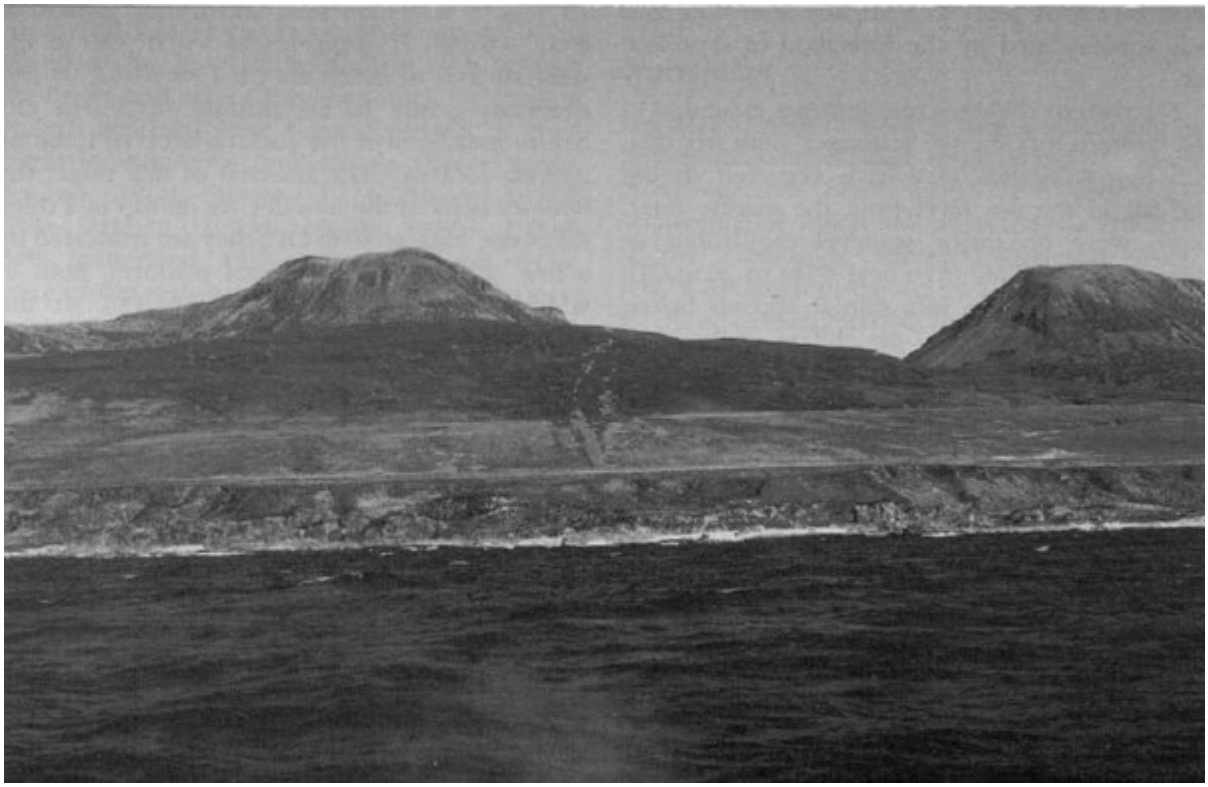

(Figure 11.13) West coast of Jura. The Sgriob na Caillich raised shoreline. (Photo: D. G. Sutherland.)

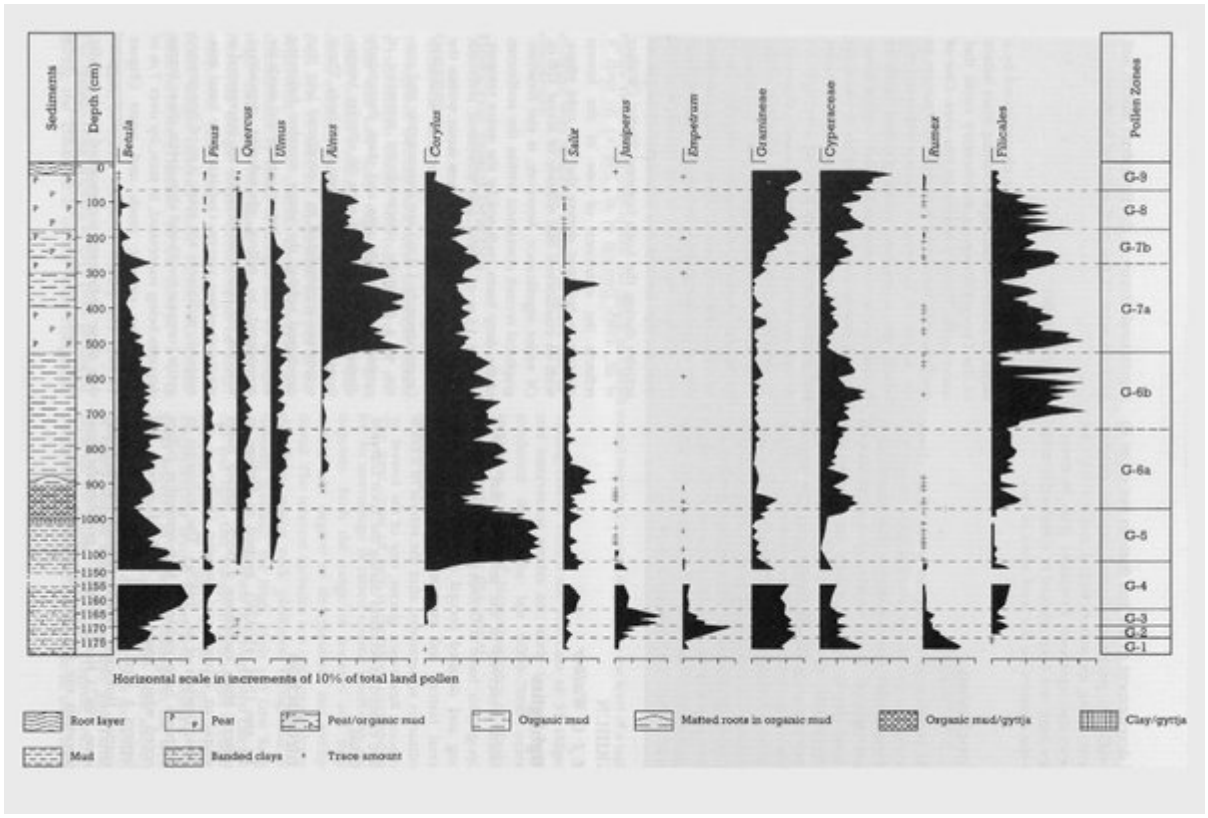

(Figure 11.14) Gribun: relative pollen diagram showing selected taxa as percentages of total land pollen (from Walker and Lowe, 1987).

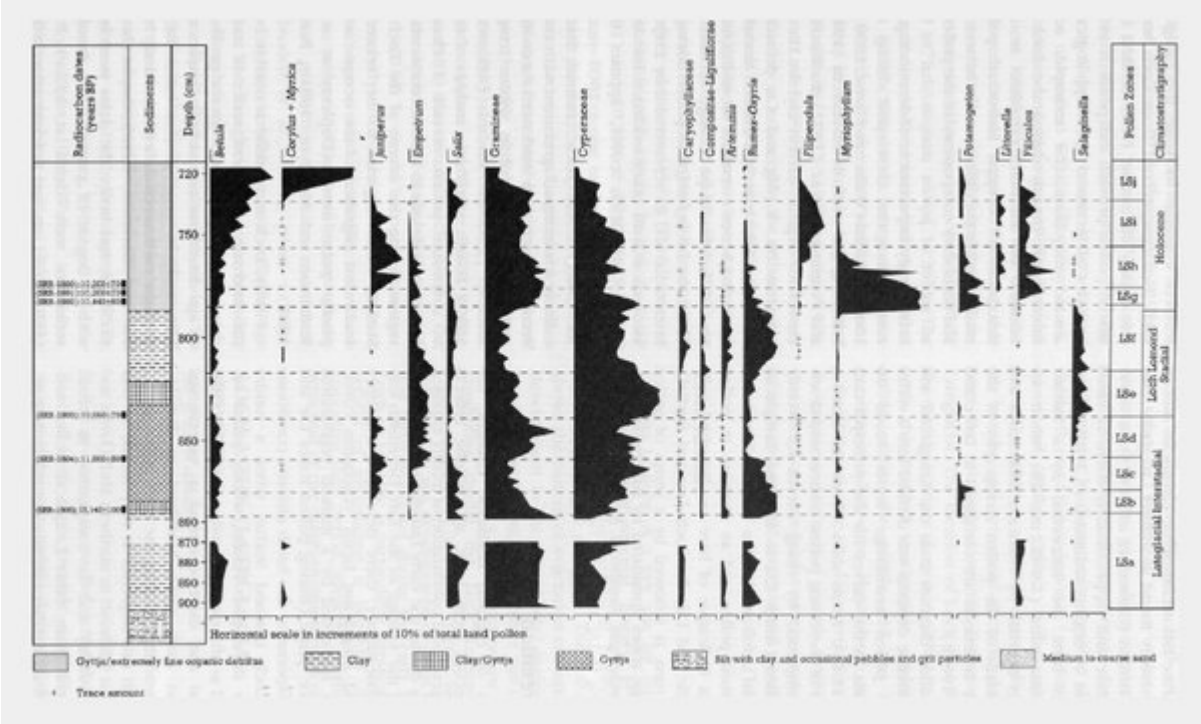

(Figure 11.15) Loch an t-Suidhe: relative pollen diagram showing selected taxa as percentages of total land pollen (from Lowe and Walker, 1986a).

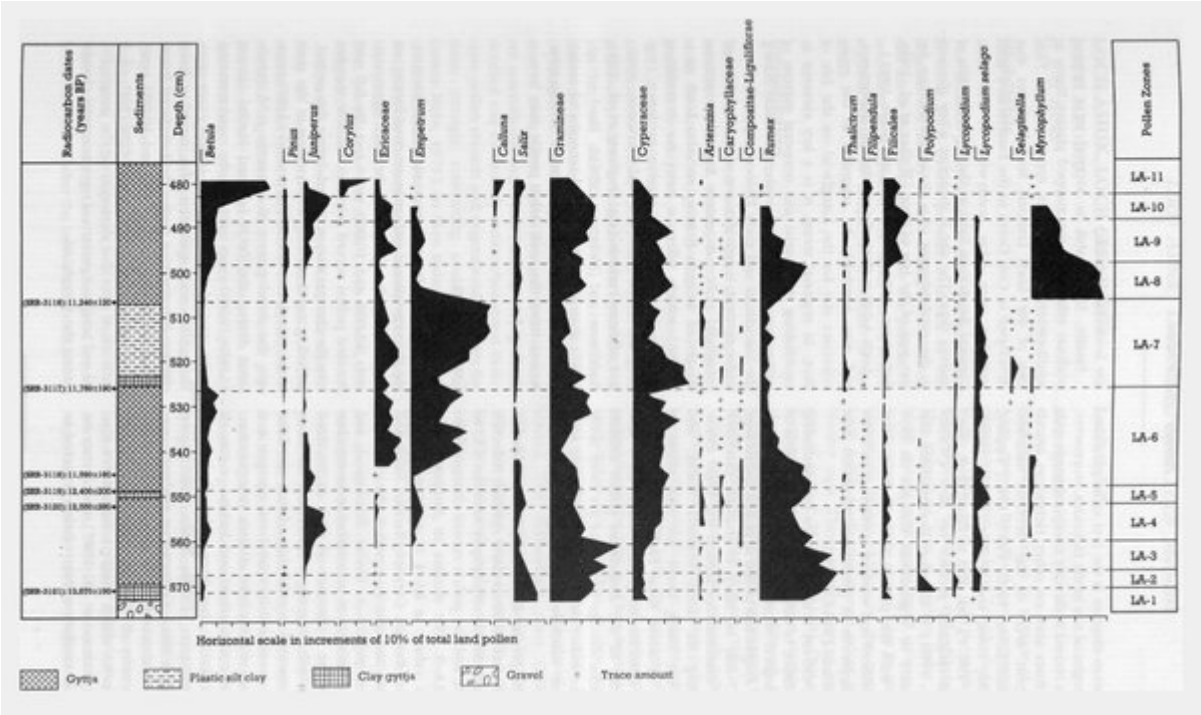

(Figure 11.16) Loch Ashik: Lateglacial relative pollen diagram showing selected taxa as percentages of total land pollen (from Walker and Lowe, 1991).

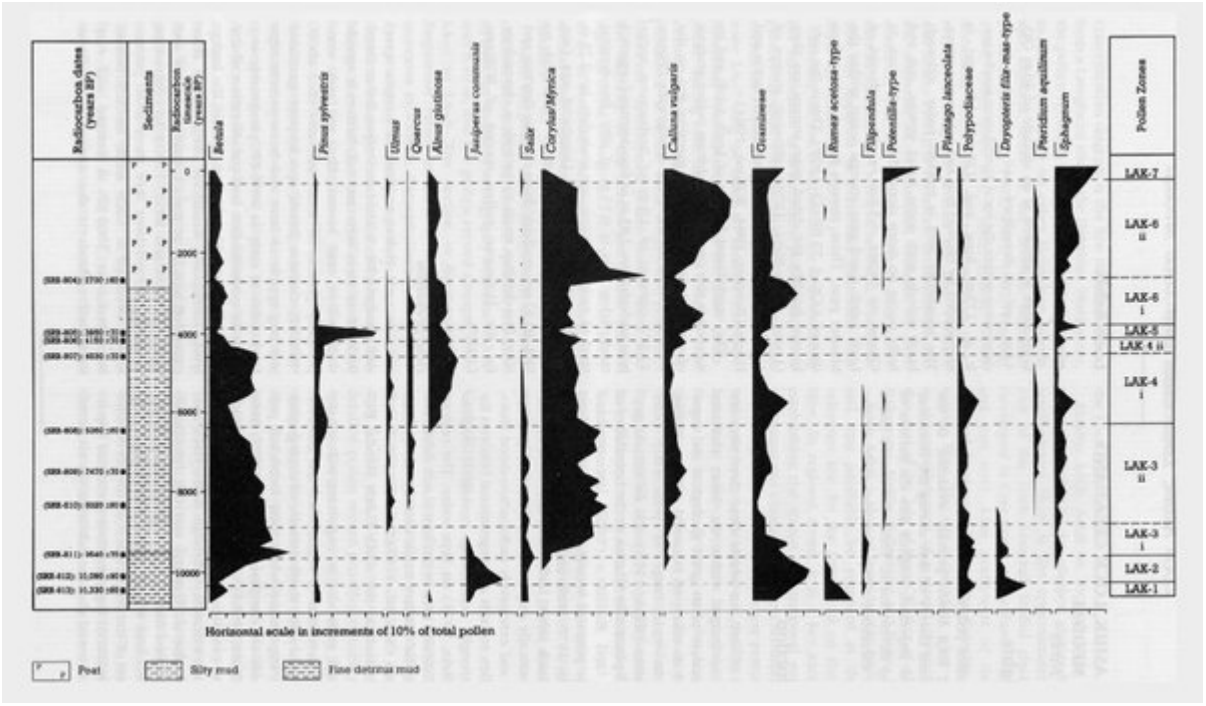

(Figure 11.17) Loch Ashik: Holocene relative pollen diagram showing selected taxa as percentages of total pollen (from Birks and Williams, 1983). Note that the data are plotted against a radiocarbon time-scale.

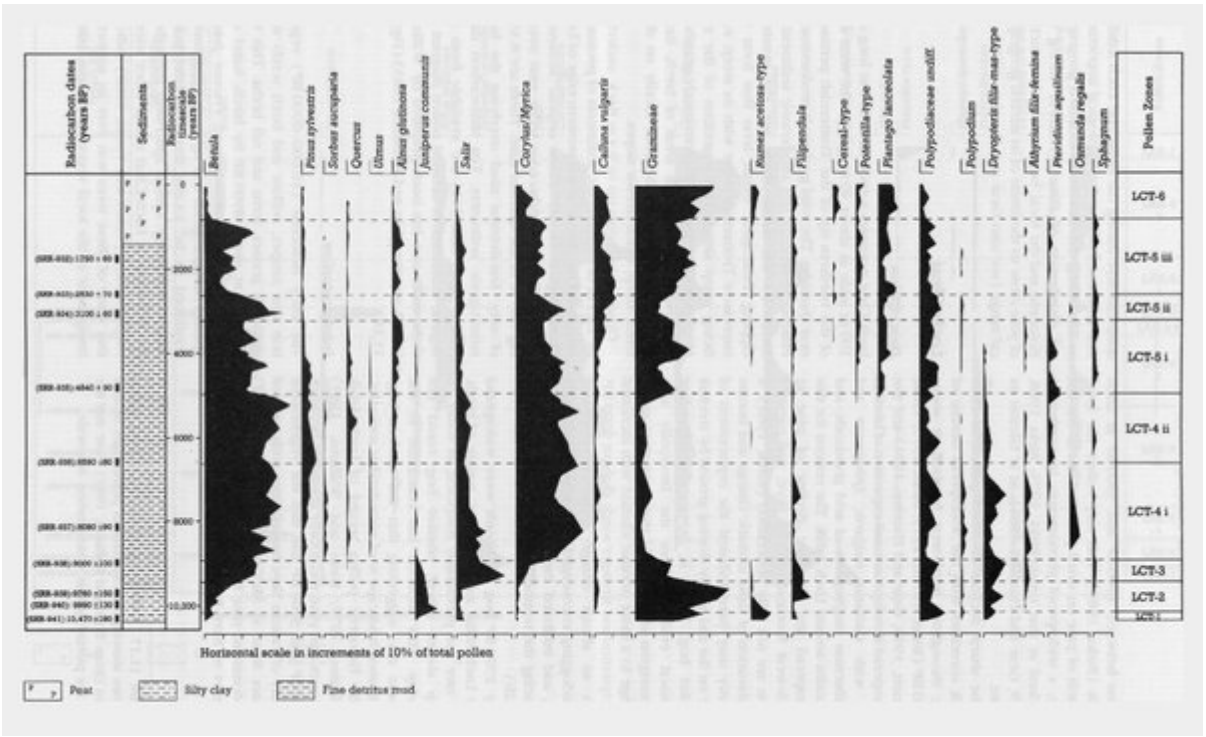

(Figure 11.18) Loch Cleat: Holocene relative pollen diagram showing selected taxa as percentages of total pollen (from Birks and Williams, 1983). Note that the data are plotted against a radiocarbon time-scale.

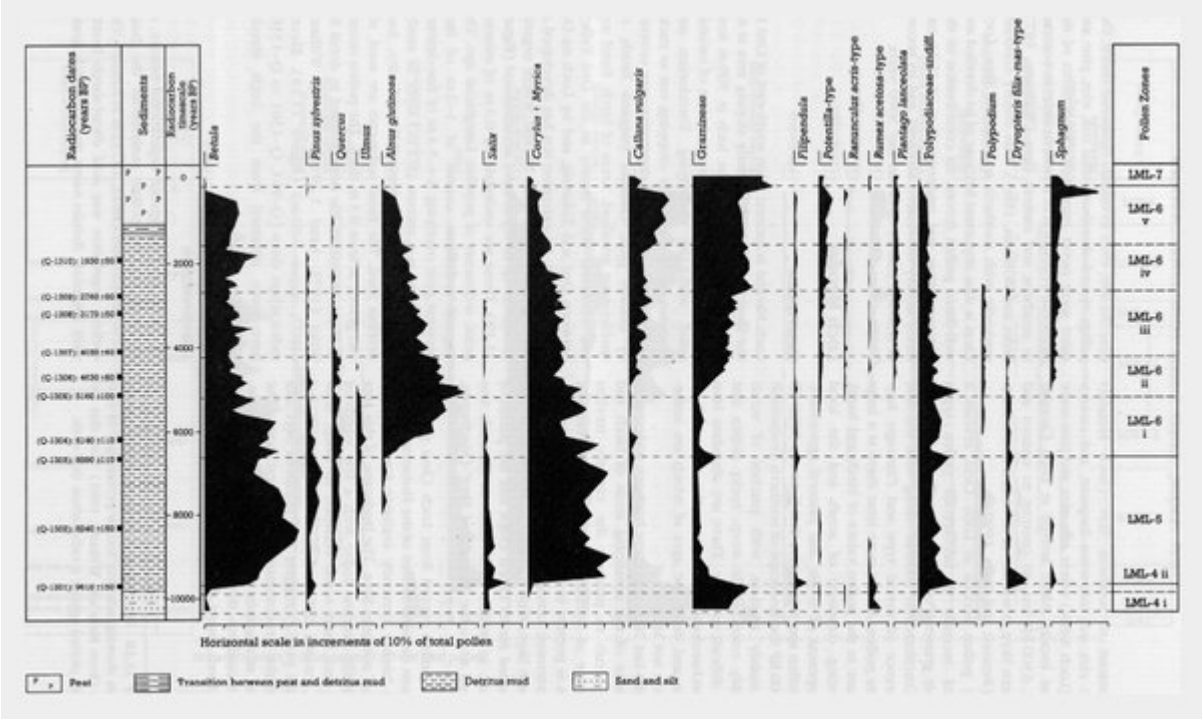

(Figure 11.19) Loch Meodal: Holocene relative pollen diagram showing selected taxa as percentages of total pollen (from Birks and Williams, 1983). Note that the data are plotted against a radiocarbon time-scale.

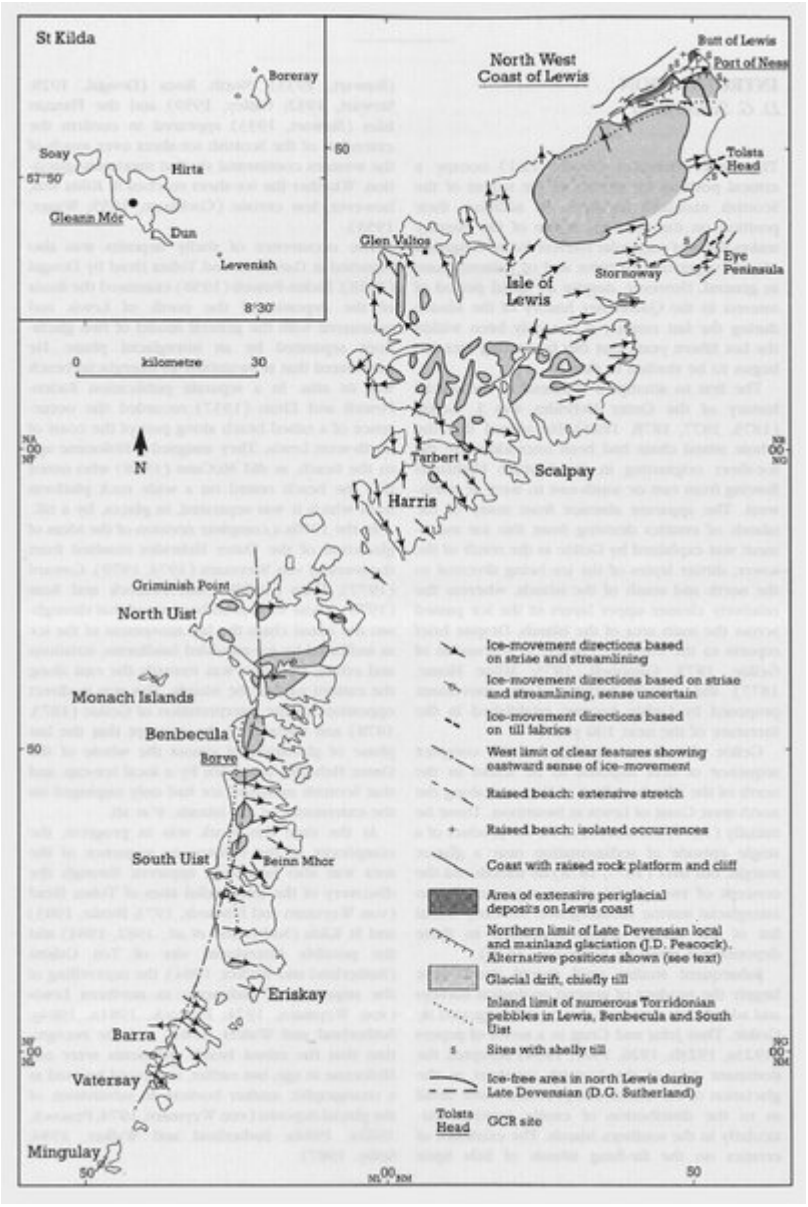

(Figure 12.1) Location map and principal Quaternary features of the Outer Hebrides (from Peacock, 1984a).

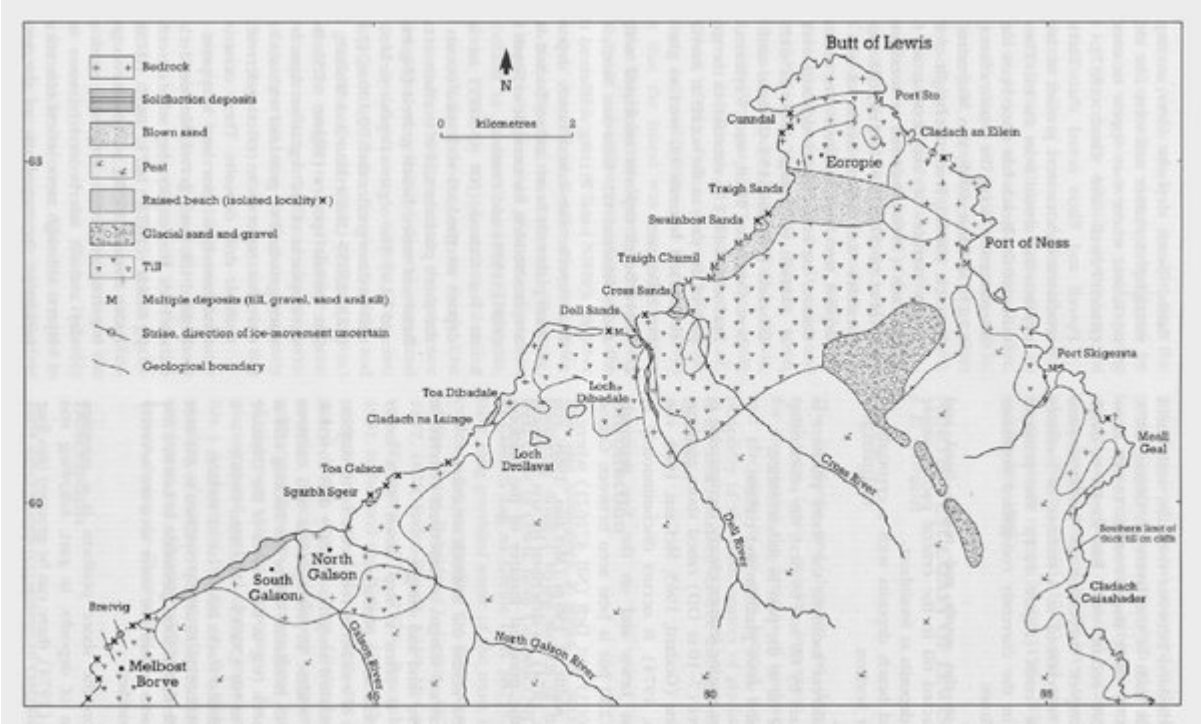

(Figure 12.2) Quaternary deposits of north-west Lewis (from Peacock, 1984a).

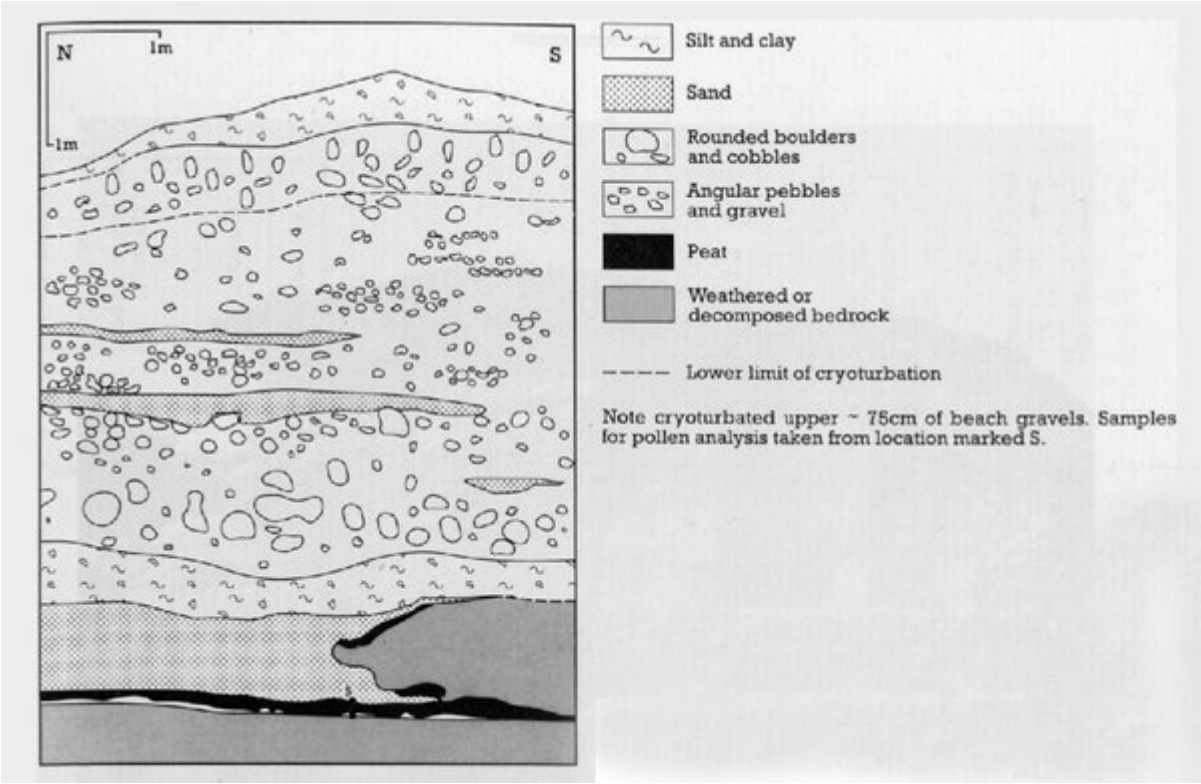

(Figure 12.3) Toa Gilson: sequence of sediments (from Sutherland and Walker, 1984).

(Figure 12.4) Section at Toa Galson, north-west Lewis, showing the interglacial peat resting on bedrock and overlain by sand, head and the Galson Beach deposits. The upper part of the beach deposits has been affected by cryoturbation. (Photo: D. G. Sutherland.)

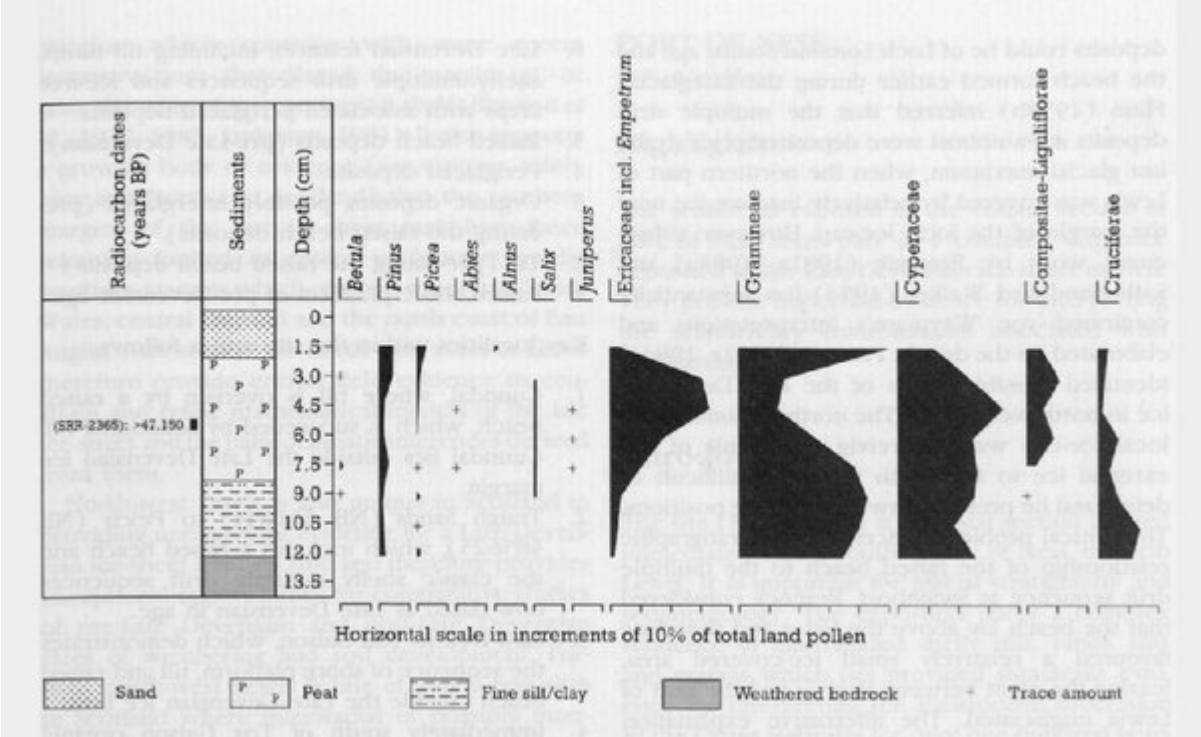

(Figure 12.5) Relative pollen diagram for the peat deposit at Toa Galson showing selected taxa as percentages of total land pollen (from Sutherland and Walker, 1984). The location of the sample is shown in Figure 12.3.

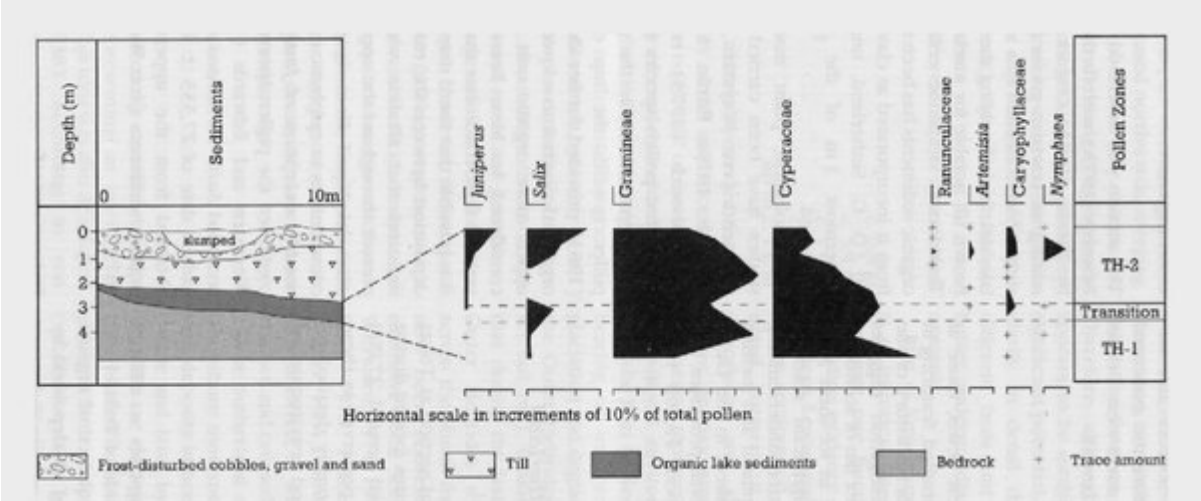

(Figure 12.6) Tolsta Head: sediments and relative pollen diagram showing selected taxa as percentages of total pollen (from von Weymarn and Edwards, 1973; Birnie, 1983; Lowe, 1984).

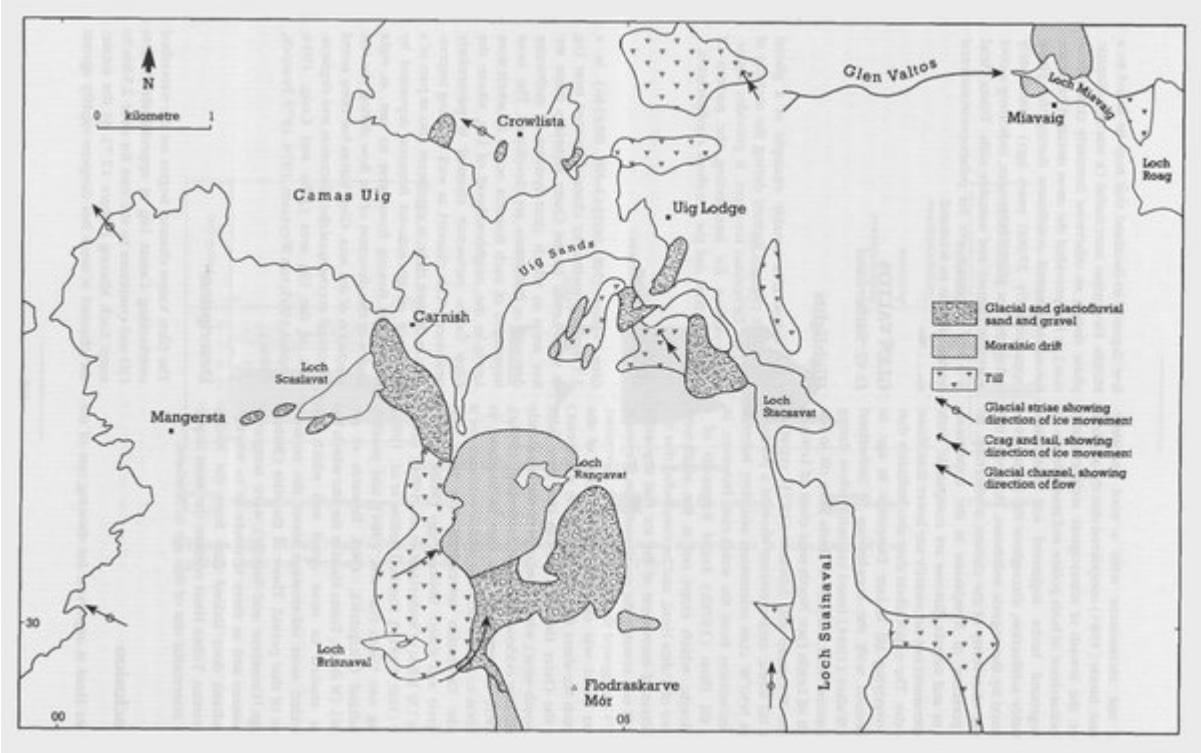

(Figure 12.7) Landforms and deposits of the Glen Valtos–Uig area (from Peacock, 1984a).

(Figure 12.8) Glen Valtos meltwater channel. The channel has the form of a single, narrow gorge. (Photo: D. G. Sutherland.)

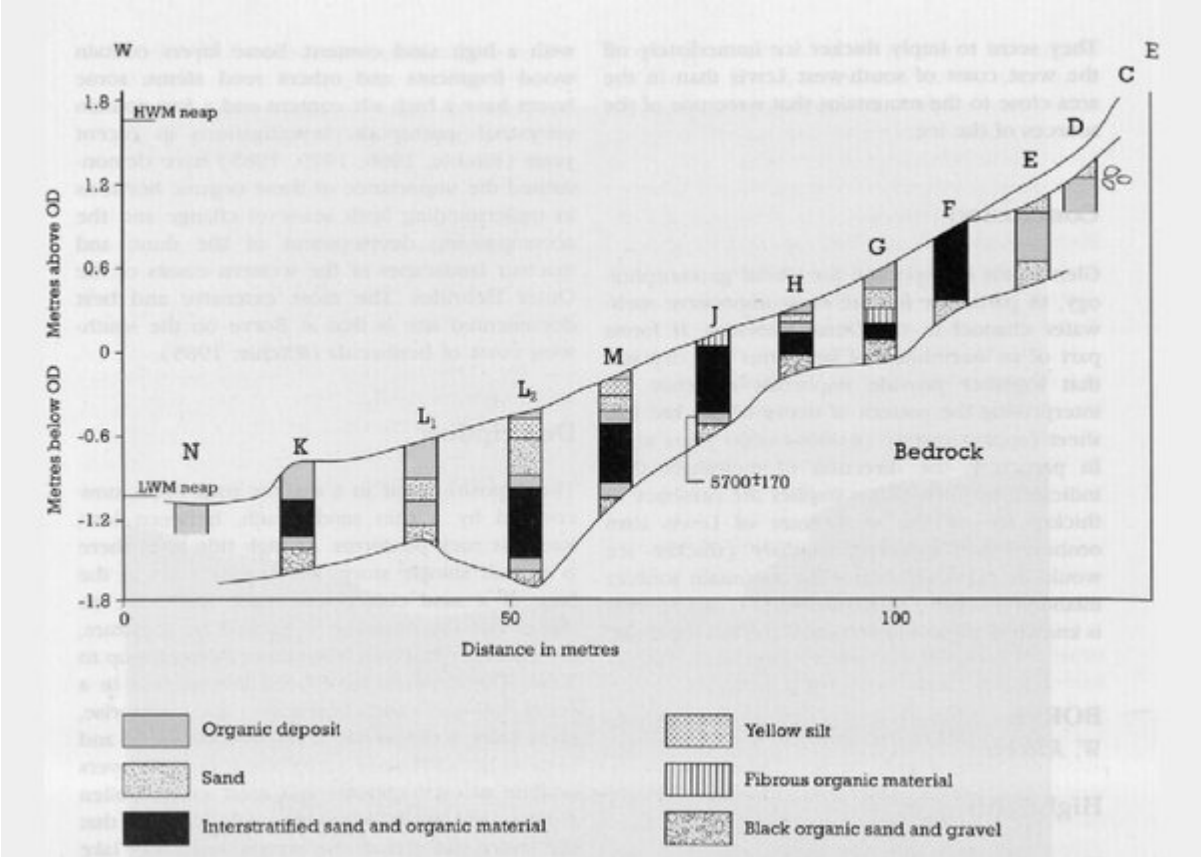

(Figure 12.9) Profile across the intertidal deposits at Borve, showing the sediment sequence and its variations (from Ritchie, 1985).

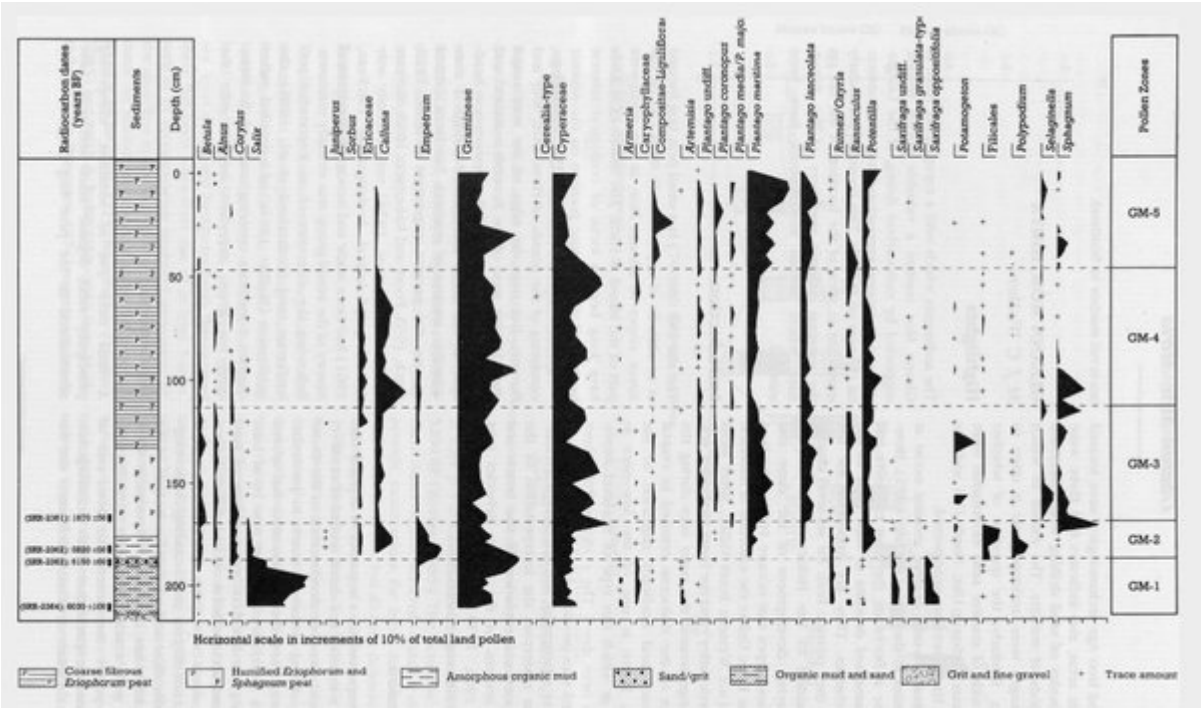

(Figure 12.10) Gleann Mor, Hirta: relative pollen diagram showing selected taxa as percentages of total land pollen (from Walker, 1984a).

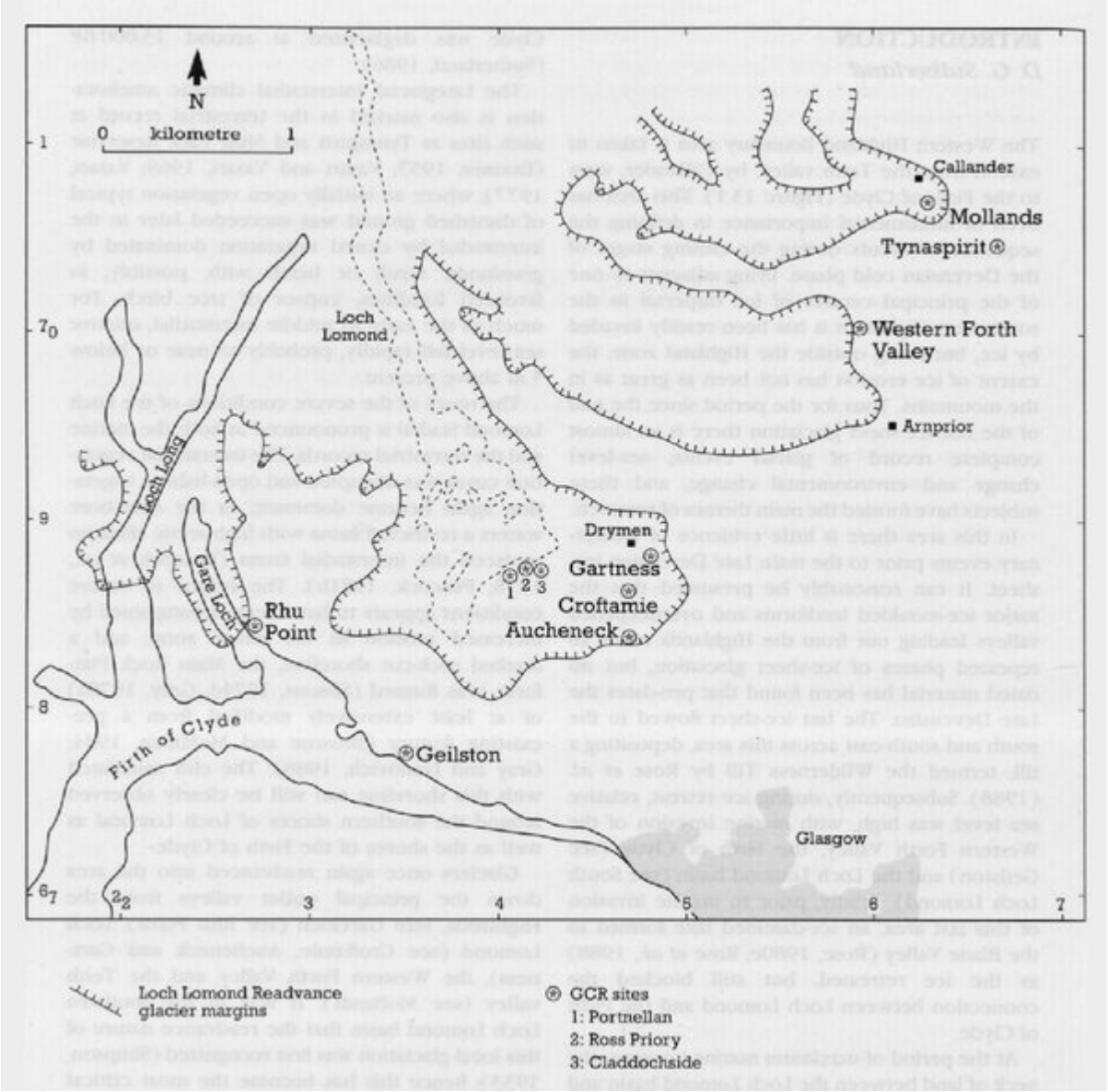

(Figure 13.1) Location map of the Western Highland Boundary area.

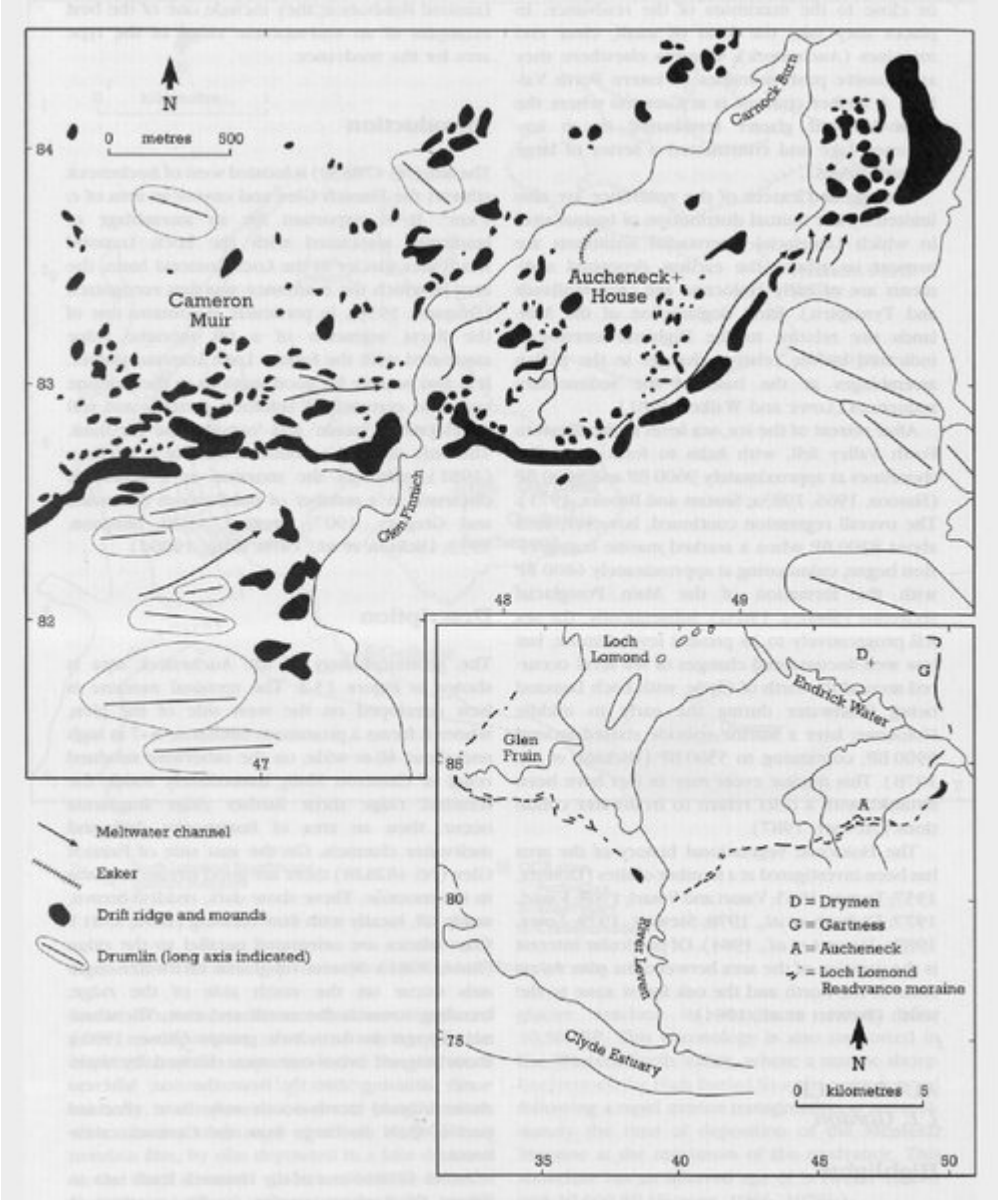

(Figure 13.2) Landforms and deposits associated with the Loch Lomond Readvance ice limit at Aucheneck (from Rose, 1981). Inset shows the wider extent of the moraine that marks the ice limit at the southern end of Loch Lomond (from Dickson et al., 1978).

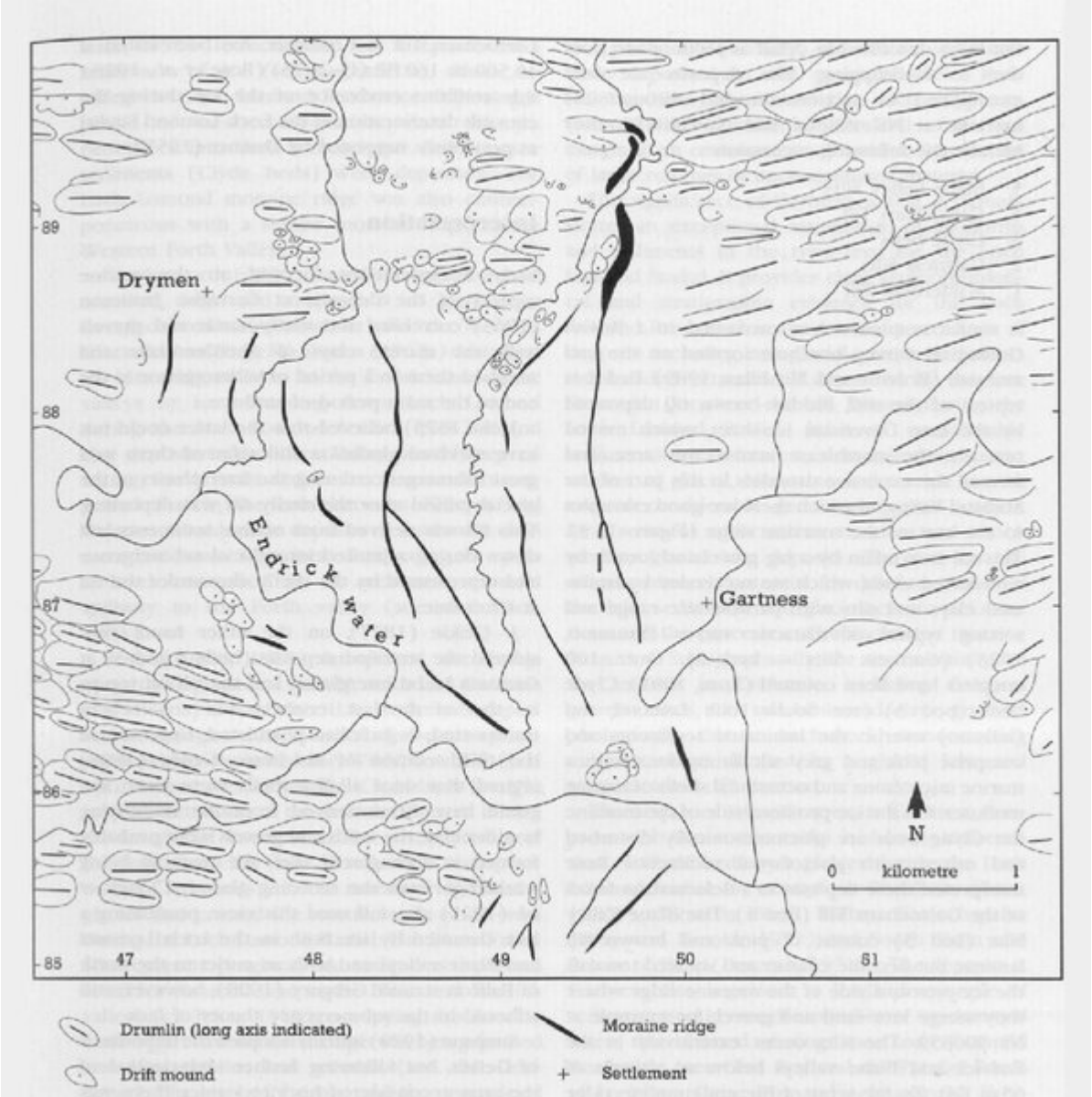

(Figure 13.3) Landforms and deposits associated with the Loch Lomond Readvance ice limit at Gartness (from Rose, 1980e, 1981).

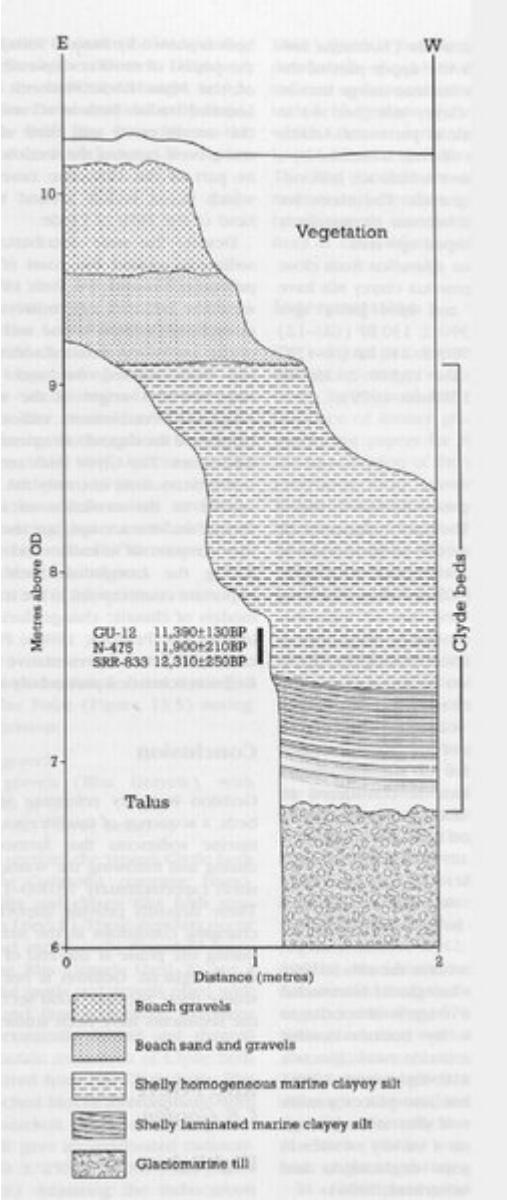

(Figure 13.4) Geilston: sequence of sediments (from Rose, 1980a).

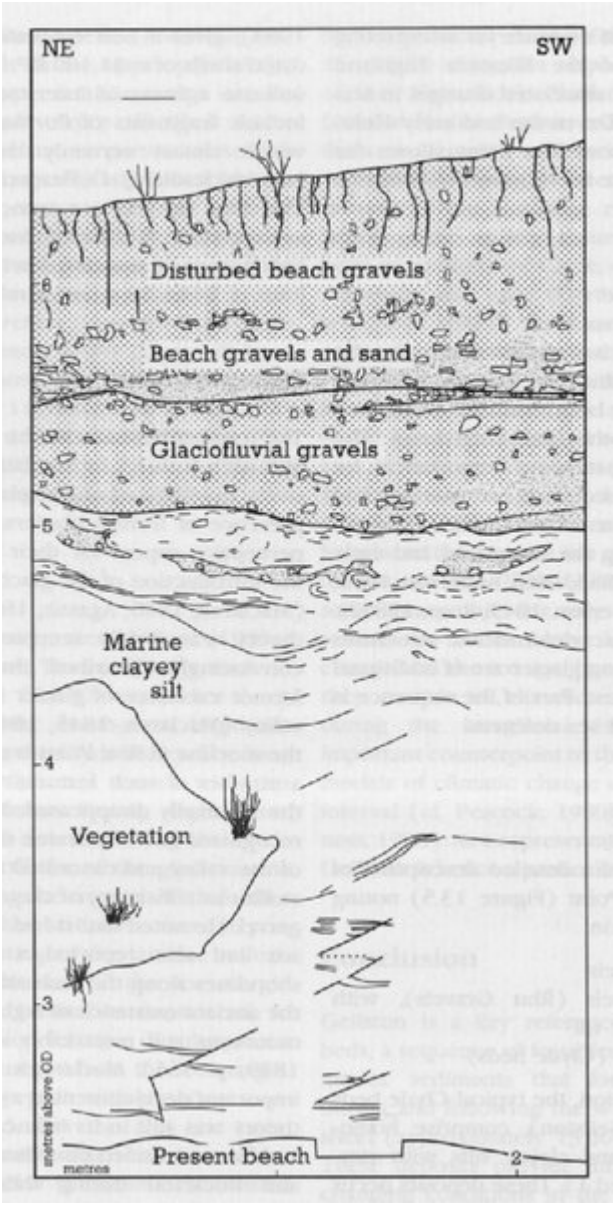

(Figure 13.5) Rhu Point: section showing glacially deformed Clyde beds, Rhu Gravels and Holocene raised beach deposits (from Rose, 1980c).

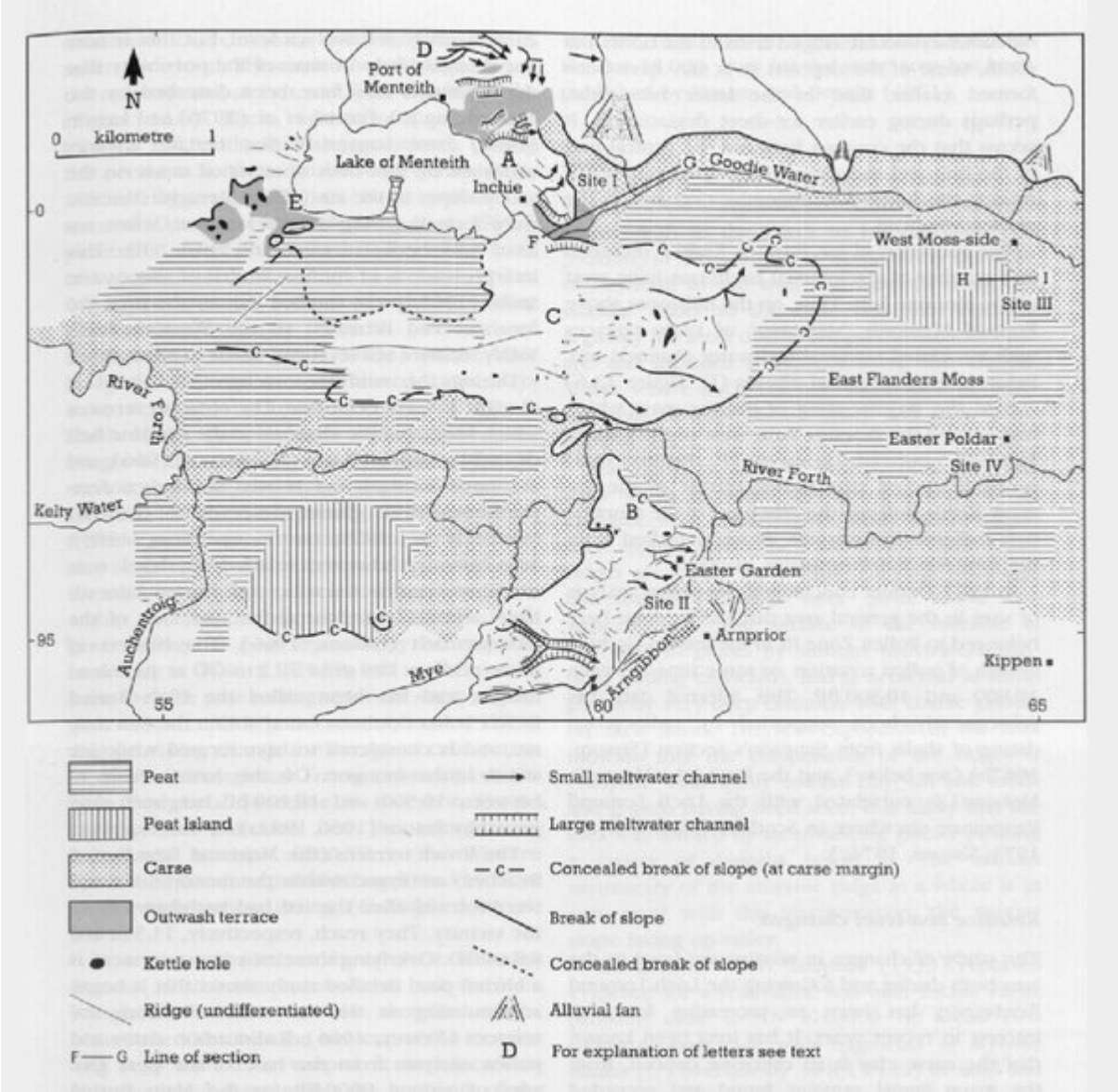

(Figure 13.6) Geomorphology of the Western Forth Valley.

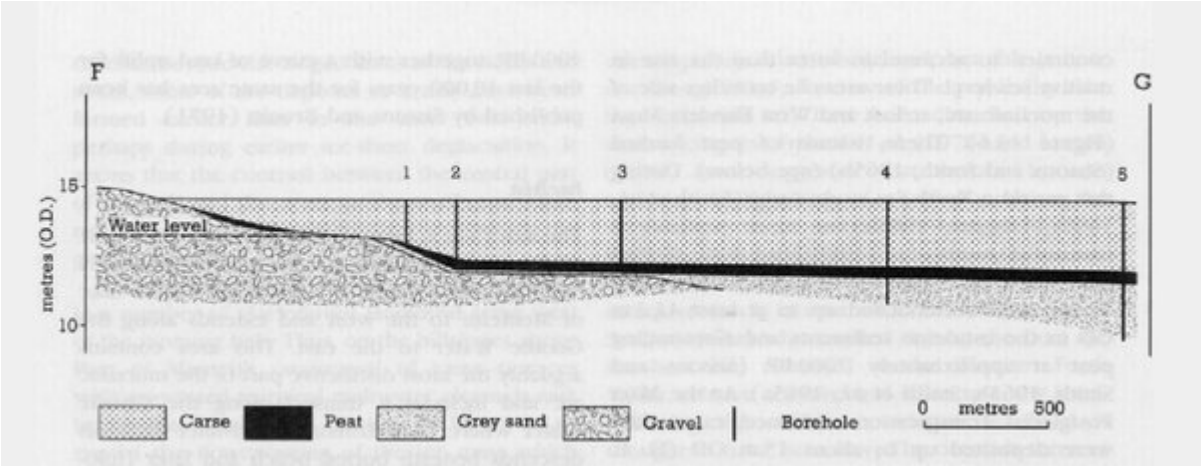

(Figure 13.7) Western Forth Valley: section along the Goodie Water (from Sissons et al., 1965). See Figure 13.6 for location of section.

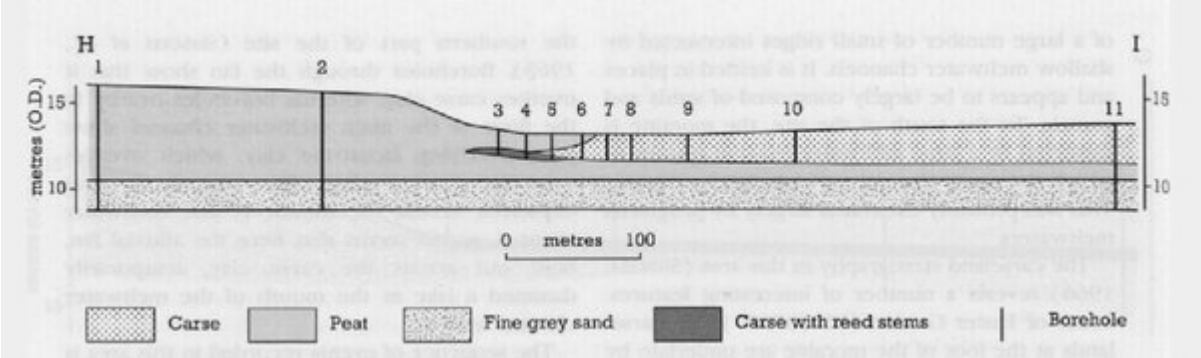

(Figure 13.8) Western Forth Valley: section at West Mossside, East Flanders Moss (from Sissons and Smith, 1965b). See Figure 13.6 for location of section.

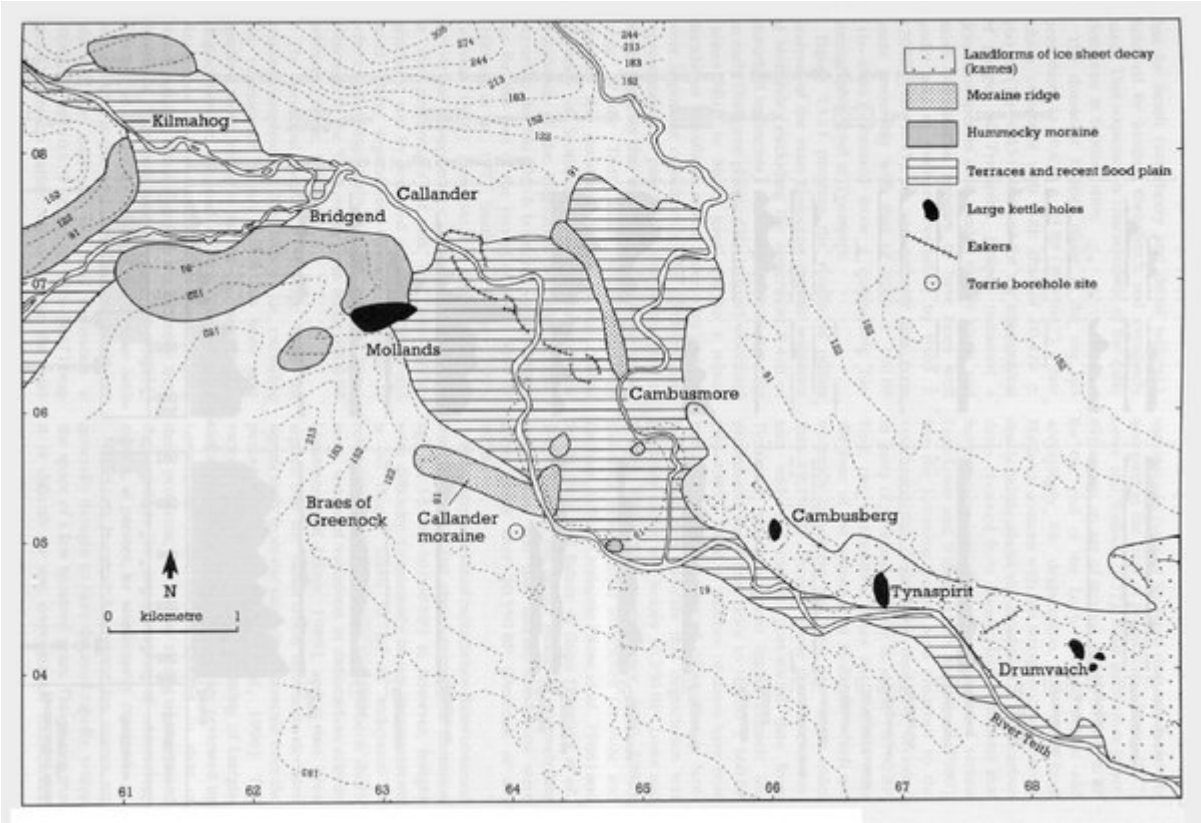

(Figure 13.9) Glacial and glaciofluvial landforms of the Callander area (from Lowe, 1978, after Thompson, 1972).

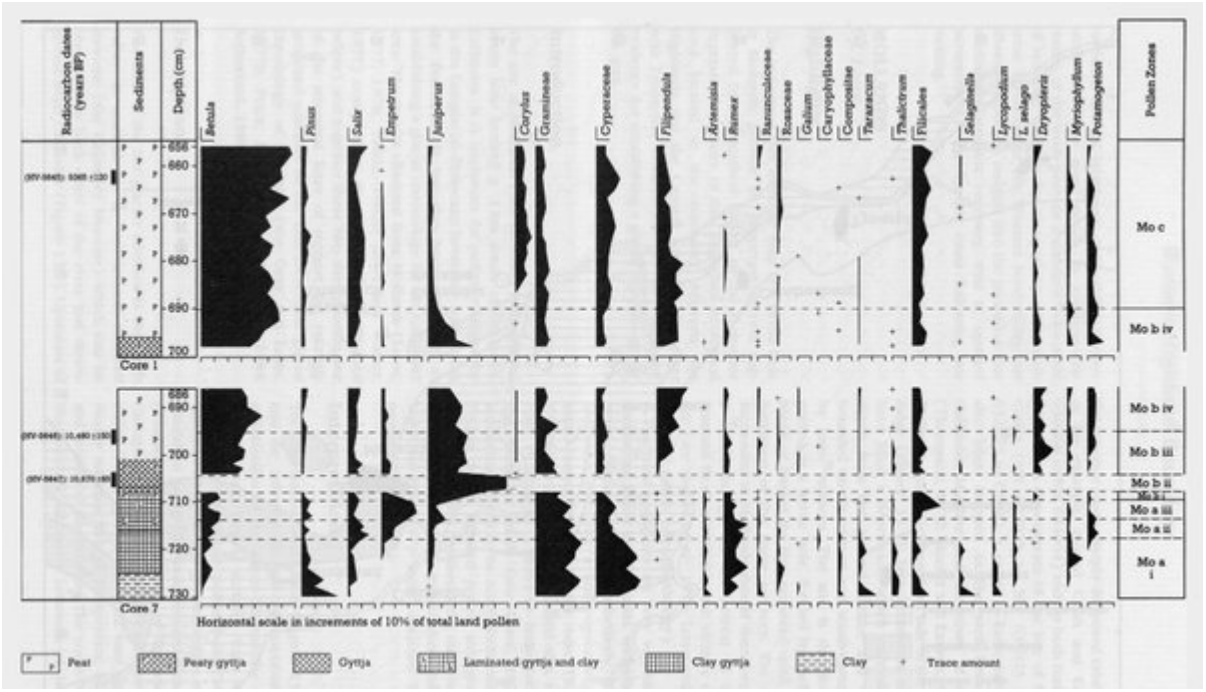

(Figure 13.10) Mollands: Lateglacial and early Holocene relative pollen diagram showing selected taxa as percentages of total land pollen (from Lowe, 1978).

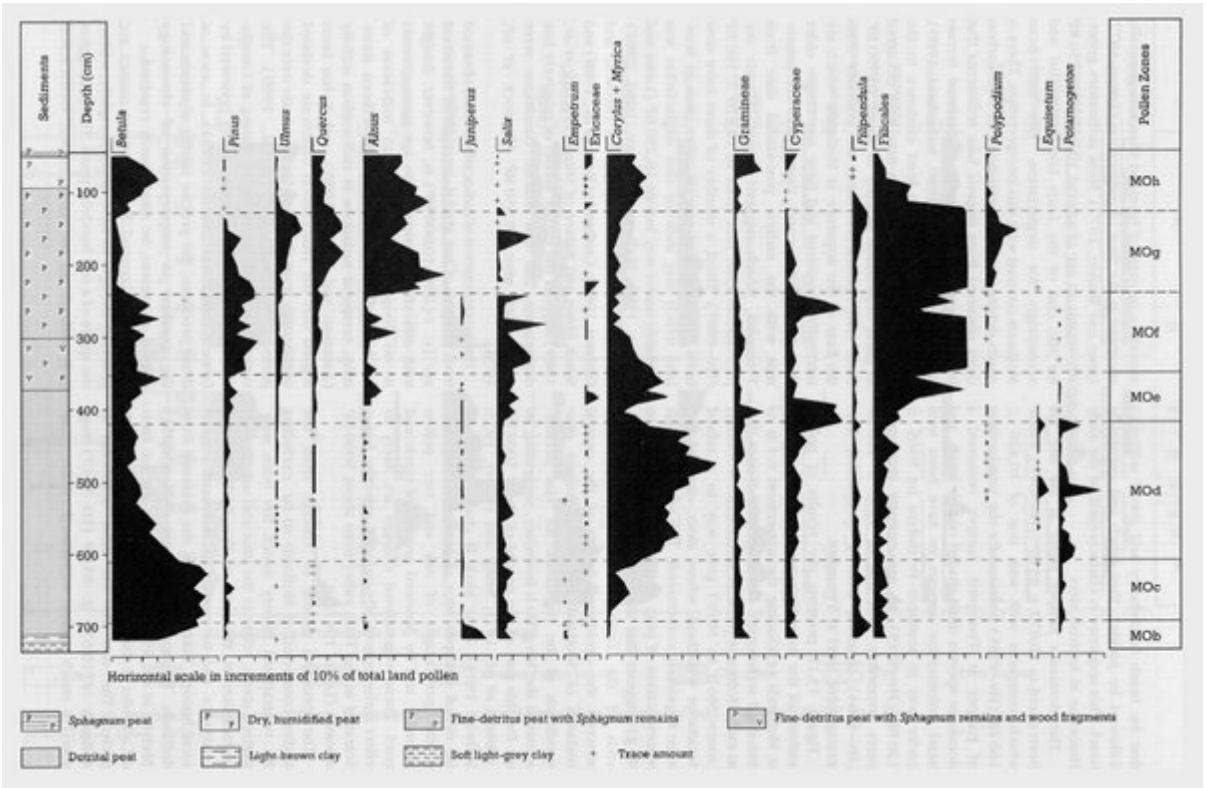

(Figure 13.11) Mollands: main Holocene relative pollen diagram showing selected taxa as percentages of total land pollen (from Lowe, 1982a).

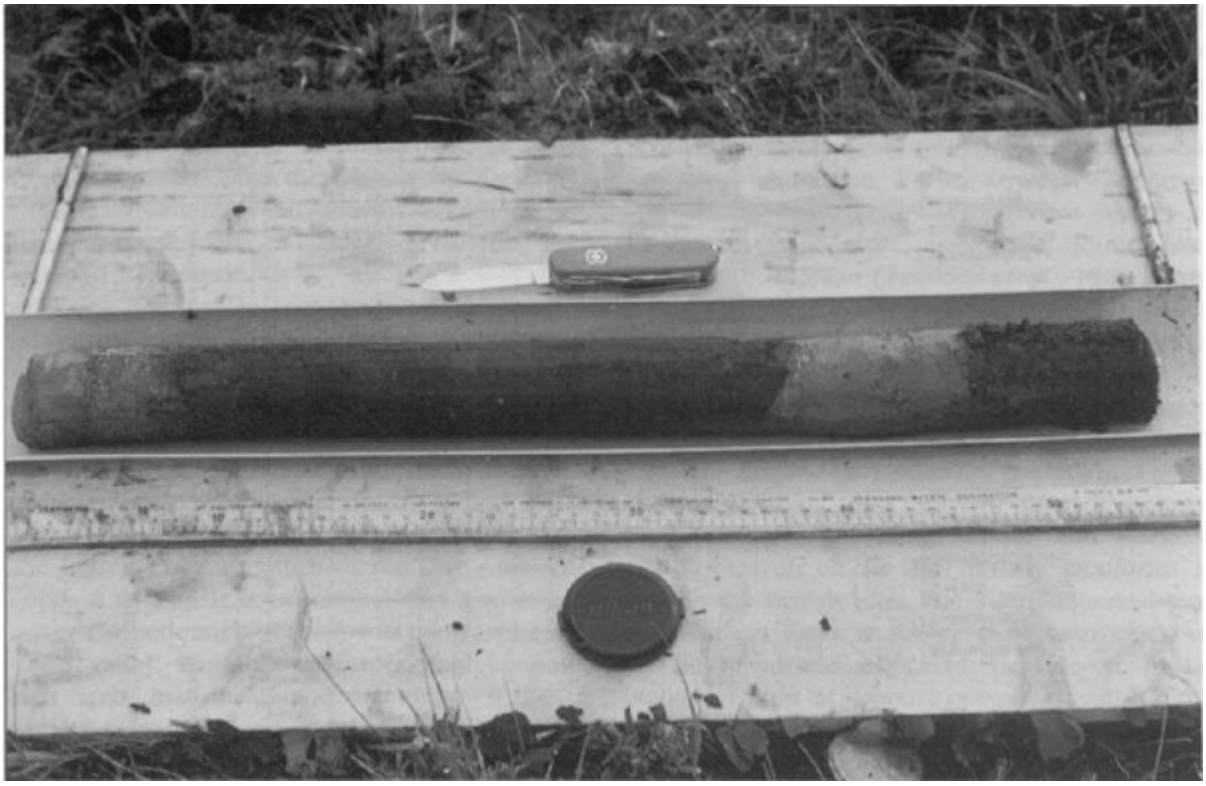

(Figure 13.12) Core from the basal sediments at Tynaspirit. From the left, the sequence comprises Late Devensian minerogenic sediments, organic Lateglacial Interstadial sediments, Loch Lomond Stadial silts and clays, and early Holocene organic lake muds. (Photo: M. J. C. Walker.)

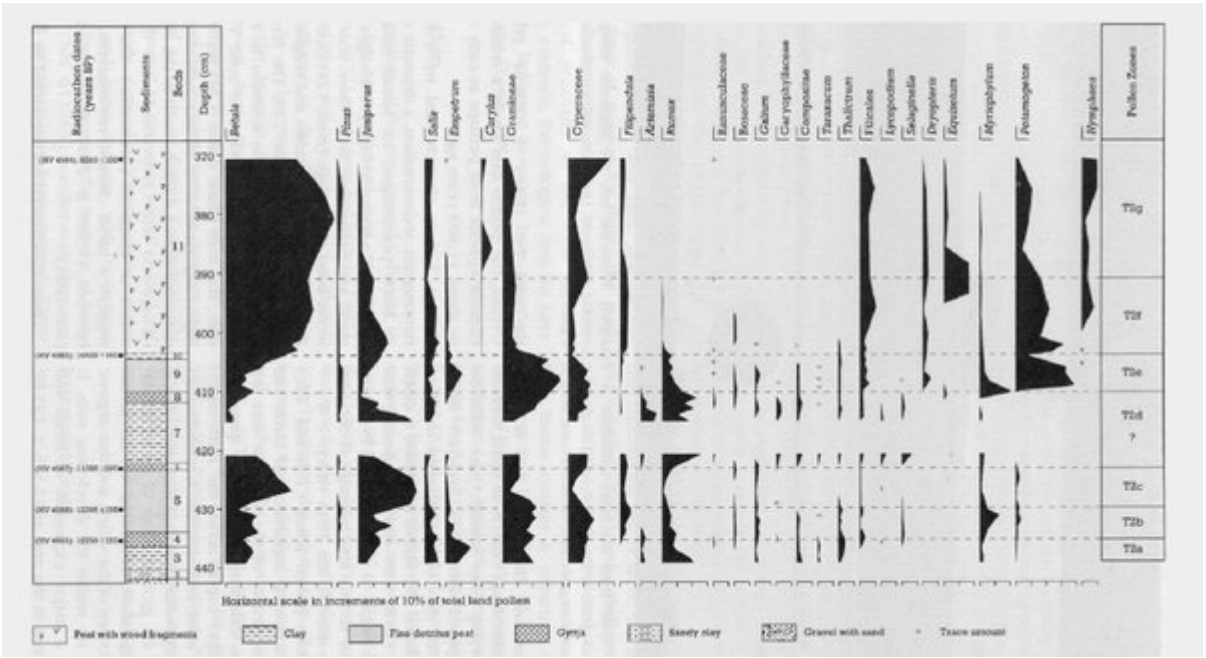

(Figure 13.13) Tynaspirit: relative pollen diagram showing selected taxa as percentages of total land pollen (from Lowe, 1978).

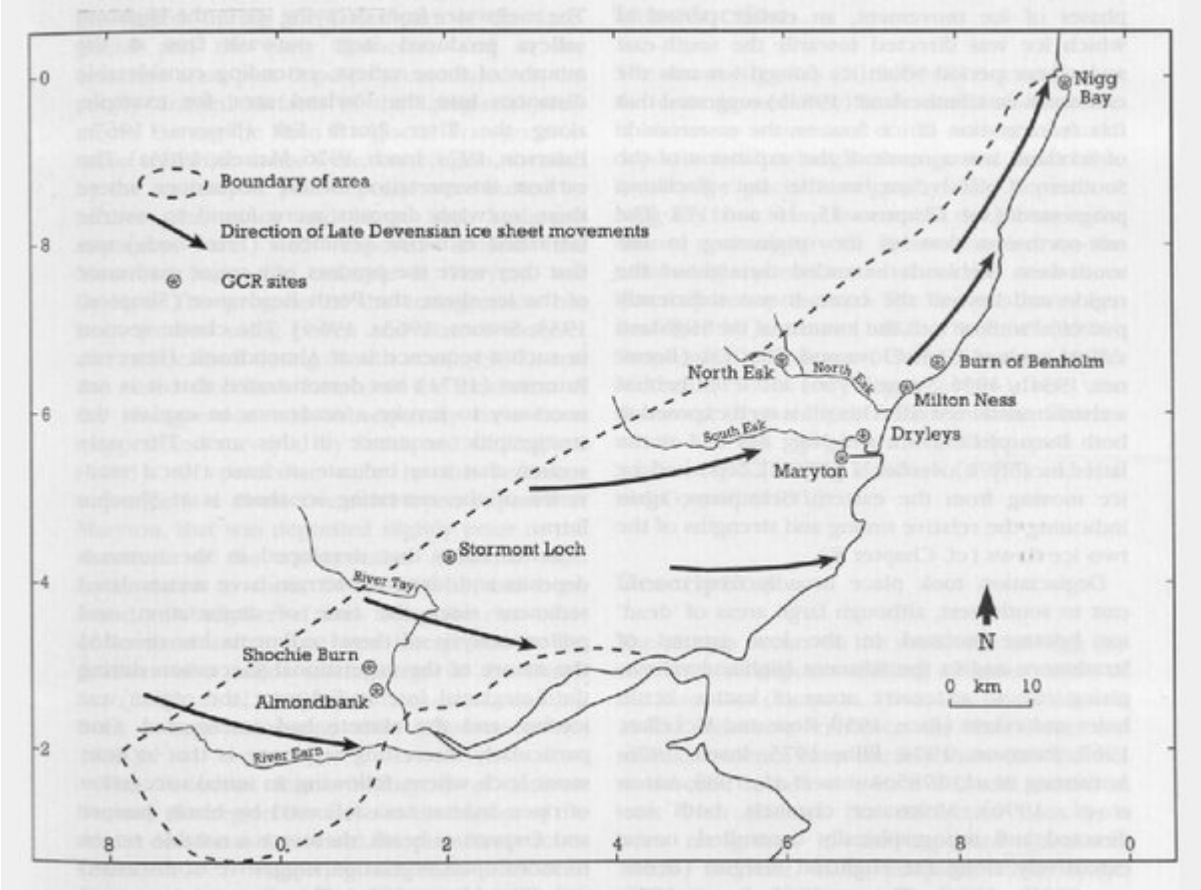

(Figure 14.1) Location map of the Eastern Highland Boundary area.

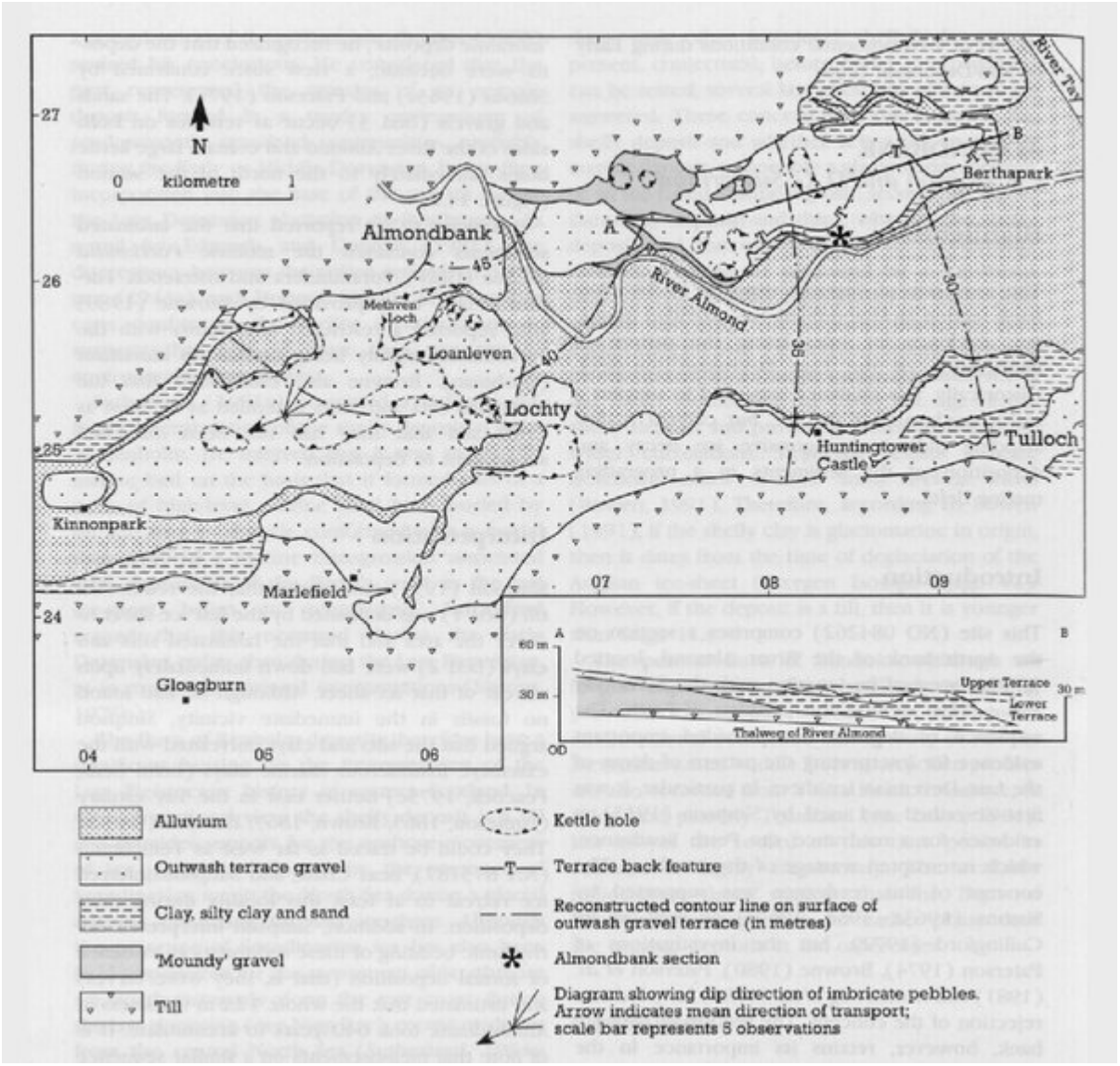

(Figure 14.2) Map and section of Late glacial deposits in the Almond Valley (from Paterson, 1974).

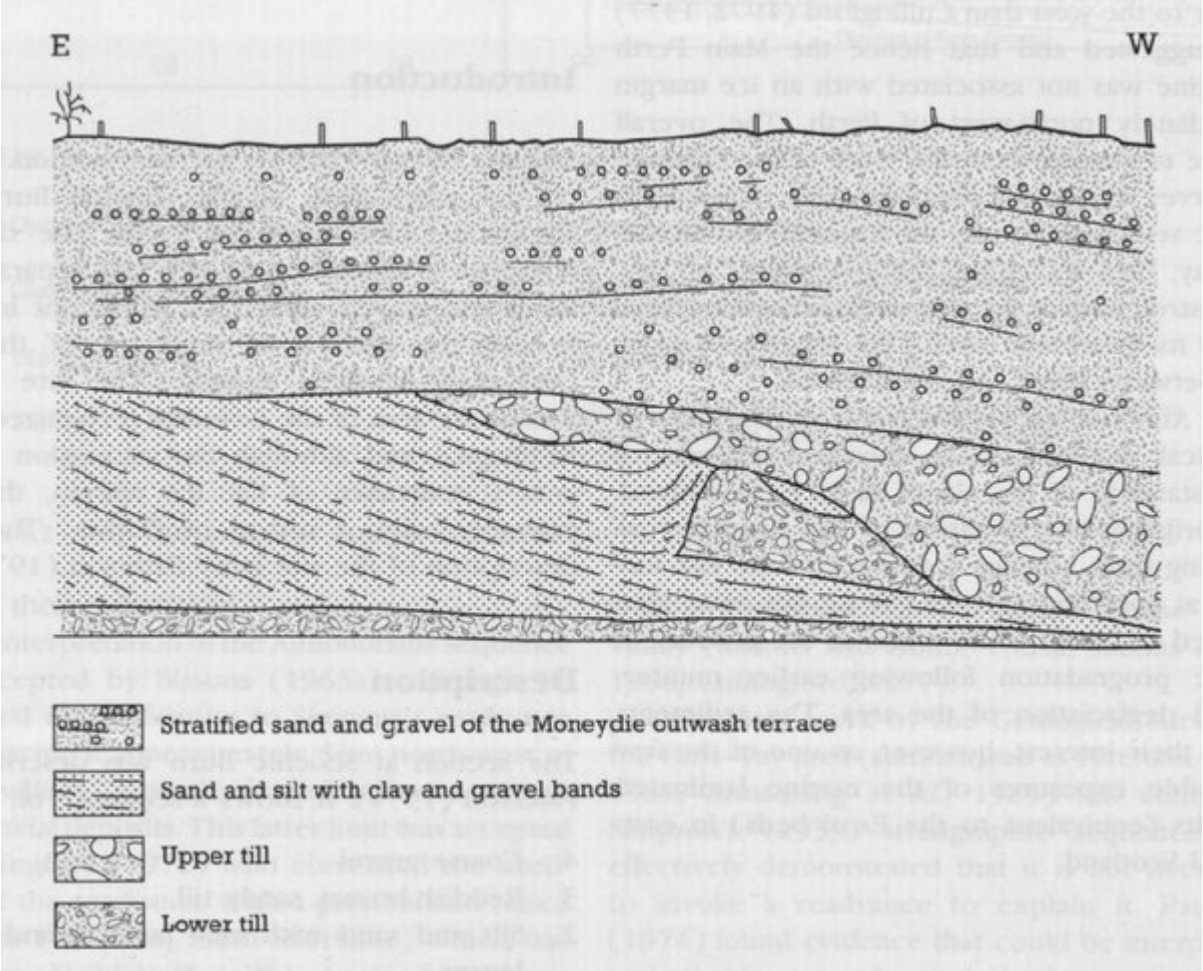

(Figure 14.3) Sketch section of glacial deposits at Shochie Burn (unscaled) (from Paterson, 1974).

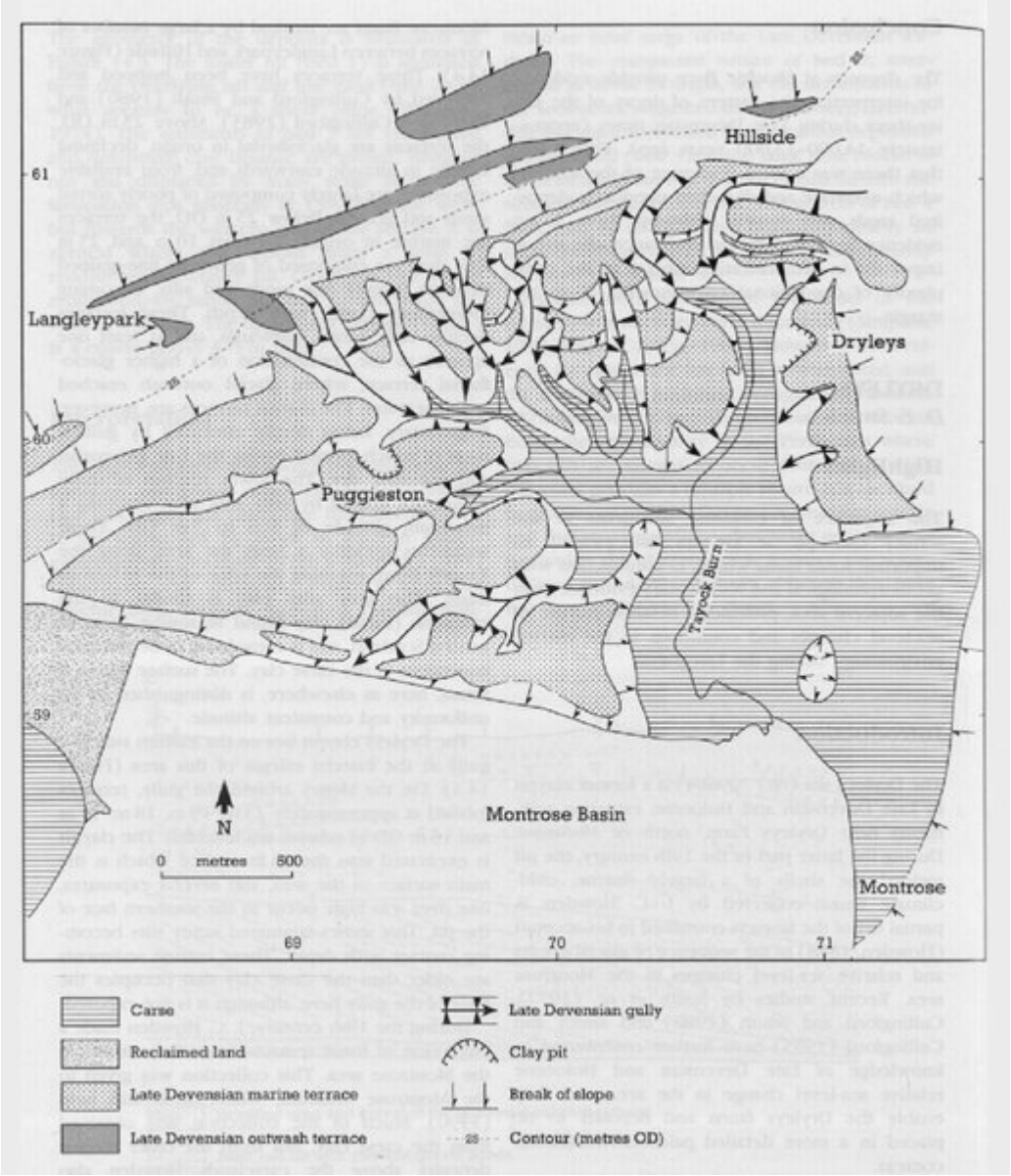

(Figure 14.4) Lateglacial and Holocene raised marine deposits in the Dryleys area.

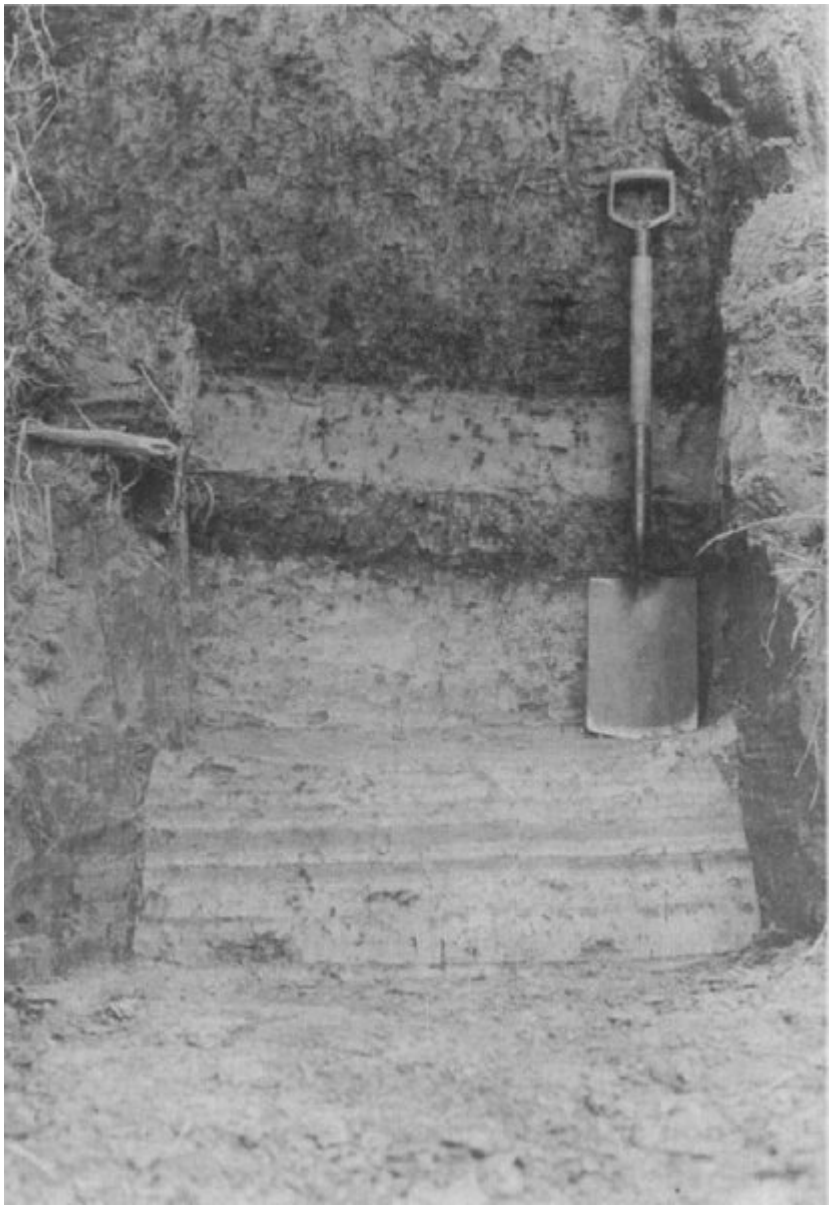

(Figure 14.5) Section at Maryton. Laminated Late Devensian marine clays are overlain by peat then a layer of grey, micaceous, silty, fine sand interpreted as a tsunami deposit. Above the latter is silty peat then carse clay. (Photo: D. E. Smith.)

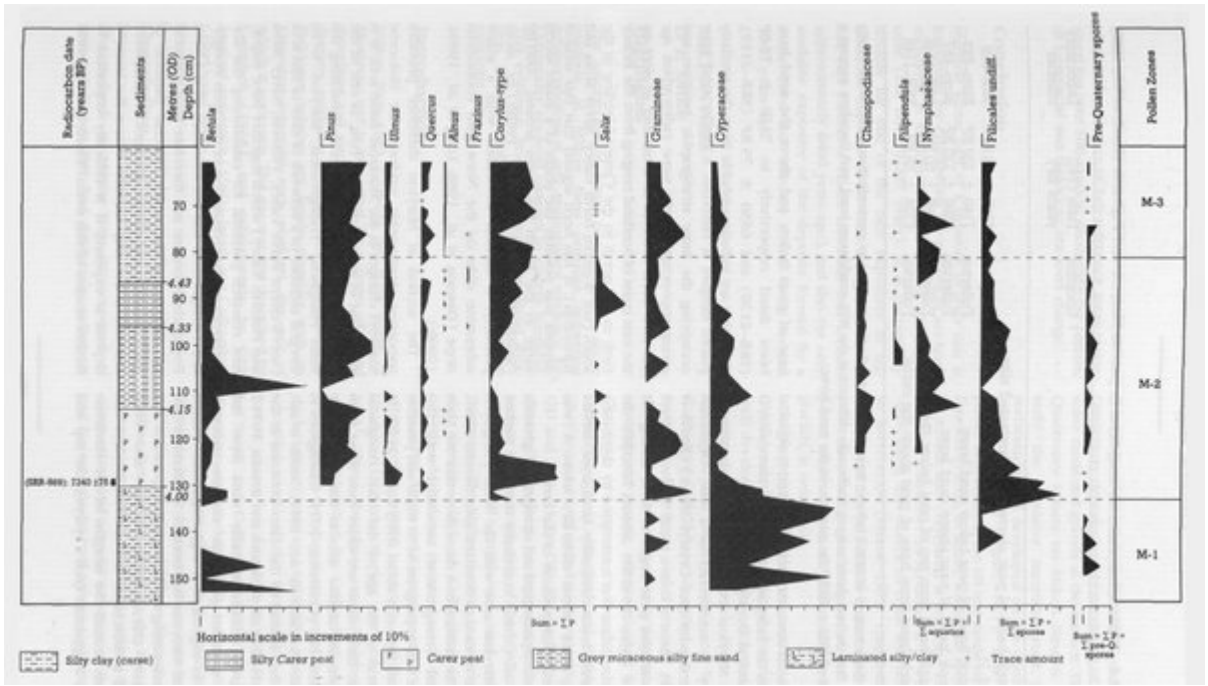

(Figure 14.6) Marylon: relative pollen diagram showing selected taxa as percentages of total pollen (from Smith et al., 1980).

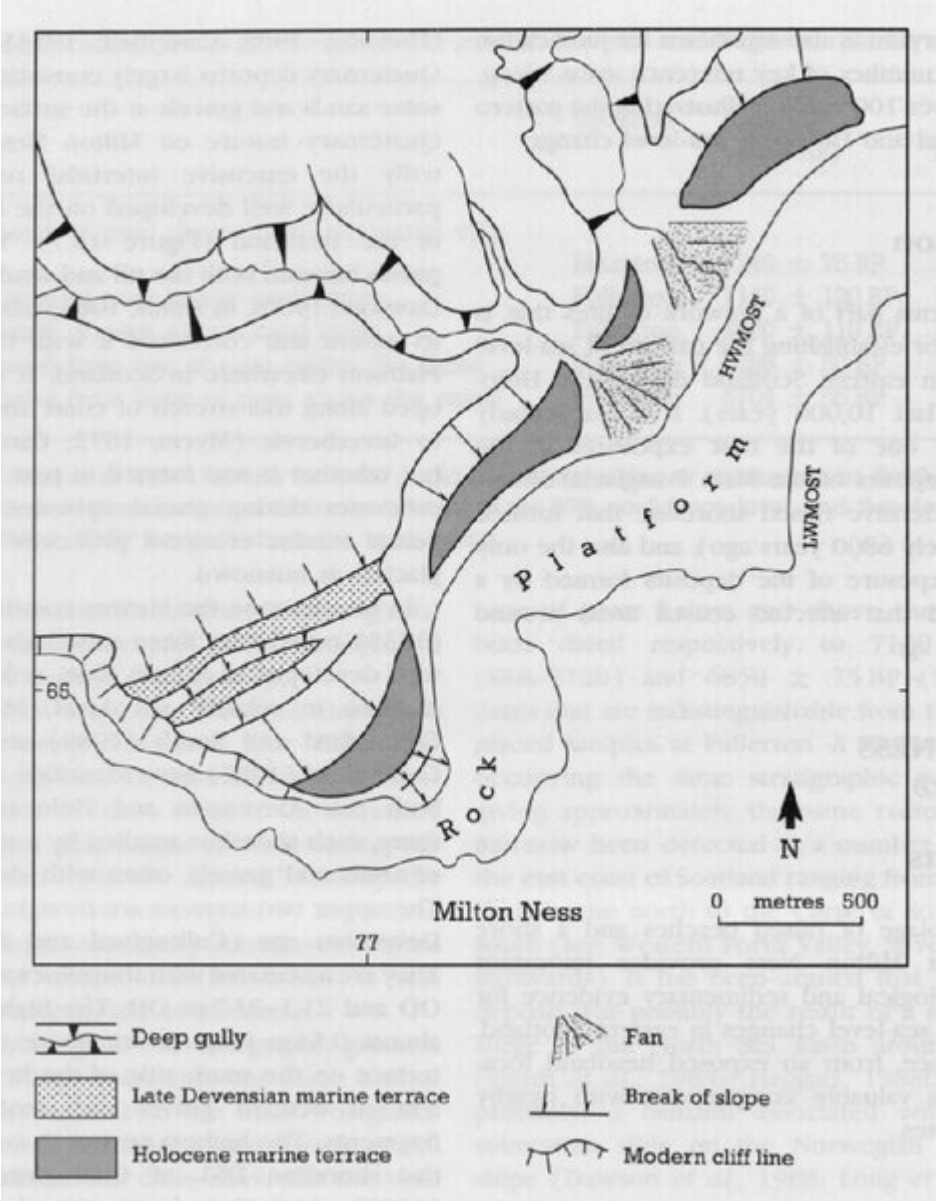

(Figure 14.7) Raised shorelines and intertidal shore platform at Milton Ness.

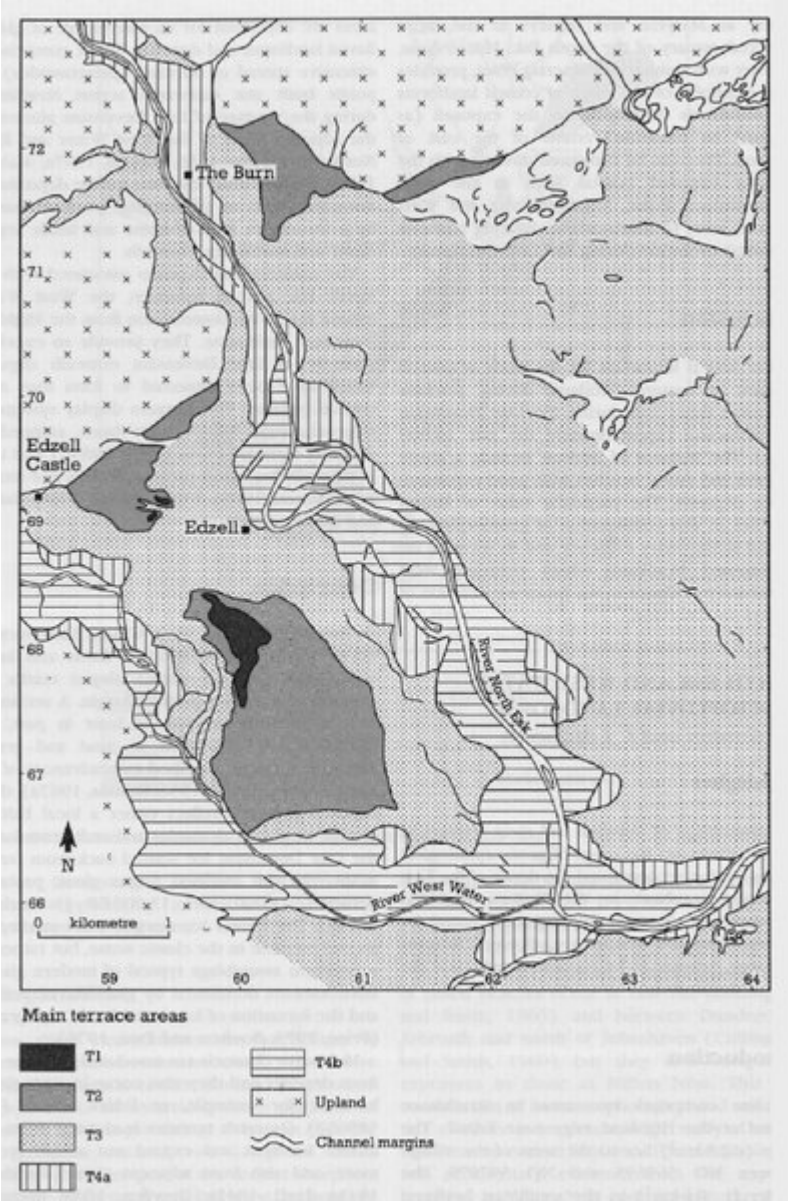

(Figure 14.8) Terraces of the River North Esk and West Water in the Edzell area (from Maizels, 1983a).

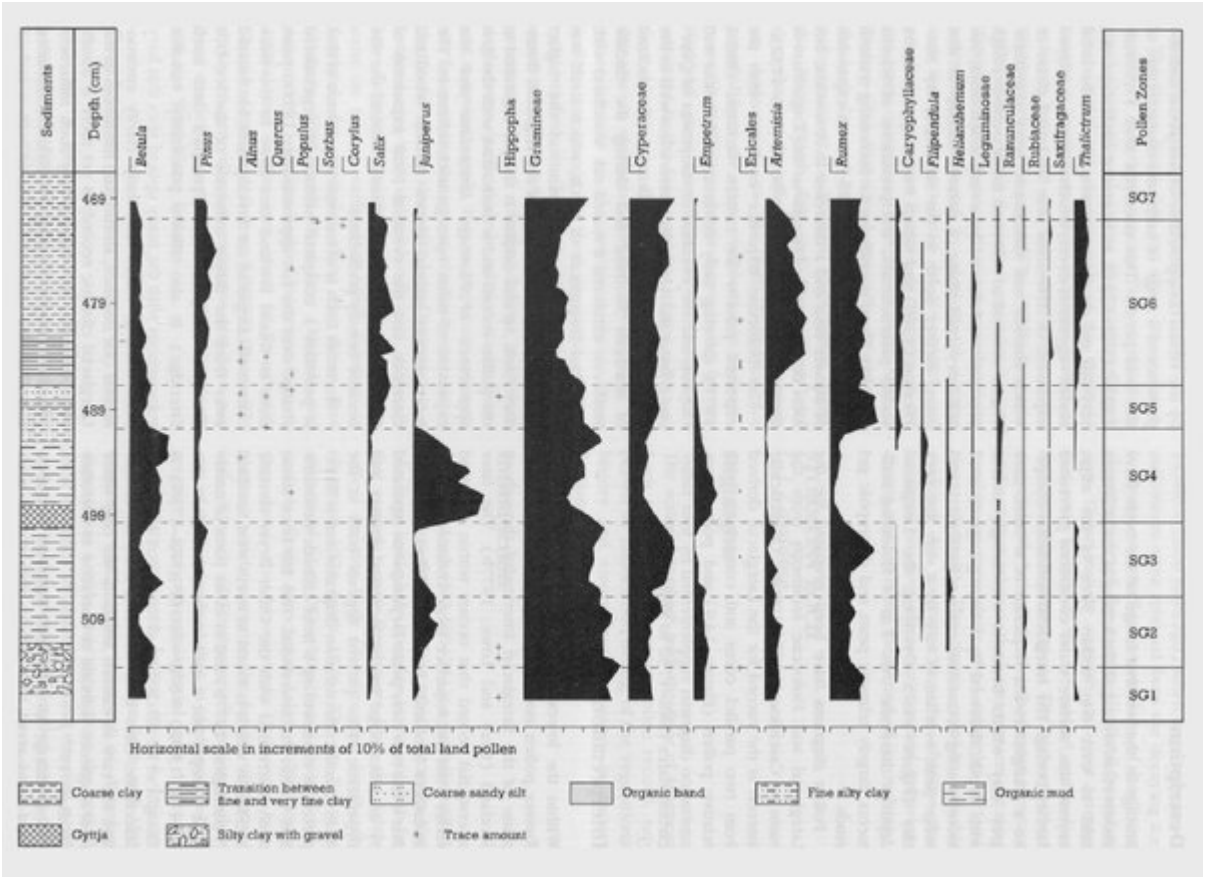

(Figure 14.9) Stormont Loch: relative pollen diagram for core SGI showing selected taxa as percentages of total land pollen (from Caseldine, 1980a).

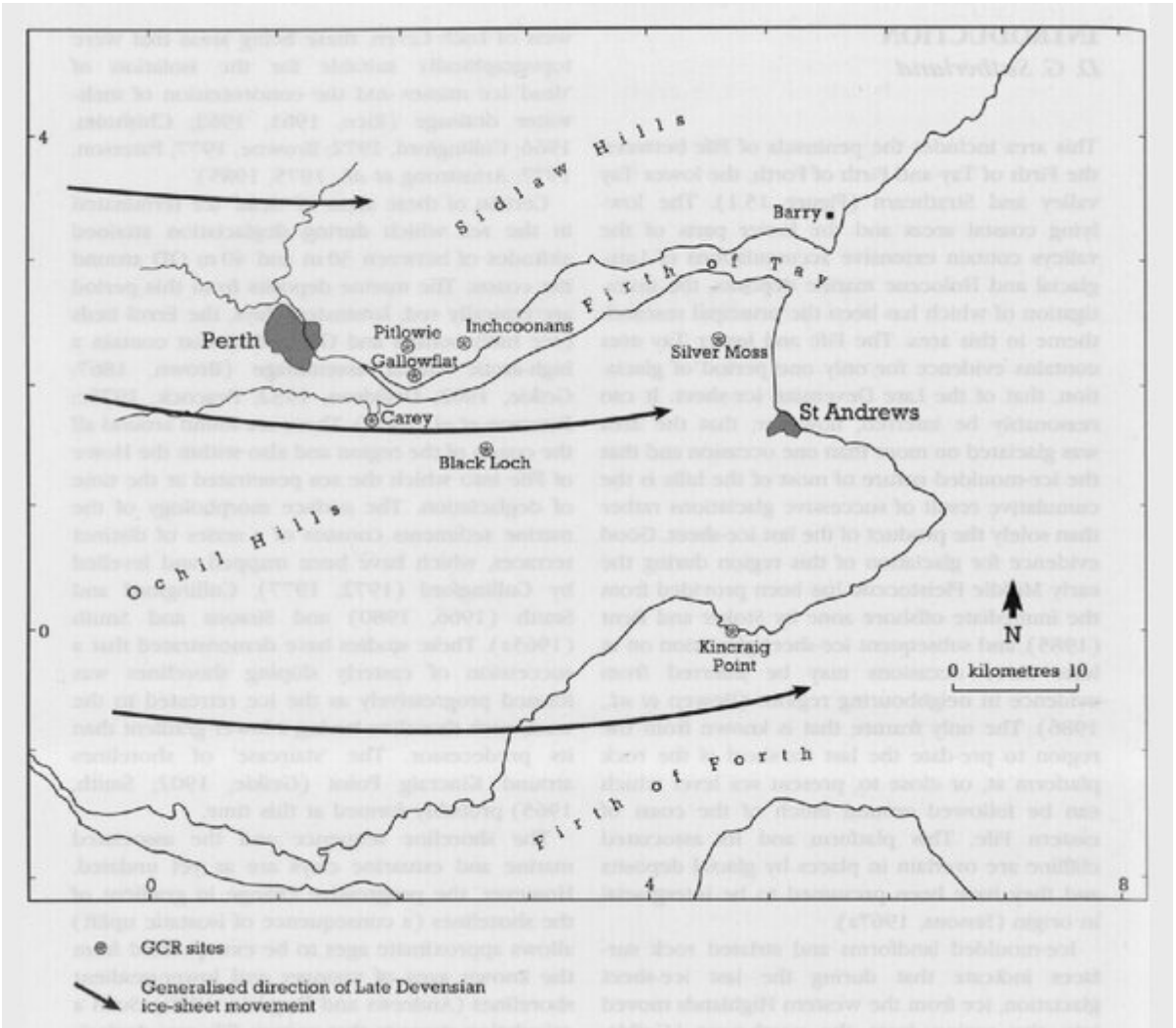

(Figure 15.1) Location map of the Fife and the Lower Tay area.

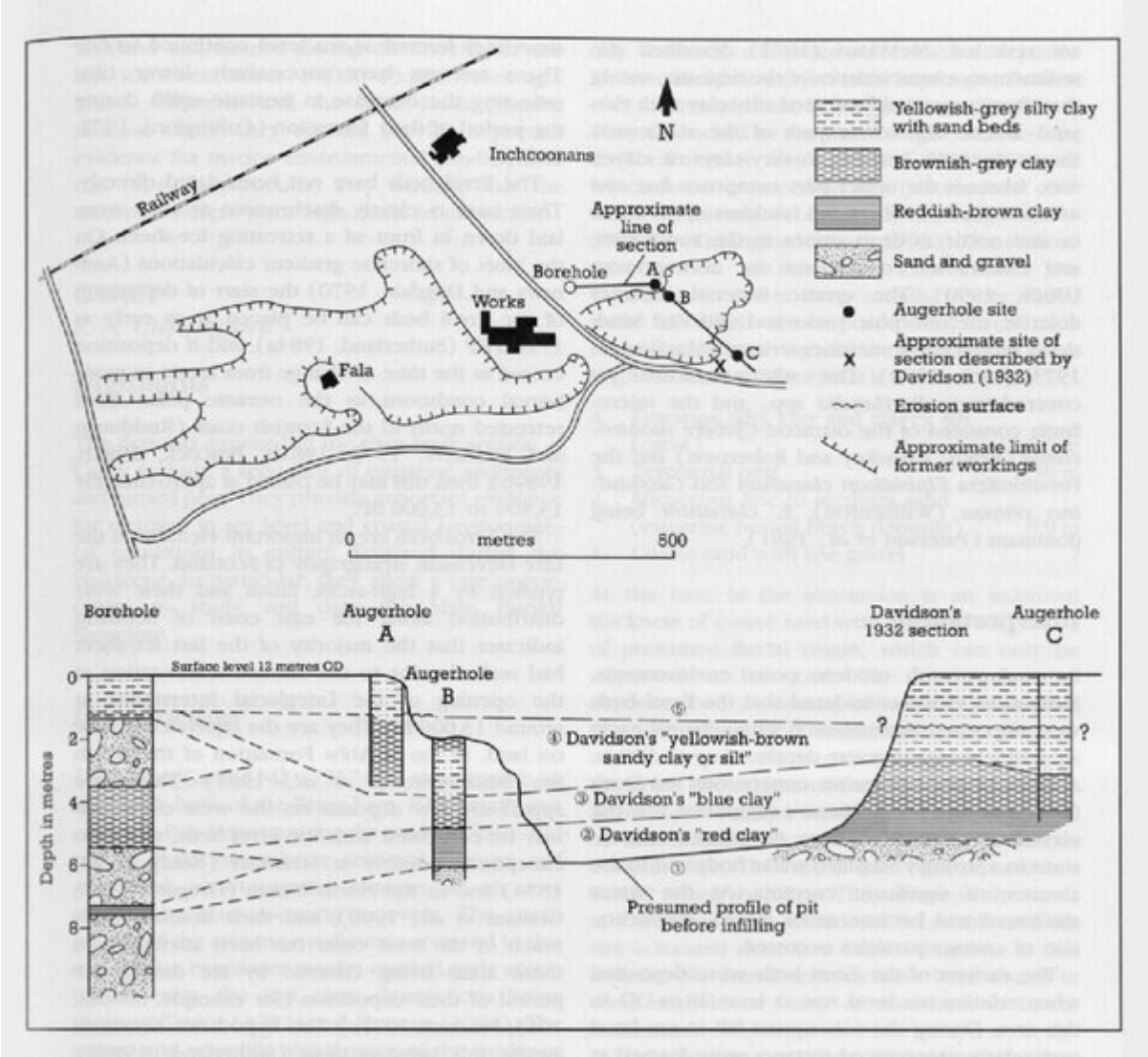

(Figure 15.2) Inferred stratigraphy of the Errol beds at Inchcoonans claypit (from Paterson et al., 1981).

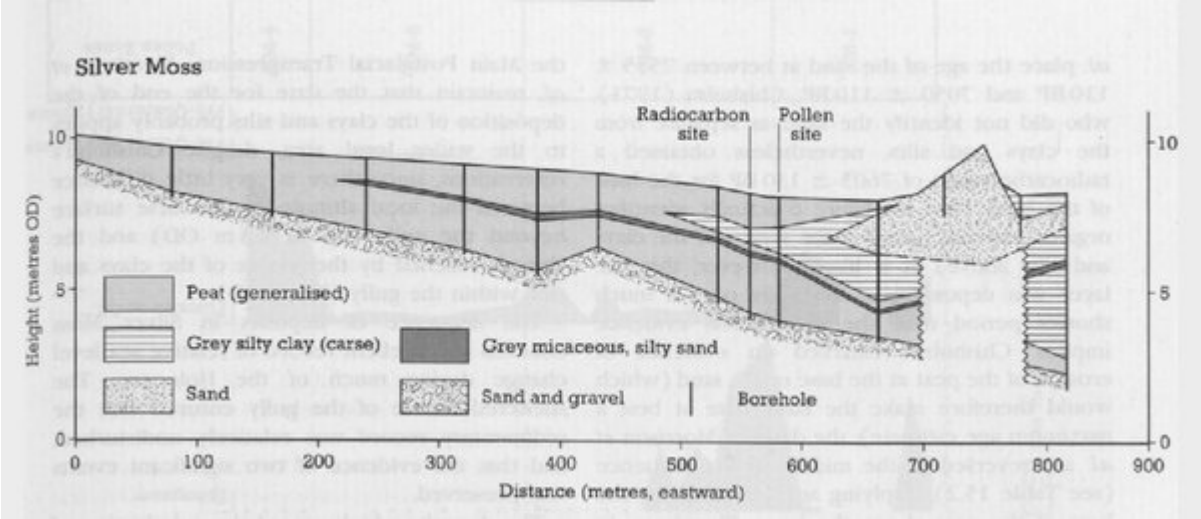

(Figure 15.3) Silver Moss: section along the gully showing the sequence of sediments (from Morrison et al., 1981).

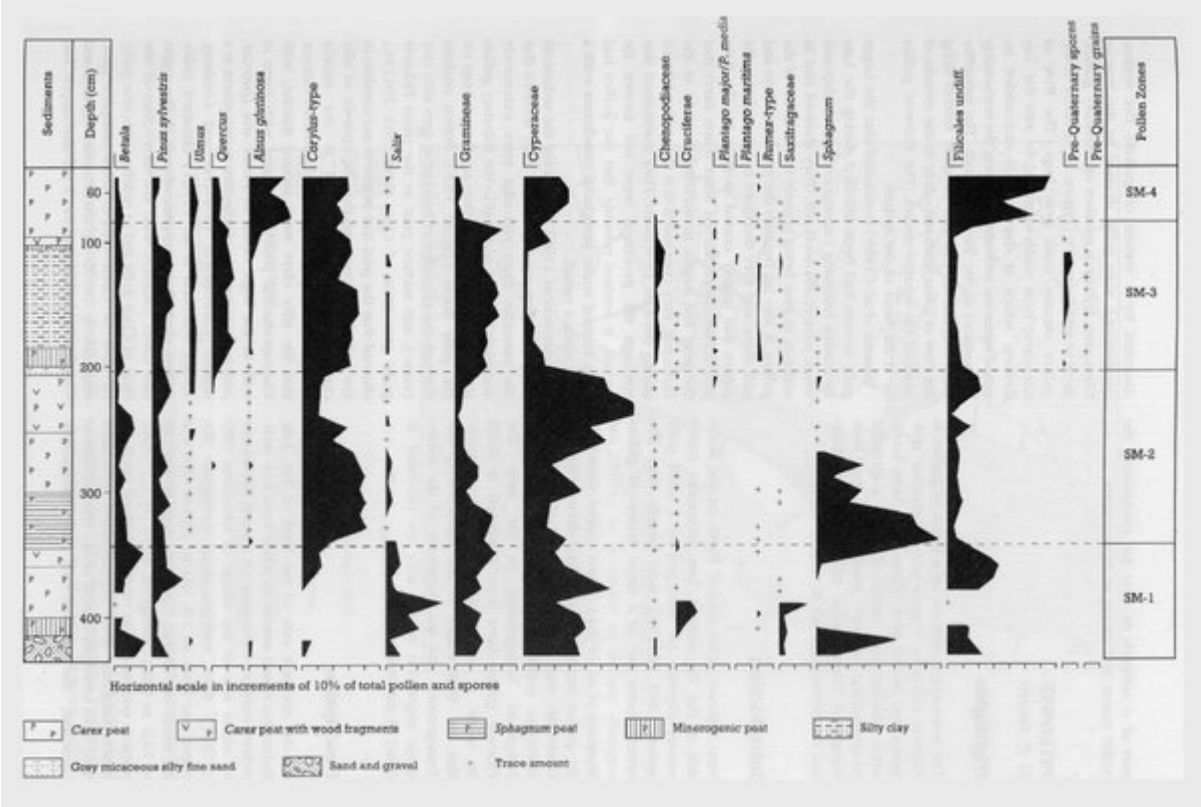

(Figure 15.4) Silver Moss: relative pollen diagram showing selected taxa as percentages of total pollen and spores (from Morrison et al., 1981).

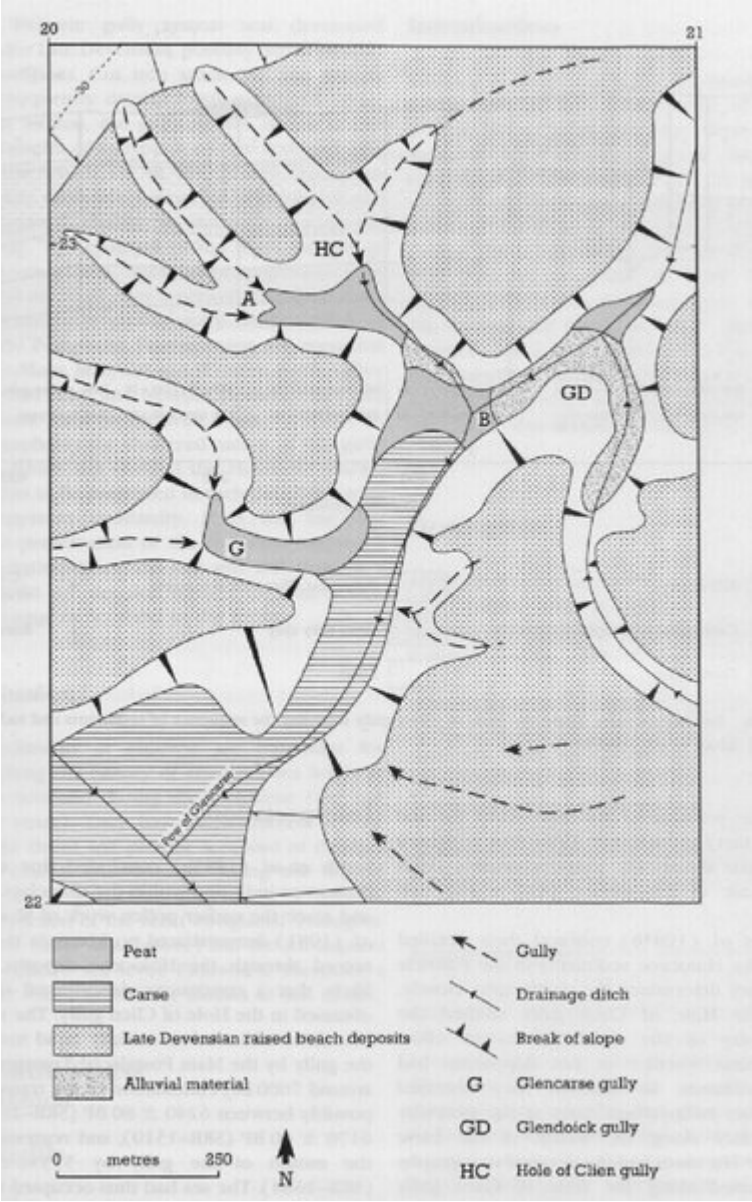

(Figure 15.5) Geomorphology of the Pitlowie gullies (from Morrison et al., 1981). The sediment sequence along the line AB is shown in Figure 15.6.

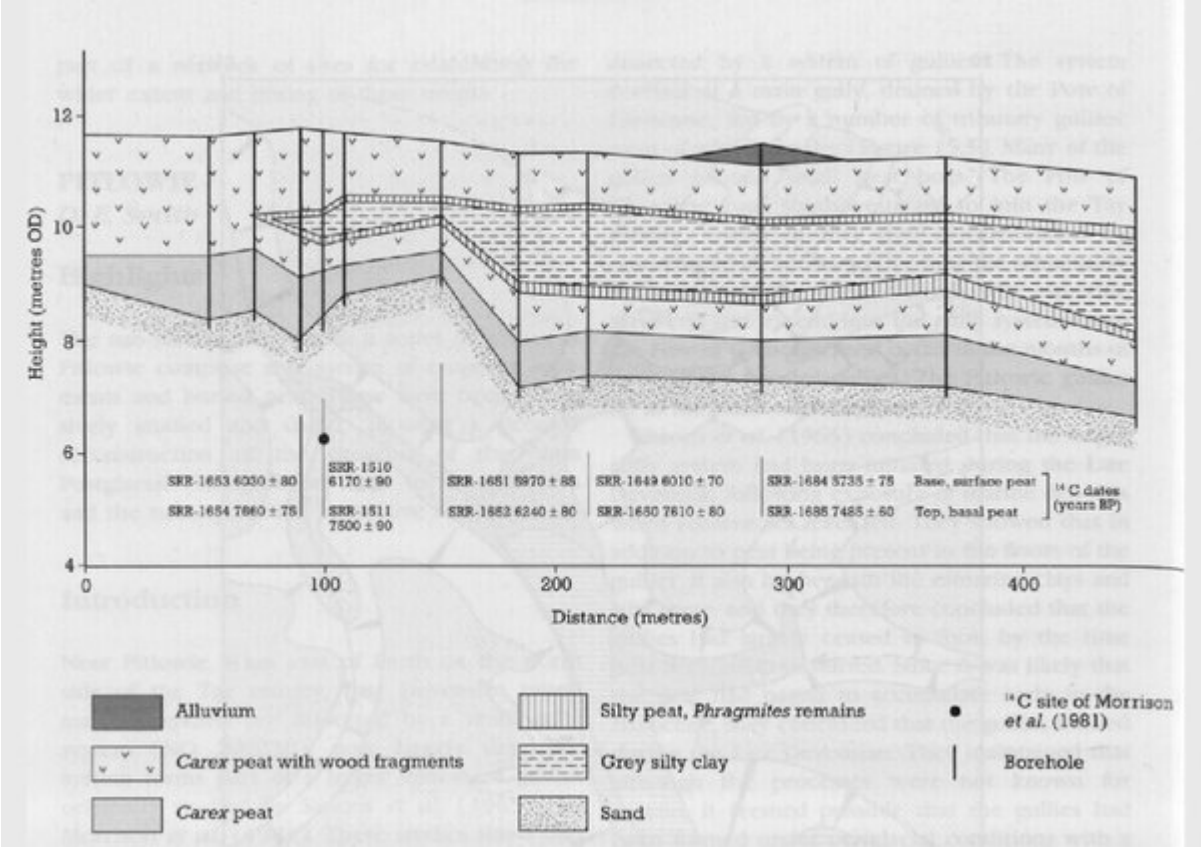

Figure 15.6 Pitlowie: section along the Hole of Clien gully showing the sequence of sediments and radiocarbon dates (from Smith et al., 1985b).

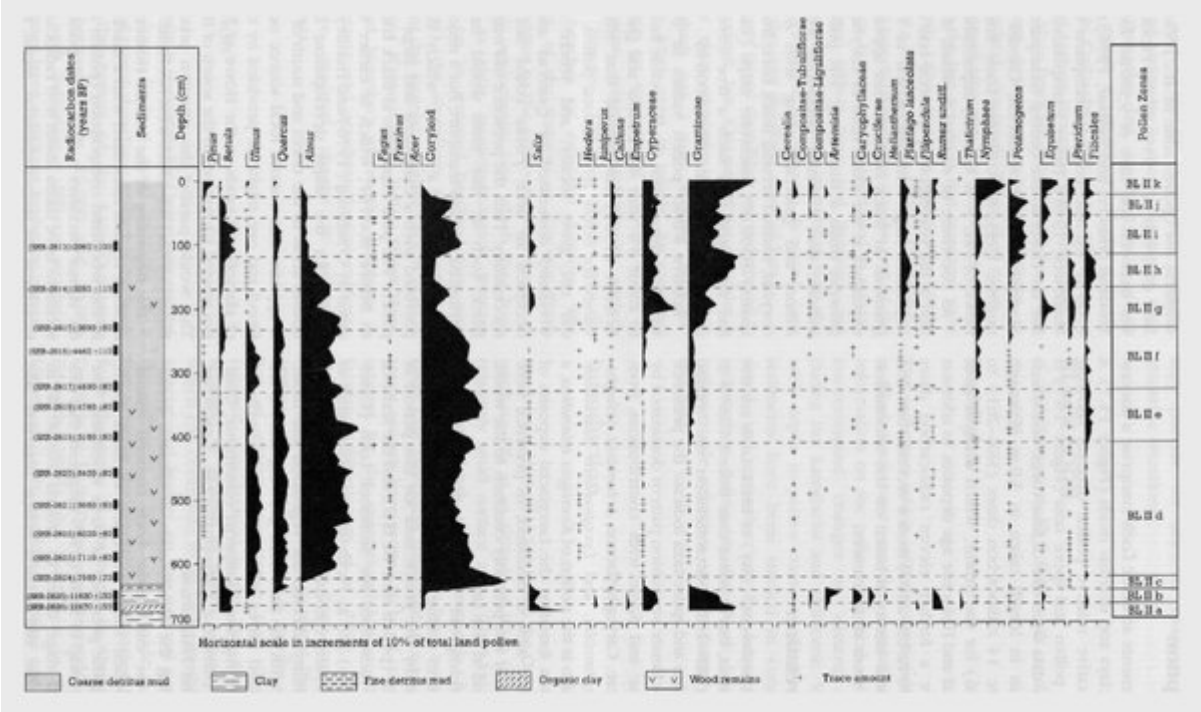

(Figure 15.7) Black Loch: relative pollen diagram at coring site BL II showing selected taxa as percentages of total land pollen (from Whittington et al., 1990). Cannabis sativa is not represented in this diagram but in the other cores occurs in zones equivalent to BL II j.

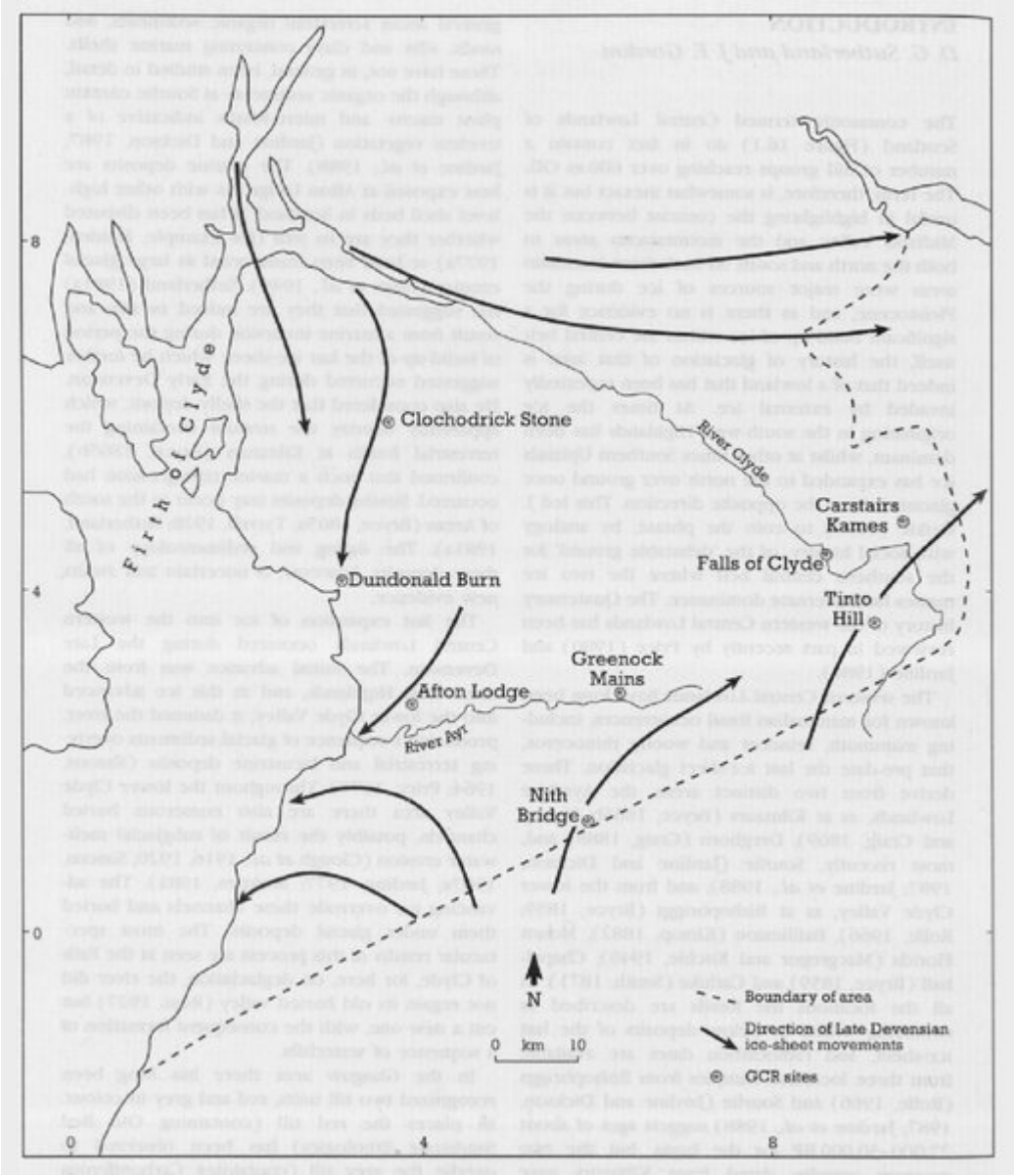

(Figure 16.1) Location map of the western Central Lowlands.

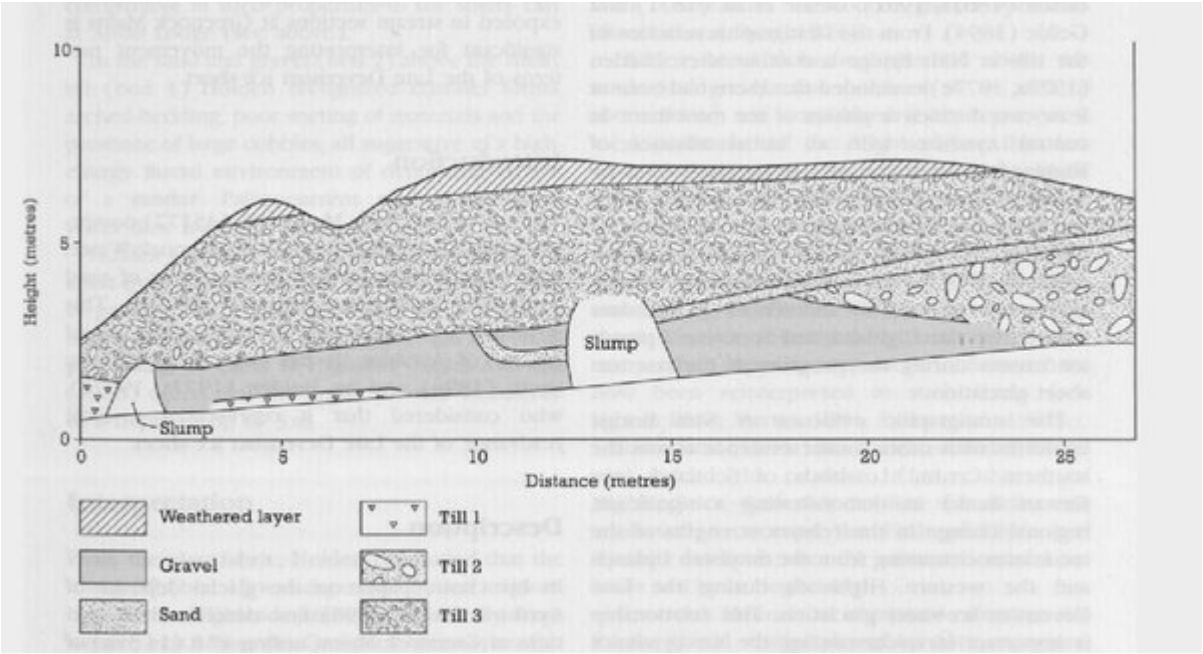

(Figure 16.2) Nith Bridge: sequence of sediments (from Holden and Jardine, 1980).

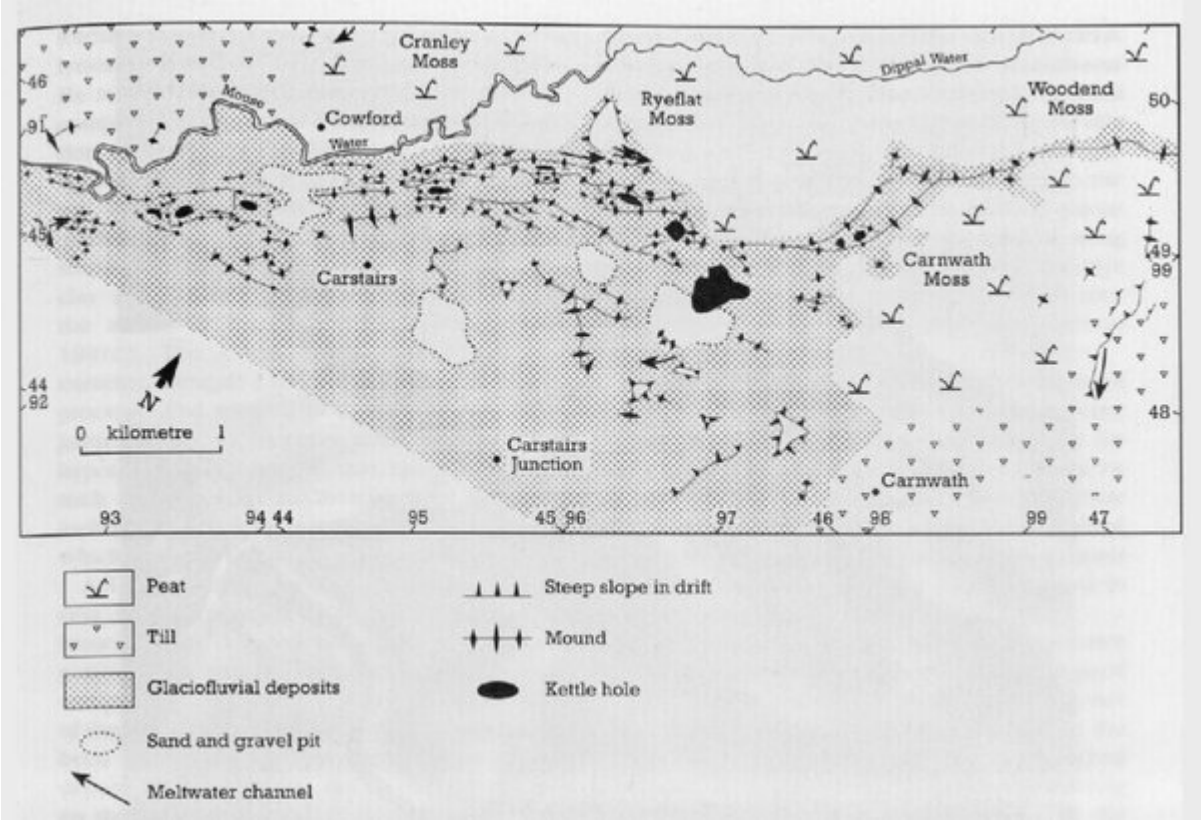

(Figure 16.3) Geomorphology of the Carstairs area (from McLellan, 1969).

(Figure 16.4) Carstairs Kames showing the interlinked form of the ridges and mounds, with intervening kettle holes. (© British Crown copyright 1992/MOD reproduced with the permission of the Controller of Her Britannic Majesty's Stationery Office.)

(Figure 16.5) Clochodrick Stone. (Photo: J E. Gordon.)

(Figure 16.6) Stone stripes are particularly well developed on Tinto Hill. (Photo: J E. Gordon.)

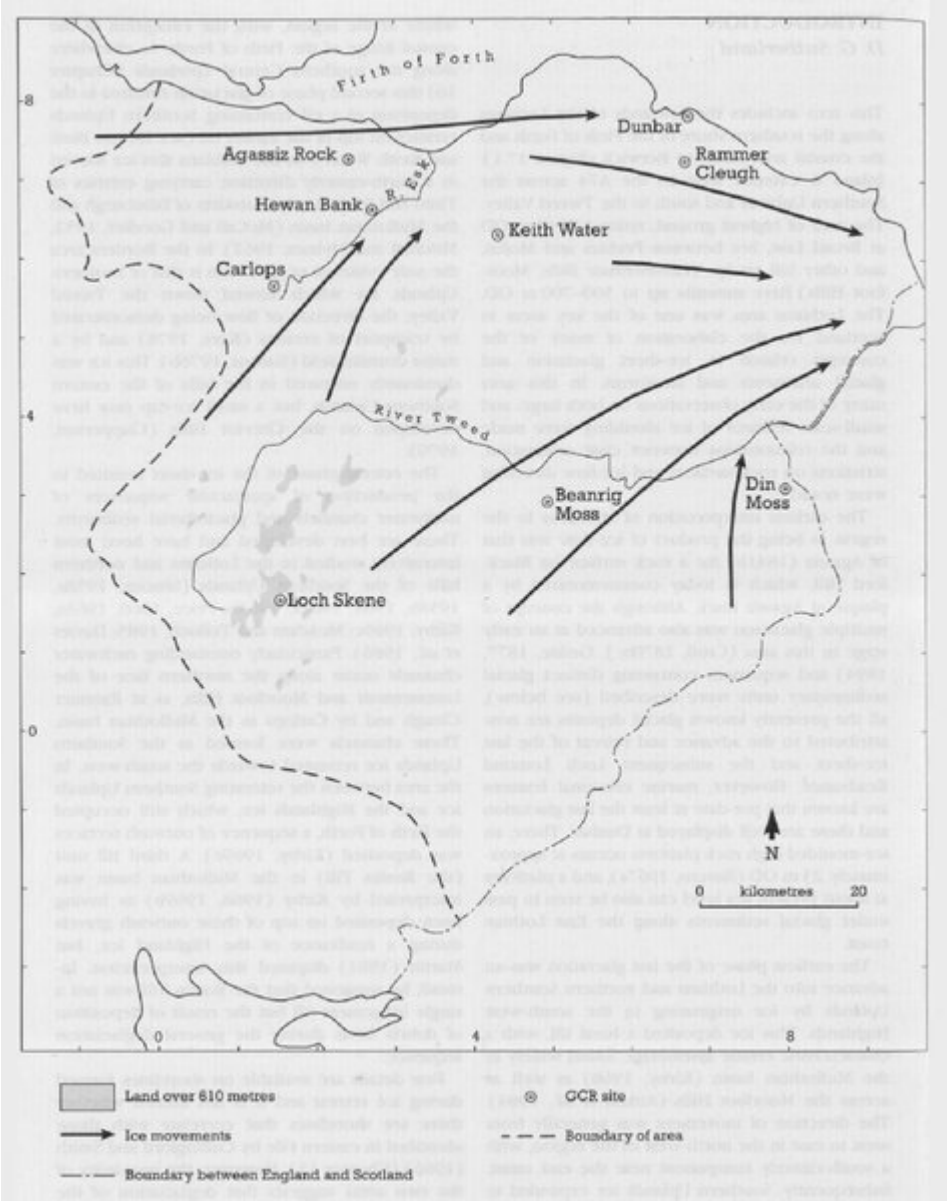

(Figure 17.1) Location map of the Lothians and Borders area.

(Figure 17.2) Part of the smoothed and grooved rock surface at Agassiz Rock, Edinburgh, which has been attributed to glacial abrasion. The form of the rock surface bears a strong resemblance to glacially abraded surfaces elsewhere in Scotland and in modern glacial environments (Photo: J E. Gordon.)

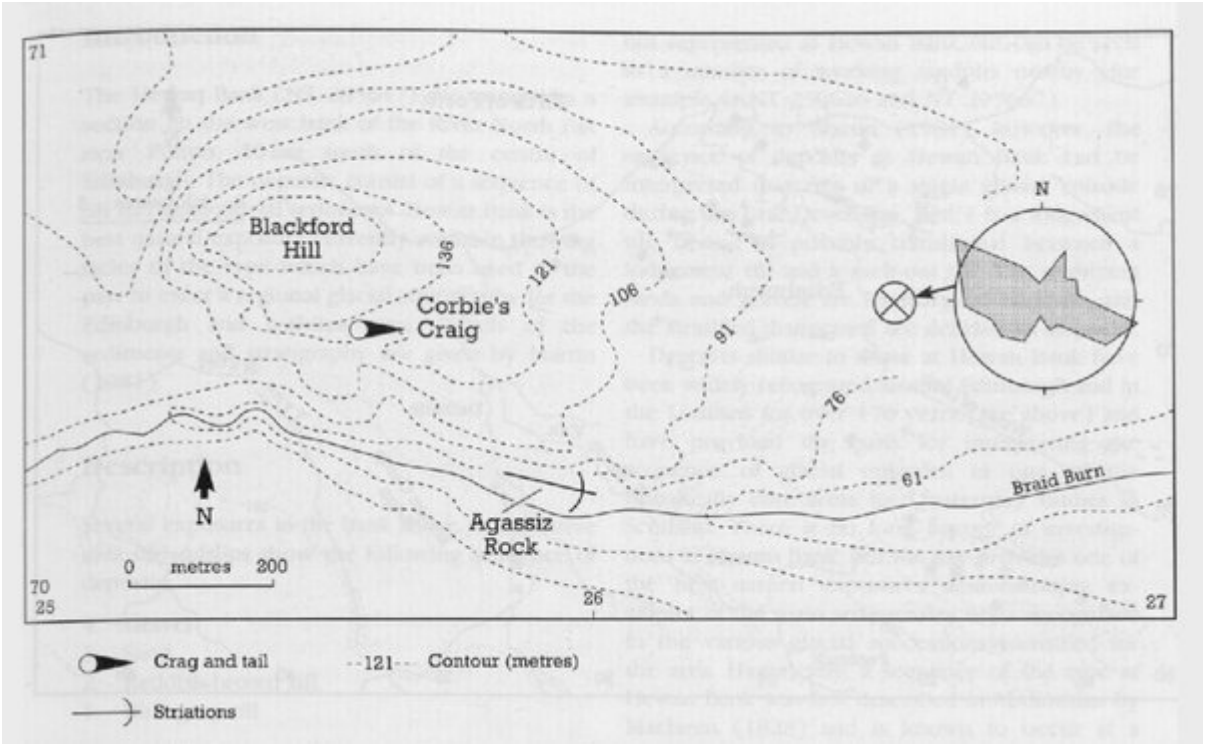

(Figure 17.3) Blackford Hill crag and tail, showing a till clast fabric in the tail, the Corbie's Craig crag and tail and the direction of ice movement inferred from the striations at Agassiz Rock (from Kirby, 1969b).

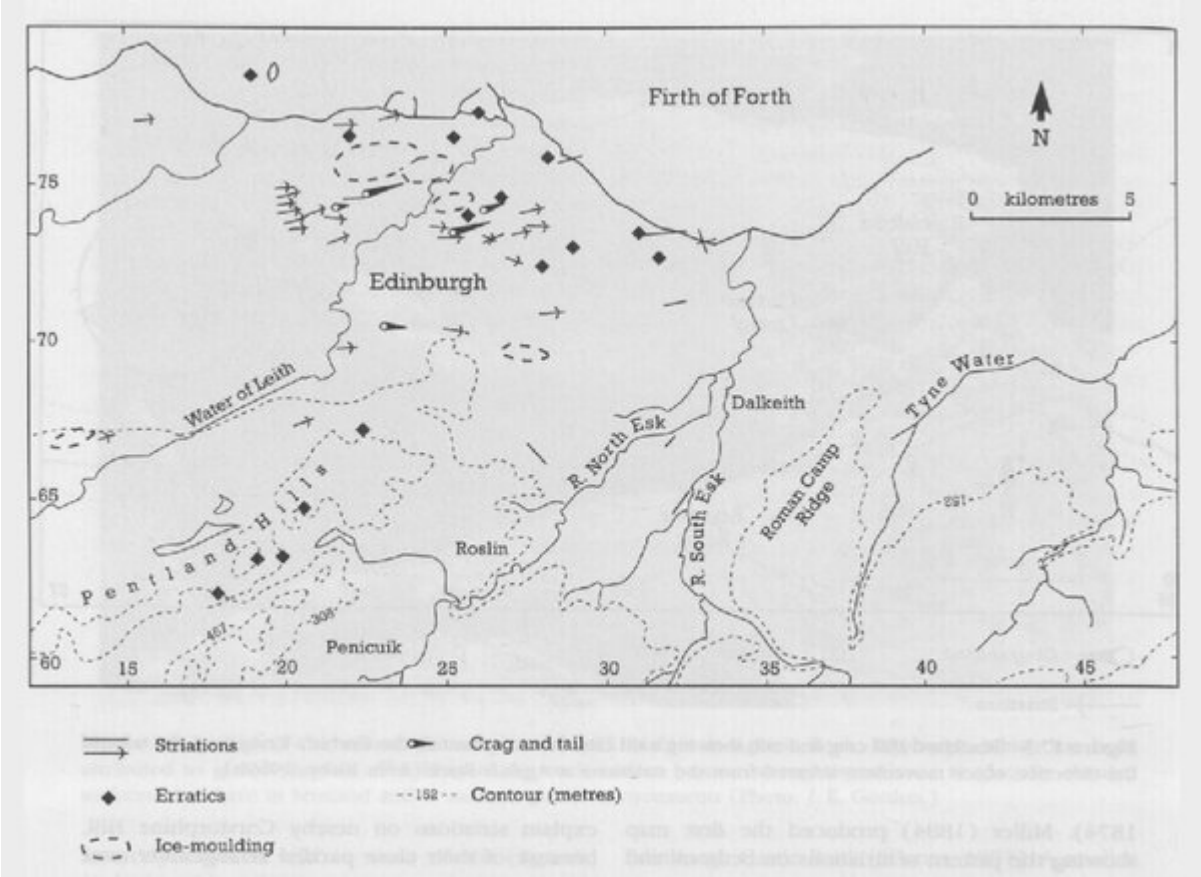

(Figure 17.4) Indicators of ice movement in the Lothians area recorded up until 1863 (from Kirby, 1969b).

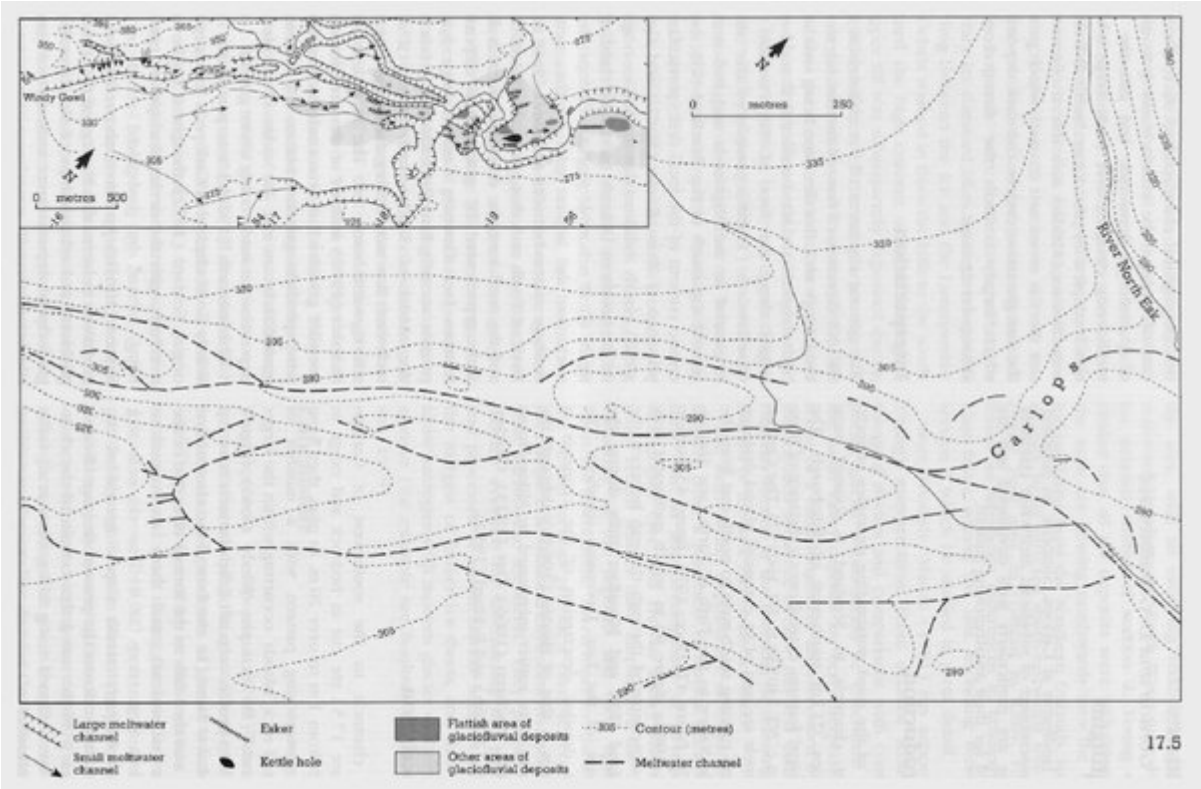

(Figure 17.5) The meltwater channel system at Carlops. The detailed pattern of channels immediately to the south-west of the village (main diagram) forms part of a more extensive glacial drainage system represented by channels and glaciofluvial deposits (inset) (from Sissons, 1963b).

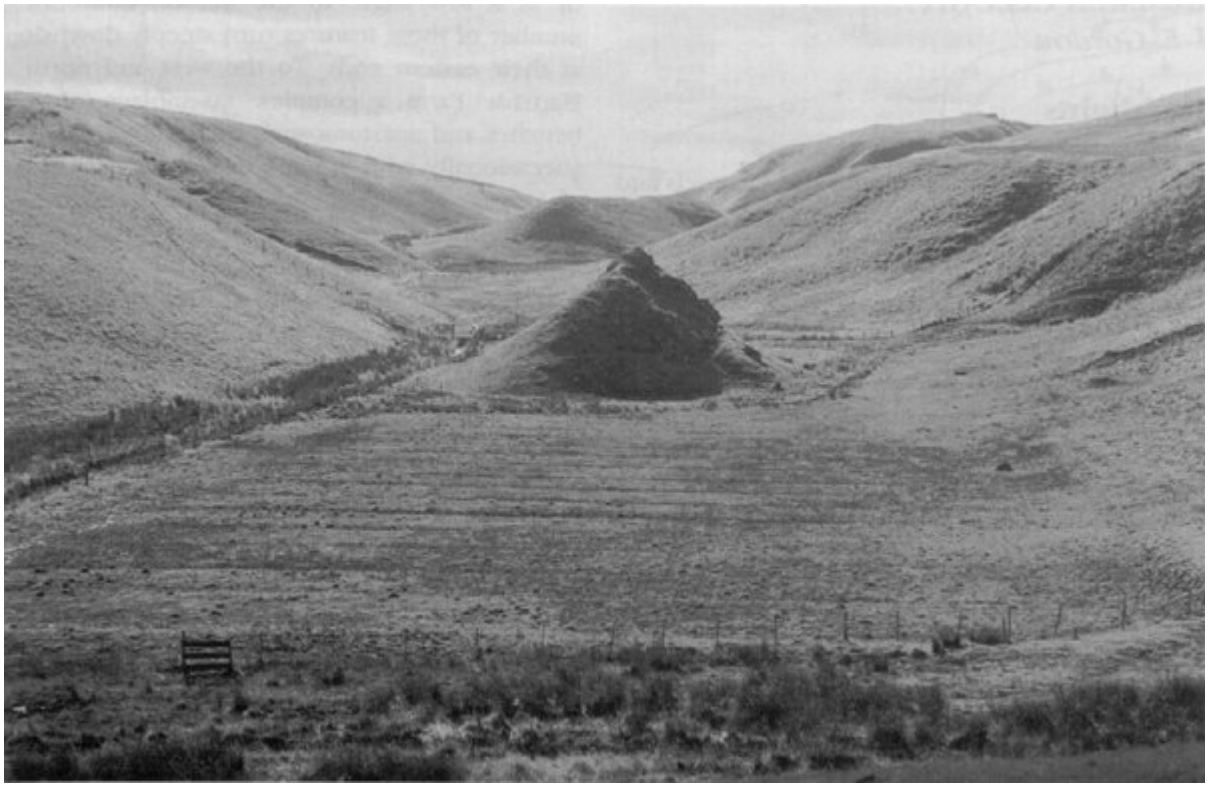

(Figure 17.6) The main meltwater channel at Carlops showing the anastomosing form of the channel system and the isolated interfluve 'islands' between constituent channels. (Photo: J E. Gordon.)

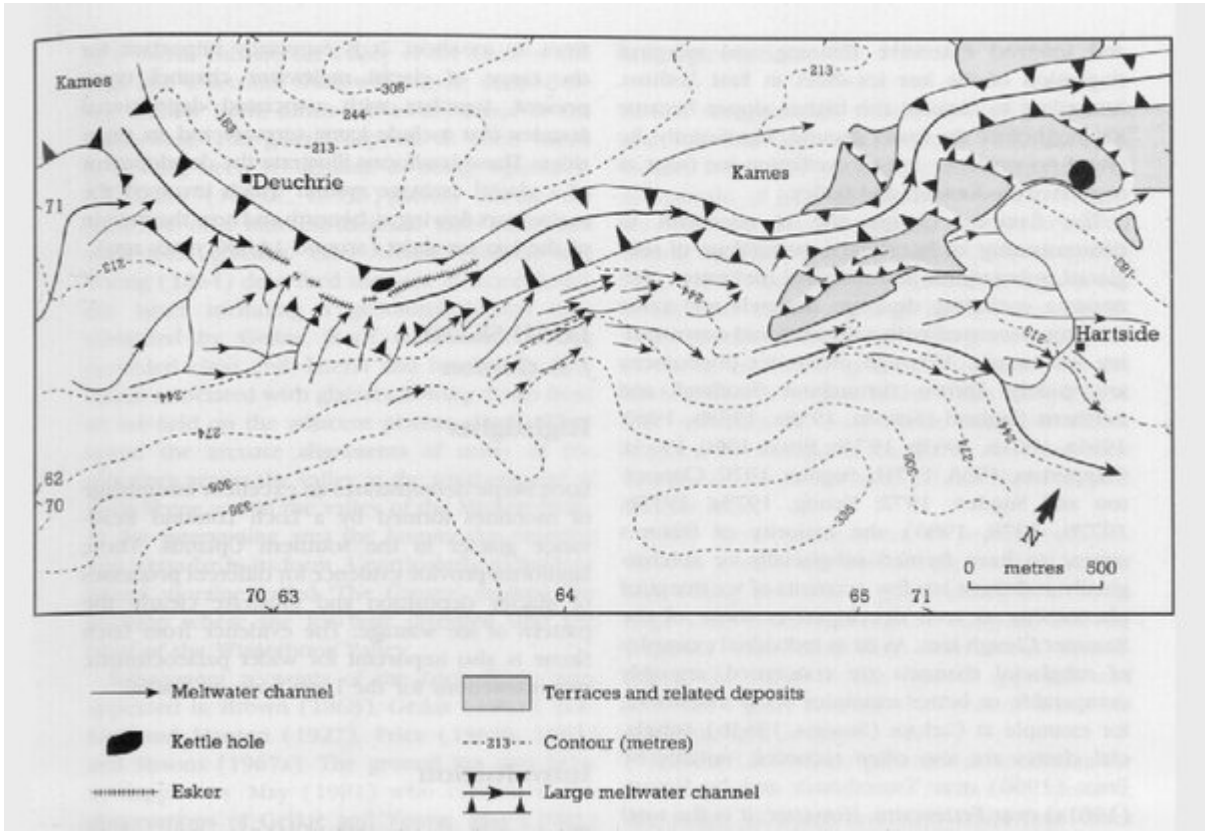

(Figure 17.7) Geomorphology of the meltwater channel system at Rammer Cleugh (from Sissons, 1958a).

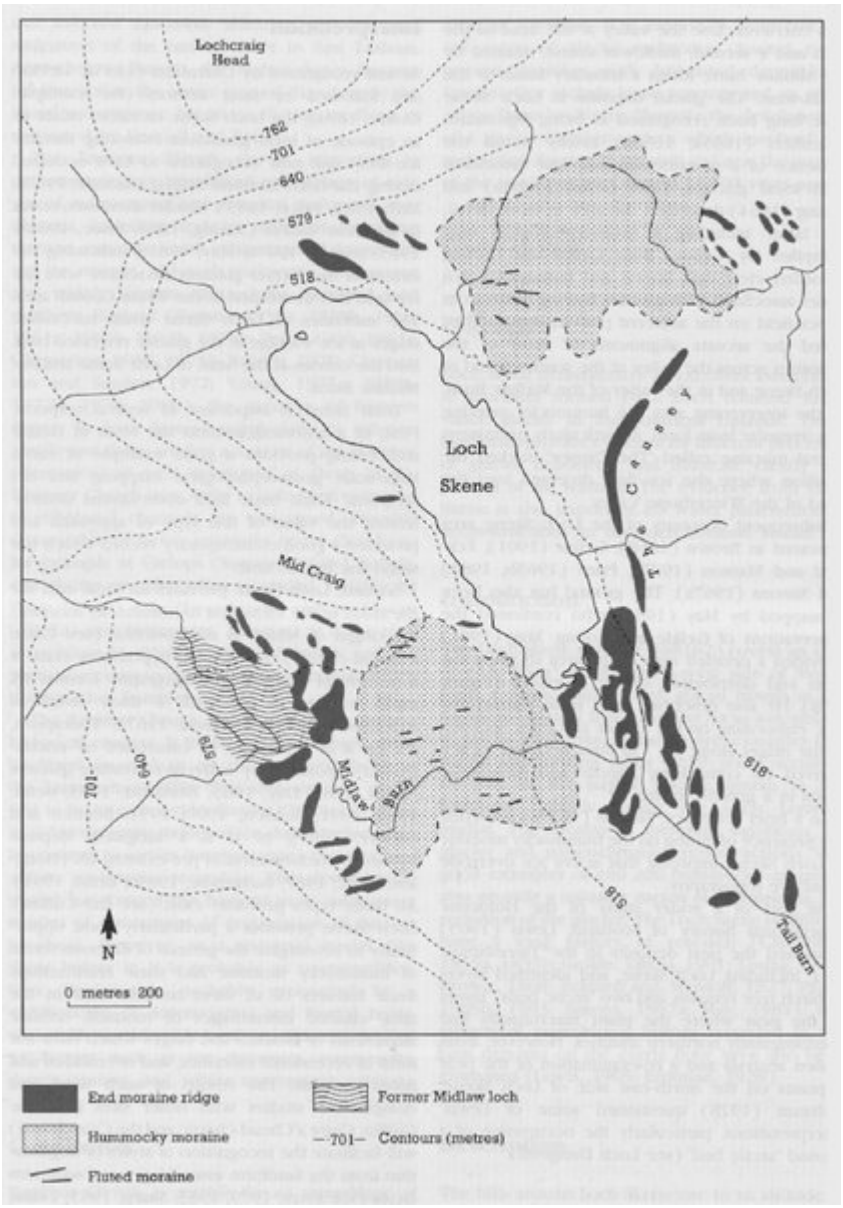

(Figure 17.8) Loch Lomond Readvance moraines at Loch Skene (from May, 1981).

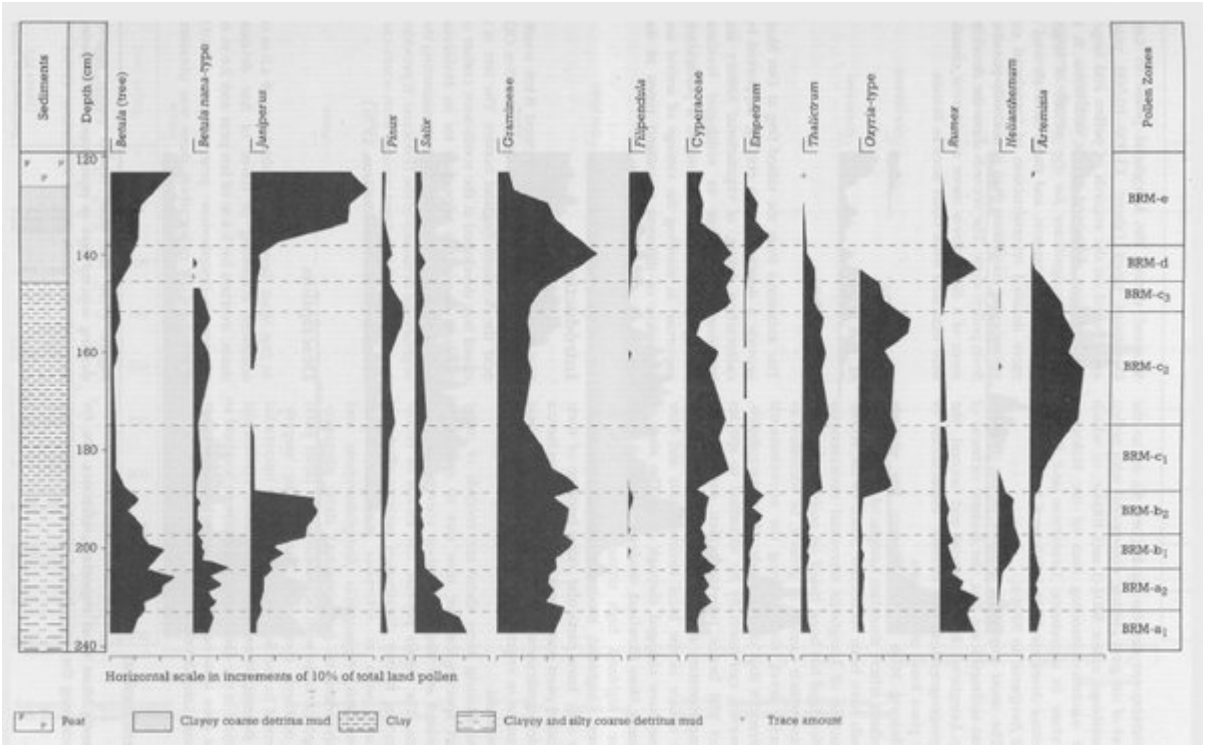

(Figure 17.9) Beanrig Moss: relative pollen diagram showing selected taxa as percentages of total land pollen (from Webb and Moore, 1982).

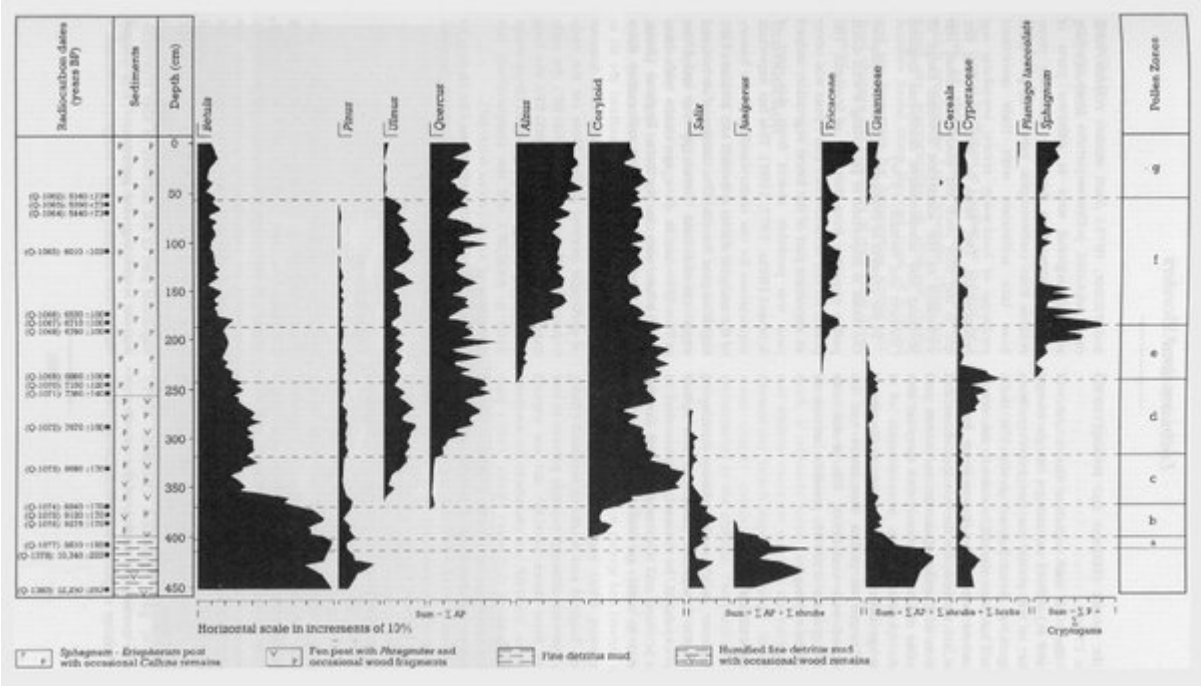

(Figure 17.10) Din Moss: relative pollen diagram showing selected taxa as percentages of the pollen sums indicated (from Hibbert and Switsur, 1976).

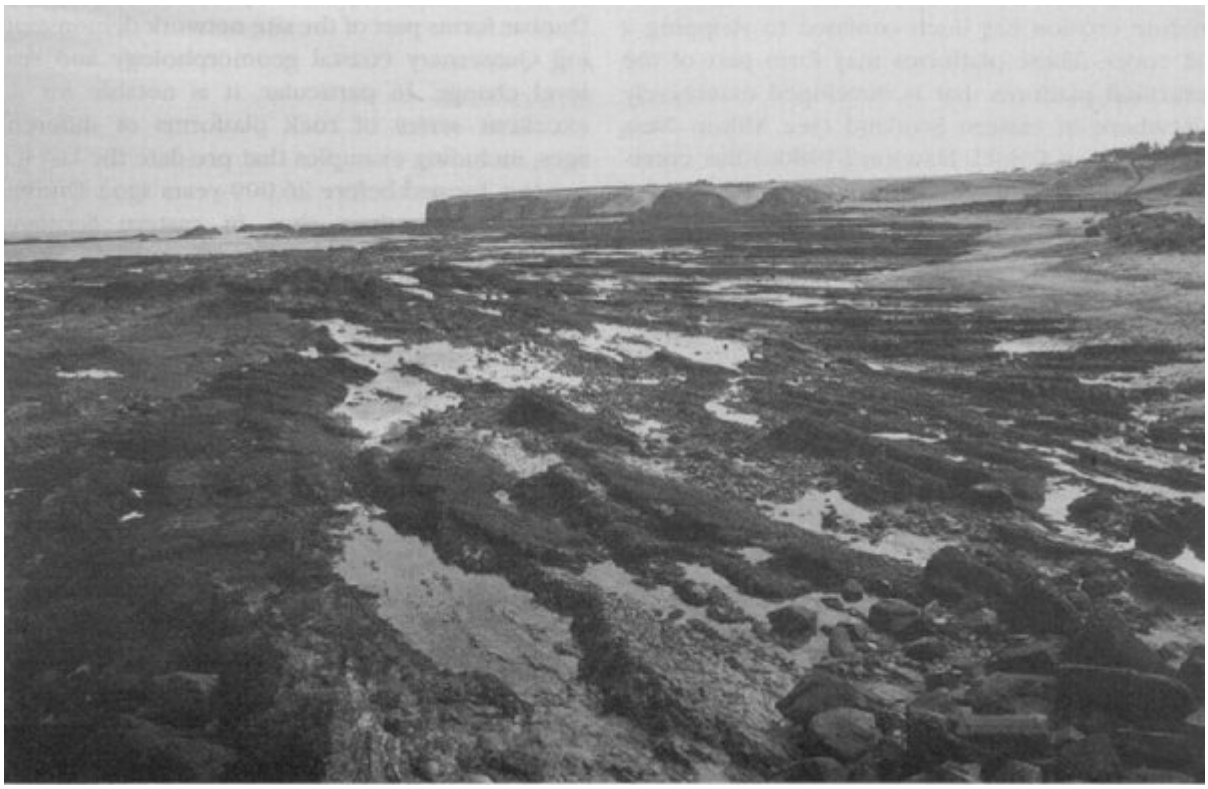

(Figure 17.11) Intertidal shore platform at Dunbar, which has been planed across a series of Devonian–Carboniferous and Carboniferous sediments and agglomerates. (Photo: J E. Gordon.)

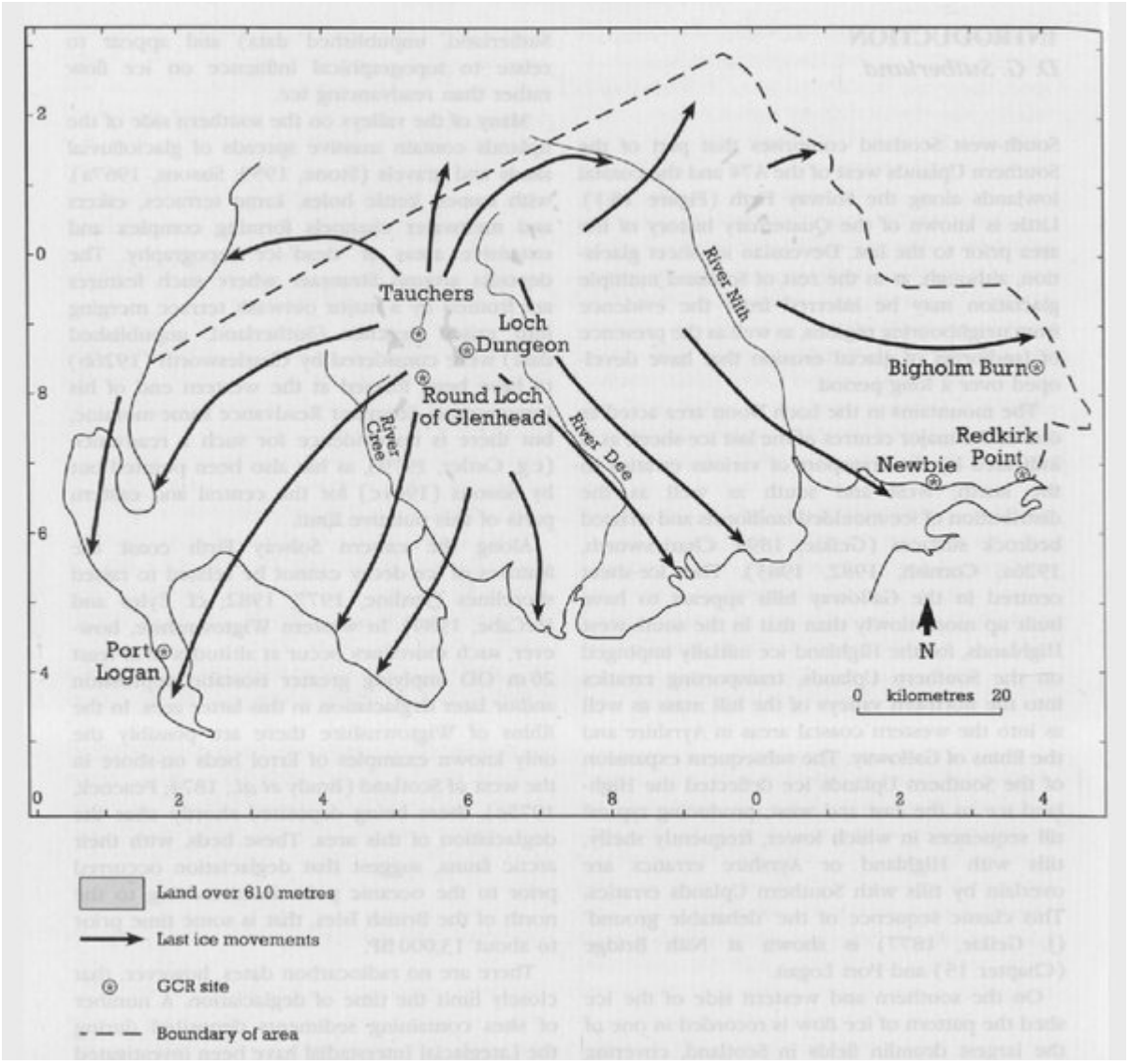

(Figure 18.1) Location map of south-west Scotland and generalized directions of ice movement.

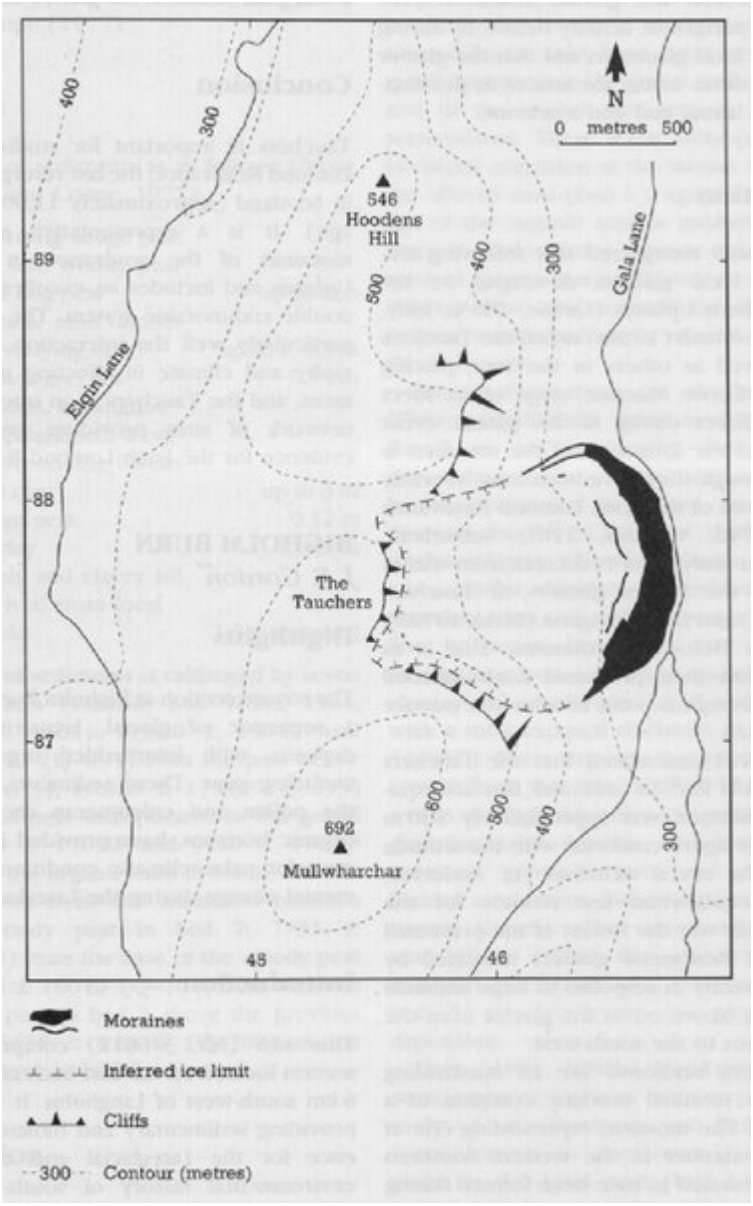

(Figure 18.2) Loch Lomond Readvance moraines and ice limits at the Tauchers (from Cornish, 1981).

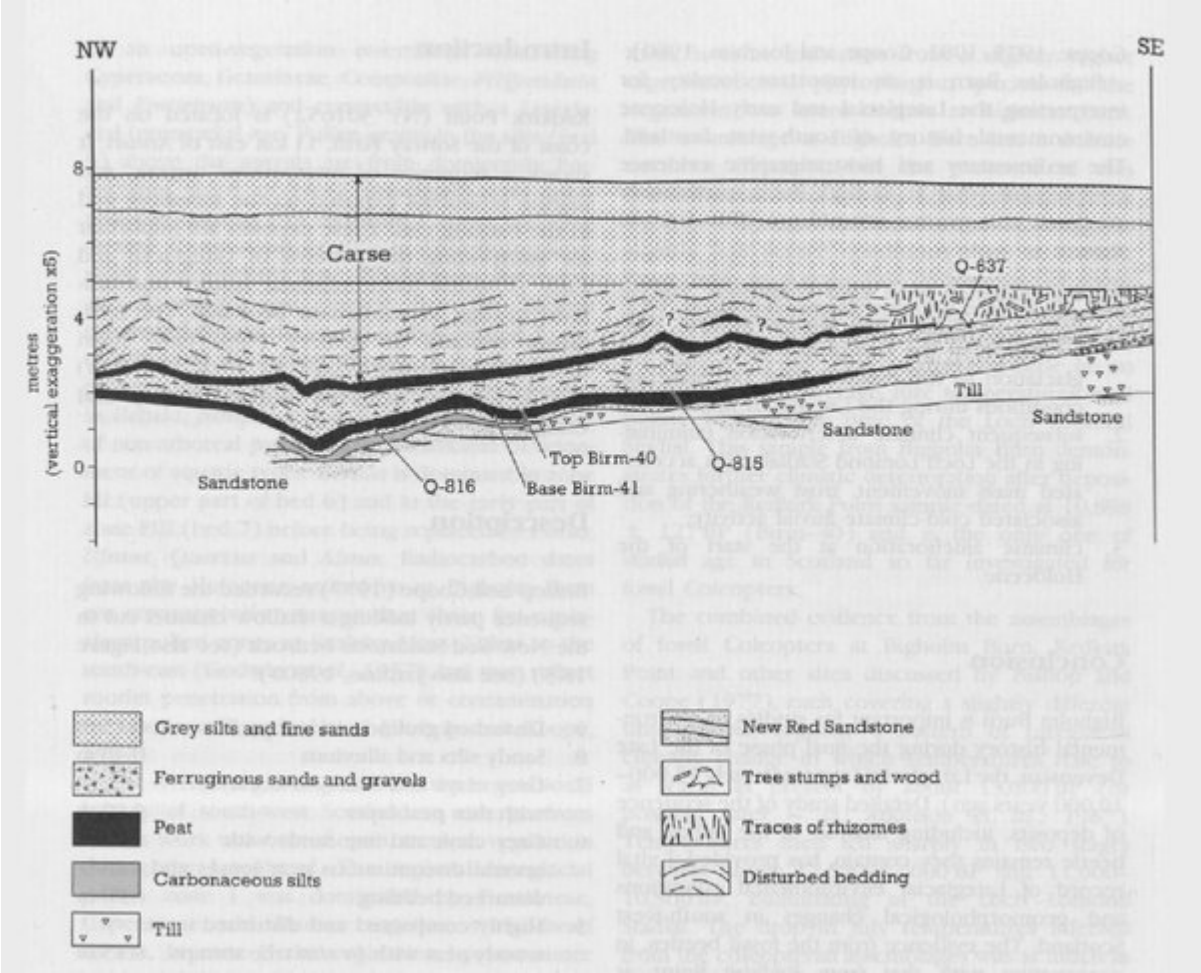

(Figure 18.3) Redkirk Point: sediment succession (from Bishop and Coope, 1977).

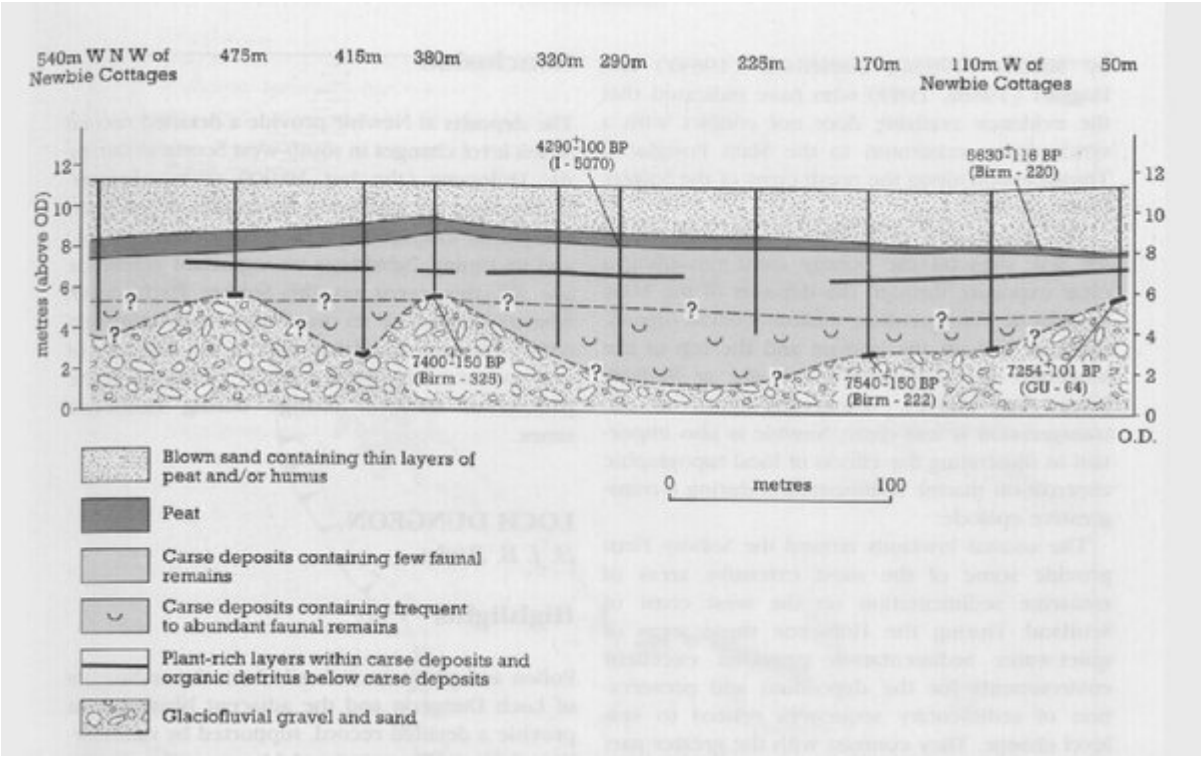

(Figure 18.4) Newbie: sediment succession (from Jardine, 1980b).

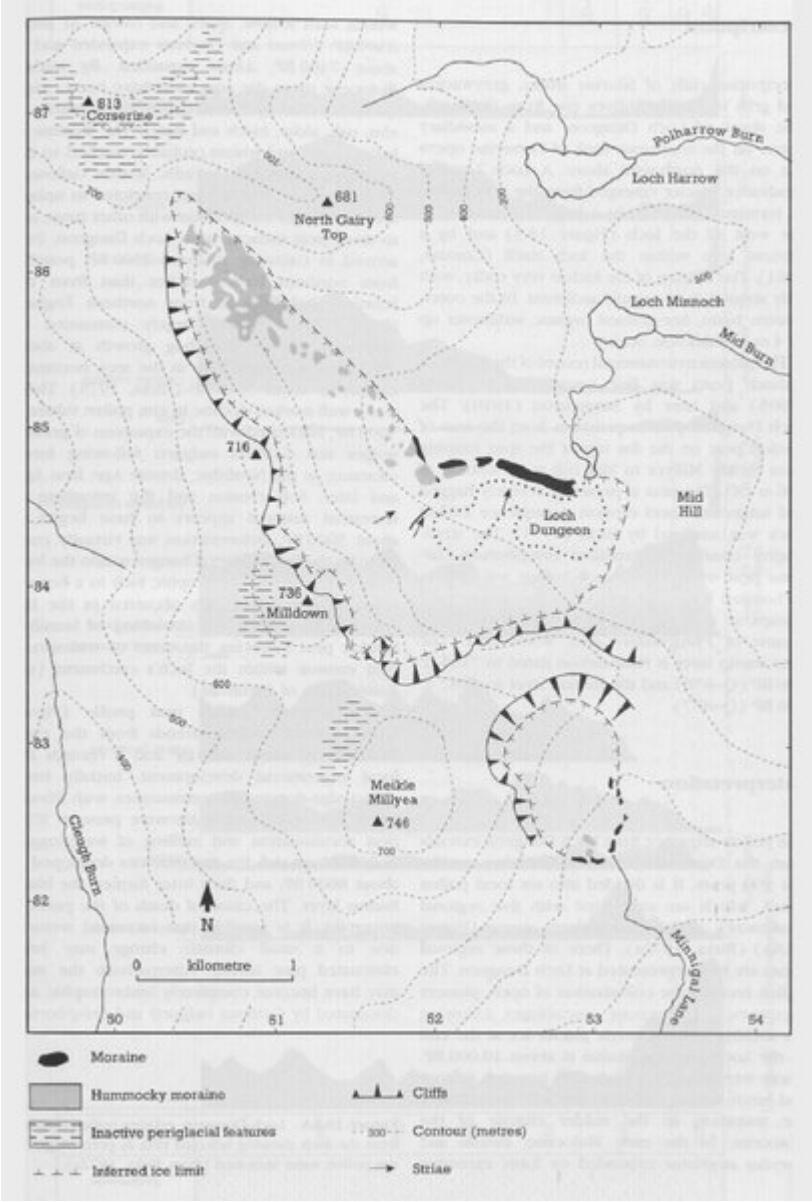

(Figure 18.5) Geomorphology of the Loch Dungeon area (from Cornish, 1981).

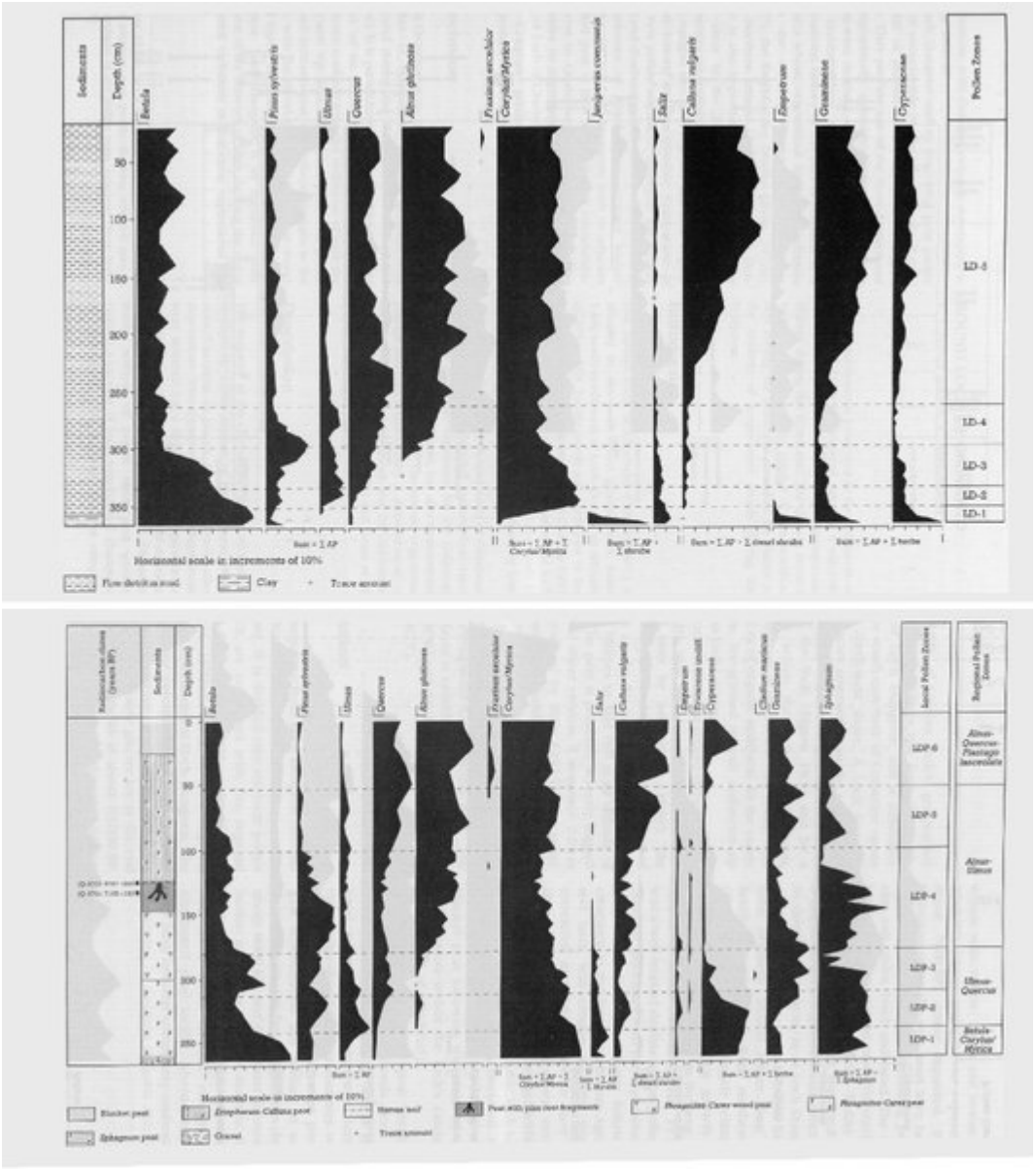

(Figure 18.6) A Loch Dungeon: relative pollen diagram from the loch showing selected taxa as percentages of the pollen sums indicated (from Birks, 1972a). B Loch Dungeon: relative pollen diagram from adjacent peat profile showing selected taxa as percentages of the pollen sums indicated (from Birks, 1975).

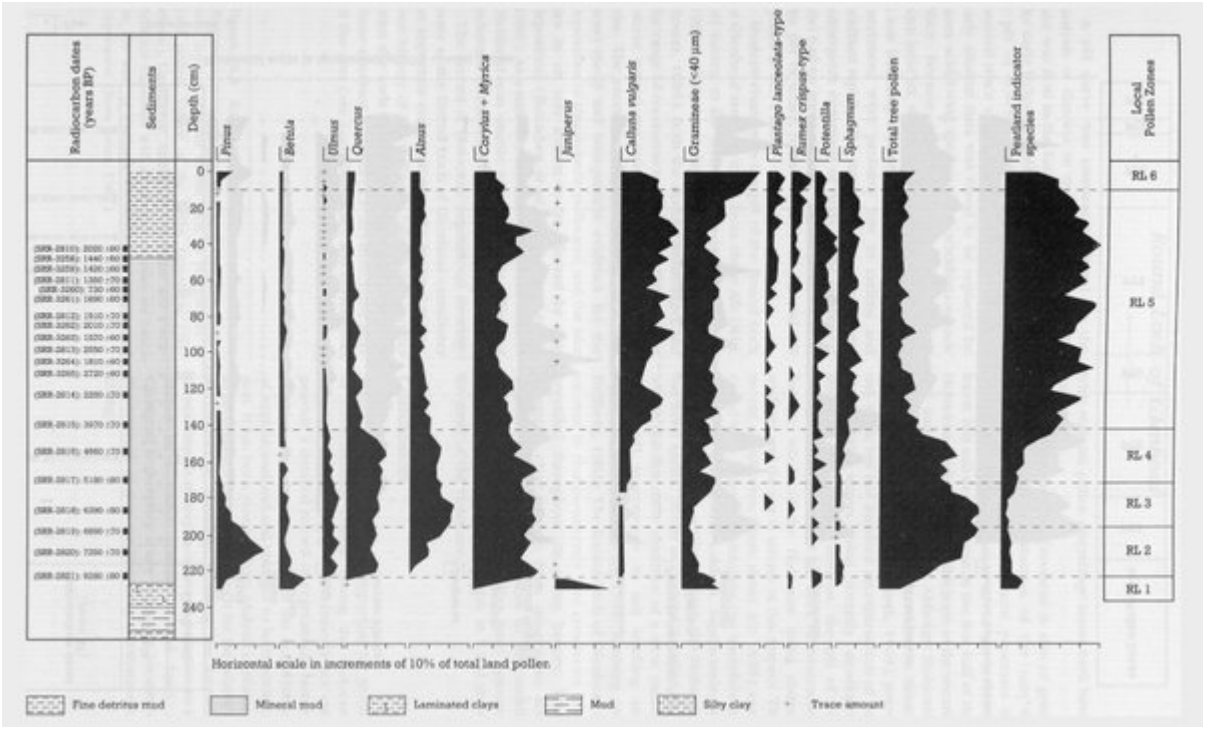

(Figure 18.7) Round Loch of Glenhead: relative pollen diagram showing selected taxa from core RLGH3 as percentages of total land pollen. Values of herbs except Gramineae and Cyperaceae are expanded X 10. Peatland indicators are based on the sum of Calluna, Potentilla, Sphagnum and Cyperaceae (from Jones, 1987).

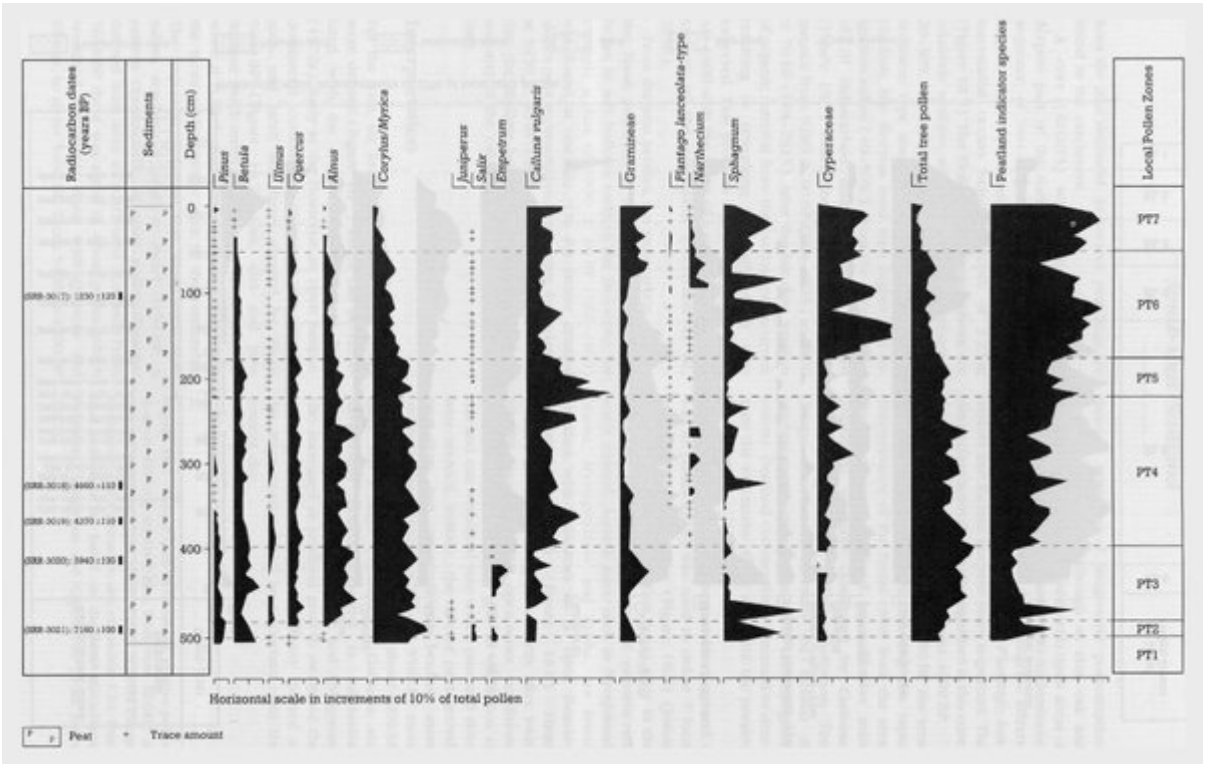

(Figure 18.8) Round Loch of Glenhead: relative pollen diagram showing selected taxa from core S18, from a peat deposit adjacent to the loch, as percentages of total pollen. Values of the herbs, Gramineae (4049 p.m), Liguliflorae, Artemisia, Cruciferae and Potentilla are expanded x 10. Peatland indicators are based on the sum of Calluna, Potentilla, Sphagnum and Cyperaceae (from Jones, 1987).

Location	Material	Radiocarbon date	Laboratory number
Garths Voe	0.02 m thick layer of peat above sand	5315 ± 45 BP	SRR–3839
Garths Voe	0.02 m thick layer of peat below sand	5765 ± 45 BP	SRR–3838
Voe of Scatsta	0.02 m thick layer of peat above sand	3815 ± 45 BP	SRR–3841
Voe of Scatsta	0.02 m thick layer of peat below sand	5700 ± 45 BP	SRR–3840

(Table 3.1) Radiocarbon dates relating to the buried sand horizon at Garths Voe and Voe of Scatsta

(a) Surface of fine-grained deposits in the inner Reindeer Cave		
Carnivora	*Ursus arctos* L.	Brown bear
	Alopex lagopus (L.)	Arctic fox
	Lynx lynx (L.)	Northern lynx
	Canis lupus L.	Wolf
Artiodactyla	*Rangifer tarandus* L.	Reindeer
Rodentia	*Dicrostonyx torquatus* (Pallas)	Arctic/collared lemming
	Microtus cf. *agrestis* L.	Field vole
	Microtus cf. *oeconomus* (Pallas)	Northern vole
	Arvicola terrestris L.	Water vole
	Apodemus sylvaticus (L.)	Wood mouse
(b) Dolomite-rich, upper gravel unit, outer Reindeer Cave		
Carnivora	*Ursus arctos* L.	Brown bear
Artiodactyla	*Rangifer tarandus* L.	Reindeer
Rodentia	*Dicrostonyx torquatus* (Pallas)	Arctic/collared lemming
	Microtus gregalis (Pallas)	Tundra vole
	Microtus sp.	Vole
(c) 'Cave earth' in Badger Cave (1), Reindeer Cave (2), Bone Cave (3)		
Insectivora	*Sorex araneus* L.	Common shrew (1)
	Sorex sp.	Shrew (2)
Primates	*Homo sapiens* L.	Man (1,2)
Carnivora	*Felis silvestris* Schreber	Wildcat (1)
	Mustela erminea L.	Stoat (3)
	Meles meles (L.).	Badger (1)
	Canis lupus L.	Wolf (3)
	Vulpes vulpes (L.).	Common fox (1,3)
	Ursus arctos L.	Brown bear (1,2,3)
Artiodactyla	*Sus* sp.	Pig (1)
	Cervus elaphus L.	Red deer (1,2)
	Capreolus capreolus (L.)	Roe deer (1)
	Rangifer tarandus L.	Reindeer (1,2,3)
	Ovis sp.	Sheep (1,2)
	Bos sp.	Ox (1,3)
Lagomorpha	*Oryctolagus cuniculus* (L.)	Rabbit (1,3)
	Lepus sp.	Hare (1)
Rodentia	*Arvicola terrestris* L.	Water vole (1)
	Microtus cf. *agrestis* L.	Field vole (1)
	Microtus oeconomus (Pallas)	Northern vole (1)
	Dicrostonyx torquatus (Pallas)	Arctic/collared lemming (2)

A variety of different unidentified bird species and fish, gastropods (including *Cepaea nemoralis* (L.) (2) and *Patella* sp. (2)) and amphibians (mainly frogs and toads) were also retrieved from this layer (c). E.T. Newton (in Peach and Horne, 1917) identified the following additional species from Bone Cave, presumably from the 'cave earth' stratum of the revised stratigraphy: weasel (*Mustela nivalis* L.), otter (*Lutra lutra* (L.)), rat vole (*Microtus ratticeps* (Keyserling and Blasius)), bank vole (*Clethrionomys glareolus* (Schreber)), ?chaffinch (*Fringilla coelebs* L.), barnacle goose (*Branta leucopsis* (Bechstein)), ?mute swan (*Cygnus olor* (Gm)), ?mallard (*Anas platyrhynchos* (L.)), teal (*Anas crecca* L.), wigeon (*Anas penelope* L.), tufted duck (*Aythya fuligula* (L.)), long-tailed duck (*Clangula hyemalis* (L.)), eider duck (*Somateria mollissima* (L.)), common scoter (*Melanitta nigra* (L.)), ptarmigan (*Lagopus mutus* (Montin)), red grouse (*Lagopus lagopus scoticus* (Latham)), golden plover (*Pluvialis apricaria* (L.)), grey plover (*Pluvialis squatarola* (L.)), little auk (*Alle alle* (L.)), puffin (*Fratercula arctica* (L.)), frog (*Rana temporaria* L.), toad (*Bufo bufo* L.), natterjack toad (*Bufo calamita* (Laurenti)), salmon or trout (*Salmo* sp.).

(Table 6.1) Faunal assemblages from the Creag nan Uamh caves.

Location	Details of sample	Altitude (metres OD) of sample at contact with minerogenic layer	14C date (years BP)	Laboratory number
Philorth Home Farm	Bottom 2 cm of peat above micaceous sandy silt	1.48	5700 ± 90	SRR–1660
Philorth Home Farm	Top 2 cm of peat below micaceous sandy silt	0.82	6300 ± 60	SRR–1661
Milltown	Bottom 2 cm of peat above micaceous sandy silt	1.82	5140 ± 60	SRR–1686
Milltown	Top 2 cm of peat below micaceous sandy silt	1.11	6095 ± 75	SRR–1687
Mains of Philorth	Top 1cm of peat below brown silty clay	2.59	4760 ± 60	SRR–1655
Mains of Philorth	Bottom 2 cm of peat above grey sand	1.51	6150 ± 250	SRR–1656
Mains of Philorth	Top 2 cm of peat below grey sand	1.47	6885 ± 90	SRR–1657
Mains of Philorth	Bottom 2 cm of peat above grey sand	1.40	7510 ± 120	SRR–1658
Mains of Philorth	Top 2 cm of peat below grey sand	1.34	8465 ± 95	SRR–1659

(Table 8.1) Radiocarbon dates from sites in the Philorth Valley (after Smith et al. 1982)

	1	2	3	4
Antalis entalis (L.)	**	*		
Boreotrophon clathratus (Ström)		*	*	
Boreotrophon truncatus (Ström)	**			
Buccinum undatum (L.)	*	*		
Gibbula cineria (L.)		*		
Lacuna parva (da Costa)			**	
Lacuna vincta (Montagu)	*			
Littorina sp	*			
Littorina saxatilis (Olivi)				*
Lora turricula (Montagu)		*	*	
Manzonia zetlandica (Montagu)	*			
Margarites costalis (Gould)	*			
Margarites helicinus (Fabricius)			*	
Moelleria costulata (Möller)	*			
Onoba aculeus (Gould)			**	
Onoba semicostata (Montagu)	*		**	
Polinices pallidus (Broderip and Sowerby)	*	*		
Puncturella noachina (L.)	*	*		
Rissoa interrupta (Adams)		*	**	
Skeneopsis planorbis (Fabricius)			**	
Tectonatica affinis (Gmelin)	*			
Velutina velutina (Müller)		*		
Abra sp.	*			
Abra alba (Wood)			**	
Acanthocardia echinata (L.)	*			
Arctica islandica (L.)	*	**		
Astarte sulcata (da Costa)		*		
Chlamys islandica (Müller)	***	***		
Heteranomia squamula (L.)	*			
Hiatella arctica (L.)	*	*		
Jupiteria minuta (Müller)	*		**	
Lyonsia arenosa (Möller)			*	
Macoma calcarea (Chemnitz)		*	**	
Mya truncata (L.)		*	**	
Nucula nucleus (L.)	*	*		
Nuculana pernula (Müller)	**	***	**	
Nuculoma sp.		*	**	
Nuculoma belloti (Adams)	*			**
Parvicardium ovale (Sowerby)	**	*		
Portlandia arctica (Gray)		*	*	****
Spisula subtruncata (da Costa)			*	
Thracia cf. *myopsis* (Möller)			*	
T. cf. *villosiuscula* (Macgillivray)	*			
Thyasira gouldi (Philippi)	*		**	
Tridonta elliptica (Brown)	***	***		
Tridonta montagui (Dillwyn)	**	**	*	
Yoldiella solidula (Warén)	**		***	
Yoldiella lenticula (Müller)	**	**	***	**

1. *Shore 10 m west of South Shian pier (NM 90834228).*
2. *Shore 10 m west of South Shian pier (NM 90834228), British Geological Survey collection.*
3. *Shore east of shellfish factory (NM 908416).*
4. *Shore west of Balure of Shian (glaciomarine bed) (NM 8962 4216).*

* *rare*
** *common*
*** *very common*
**** *dominant*

(Table 10.1) Mollusca from South Shian and Balure of Shian

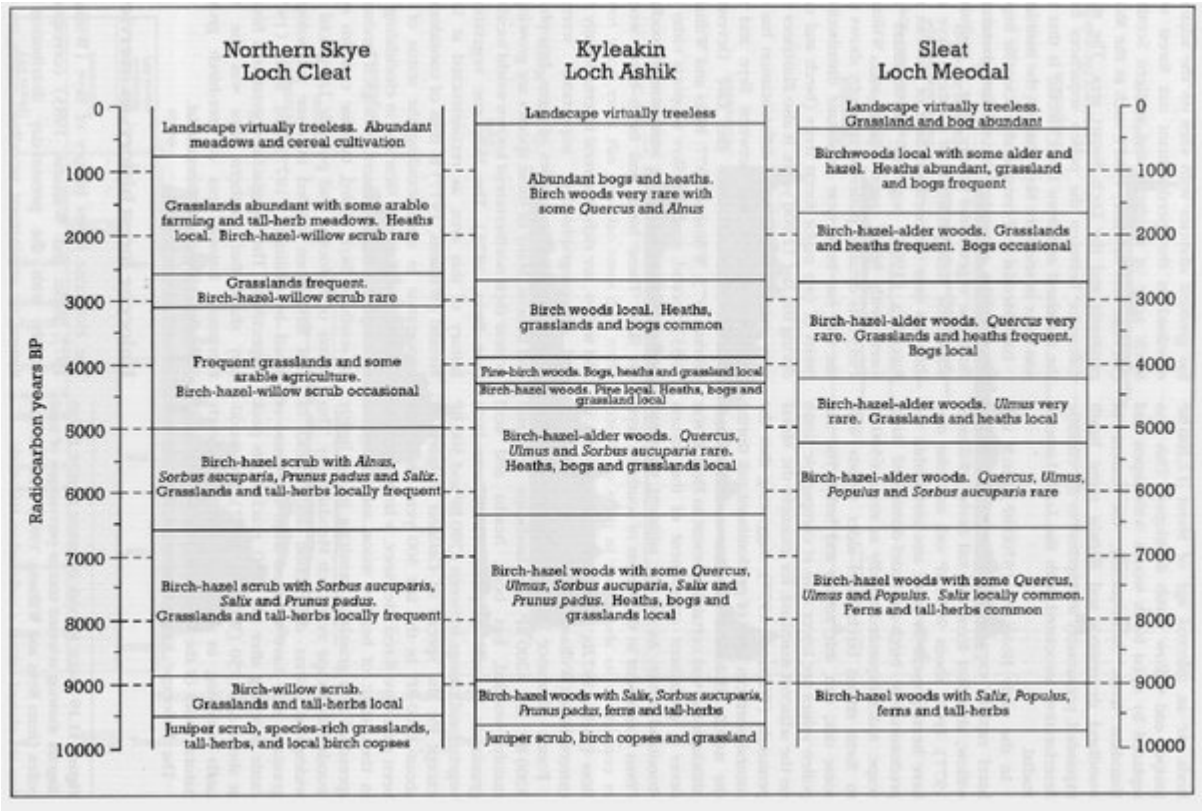

(Table 11.1) Generalized comparison of the inferred Holocene vegetational history of the Isle of Skye based on the pollen records from Loch Cleat, Loch Ashik and Loch Meodal (from Birks and Williams, 1983)

Museum specimen	Location	Modern name
Cyprina islandica	Dryleys	*Arctica islandica* (L.)
Leda arctica	Not given	*Portlandia arctica* (Gray)
Nucula tenuis	Not given	*Nuculoma tenuis* (Montagu)
Pecten greenlandicus	Dryleys	*Arctinula greenlandica* (Sowerby)
Saxicava sulcata	Dryleys	*Hiatella arctica* (L.)
Yoldia arctica	Dryleys	*Portlandia arctica* (Gray)
Somateria sp.	Puggieston	
Cythere sp.	Not given	
Ophiolepis gracilis	Dryleys	
Phoca vitellinus	Balwyllo	*Phoca vitulina* L.

An investigation of the Howden Collection in the Montrose Museum showed the following molluscan fauna to be present (J.D. Peacock, unpublished data).

Dryleys: *Arctinula greenlandica* (Sowerby), *Hiatella arctica* (L.), *Mya truncata* (L.) *Nuculoma belloti* (Adams), *Portlandia arctica* (Gray) and *Yoldiella* cf. *lenticula* (Müller).

Puggieston: *Arctica islandica* (L.), *Hiatella arctica* (L.), *Nuculoma* cf. *belloti* (Adams), *Yoldiella solidula* Warén and *Y. lenticula* (Müller).

Ballwyllo: *Arctinula greenlandica* (Sowerby).

Unplaced specimens: *Arctica islandica* (L.), *Arctinula greenlandica* (Sowerby), *Hiatella arctica* (L.) and *Portlandia arctica* (Gray).

(Table 14.1) Faunal remains (collected by J. C. Howden) in the Montrose area and attributed to a cold-climate environment

Sample	Location	Age (14C years BP)	Laboratory number
[1]*Somateria mollissima*	Puggieston	10,610 ± 220	Birm–660
[1]*Somateria* sp. or *Melanitta* sp.	Puggieston	11,110 ± 210	Birm–661
[2]*Arctica islandica*	Dryleys		
Outer fraction		3830 ± 140	Birm–737(1)
First middle fraction		4180 ± 120	Birm–737(2)
Second middle fraction		4170 ± 160	Birm–737(3)
Inner fraction		4020 ± 200	Birm–737(4)

[1]Smith *et al.* (1977); Williams and Johnson (1976).
[2]Smith (1986).

(Table 14.2) Radiocarbon dates from faunal remains in the Montrose area

Sample	Date (14C years BP)	Laboratory number
0.02 m thick slice of peat above layer	6850 ± 75	SRR–2119
0.02 m thick slice of peat below layer	7120 ± 75	SRR–2120

(Table 14.3) Radiocarbon dates on a possible storm surge layer at Puggieston, after Smith and Cullingford (1985)

Sample	Location	Date (14C years BP)	Laboratory number
0.02 m thick band of peat above basal laminated silty clay (bed 1)	Maryton	7340 ± 75 BP	SRR–869
0.02 m thick band of peat below sand layer	Fullerton	7140 ± 120 BP	Birm–823
0.02 m thick band of peat above sand layer	Fullerton	6880 ± 110 BP	Birm–867
0.02 m thick band from top of peat below the carse	Fullerton	7086 ± 50 BP	SRR–1149
0.02 m thick band from base of peat above the carse	Fullerton	6704 ± 55 BP	SRR–1148

Although the inversion of SRR–1149 and Birm–867 could reflect reworking or contamination, Smith *et al.* (1980) point out that the two dates are not statistically different at the 95% confidence level, and therefore suggest a mean age of 6983 ± 60 BP for peat above the sand layer.

(Table 14.4) Radiocarbon dates on sand layer in peat at Maryton and Fullerton (Smith et al., 1980)

Sample	Altitude OD (m)	Date (^{14}C years BP)	Laboratory number
Bottom 0.01 m of peat	3.19	9640 ± 140	I–2796
Bottom 0.04 m of peat	3.19	9524 ± 67	SRR–72
Top 0.01 m of peat	3.78	7605 ± 180	NPL–127
Top 0.04 m of peat	3.78	7778 ± 55	SRR–71

(Table 15.1) Radiocarbon dates on the buried peat layer at Carey

Sample	Altitude (m) OD (surface = 8.30 m)	Date (^{14}C years BP)	Laboratory number
Bottom 0.01 m of surface peat	7.23–7.24	5890 ± 5	SRR–1331
Top 0.01 m of peat beneath grey silty clay ('carse')	6.75–6.76	7310 ± 100	SRR–1332
Bottom 0.01 m of peat above grey, micaceous, silty fine sand	6.38–6.39	7050 ± 100	SRR–1333
Top 0.01 m of peat below grey, micaceous, silty fine sand	6.19–6.20	7555 ± 110	SRR–1334

(Table 15.2) Radiocarbon dates at Silver Moss (from Morrison et al., 1981)

Specimen	Modern name
Astarte compressa Mont.	*Tridonta montagui* (Dillwyn)
A. sulcata da Costa	*Astarte sulcata* (da Costa)
Cyprina islandica L.	*Arctica islandica* (L.)
Pecten islandicus Chemnitz	*Chlamys islandica* (Müller)
Leda pernula Müller	*Nuculana pernula* (Müller)
Hydrobia ulvae Pennant	
Natica affinis Gmelin	*Tectonatica clausa* (Broderip and Sowerby)
Drillia turricula Sowerby	*Oenopota turricula* (Montagu)
Trophon clathratus L.	*Boreotrophon clathratus* (L.)

(Table 16.1) List of mollusc shells recorded at Afton Lodge by Eyles (1922) and Eyles et al. (1949). (Modern names are from J. D. Peacock, unpublished data.)

Mollusca

Arctica islandica (L.)
Astarte elliptica (Brown)

Foraminifera

Ammonia beccarri (L.)
Quinqueloculina seminulum (L.)
Elphidium excavatum (Terquem)
Elphidium articulatum (d'Orbigny)
Elphidium clavatum (Cushman)
Elphidium sp.
Fissurina cf. *lucida* (Williamson)

Ostracoda

Cyprideis torosa Jones
Cytheropteron latissimum (Norman)

(Table 16.2) Fauna recovered from the Afton Lodge marine clay listed in Holden (1977a)